NOVEL BIONANOCATALYSIS FOR CHROMIUM(VI) REMEDIATION

By Andrea Claire Humphries

A thesis submitted to

The University of Birmingham

for the degree of

DOCTOR OF PHILOSOPHY

School of Biosciences

The University of Birmingham

January 2005

UNIVERSITY OF
BIRMINGHAM

University of Birmingham Research Archive

e-theses repository

This unpublished thesis/dissertation is copyright of the author and/or third parties. The intellectual property rights of the author or third parties in respect of this work are as defined by The Copyright Designs and Patents Act 1988 or as modified by any successor legislation.

Any use made of information contained in this thesis/dissertation must be in accordance with that legislation and must be properly acknowledged. Further distribution or reproduction in any format is prohibited without the permission of the copyright holder.

STATEMENT

I declare that this thesis contains no material which has been accepted for the award of any other degree or diploma in any University and that, to the best of my knowledge, this thesis contains no material previously published or written by any person except where due reference is given in the text of this thesis.

Andrea Humphries BSc (Hons) Msc (Eng).

To my family

ACKNOWLEDGEMENTS

I would like to thank Prof. Lynne Macaskie, my supervisor, for her guidance and support during this PhD.

I would like to thank my family and friends, in particular my mother and father, for their love, support and encouragement.

Lastly, but by no means least, all members of laboratory T102 past and present. Their good humour, advice, support and encouragement has been invaluable.

ABSTRACT

Many industrial wastewater's contain carcinogenic and mutagenic Cr (VI). Conversion to Cr(III) reduces toxicity. *Desulfovibrio vulgaris* NCIMB 8303 and *Microbacterium* sp. NCIMB 13776 immobilized in agar reduced Cr(VI) at initial rates of 127 and 15 nmol h^{-1} mg dry cell wt^{-1} in batch, and for 160 h in continuous-flow packed-bed columns. Similar columns containing agar-immobilized Bio-Pd(0) (Pd(II) was reduced to cell-bound Pd(0) using growth decoupled cells of *D. vulgaris*) reduced Cr(VI) in excess of 1334 h. Bio-Pd(0) produced using *Desulfovibrio* species was catalytically superior to Bio-Pd(0) produced using *Escherichia coli* species. Application of enzyme kinetics to the immobilized Bio-Pd(0) system gave an apparent K_m value of 650 μM for batch reduction, and 430 μM for continuous-flow.

Magnetic Resonance Imaging (MRI) was used to demonstrate immobilization matrix integrity, homogeneity within agar beads, and to distinguish between columns containing Cr(III) and Cr(VI), suggesting it may be possible to study Cr(VI) reduction non-invasively *in vivo* using MRI.

Biologically produced hydrogen was used in conjunction with resting and palladised cells of *D. vulgaris* for Cr(VI) reduction, and a system proposed for the concurrent treatment of industrial sugar wastes, precious metal scrap and Cr(VI).

TABLE OF CONTENTS

SECTION 1: GENERAL INTRODUCTION.	**1**
1.0 Heavy metal pollution.	2
1.1 Sources of chromium.	2
1.2 Chromium chemistry.	3
2.0 Reduction of Cr(VI) as a means to its removal from solution.	7
2.1 Mechanism of Cr(VI)-resistance.	8
2.2 Cr(VI) removal.	8
2.3 Occurrence of microbial Cr(VI) reduction.	9
2.3.1 Cr(VI) reduction by *Escherichia coli.*	10
2.3.2 Cr(VI) reduction by *Pseudomonas.*	12
2.3.3 Cr(VI) reduction by *Agrobacterium.*	14
2.3.4 Cr(VI) reduction by *Enterobacteria.*	14
2.3.5 *Microbacterium* sp. NCIMB 13776.	16
2.4 Sulfate-reducing bacteria (SRB).	17
2.4.1 Bioenergetics of dissimilatory sulfate reduction.	18
2.4.2 Hydrogenases.	20
2.4.3 Cytochromes.	20
2.4.4 Reduction of Cr(VI) by SRB's.	21
2.4.5 Reduction by Pd(II) by SRB's.	23
3.0 Cell immobilization.	25

3.1 Immobilization by surface attachment.	27
3.1.1 Immobilization by natural adsorption.	27
3.1.2 Artificially induced immobilization.	28
3.2 Entrapment in a porous matrix.	29
3.2.1 Gel entrapment.	29
3.2.1.1 Gel entrapment with alginate.	29
3.2.1.2 Gel entrapment with carrageenan.	30
3.2.1.3 Gel entrapment with agar and agarose.	31
3.2.1.4 Gel entrapment with chitosan.	32
3.2.1.5 Gel entrapment with polyacrylamide.	32
3.2.1.6 Gel entrapment with polyvinyl alcohol (PVA).	33
3.2.1.7 Gel entrapment with Lentikats®.	34
3.2.2 Entrapment with a preformed support.	35
3.3 Containment behind a barrier.	35
3.4 Self-aggregation of cells.	36
3.5 Biofilm formation.	36
3.6 Factors affecting the activity of immobilized cell particles.	38
3.6.1 Activity of immobilized cells.	38
3.6.2 Concentration in the bulk liquid.	39
3.6.3 Effective diffusion coefficients.	40
3.7 Operational considerations in the use of immobilized cells.	40
3.7.1 Stability in immobilized bioreaction systems.	40
3.7.2 Support matrix stability.	40

4.0 Objectives of the research programme.	41
4.1 Aims of this study.	42
5.0 Layout of the thesis.	43
References cited in Introduction.	44
SECTION 2: Chromate reduction by *D. vulgaris* NCIMB 8303 and *Microbacterium* sp. NCIMB 13776.	**51**
SECTION 2.1: Reduction of Cr(VI) by *Desulfovibrio vulgaris* and *Microbacterium* sp.	52
SECTION 2.2: Reduction of Cr(VI) by immobilized cells of D*esulfovibrio vulgaris* NCIMB 8303 and *Microbacterium* sp. NCIMB 13776.	60
SECTION 3: Chromate reduction by palladised biomass.	**88**
SECTION 3.1: Continuous removal of Cr(VI) from aqueous solution catalysed by palladised biomass of *Desulfovibrio vulgaris* NCIMB 8303.	89
SECTION 3.2: Reduction of Cr(VI) by palladised biomass of *Desulfovibrio vulgaris* NCIMB 8303.	102
SECTION 3.3: Chromate reduction by immobilized palladised bacteria.	122
SECTION 4: Cr(VI) reduction by bio- and bioinorganic catalysis via use of Bio-H_2: a sustainable approach for remediation of wastes from the metal finishing and food processing sectors.	167

SECTION 5: Discussion.	**191**
General Discussion.	192
Conclusions.	204
Further work.	205
References cited in discussion.	207
APPENDICES	**210**
APPENDIX I: Chromate reduction by immobilized cells of *Desulfovibrio vulgaris* using biologically produced hydrogen.	211
APPENDIX II: Principles of Magnetic Resonance Imaging.	224
1.0 Magnetic Resonance Imaging (MRI).	225
2.0 Principles of MRI.	225
2.1 Nuclear spin and magnetic moment.	225
2.2 Bulk magnetisation in a magnetic field.	226
2.3 Resonance.	227
2.4 The MR signal.	228
2.5 The free induction signal.	228
2.6 Relaxation processes.	229
2.7 Pulse timing parameters.	229
2.8 Spin Echo Imaging.	230
2.9 Gradient Echo Techniques.	231
2.10 Spoiled GRASS (SPGR) sequence.	231

2.11 Image contrast.	231
2.12 The use of metal ions as contrast agents.	232
2.13 Use of paramagnetism as a way to determine metal speciation within a reactor	232
3.0 Examples of MRI relevant to this project.	233
References cited in Appendix II.	236
APPENDIX III: Visualisation of the biosorption of Cr^{6+} and Cr^{3+} by Magnetic Resonance Imaging.	237
APPENDIX IV: Supplementary Materials and Methods.	248
1.0 Materials.	249
1.1 Bacterial strains.	249
1.2 Media.	249
2.0 General methods in Biochemistry.	252
2.1 Assay for Cr(VI) – The diphenylcarbazide method.	252
2.1.1 Cr(VI) calibration curve.	253
2.2 Determination of protein concentration – The bicinochoninic acid method.	254
2.2.1 Protein calibration curve.	255
2.3 Determination of Pd(II) concentration.	256
2.3.1 Pd(II) calibration curve.	256
2.4 Cell density.	257
2.5 Determination of dry cell weight.	257
2.6 Relationship between OD_{600}, protein concentration and dry cell weight.	257

APPENDIX V: Application of bacterial hydrogenases in waste decontamination, manufacture of novel bionanocatalysts and in sustainable energy.	259

Table of Figures

SECTION 1: INTRODUCTION	
Fig. 1: Cellular reduction of Cr(VI).	4
Fig. 2: Hydrogen cycling in SRB.	18
Fig. 3: Immobilization methods for microbial cells.	26
Fig. 4: Geometry of a Lentikat®.	35
Fig. 5: Substrate concentration profile of an immobilized cell particle.	38
SECTION 2:	
SECTION 2.1:	
Fig. 1: Reduction of 500 µM Cr(VI) by resting cells of *D. vulgaris* (A) and *Microbacterium* sp. (B) at pH 7 and 30 °C using different electron donors.	55
Fig. 2: Reduction of 500 µM Cr(VI) by resting cells of *D. vulgaris* (A) and *Microbacterium* sp. (B) at 30 °C at different pH's.	57
Fig. 3: Comparative reduction of 500 µM Cr(VI) by resting cells of *D. vulgaris* and *Microbacterium* sp. in the presence and absence of 3-(N-Morpholino)propanesulfonic acid.	57
SECTION 2.2:	
Fig. 1: Reduction of 500 µM Cr(VI) by resting cells of *D. vulgaris* and *Microbacterium* sp. immobilized in agar, agarose, Lentikats® and *k*-carrageenan.	85
Fig. 2: Continuous removal of Cr(VI) by cells of *D. vulgaris* (A) and *Microbacterium* sp. (B) immobilized in agar and agarose beads.	86

Fig. 3: Proton magnetic resonance imaging of the columns shown in Fig. 2.	87
SECTION 3:	
SECTION 3.1:	
Fig. 1: Magnetic resonance images of Bio-Pd(0) immobilized in chitosan and agar.	100
Fig. 2: Continuous reduction of 100 μM Cr(VI) by agar-immobilized Bio-Pd(0) and Chemical-Pd(0).	101
SECTION 3.2:	
Fig. 1: Reduction of 500 μM Cr(VI) by suspended Bio-Pd(0) and Chemical-Pd(0) at 22 and 30 °C.	118
Fig. 2: Effect of pH on the initial rate of reduction of 500 μM Cr(VI) by suspended Bio-Pd(0) and Chemical-Pd(0).	119
Fig. 3: Reduction of 500 μM Cr(VI) by agar-immobilized Bio-Pd(0) at 22°C at pH 3 and 7.	120
Fig. 4: Effect of initial Cr(VI) concentration on the initial rate of Cr(VI) reduction by suspended and agar-immobilized Bio-Pd(0).	121
SECTION 3.3:	
Fig. 1: Deposits of Pd(0) on the surface of *D. desulfuricans* (a), *D. vulgaris* (b) *E. coli* strain MC4100 (c) and *E. coli* strain HD701 (d).	160

Fig. 2: Aerobic vs. anaerobic batch reduction of 500 μM sodium chromate by free and agar-immobilized Bio-Pd(0) produced with **(A)** *D. vulgaris*, **(B)** *D. desulfuricans*, **(C)** *E. coli* strain HD701, **(D)** *E. coli* strain MC4100.	161
Fig. 3: Correlation between the % by which the amount of Cr(VI) reduced in the initial 1.5 h is affected by immobilization and the initial rate of Cr(VI) reduction by immobilized Bio-Pd(0).	162
Fig. 4: Continuous Cr(VI) reduction by agar-immobilized Bio-Pd(0), produced using *D. vulgaris*, *D. desulfuricans*, and *E. coli* strains MC4100 and HD701.	163
Fig. 5: Effect of Cr(VI) concentration on continuous reduction by *D. vulgaris* Bio-Pd(0) immobilized in agar.	164
Fig. 6: Flow rate/ activity plots for Cr(VI) reduction by packed-bed columns containing *D. vulgaris* Bio-Pd(0) immobilized in agar at loadings of 0, 1.25, 2.5, 5.0, and 7.5 mg Bio-Pd(0) mL agar^{-1}.	165
Fig. 7: Model depicting transcriptional regulation by HycA.	166
SECTION 4:	
Fig. 1: Cr(VI) reducing dual reactor system for batch (a) and continuous (b) Cr(VI) reduction.	187
Fig. 2: Example TEM of (a) native and (b) palladised cells of *D. vulgaris*.	188
Fig. 3: Batch reduction of 500 μM Cr(VI) by suspended and immobilized resting cells of *D. vulgaris* NCIMB 8303 (a,b) or Bio-Pd(0) (c,d,e) using chemical hydrogen (a,c) or Bio-H_2 (b,d,e) as electron donor.	189
Fig. 4: Continuous reduction of 100 μM Cr(VI) by agar-immobilized Bio-Pd(0) using Bio-H_2 as electron donor.	190

SECTION 5:	
Fig. 1: System for the treatment of 3 industrial wastes.	203
APPENDICES	
APPENDIX I:	
Fig. 1: The Cr(VI) reducing dual reactor system.	217
Fig. 2: Reduction of 500 μM Cr(VI) by free and agar-immobilized resting cells of *D. vulgaris* NCIMB 8303 using biologically produced hydrogen as electron donor.	219
Fig. 3: Reduction of 500 μM Cr(VI) by free and agar-immobilized resting cells of *D. vulgaris* NCIMB 8303 using chemical hydrogen as electron donor.	220
APPENDIX II:	
Fig. 1: Low and High energy alignment of nuclei with applied magnetic field.	226
Fig. 2: Precession.	227
Fig. 3: Phase of magnetic moments around their precessional path.	228
Fig. 4: A basic pulse sequence.	230
Fig. 5: The formation of a spin echo.	230
Fig. 6: A 2D slice through a 3D MRI data set of reticulated polyurethane foam in the absence (A) and presence (B) of *Serratia* biofilm.	233
Fig. 7: 2D images of reactors packed with reticulated foam containing immobilized *Serratia* sp. biofilm and challenged with 2 mM citrate buffer, pH 6 in the presence of 5 mM glycerol-2-phosphate, and with or without metal: (a) metal unsupplemented flow (b) La^{3+} supplemented (c) control cell free reactor + La^{3+} + Cu^{2+} (d) Cu^{2+} supplemented (e) La^{3+} + Cu^{2+} supplemented.	235

APPENDIX III:	
Fig. 1: 2D slices taken from 3D MR image data sets of packed-bed columns containing polyurethane foam cubes with and without *Serratia* biofilm, challenged with Cr^{6+} or Cr^{3+} in the presence of glycerol-2-phosphate.	246
Fig. 2: Variation of image intensity of solutions present in Fig. 1.	247
APPENDIX IV:	
Fig. 1: Cr(VI) calibration curve.	253
Fig. 2: Protein calibration curve.	255
Fig. 3: Pd(II) calibration curve.	256
Fig. 4: Relationship between protein concentration and OD_{600} for (A) *D. vulgaris* NCIMB 8303 and (B) *Microbacterium* sp. NCIMB 13776.	258
APPENDIX V:	
Fig. 1: Accumulation of Pd(0) by *D. desulfuricans* at the expense of H_2.	271
Fig. 2: Illustration of Bio-Pd(0) made on *D. desulfuricans.*	272

List of Tables

SECTION 1: INTRODUCTION	
Table 1: Possible oxidation/ reduction reactions for Cr(VI).	5
Table 2: Comparison of metal uptake by biosorption and bioaccumulation.	9
Table 3: Microbial aerobic Cr(VI) reduction.	10
Table 4: Pathway of dissimilatory sulfate reduction.	19
Table 5: Aspartase activities of immobilized *E. coli* cells formed in various shapes and their activity yields.	39
SECTION 2:	
SECTION 2.1:	
Table 1: Effect of electron donor on initial rates of Cr(VI) reduction by *D. vulgaris* NCIMB 8303 and *Microbacterium* sp. NCIMB 13776.	54
Table 2: Significance of electron donor on initial rates of Cr(VI) reduction.	56
Table 3: Effect of temperature and pH on initial rates of Cr(VI) reduction by *D. vulgaris* NCIMB 8303 and *Microbacterium* sp. NCIMB 13776.	58
SECTION 2.2:	
Table 1: First stage evaluation of different support matrices using beads in batch suspensions.	80
Table 2: Effect of immobilization of *D. vulgaris* NCIMB 8303 and *Microbacterium* sp. NCIMB 13776 on initial rates of Cr(VI) reduction in batch.	81
Table 3: Significance of immobilization matrix on initial rate of Cr(VI) reduction by *D. vulgaris* (a) and *Microbacterium* sp. (b).	82

SECTION 3:	
SECTION 3.3:	
Table 1: Effect of Bio-Pd(0) bacterial source on initial rates of Cr(VI) reduction by Bio-Pd(0) in batch suspensions.	152
Table 2: Cr(VI) removal after 24 h of continuous-flow by packed-bed columns containing immobilized *D. vulgaris* Bio-Pd(0).	153
Table 3: Equations relating $[Cr(VI)]_{inlet}$ to % Cr(VI) reduction for continuous-flow packed-bed columns containing agar-immobilized Bio-Pd(0).	154
Table 4: Comparison of experimentally determined and predicted values for % Cr(VI) reduction by agar-immobilized Bio-Pd(0) in flow-through packed-bed columns.	155
Table 5: Effect of Bio-Pd(0)/ agar loading on the flow rate at which 50 % Cr(VI) is reduced ($FA_{1/2}$ value) and the residence time needed for 50 % Cr(VI) reduction to occur ($RA_{1/2}$ value).	156
Table 6: Comparison of expected and actual bioreactor activities.	157
SECTION 4:	
Table 1: Nougat and Caramel waste composition.	184
Table 2: Effect of H_2 source and immobilization on Cr(VI) reduction by unpalladised and palladised cells of *D. vulgaris*.	185
SECTION 5:	
Table 1: Stability constants of Cr(III) amino acid complexes.	199

APPENDICES	
APPENDIX I:	
Table 1: Caramel waste composition.	218
APPENDIX IV:	
Table 1: Composition of PGB.	250
Table 2: Composition of PGC.	250

List of Abbreviations

AMM	Acetate Minimal Medium
AMP	Adenosine Monophosphate
APS	Adenosine Phosphosulfate
ATP	Adenosine Triphosphate
BBSRC	Biotechnology and Biological Sciences Research Council
BOD	Biological Oxygen Demand
BSA	Bovine Serum Albumin
CRB	Cr(VI) Reducing Bacteria
Cyt	Cytochrome
DNA	Deoxyribonucleic Acid
DNP	2,4-dintitrophenol
DTPA	Diethylenetriaminepentaacetic acid
EDAX	Energy-Dispersive X-Ray Analysis
EDTA	Ethylenediaminetetraacetic acid
EM	Electron Microscopy
EPSRC	Engineering and Physical Sciences Research Council
FADH	Flavin Adenine Dinucleotide (reduced form)
FHL	Formate Hydrogenlyase
FhlA	Transcriptional regulator needed for expression of the *hyc, hyp, hyf* operons and the gene *fhfF*
FHL-1	FHL system 1
FHL-2	FHL system 2
FID	Free Induction Decay
GC	Gas Chromatography
G2P	Glycerol-2-phosphate
ICP-MS	Inductively Coupled Plasma Mass Spectrometry
MOPS	3-(N-Morpholino)propanesulfonic acid
MRI	Magnetic Resonance Imaging
NADH	Nicotinamide Adenine Dinucleotide (reduced form)
NADPH	Nicotinamide Adenine Dinucleotide Phosphate (reduced form)
NCIMB	National Collection of Industrial, Food and Marine Bacteria, Scotland

NMR	Nuclear Magnetic Resonance
NTA	Nitrilotriacetic acid
OFN	Oxygen Free Nitrogen
PBS	Phosphate Buffered Saline
PCB	Polychlorinated Biphenyl
PEM	Proton Exchange Membrane
PGB	Postgate Medium B
PGC	Postgate Medium C
PGM	Platinum Group Metals
PVA	Polyvinyl Alcohol
RF	Radio-Frequency
SEM	Scanning Electron Microscopy
SEM	Standard Error Mean
SRB	Sulfate-Reducing Bacteria
TEM	Transmission Electron Microscopy
UK	United Kingdom
USA	United States of America
XRD	X-Ray Diffraction

List of Symbols

$Bio\text{-}H_2$	Biologically produced hydrogen
$Bio\text{-}H_{2\ caramel}$	$Bio\text{-}H_2$ produced by *E. coli* using caramel waste as oxidisable substrate
$Bio\text{-}H_{2\ glucose}$	$Bio\text{-}H_2$ produced by *E. coli* glucose solution as oxidisable substrate
$Bio\text{-}H_{2\ nougat}$	$Bio\text{-}H_2$ produced by *E. coli* using nougat waste as oxidisable substrate
Bio-Pd(0)	Biologically synthesised elemental palladium
B_0	Magnetic field
Chemical-Pd(0)	Chemically synthesised elemental palladium
$[Cr(VI)]_{inlet}$	Concentration of Cr(VI) entering reactor
$[Cr(VI)]_{outlet}$	Concentration of Cr(VI) leaving reactor
Cr_{total}	Total concentration of all chromium species present
d	Radius of gel particle
e^-	Electron
E_o	Total enzyme present
F	Larmor frequency
F	Flow Rate
FA½	Flow rate giving 50 % removal of Cr(VI)
H_2ase	Hydrogenase
$H_{2\ commercial}$	Commercially supplied hydrogen (from a cylinder)
i.d	Internal Diameter
I	Spin quantum number
K_m	Concentration of substrate at half V_{max} of reaction catalysed by an enzyme
$K_{m\ app}$	Experimentally determined concentration of substrate at half V_{max} of reaction catalysed by an enzyme
K_3	Intrinsic kinetic constant
logβ	Stability constant
M_0	Bulk magnetisation
n	Number of replicates
OD_{600}	Optical Density at 600 nm
pH	The logarithm of the reciprocal of hydrogen ion concentration
pK_a	The negative logarithm of the acid dissociation constant, K_a.
$pLHB1^+$	Chromate resistance plasmid

Pi	Inorganic Phosphate
PPi	Pyrophosphate
r	Thickness of stagnant region surrounding gel particle
RA½	Residence time needed for 50 % Cr(VI) reduction
R^2	Correlation Coefficient
S	Substrate concentration at time t
S_{bulk}	Substrate concentration in bulk medium
S_0	Substrate concentration at time t = 0
T_1	Longitudinal relaxation (spin-lattice relaxation)
T_2	Transverse relaxation (spin-spin relaxation)
TE	Echo Time
TR	Repetition Time
V	Reaction velocity
V_{max}	Maximum velocity of an enzyme catalysed reaction
X	Conversion factor ($X = (S_0-S)/S_0$)
θ	Flip Angle

SECTION 1

GENERAL INTRODUCTION

1.0 Heavy metal pollution

Heavy metals occur naturally in the environment, but concentrations are greatly increased where heavy metals have been extracted and used for industrial processes. Widespread pollution by heavy metals is of great environmental concern because these metals are non-degradable and thus persist in the environment. The most common heavy metal pollutants are arsenic, cadmium, chromium, copper, nickel, lead and mercury. The problems posed by heavy metals vary. For example, the lower trophic levels (e.g. phytoplankton) are affected by dissolved copper, whilst lead, cadmium and mercury pose a risk to species higher in the food chain (e.g. humans) (Nriagu 1996).

The Dangerous Substances Directive has been implemented in developed countries to control heavy metal pollution, and has resulted in certain environmental protection acts and regulations, which are enforced by environmental agencies (Gupta *et al.* 2000). For example, the UK maximum permitted release concentration for hexavalent chromium, Cr(VI), in wastewater is 50 $\mu g\ L^{-1}$, and for trivalent chromium, Cr(III), is 1000 $\mu g\ L^{-1}$ (http://acornusers.org/education/HNC-Web/Theory.html 2004).

1.1 Sources of chromium

Chromium is recovered from chromite ore (typically composed of 46 % chromic oxide) by fusing the ore with lime and soda ash in the presence of air to give a yellow mixture (Shupack 1991). This mixture is leached with water and filtered to separate the chromium from the aluminium impurities. Acidification and concentration of this filtrate produces sodium chromate (Shupack 1991).

Mining chromite in the USA ceased to be economically feasible in 1961, although the US still consumes 12 % of the world's output (14 million tonnes in 2002: www.chromium-

asoc.com 2004) (Zayed and Terry 2003). Currently, South Africa produces 46 % of annual world chromate needs, whilst Kazakhstan and India provide 17 % and 19 %, respectively (www.chromium-asoc.com 2004).

Although there are natural sources of chromium, the majority of Cr(VI) originates from industrial activities. Chromium is used by a variety of industries ranging from chromium plating and polishing operations, aluminium conversion coating operations, to wood-preserving facilities and the colourisation of rubies and emeralds (Chen and Hao 1998). Chromium is rarely used alone. It is the supreme additive, endowing alloys or materials with properties of resistance to corrosion, temperature, decay, strength, hardness, permanence, and colour (www.chromium-asoc.com 2004). On a worldwide scale, 80 % of chromium that is mined is used for metallurgical operations, 15 % for chromium chemical manufacture, and the remainder used in refractory applications (Barnhart 1997).

1.2 Chromium chemistry

Chromium was first discovered in 1797 by Nicolas-Louis Vauquelin when he analysed chromite ore. It was named chromium from the Greek word chroma, meaning colour, because of the many different colours characteristic of its compounds. Chromium is a transition metal, existing in a variety of transition states ranging from -2 to +6, with the trivalent and hexavalent state being predominant in solution (Barnhart 1997).

Cr(VI) is toxic, mutagenic and carcinogenic to humans and animals (Komori *et al.* 1989). When present as CrO_4^{2-}, hexavalent chromium can enter the cell by crossing the cell membrane through various transport pathways due to its structural similarity to SO_4^{2-} (see Pattanapipitpaisal *et al.* 2001b). Once within the cell, Cr(VI) can be converted to the more reactive and oxidizing Cr(V) and Cr(IV) species (Liu and Shi 2001) by physiological reducing

agents NAD(P)H, $FADH_2$, several pentose sugars and glutathione (Cervantes *et al.* 2001). Fig. 1 illustrates cellular reduction of Cr(VI) to Cr(V) and Cr(IV) with consequent production of hydroxyl and glutathionyl free radicals. These free radicals attack DNA, causing DNA single-strand breaks, DNA-protein crosslinks and glutathione reductase inhibition. Ultimately these mutations result in uncontrolled cell division (i.e. cancer). Intracellular Cr(III) may be sequestered by DNA phosphate groups affecting replication and transcription causing mutagenesis (Cervantes *et al.* 2001). Cr(III) may also react with carboxyl and sulfhydryl groups of enzymes causing alterations in their structures and activities. Additionally, modification of DNA polymerase and other enzyme activities may be caused by displacement of magnesium ions by Cr(III) (Cervantes *et al.* 2001).

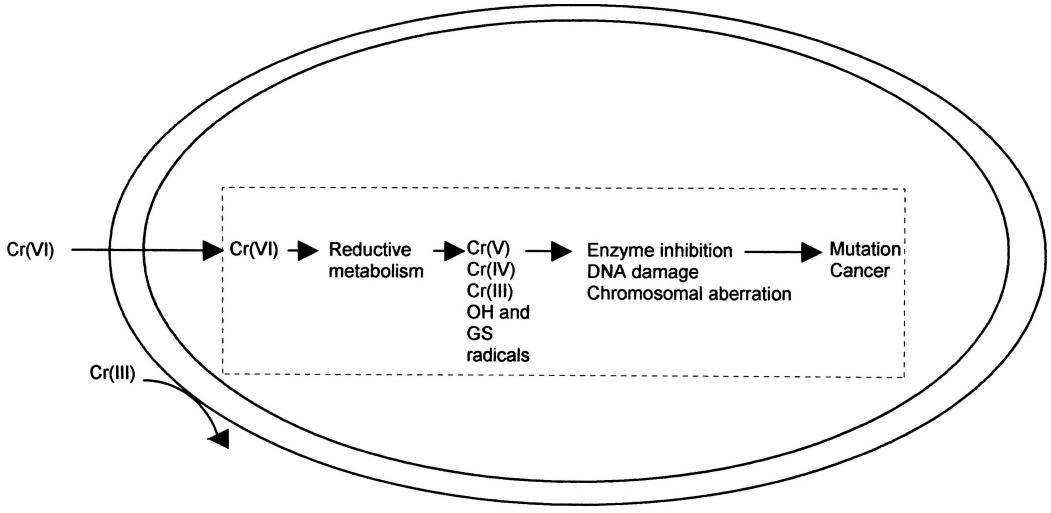


Fig. 1: Cellular reduction of Cr(VI) (Taken from Sugiyama 1991).

Cr(VI) can be converted to Cr(III) by the addition of three electrons. In contrast to Cr(VI), Cr(III) is non-toxic, relatively insoluble and immobile, and is an essential trace element in human nutrition, being involved in glucose metabolism by enhancing the effects of insulin (adult recommended daily intake: 200 μg: www.chromium-asoc.com 2004) (Shupack 1991). Cr(III) consists of an octahedral complex with single occupation of each t_{2g} level. This gives a

type of half-filled shell stability (Cary 1982) leading to the relative kinetic inertness of Cr(III) complexes. Biological membranes are virtually impermeable to Cr(III). This is probably due to Cr(III) forming water insoluble compounds in non-acidic aqueous solutions, thus Cr(III) present in solution cannot enter the cell (Cervantes and Silver 1992). Studies have shown that Cr(III) is approximately 1000 times less cytotoxic and mutagenic than Cr(VI) compounds cultured in diploid human fibroblasts (Bagchi *et al.* 2001).

The conversion of Cr(III) to Cr(VI) and *vice versa* is controlled by several factors, such as the concentrations of the chromium species and oxidising and reducing agents present. Other factors include the redox potentials of the oxidation and reduction reactions, temperature, light, acid-base reactions, the presence of complexing agents, and precipitation reactions (Kimbrough *et al.* 1999).

The capacity of a chemical reagent for donating or accepting electrons governs redox reactions between a given chromium species and the reducing agent. Examples of possible oxidation/ reduction reactions are given in Table 1 (Kimbrough *et al.* 1999).

Table 1: Possible oxidation/ reduction reactions for Cr(VI)

	Redox potential (volts)
A) $Cr^{3+} + 5H_2O + 3O_3 \leftrightarrow 2CrO_4^{2-} + 10H^+ + 3O_2$	0.87
B) $2Cr^{3+} + 2H_2O + 3H_2O_2 \leftrightarrow 2CrO_4^{2-} + 10H^+$	0.58
C) $3MnO_2 + 2Cr(OH)_3 \leftrightarrow 3Mn^{2+} + 2CrO_4^{2-} + 2H_2O + 2OH^-$	1.328
D) $2Cr^{3+} + 3H_2O + 2MnO_4^- \leftrightarrow Cr_2O_7^{2-} + 6H^+ + 2MnO_2$	0.35
E) $2Cr^{3+} + 7H_2O + 6Mn^{3+} \leftrightarrow Cr_2O_7^{2-} + 14H^+ + 6Mn^{2+}$	0.18
F) $2Cr^{3+} + H_2O + 3PbO_2 \leftrightarrow Cr_2O_7^{2-} + 2H^+ + Pb^{2+}$	0.13

(Taken from Kimbrough *et al.* 1999)

Chromium oxidation and reduction is governed by water chemistry, for example solution pH. In solution Cr(VI) is present in anionic compounds that are soluble over a wide range of pH values. At low pH, chromates dimerize to the dichromate species ($H_2Cr_2O_7$ or $HCr_2O_7^-$);

strong oxidizing agents that are reduced rapidly when a reducing agent is present. At higher pH values, chromates exist as CrO_4^{2-}, a poor oxidizing agent. Consequently this species is more stable (Kimbrough *et al.* 1999).

In aqueous solutions the main Cr(III) species present are Cr^{3+}, $Cr(OH)^{2+}$, $Cr(OH)_2^{+}$, whilst polymeric forms include $Cr_2(OH)_2^{4+}$, $Cr_3(OH)_4^{5+}$ and $Cr_4(OH)_6^{6+}$ (Chen and Hao 1998). At neutral to basic pH, Cr(III) has a tendency to form polynuclear complexes because of the ability of Cr(III) complexes to undergo hydrolysis, as illustrated below:

$$[Cr(H_2O)_6]^{3+} \rightarrow [Cr(H_2O)_5OH]^{2+} + H^{+} \qquad k \approx 10^{-4}$$

Increasing pH causes a shift in equilibrium to the right of the above equation, resulting in conversion of more co-ordinated water molecules to hydroxyl groups. Olation can then occur, whereby Cr(III) ions are connected by bridging OH^- groups. Continued olation leads to the formation of larger molecules of colloidal dimensions, resulting in precipitation of chromium hydroxide. Chelating agents, such as citrate, prevent olation by forming stable soluble complexes with Cr(III) (Mabbett *et al.* 2002).

Another important factor in chromium oxidation/ reduction is the concentration of oxidizing and reducing agents present in solution. There are many oxidizing agents capable of oxidizing Cr(III) to Cr(VI), but many of these agents are not present at high enough concentrations in the environment. In contrast there are many reducing agents for which reduction of Cr(VI) to Cr(III) is thermodynamically less favourable, but these are present in sufficient concentrations to play a role in Cr(VI) reduction. For example Cr(III) can be oxidized to Cr(VI) by ozone (redox potential 0.87 volts), but ozone is not present in high enough concentrations for this oxidation to occur. In contrast, reduction of Cr(VI) to Cr(III)

by Fe(II) has a low redox potential (0.56 volts), but the concentration of Fe(II) in the environment is high enough for the reduction reaction to occur (Kimbrough *et al.* 1999).

2.0 Reduction of Cr(VI) as a means to its removal from solution

Cr(VI) rich wastewater is treated by conventional aerobic and anaerobic processes by many industrial plants, which lower the chromium concentration, although not to a low enough level to deem it non-toxic to flora and fauna (Srinath *et al.* 2002). Alternatively, metals may be separated by precipitation by increasing the solution pH (see above). However this process is non-selective and consequently produces large quantities of sludge for disposal (Eccles 1999). Another method to treat wastewaters with low Cr(VI) concentrations is to use ion-exchange resins, but the high cost of the resin limits their use (Srinath *et al.* 2002).

The use of biological methods to remediate metal-containing industrial wastes is an emerging field. The large-scale use of microorganisms for the reduction of Cr(VI) is an attractive option because the methods involved are relatively cheap, simple and do not require toxic chemical reagents, and native, non-hazardous bacterial strains may be used. New industrial wastewater treatment methods must be compatible with existing operations, be cost-effective, flexible to handle fluctuations in quantity and composition of effluent, and reliable, as wastewater treatment generally operates on a continuous basis. Treatment must also be simple in order to minimize the need for skilled operators. Laboratory-scale investigations have identified several different types of bacteria that are capable of reducing hexavalent chromium to the less toxic trivalent form.

2.1 Mechanism of Cr(VI)-resistance

Usually the low levels of Cr(VI) present in the environment are reduced by organic matter and other reductants, to produce Cr(III). When Cr(VI) is present at higher levels, its presence inhibits the reducing ability of the environment, resulting in the persistence of Cr(VI) in the ecosystem to potentially toxic levels. When this occurs, natural selection promotes the survival of bacterial strains with Cr(VI) resistance determinants. For example, bacteria isolated from sediments of metal processing waste evaporation ponds are more tolerant than bacteria isolated outside the pond (Losi *et al.* 1994).

Bacterial resistance to Cr(VI) is either conferred as a chromosomal mutation affecting sulfate transport pathways, or alternatively is plasmid-borne. Studies suggest that chromosomal and plasmid determinants confer Cr(VI) resistance by different mechanisms as cells that possess both determinants show additive effects with respect to Cr(VI) resistance (Cervantes and Silver 1992). Examples where Cr(VI) resistance is conferred by plasmid determinants include *Streptococcus, Pseudomonas* and *Alcaligenes* species (Cervantes and Silver 1992). In these cases, decreases in chromate accumulation by cells results in resistance to Cr(VI) (Cervantes and Silver 1992).

2.2 Cr(VI) removal

Some microorganisms interact with toxic metals to allow their removal by biosorption, bioaccumulation and enzymatic reduction. Biosorption is a rapid process in which pollutants are removed from solution by passive binding to biological material. Biosorption may occur through adsorption, ion exchange, co-ordination, complexation, chelation and microprecipitation (Cetinkaya *et al.* 1999).

Microbial heavy metal accumulation (bioaccumulation) generally involves two phases. An initial rapid metabolism-independent phase involving physical adsorption or ion-exchange at the cell surface is followed by the slower metabolism-dependent transport of metal into the bacterial cell (Srinath *et al.* 2002). Once metal ion concentrations become too high, the microorganism's metabolism is disrupted leading to cell death (Eccles 1995). Metabolism-dependent intracellular uptake of metals is inhibited by low temperatures, metabolic inhibitors and uncouplers and is also influenced by the physiological state of the cell (Gadd 1988). Table 2 compares features of biosorption and bioaccumulation.

Table 2: Comparison of metal uptake by biosorption and bioaccumulation

Feature	Biosorption	Bioaccumulation
Metal affinity	Higher under favourable conditions.	Toxicity affects metal uptake by living cells. In some instances high metal accumulation.
Rate of metal uptake	Usually rapid, a few seconds for outer wall accumulation.	Usually slower than biosorption.
Selectivity	Variety of ligands involved, hence poor.	Better than biosorption.
Temperature tolerance	Within a modest range.	Inhibited by low temperatures.
Versatility	Anions or other molecules may affect metal uptake. Extent of metal uptake is usually pH dependent.	Requires an energy source. Dependent on plasma membrane ATP-ase activity. Often accompanied by metal efflux.

(Taken from Eccles, 1995)

2.3 Occurrence of microbial Cr(VI) reduction

Some bacteria that are resistant to hexavalent chromium are also capable of enzymatically reducing it to the less toxic trivalent form to various extents. Cr(VI) reduction may be an additional Cr(VI) resistance mechanism that is chromosomally encoded (Cervantes *et al.* 2001). A wide variety of bacteria have been reported to reduce Cr(VI) aerobically or

anaerobically (Shen and Wang 1997). Table 3 summarises five bacterial systems that are capable of Cr(VI) reduction under aerobic conditions.

Generally, microbial Cr(VI) reduction to Cr(III) can be illustrated as follows:

$$\overset{\text{CRB}}{\leftrightarrow} \qquad \overset{\text{Neutral pH}}{\rightarrow}$$

$$CrO_4^{2-} + 8H^+ + 3e^- \leftrightarrow Cr^{3+} + 4H_2O \rightarrow Cr(OH)_{3(s)} + 3H^+ + H_2O$$

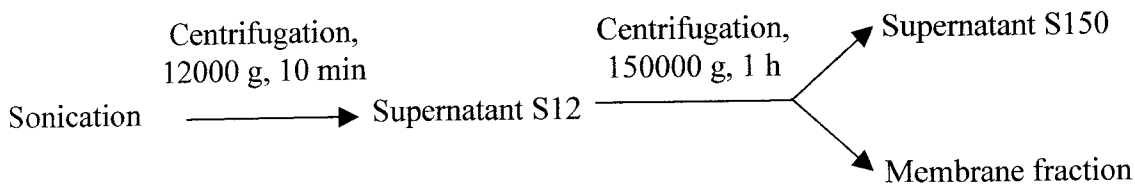
CRB = Cr(VI) reducing bacteria or enzymes.

Table 3: Microbial aerobic Cr(VI) reduction

Bacteria	V_{max} (nmol/min/ mg protein)	Reference	Reduction conditions
Pseudomonas putida PRS2000	6	(Ishibashi *et al.* 1990)	pH 6.5 - 7.5, heat labile
Pseudomonas ambigua G-1	27	(Suzuki *et al.* 1992)	Optimal conditions: 50 °C, pH 8.6, heat stable
Pseudomonas aeruginosa HPO14	330	(Oh and Choi 1997)	Not Determined
Pseudomonas putida MK1	1720	(Park *et al.* 2000)	Optimal conditions 80 °C, pH 5.0, heat stable
Bacillus subtilis	ND	(Garbisu *et al.* 1998)	Heat labile

2.3.1 Cr(VI) reduction by *Escherichia coli*

Escherichia coli ATCC 33456 can reduce Cr(VI) aerobically and anaerobically, with reduction rate highest under anaerobic conditions (Shen and Wang 1993). Shen and Wang (1993) investigated the biological characteristics and cellular location of Cr(VI) reductase in *E. coli* strain ATCC 33456. They showed that whole cells could completely reduce 0.3 mM Cr(VI) in 12.5 h using NADH as the electron donor, with Cr(III) predominantly present in the external medium. For further studies Shen and Wang (1993) produced cell extracts as follows;



No Cr(VI) reduction occurred in membrane fractions. Similar levels of reduction occurred by supernatant fractions S12 and S150 when NADH was present as electron donor leading Shen and Wang (1993) to suggest Cr(VI) reduction was predominantly carried out by soluble reductase activity.

This idea was supported when addition of respiratory inhibitors (cyanide, azide and rotenone) did not affect Cr(VI) reduction by intact cells or by supernatant fractions of cell extract. Addition of DNP (2,4-dinitrophenol: an electron transport uncoupler) stimulated Cr(VI) reduction by intact cells under aerobic and anaerobic conditions, suggesting the involvement of intracellular Cr(VI) mechanisms. A possible explanation is that DNP increases the permeability of the inner membrane to H^+ ions. Increased intracellular concentrations of H^+ could lead to increased Cr(VI) reduction through the respiratory-chain-linked activity of the reaction (Shen and Wang 1993):

$$CrO_4^{2-} + 8H^+ + 3e^- \rightarrow Cr^{3+} + 4H_2O$$

Spectroscopic studies used to characterise the involvement of respiratory chain enzymes in Cr(VI) reduction identified cytochromes *b* and *d* in both supernatant S12 and the membrane fraction, with no identifiable peaks in supernatant fraction S150. The spectroscopic studies suggest that cytochrome *b* and *d* are present in the membrane of *E. coli* ATCC 33456. Studies showed that hydrogen-reduced cytochromes *b* and *d* in the membrane fraction could only be

reoxidized by oxygen and not Cr(VI), whilst these cytochromes in the supernatant fraction could be reoxidized by both. From these results it was concluded cytochromes *b* and *d* were involved in the transport of electrons to Cr(VI) through the mediation of the soluble Cr(VI) reductase (Shen and Wang 1993).

The optimum conditions for Cr(VI) reduction by *E. coli* ATCC 33456 in aerobic batch culture were investigated by Bae *et al.* (2000). These were shown to be pH 7 and 30 °C using tryptone as the nutrient source for bacterial growth. Cr(VI) reduction was inhibited by the presence of the following metal cations (1 mM) in the order;

$$Hg^{2+} > Ag^{2+} > Mn^{2+} > Zn^{2+} > Pb^{2+} > Cd^{2+} > Ca^{2+} > Mg^{2+}$$

Reduction was completely inhibited by the presence of Hg^{2+}, with marginal inhibition in the presence of Mg^{2+} (Bae *et al.* 2000). Further studies investigated the potential to reduce Cr(VI) in continuous aerobic culture using glycerol as the carbon source. Cr(VI) reduction efficiency reduced from 99.3 % to 84.3 % as the concentration of Cr(VI) in the inlet increased from 50 to 200 μM. However the specific Cr(VI) reduction rate increased from 0.72 to 2.41 mg Cr(VI) g dry cell wt.$^{-1}$ h^{-1}.

2.3.2 Cr(VI) reduction by *Pseudomonas*

Pseudomonas fluorescens sp. LB300 contains a chromate resistance plasmid (pLHB1^{+}), and can reduce chromate aerobically or anaerobically (Bopp and Ehrlich 1988). Bopp and Ehrlich (1988) conducted a study to determine the relationship between chromate resistance and reduction. They showed the minimum inhibitory concentration of K_2CrO_4 in Vogel-Bonner broth for *P. fluorescens* sp. LB300, resulting in significantly slower growth and lower growth yield, was 5.15 mM (1% (v/v) overnight *P. fluorescens* inoculum). In the presence of 1.29 mM K_2CrO_4 the growth was identical to that seen in the absence of Cr(VI). In the presence of

2.58 mM K_2CrO_4 a high growth yield was attained, although this was lower than in the absence of Cr(VI) (Bopp and Ehrlich 1988).

Resting cells of *P. fluorescens* reduced Cr(VI) aerobically only when glucose or another suitable electron donor was present, with similar initial rates of Cr(VI) reduction at glucose concentrations of 0.25 and 0.5 % (w/v). Cr(VI) reduction by crude extracts of *P. fluorescens* was completely inhibited in the presence of 10 mM potassium cyanide or 1 mM azide, suggesting that a membrane-associated Cr(VI) reductase that mediates electron transfer from NADH to Cr(VI) was involved (Bopp and Ehrlich 1988). *P. fluorescens* was unable to reduce Cr(VI) anaerobically, except when grown on acetate at concentrations lower than 257 μM K_2CrO_4. Bopp and Ehrlich (1988) suggested the enzyme that catalyzes Cr(VI) reduction is repressed in the presence of glucose under anaerobic conditions.

Further studies involved batch cultures of *P. fluorescens* strain LB300 grown aerobically in the presence of Cr(VI) at concentrations of 1.93, 1.23, and 0.69 mM Cr(VI), with 61, 69, and 99.7 % reduction, respectively, in 289 h (Deleo and Ehrlich 1994). DeLeo and Ehrlich (1994) also investigated the effect of shaking on Cr(VI) reduction and found that 80 % Cr(VI) was reduced in 147 h by stationary cultures, and in 122 h for shaken cultures. DeLeo and Ehrlich (1994) also investigated Cr(VI) reduction by a continuous culture of *P. fluorescens* strain LB300, with 28 % Cr(VI) removed at a flow rate of 3.85 mL h^{-1}, 39 % at 2.26 mL h^{-1}, and 57 % at 1.17 mL h^{-1} (initial Cr(VI) concentration: 0.06 mM).

Studies on Cr(VI) reduction by *Pseudomonas putida* PRS2000 demonstrated that reduction can occur aerobically or anaerobically using either NADH or NADPH as electron donor (Ishibashi *et al.* 1990). Fractions of cell extract and supernatant produced by cell disruption and centrifugation (150000 g, 1 h) were used for Cr(VI) reduction tests. Reduction occurred in both fractions, but to a lower extent in the membrane fraction. Cr(VI) reduction by the

supernatant increased linearly with NADH or NADPH addition until saturation at a concentration of 200 μM. From these results Ishibashi *et al.* (1990) concluded that chromate reduction was a secondary activity of a soluble enzyme reductase.

2.3.3 Cr(VI) reduction by *Agrobacterium*

Resting cell suspensions of the Gram-negative bacterium *Agrobacterium radiobacter* strain EPS916 suspended in phosphate buffer were used for chromate reduction assays at 30 °C. Llovera *et al.* (1993a) showed *Agrobacterium radiobacter* strain EPS916 can reduce Cr(VI) in the absence of exogenous electron donors in aerobic and anaerobic conditions, at concentrations as high as 0.5 mM Cr(VI) (Llovera *et al.* 1993a,b). At a cell concentration of 2 x 10^9 cells mL^{-1}, 0.3 mM Cr(VI) was reduced in 6 hours (Llovera *et al.* 1993a).

Llovera *et al.* (1993b) studied the effect of culture medium ions on Cr(VI) reduction by *A. radiobacter* strain EPS916. Inhibition of Cr(VI) reducing activity was observed in the presence of 200 μM Na_2MoO_4, 10 mM Na_2SO_4 and 89 μM ferric citrate. No significant inhibition was observed in the presence of 500 μM $MgCl_2$, 500 μM $CdCl_2$, 500 μM $ZnCl_2$ or 200 μM $MnCl_2$. Cells showed maximum Cr(VI) reducing ability when pre-grown in the presence of 0.243 μM Mg^{2+}, 20 μM Ca^{2+} and 3.6 μM Mn^{2+}. Addition of Fe(III) (89 μM and 357 μM) to the reduction assay inhibited chromate reduction by 25 and 40 %, respectively. Llovera *et al.* (1993b) suggested inhibition may be due to competition between Fe(III) and Cr(VI) by the uptake system.

2.3.4 Cr (VI)reduction by *Enterobacteria*

The Gram-negative bacterium *Enterobacter cloacae* strain H01, isolated from an activated sludge sample from a municipal waste treatment plant, is resistant to high chromate

concentrations (10 mM) under aerobic and anaerobic conditions. Komori *et al.* (1989) demonstrated that *E. cloacae* cells in KSC medium could reduce up to 2 mM K_2CrO_4 anaerobically, with the time required for complete reduction increasing with Cr(VI) concentration and viable cell concentration. Reduction occurred at 3 – 5 mM Cr(VI), although reduction did not go to completion in 5 days. At concentrations above 5 mM chromate, cell death occurred and reduction was inhibited (Komori *et al.* 1990). When an inhibitor of cell growth was added (e.g. penicillin, chloramphenicol), Cr(VI) reduction did not occur under anaerobic conditions proving that Cr(VI) reduction in growing anaerobic cultures was due to the biochemical activity of HO1 cells and not due to chemical redox reactions in the medium (Komori *et al.* 1989).

Komori *et al.* (1990) studied the factors affecting Cr(VI) reduction by *E. cloacae* strain H01 and found the optimum conditions were pH 7 - 7.8, and 30 - 37 °C, with the highest reducing activity occurring when acetate, ethanol, malate or glycerol were present as electron donors (Komori *et al.* 1990). Further studies investigating the mechanism of cellular Cr(VI) reduction showed Cr(VI) reducing activity was lost by the addition of metabolic poisons (formaldehyde) (Wang *et al.* 1990).

To determine the location of the Cr(VI) reducing activity, *E. cloacae* HO1 cells were disrupted and separated to give various fractions. The chromate reductase activity was found to be preferentially associated with the membrane fraction of *E. cloacae* cells prepared as right-side-out membrane vesicles (Wang *et al.* 1990). Reduction occurred, but at a significantly lower level in the absence of electron donors in the membrane vesicles suggesting that the vesicles were not depleted of endogenous electron donors. It was concluded that reductase activity in *E. cloacae* is membrane-associated with chromate utilized

as electron acceptor under anaerobic conditions. Reduction occurs on the cell surface with the Cr(III) product precipitated as hydroxide in solution (Wang *et al.* 1990).

Spectral adsorption studies investigated the role of Cr(VI) in the respiratory system of *E. cloacae* strain HO1. This study indicated that chromate and oxygen both acted as electron acceptors in the respiratory system of *E. cloacae* cells (Wang *et al.* 1991). It was postulated that cytochrome c_{548} may be specifically involved in chromate reduction, but not oxygen reduction, and may play a role in dividing the electron transfer between the chromate and oxygen respiratory system (Wang *et al.* 1991). This was confirmed by examining the spectral changes of cytochromes in membrane vesicles of anaerobically grown cells oxidized by chromate and oxygen (Wang *et al.* 1991).

2.3.5 *Microbacterium* sp. NCIMB 13776

A new Gram-positive organism (isolated from a Pakistan tannery factory sample) identified as a species of *Microbacterium* (shown to be closely related to *M. liquefaciens* by 16S rRNA sequence homology and deposited as *Microbacterium* sp. NCIMB 13776) can reduce hexavalent chromium anaerobically at the expense of acetate as the electron donor, without significant growth. This organism is known to be resistant to chromate at concentrations up to 10 mM (Pattanapipitpaisal *et al.* 2001a). It is believed that Cr(VI) reduction by *Microbacterium* sp. NCIMB 13776 occurs by a detoxification mechanism, although no sequences corresponding to known Cr(VI) resistance mechanisms have been detected using appropriate probes (Pattanapipitpaisal *et al.* 2001a).

For Cr(VI) reduction tests (Pattanapipitpaisal 2001), acetate minimal medium (AMM) containing 100 μM chromate was inoculated with *Microbacterium* sp. at 30 °C under anaerobic conditions, with 99 % Cr(VI) removed from solution over 72 h. Further studies on

Microbacterium sp. NCIMB 13776 investigated Cr(VI) reduction under aerobic and anaerobic conditions at Cr(VI) concentrations in the range 100 – 500 μM. The results indicated that aerobic growth was not affected by the presence of Cr(VI), although reduction of Cr(VI) did not occur. Under anaerobic conditions Cr(VI) was reduced at all Cr(VI) concentrations, with no biosorptive uptake.

The effect of initial cell density on Cr(VI) reduction was studied by anaerobic incubation in AMM in the presence of 100 μM chromate, at cell densities in the range $2.7 \times 10^6 - 2.4 \times 10^9$ cells mL^{-1}. Reduction rate increased with escalating cell concentration, with a reduction rate of 3.9 nmol h^{-1} at 2.4×10^9 cells mL^{-1}, and 2.2 nmol h^{-1} at 2.7×10^6 cells mL^{-1} after 24 h (Pattanapipitpaisal 2001).

2.4 Sulfate-reducing bacteria (SRB)

The sulfate-reducing bacteria are a versatile group of microorganisms. Normally these bacteria use either an organic compound (for example lactate) or molecular hydrogen as an electron donor and sulfate as an electron acceptor, with consequent reduction to hydrogen sulfide. Certain metal ions can be used as electron sinks in place of sulfate, resulting in reduction of the metal ion, although the microorganisms are usually unable to couple growth to metal reduction.

For example members of the sulfate reducing family have been utilised for the reduction of molybdenum, uranium, iron, and technetium. Soluble U(VI) was reduced to insoluble U(IV) by *Desulfovibrio desulfuricans* using hydrogen or lactate as the electron donor, with U(IV) precipitated as $UO_{2(s)}$ (Tucker *et al.* 1998). In the absence of an electron donor, hexavalent uranium was not reduced (Tucker *et al.* 1998).

Only one SRB has been identified that conserves energy through metal reduction, *Desulfotomaculum reducens*, which was isolated from heavy metal contaminated sediment. This microorganism is able to grow with Cr(VI), Mn(IV), Fe(III) and U(VI) as electron acceptors in place of sulfate (Lloyd *et al.* 2001).

2.4.1 Bioenergetics of dissimilatory sulfate reduction

The ability of sulfate-reducing bacteria to couple H_2 oxidation to sulfate reduction, with subsequent ATP synthesis, has been extensively studied (Peck and Lissolo 1988). The accepted scheme for energy production in *Desulfovibrio* is shown in Fig. 2.

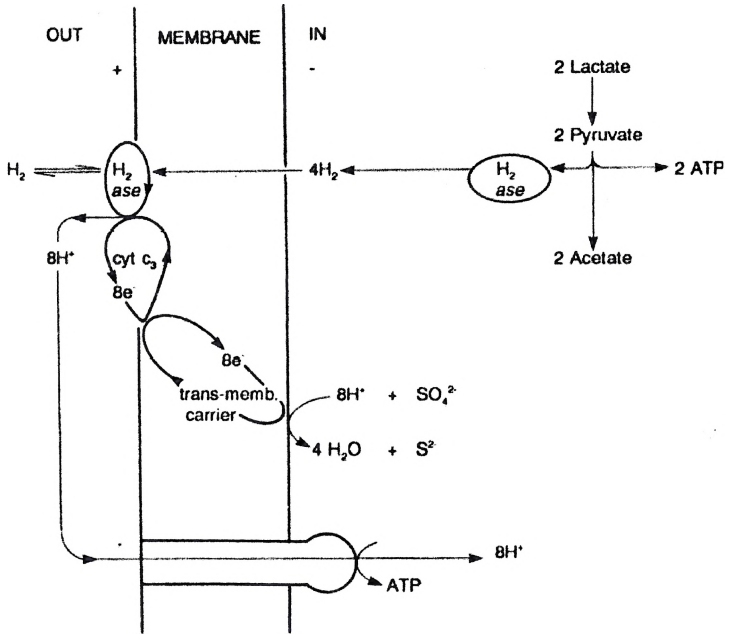


Fig. 2: Hydrogen cycling in SRB (Odom and Peck 1981).

In this scheme, lactate enters the cell and is oxidized to pyruvate by lactate dehydrogenase (located either on the internal face of the cytoplasmic membrane or in the cytoplasm). Electrons are also produced, which are used to reduce $2H^+$ to H_2. This reaction is

thermodynamically unfavourable and probably occurs due to maintenance of low partial pressure of H_2 (e.g. by interspecies hydrogen transfer). Further oxidation occurs with pyruvate converted to CO_2, acetyl phosphate and lower potential electrons. In the presence of an internal hydrogenase these electrons are used to reduce $2H^+$ to H_2. Cytoplasmic H_2 diffuses rapidly across the membrane. In the presence of electron acceptor (e.g. sulfate), hydrogen is reoxidized to H^+ and electrons by periplasmic hydrogenase and its cofactor cytochrome c_3 (Odom and Peck 1984). The electrons are transferred across the cytoplasmic membrane, leaving H^+ at the external of the membrane. This establishes a proton gradient and the energy can be used for the synthesis of ATP (Odom and Peck 1984).

In the cytoplasm electrons are used for reduction of adenylyl sulfate to sulfide as shown in Table 4.

Table 4: Pathway of dissimilatory sulfate reduction (Peck and Lissolo 1988).

	Reaction	Enzyme
1	$ATP + SO_4^{2-} \leftrightarrow APS + PPi$	ATP Sulphurylase
2	$PPi + H_2O \rightarrow 2Pi$	Inorganic Pyrophosphatase
3	$APS + 2e^- \leftrightarrow SO_3^{2-} + AMP$	APS Reductase
4	$H^+ + SO_3^{2-} \leftrightarrow HSO_3^-$	(Chemical reaction)
5	$HSO_3^- + 6H^+ + 6e^- \rightarrow HS^- + 3H_2O$	Bisulfate Reductase

Equilibrium of reaction (1) lies to the left and so PPi must be removed to drive the reaction to the right (Peck and Lissolo 1988).

2.4.2 Hydrogenases

The presence of distinct hydrogenases in the same bacterium, with different cellular locations, is poorly understood (Romao *et al.* 1997). Three hydrogenases have been identified in species of *Desulfovibrio*, all of which require tetraheme cytochrome c_3 for the reduction of electron transfer proteins (e.g. ferrodoxin, flavodoxin) (Odom and Peck 1984). These hydrogenases can be distinguished according to their metal centre content, sensitivity to inhibitors, amino acid sequences and immunological properties (Romao *et al.* 1997). The 3 hydrogenases identified are: [Fe] hydrogenase, [NiFe] hydrogenase and [NiFeSe] hydrogenase. Different species of *Desulfovibrio* contain different types of hydrogenase, although [NiFe] hydrogenase is uniformly present in SRB, and is characterised by its high affinity for H_2. For example, *D. vulgaris* contains periplasmic [Fe] hydrogenase, a membrane bound [NiFe] hydrogenase and a cytoplasmic facing membrane bound [NiFeSe] hydrogenase (Romai *et al.* 1997).

2.4.3 Cytochromes

Cytochromes are characterised by the presence of one or several *c*-type hemes, exhibiting low oxidoreduction potential compared to mitochondrial *c*-type cytochromes (Odom and Peck 1984). Five types of periplasmic soluble *c*-type cytochromes have been isolated from SRB. These are tetraheme cytochrome c_3 (Mr 13000), octaheme cytochrome c_3 (Mr 26000), dodecaheme Hmc, nine-heme cytochrome, and monoheme cytochrome c_{553} (Aubert *et al.* 2000). Cytochrome c_3 (Mr 13000) is the most abundant cytochrome and is found in all species of *Desulfovibrio*, although the degree of sequence homology between species is limited (Voordouw 1988). A study of the 3D structures of cytochrome c_3 (Mr 13000) from *D. vulgaris* (Miyazaki) and *D. desulfuricans* (Norway) showed that despite a sequence homology

of only 30 %, the two proteins fold into very similar structures, with the relative positions of the hemes being identical (Voordouw 1988).

Aubert *et al.* (2000) investigated the interaction of [NiFeSe] hydrogenase, octaheme cytochrome c_3 (Mr 26000) and tetraheme cytochrome c_3 (Mr 13000), which is now described in *Desulfovibrio* and *Desulfomicrobium*. The study suggested that cytochrome c_3 (Mr 13000) acts as an electron shuttle between hydrogenase and polyheme cytochromes.

Loujou *et al.* (1998) demonstrated that reduced triheme cytochrome c_7 from *Desulfovibrio acetoxidans* acts as an efficient metal reductase for various metal oxides e.g. chromium (VI) oxide. The catalytic process requires hemin-type molecules that exhibit low redox potentials (e.g. cytochrome c_7 or c_3). Reduction of the cytochrome can be performed by hydrogen-reduced hydrogenase (Loujou *et al.* 1998).

2.4.4 Reduction of Cr(VI) by SRB's

Hydrogen sulfide, produced during sulfate reduction by sulfate-reducing bacteria is a powerful reductant and can reduce heavy metal ions such as Cr(VI) to produce metal sulfides (Pettine *et al.* 1998). Some SRB's may be used to enzymatically reduce Cr(VI) in the absence of sulfate.

Lovley and Phillips (1994) investigated the enzymatic mechanism of Cr(VI) reduction in *D. vulgaris* NCIMB 8303. To localize H_2-dependent Cr(VI) reducing activity, they produced soluble and membrane-bound protein fractions through cell disruption and centrifugation. The soluble protein fraction accounted for 86 % of the cell protein, and reduced Cr(VI) faster than the membrane-bound protein fraction. In further studies, cytochrome c_3 was selectively removed from the soluble protein fraction by flow through a cation exchange column. This resulted in loss of Cr(VI) reduction and it was suggested cytochrome c_3 can function as a

Cr(VI) reductase. Cr(VI) reduction occurred when pure cytochrome c_3 was combined with excess hydrogenase (purified from soluble protein fraction) in the presence of H_2. When only cytochrome c_3 or hydrogenase was present (with H_2), reduction did not occur. It was concluded that cytochrome c_3 and hydrogenase must be present for Cr(VI) reduction in *D. vulgaris* (Lovley and Phillips 1994).

The experiments conducted by Lovley and Phillips contained bicarbonate buffer; bicarbonate is known to complex metal cations and could conceivably have removed the toxic Cr^{3+} product of the reaction; formation of chromium hydroxide is slower than the likely release of Cr(III) from the reduction 'reaction' (Mabbett 2001). Similar to Cu(II) it was suggested Cr(III) is able to gain access to the sensitive sites of periplasmic hydrogenase, resulting in inhibition of Cr(VI) reduction (Mabbett *et al.* 2002). Accordingly, Mabbett *et al.* (2002) have shown that for SRB's to reduce Cr(VI) a chelating agent must be present. Chromate reduction was studied under anaerobic conditions, with resting cells of *Desulfovibrio vulgaris* ATCC 29579 suspended in MOPS/ NaOH buffer, using hydrogen as an electron donor. The initial cell concentration was 0.5 mg dry cell wt mL^{-1} and initial chromate concentration, 0.5 mM. In the absence of ligands approximately 30 % Cr(VI) was removed from solution due to biosorption. Cr(VI) reduction occurred in the presence of ligands in the order Citrate > DTPA > HCO_3^- ≅ EDTA ≅ NTA. When citrate and DTPA were present, 90 % of hexavalent chromium was removed in the first 3 h (Mabbett *et al.* 2002). Mabbett *et al.* (2002) took $\log_{10}$ values of stability constants for the Cr(III) complexes formed with DTPA, EDTA, and NTA with the corresponding rates of Cr(VI) reduction, and found a correlation coefficient of 0.988. They proposed that the Cr(VI) reducing ability of *D. vulgaris* was related to the extent Cr(III) could be removed from the bioreduction reaction by its complexation (Mabbett *et al.* 2002).

When chelating agents and ligands are present in the Cr(VI) reducing solution, they probably form stable soluble complexes with Cr(III) as it is produced (Mabbett *et al.* 2002). Mabbett *et al.* (2002) suggested that Cr(III)-chelate complexes might promote Cr(VI) reduction by removal of the toxic effects of Cr^{3+} and also by a chemical reaction according to the equation:

$$n(\text{Chelator/ligand}) + \text{Cr(VI)} + H_2 \xrightarrow[\text{Cells/ hydrogenase}]{} \text{Cr(III)} \rightarrow \text{Cr(III)(Chelate/ligand)}_n$$

They proposed that the equation would move to the right so those Cr(III) ions lost in complex formation were replaced by Cr(VI) reduction. If a complexing agent is absent the trivalent chromium that is formed probably inhibits hydrogenase activity, and thus chromium reduction ceases (Mabbett *et al.* 2002).

2.4.5 Reduction of Pd(II) by SRB's

Chromium is a heavy metal, which can threaten the environment by virtue of its toxicity. In contrast, other metals can be used to protect the environment. For example, environmental concerns about greenhouse gas productions have led to an increase in the demand for the platinum group metals (PGM's) since these are used in automotive catalysts. This has led to a steep increase in the price of palladium, and a potential depletion in global reserves. The catalyst manufacturing industry is the second largest consumer of platinum, palladium and rhodium after the jewellery industry. PGM's are also used in the electronics industry and for the production of dental tools, ornaments, and wear-resistant alloys (Nowottny *et al.* 1997). The current demand for PGM's exceeds production so recovery and recycling of these metals is required. Traditional methods for recovery of PGM's are not environmentally friendly and involve complex solution chemistry, as the metals are usually present in solution as

complexes. Chelating ion exchange resins can be used to recycle PGM's, eluting the PGM with thiourea, but the use of hydrometallurgical separation is still required. Solvent extraction techniques have been used for the recovery of PGM's but the extraction rates of the metals are generally low and the process expensive (Yong *et al.* 2002; Yong *et al.* 2003). Alternatively PGM's can be recovered by electrochemical methods, but the surface area of the electrode must be large and the metal deposit must be removed from the electrode, introducing another undesirable factor. Recently microbial systems, which use metal ions as electron acceptors, have been used for the recovery of metals from solution. An example is hexavalent uranium, which can be enzymatically reduced by *Desulfovibrio desulfuricans* (a member of the SRB group) and the iron reducing species *Geobacter metallireducens* (Lloyd *et al.* 1998).

Studies have demonstrated growth decoupled SRB cells can be used to reduce Pd(II), via cellular hydrogenase activity, to cell bound Pd(0) (Bio-Pd(0)) using hydrogen as electron donor (Lloyd *et al.* 1998). Initial tests showed *D. desulfuricans* NCIMB 8307 could completely reduce 0.5 mM $Pd(NH_3)_4Cl$ in 24 h using formate, pyruvate or hydrogen as an electron donor (Lloyd *et al.* 1998). Pd(II) reduction was inhibited by the presence of Cu(II), suggesting the involvement of hydrogenase and possibly cytochrome c_3. Bio-Pd(0) crystals are approximately 50 % smaller than their chemically manufactured counterpart, with higher catalytic activity (as demonstrated by H_2 evolution from sodium hypophosphite) (Yong *et al.* 2002).

Mikheenko (2004) suggested $PdCl_4^{2-}$ crosses the outer cell membrane, penetrating the periplasmic space via porins. Following the addition of an electron donor biosorbed $PdCl_4^{2-}$ acts as an electron sink for formate/ hydrogen derived electrons, which are transported by cytochromes in the absence of sulfate or other electron acceptors. Mikheenko (2004) showed with *D. desulfuricans* nucleation of Pd(0) occurs in the periplasmic space. The growing Pd(0)

clusters erupt through the outer membrane and form dense agglomerates on the outer surface of the cell, attributable to subsequent autocatalysis of Pd(II) reduction (Mikheenko 2004). It is likely that hydrogenase/ cytochrome c_3 activity is only required for the initial reduction step, after which reduction is self-sustaining and cell viability is no longer required. Reduction of Pd(II) in the periplasmic space creates a concentration gradient, which may further facilitate Pd(II) influx (Mikheenko 2004).

Reduction of Cr(VI) by Bio-Pd(0) was investigated by Mabbett *et al.* (2001). In the absence of a Cr(III) complexing agent, Cr(VI) was completely reduced by palladised biomass in 25 h, whilst Cr(VI) reduction by unpalladised biomass ceased after 2 h with only 80 % of the Cr(VI) reduced. In the presence of H_2, an equivalent mass of chemically reduced palladium did not reduce Cr(VI) (Mabbett 2001). Further studies investigated Cr(VI) reduction by continuous flow-through columns at pH 3 by Bio-Pd(0). Two reactor set-ups were used. The first contained a cylinder of Bio-Pd(0) running the length of the column. The column was challenged with 1 mM CrO_4^{2-} at a threshold flow rate of 0.82 mL h^{-1} with 100 % reduction maintained for 3 months. Reactor 2 contained a 'plug' of Bio-Pd(0) spanning the width of the column. Reduction remained at 100 % for 1 week at a threshold flow rate of 13 mL h^{-1} (Mabbett 2004). Palladised biomass is also effective at the dehalogenation of chlorophenols and polychlorinated biphenyls, although the mechanism for this is unknown (Baxter-Plant *et al.* 2003). Bio-Pd(0) could therefore be used for the bioremediation of wastes containing metal and chlorinated aromatics.

3.0 Cell immobilization

Ultimately Cr(VI) reducing microbial systems will be used on an industrial scale for bioremediation of wastewaters. However Cr(VI) reduction using freely suspended cells is

disadvantageous because of downstream difficulties in biomass/ effluent separation. Retention of microbial biomass in an immobilized cell system can be used to overcome this problem.

Using immobilized cell technology, bioreactors can be operated on a continuous basis rather than in batch suspensions resulting in a drastic decrease in plant size and costs. Additionally, continuous processes lead to better process control, minimal down time, and product uniformity (Brodelius and Vandamme 1987).

The immobilized cell system is the region in which the cells are localised. It is composed of the cells, the support material and the solution that fills the remainder of the space (known as the interstitial solution). The chemical properties of the interstitial solution may be different to the bulk solution present, and therefore the space around the cells is often referred to as the microenvironment (Willaert and Baron 1996b).

There are a wide variety of immobilization procedures available for the immobilization of microbial cells, as illustrated in Fig. 3. Four general categories can be used to classify all immobilization systems, depending on the systems mechanism for cell immobilization and the nature of the support material. Each of these four general categories can be subdivided into more specific groups.

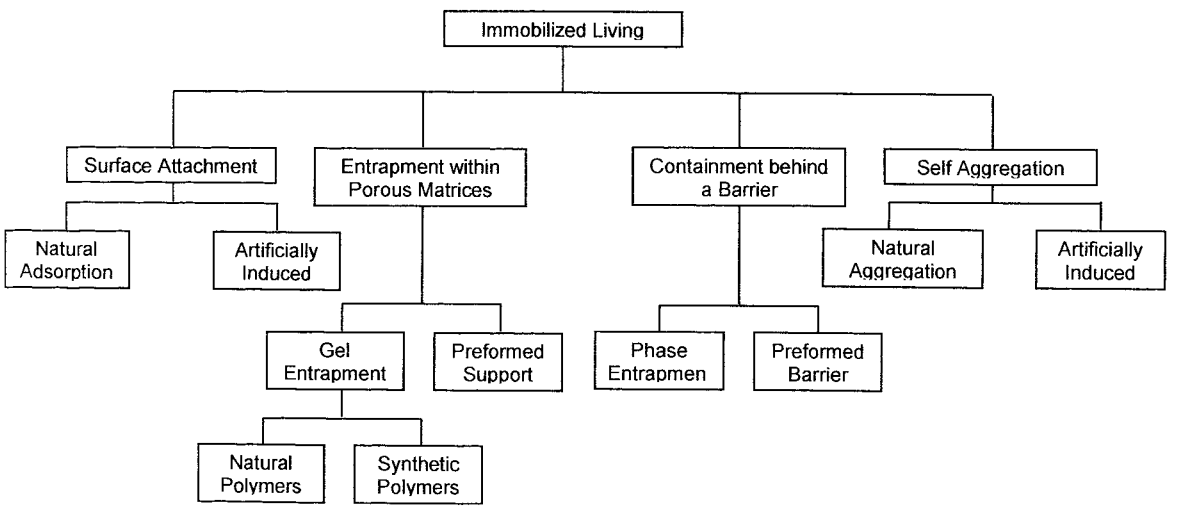


Fig. 3: Immobilization methods for microbial cells (Willaert and Baron 1996).

The type of immobilization system utilised depends on application and operational conditions (e.g. pH, temperature). The ideal immobilization system would possess the following properties (note: there is no system that possesses all these properties):

1) High cell mass loading capacity
2) Easy access to nutrients and removal of products
3) Simple and mild immobilization procedure
4) High surface area to volume ratio
5) Mechanical stability
6) Sterilisable
7) Economical

3.1 Immobilization by surface attachment

Immobilization of cells by surface attachment can be subdivided into two categories, namely natural adsorption and artificially induced attachment.

3.1.1 Immobilization by natural adsorption

Natural adsorption occurs frequently in natural environments where microbial films develop on a variety of supports, including clay particles, teeth, and metal supports.

Adsorption is the simplest method of cell immobilization, involving reversible surface interactions between cells and the support material. The charge conferred on a cell depends on the chemical nature of a cell surface, where constituents such as peptides, hexosamines, and diaminopimelic acid provide the necessary ionic sites for attachment to a support material (Brodelius and Vandamme 1987). The charge on the cell wall changes with age and

environmental conditions (e.g. cationic or anionic, depending on solution pH) (Brodelius and Vandamme 1987). Surface interactions take the form of electrostatic forces (e.g. Van der Waals forces, ionic and hydrogen bonding) (Bickerstaff 1997). Although these forces are weak, they occur in significant number to enable binding. Natural adsorption makes use of existing surface chemistry between the cell and the support, with no chemical activation or modification-taking place. Immobilization by natural adsorption is simple, cheap and high cell viability is maintained due to mild immobilization conditions. Additionally the immobilization is reversible, so the support material may be recovered and reused.

However, this method of immobilization has a number of disadvantages. As cells are only bound to the support material by relatively weak interactions, there may be leakage of cells into the aqueous environment, which can lead to downstream processing difficulties in some applications. There may be several factors contributing to desorption, such as flow rate, particle-particle abrasion, and scouring of particulate materials on vessel walls. Another disadvantage is that the support material may become overloaded, leading to mass and heat transfer difficulties, and consequent sloughing of cells from the support material. Lastly, steric hindrance of the support may occur (Bickerstaff 1997). Following the initial adhesion attachment can be rendered more permanent by the formation of an adhered biofilm (see 3.5).

3.1.2 Artificially induced immobilization

Artificially induced immobilization requires a linking agent to covalently bind microbial cells to a support material. A covalent bond is generally formed between functional groups on the support and free amino (usually on lysine or arginine) and/or carboxyl groups (from aspartic acid or glutamic acid) on the surface of the microbial cell. These amino and/or carboxyl groups are easily cross-linked by a bi- or multifunctional reagent, such as glutaraldehyde

(Brodelius and Vandamme 1987). Although cells are bound more strongly to the support material than in natural adsorption, cell viability may be reduced by the use of chemicals such as glutaraldehyde.

3.2 Entrapment in a porous matrix

Cell entrapment can be subdivided into gel entrapment and entrapment in a preformed support. It is important to ensure the pores of the support material are sufficiently small to prevent cells leaving the entrapment matrix, but sufficiently large to avoid mass and heat transfer difficulties (Bickerstaff 1997).

3.2.1 Gel entrapment

Gel entrapment involves entrapping cells in either a natural or synthetic polymer gel. This produces immobilized systems with high biomass loadings, which are formed under mild conditions to maintain high cell viability. Disadvantages of gel entrapment include poor mechanical strength and mass transfer limitations. Examples of materials used for gel entrapment include alginate, carrageenan, agar, agarose, chitosan, polyvinyl alcohol and Lentikats® (Willaert and Baron 1996).

3.2.1.1 Gel entrapment with alginate

Alginate is a popular cell immobilization technique because it is cheap, fast, simple, easy, and high cell viability is maintained due to mild immobilization conditions (Willaert and Baron 1996). Alginic acid is a constituent of brown marine algae, obtained from genera such as *Ascophyllum, Fucus,* and *Macrocystis.* Alginic acid is a copolymer composed of 1,4-linked β-

D-mannuronic acid (M) and α-L-gluronic acid (G). The polymer contains homopolymeric regions (G and M blocks) and regions of alternating structure (MG blocks).

Gelation of alginates involves ionic binding and conformational changes in the polymer structure. Divalent cations preferentially bind to G blocks, followed by the formation of crystalline aggregates in a two-fold ribbon form. Ions that have bound during the process are placed in electronegative cavities, similar to eggs in an egg box. Between these cavities and other polymer chain sequences, bonds form, giving rise to junction zones in the gel network. The composition, sequential structure, and molecular size of the polymers strongly affect the properties of the alginate beads (Willaert and Baron 1996a).

Calcium alginate beads are disrupted by the presence of chemicals that can chelate calcium ions (for example citrate). Use of divalent cations with a higher affinity for alginate than Ca^{2+}, (e.g. Ba^{2+}) overcomes this problem (Willaert and Baron 1996).

3.2.1.2 Gel entrapment with carrageenan

Carrageenans are naturally occurring hydrocolloids composed of high molecular weight, linear, sulfated polysaccharides (Chibata *et al.* 1986). They are extracted from red algae seaweeds, from species such as *Chondrus, Gigartina,* and *Hypnea*. There are three main types of carrageenan; lambda (λ) carrageenan, kappa (κ) carrageenan and iota (ι) carrageenan, each with distinct properties. In the potassium form, kappa-carrageenan is insoluble in cold water, and is considered the most suitable for cell immobilization due to the rigidity of the thermally reversible gel that it forms. The potassium salt of iota-carrageenan is insoluble in cold water, and forms compliant, thermally reversible gels with calcium ions. Lambda-carrageenan is soluble in all salt forms, forming viscous solutions, but it does not forma a gel, and thus is of little use as a gel immobilization material on its own (Chibata *et al.* 1986).

Carrageenans are composed predominantly of D-galactose, 3,6-linked β-D-galactose and 1,4-linked α-D-galactose. The number and location of ester sulfate groups on these sugars, and the extent to which the 1,4-linked residue exists as the 3,6-anhydro derivative causes differences in structure between the carrageenans (Willaert and Baron 1996).

Gelation occurs either by cooling the gel, or by the presence of gel inducing reagents, such as potassium ions. Double helix formation results in the formation of a carrageenan hydrocolloidal gel. Above the melting temperature of the gel, thermal agitation overcomes helix formation and so the polymer exists as a random coil. During the first stage of cooling a 3D polymer network builds up with helices forming junction zones between polymer chains. When cooled further, these junction zones aggregate (Willaert and Baron 1996). The gelation mechanism for carrageenan is similar to that of agar and agarose. The main advantages of this type of immobilization method are that it is easy, mild (so results in high cell viability), and the gel can be produced in a variety of shapes.

3.2.1.3 Gel entrapment with agar and agarose

The polysaccharides, agar and agarose, are isolated from marine red algae. Agar extracted from *Gracilaria* gels at temperatures in the 40 °C's and contains methyl ether groups. Comparatively, agar obtained from *Gelidium* and *Pterocladia* forms a gel in the low 30 °C's and is essentially devoid of methyl ether groups.

Agar contains a mixture of polysaccharides, with the more ionic polymers called agaropectins, and the more neutral polymers called agarose. Agarose is a linear polysaccharide consisting of alternating 1,3-linked β-D-galactopyranose and 1,4-linked 3,6-anhydro-α-galactopyranose. The gelation mechanism of agar, agarose and carrageenan

involves a shift from a random coil to a double helix during the early stages of gelation, to bundles of helices in the final stages.

An essential feature of agarose supports is the presence of pentagonal pores that are large enough to be penetrated by protein and high molecular weight compounds, thus reducing mass transport problems often associated with gel supports (Willaert and Baron 1996). A major disadvantage of using agarose for the immobilization of microbial cells is the relatively high cost of this polymer.

3.2.1.4 Gel entrapment with chitosan

Chitosan presents an alternative immobilization technique, with immobilization occurring at room temperature. Chitosan, a partially deacetylated chitin, is formed by reaction of chitin with a concentrated alkali. Chitosan is a high molecular weight polymer consisting of β-1-4-linked glucosamine molecules, containing amino groups that are used as reactive species during the immobilization process (Willaert and Baron 1996).

Gel formation occurs when chitosan solutions are added dropwise to a cross-linking solution (containing multivalent anion counterions) with a pH of less than 6. The amino groups of chitosan become protonated and ionic cross-linking occurs (Willaert and Baron 1996). If chitosan is cross-linked with high molecular weight counter-ion, capsules are formed, whilst globules are formed when chitosan is cross-linked with low molecular weight counter-ions (Vorlop and Klein 1986).

3.2.1.5 Gel entrapment with polyacrylamide

Polyacrylamide was the first synthetic gel used to entrap living microbial cells. This immobilization technique is easy and simple to do, but often results in decreased cell viability

due to the toxicity of the monomers and the heat evolved during the reaction. During the polymerisation process, linear chains of polyacrylamide are formed by a free radical process. Polyacrylamide is cross-linked by inclusion of a bifunctional reagent, such as N-N'-methylene-bisacrylamide, which contains two unsaturated double bonds. The porosity and fragility of the polyacrylamide gel formed depends on the degree of cross-linking, which is a function of the amounts of acrylamide and bifunctional reagent present (Willaert and Baron 1996).

Tucker *et al.* (1998) investigated Cr, Mo, Se, and U reduction by *Desulfovibrio desulfuricans* DSM 642 immobilized in polyacrylamide gel. Immobilized cells were placed in 10 mL columns (550 - 750 mg L^{-1} cell protein per vial). Anaerobic solutions of 0.5 mM Cr(VI), and 1 mM of each Mo(VI), Se(VI), and U(VI) were added using hydrogen or lactate as electron donor. Metal removal efficiencies of 86 – 96 % occurred over a 24 h period. Optimum conditions for reduction were 37 °C, and pH 7. Metal reduction was slower in immobilized cells than free cells, where reduction occurred in 7 h. The pseudo first order rate constant for Cr(VI) reduction by free cells was 0.9 h^{-1}, and for immobilized cells 0.13 h^{-1}. The reduced rates were probably due to transport limitations (Tucker *et al.* 1998).

3.2.1.6 Gel entrapment with polyvinyl alcohol (PVA)

PVA cell immobilization is cheap, easy, and results in the retention of high cell viability due to the mild conditions involved. PVA is a raw material of vinylon. Elastic, high strength gels are formed by cross-linking PVA with boric acid to produce a monodiol-type PVA-boric acid gel lattice. A disadvantage of PVA cell beads is that they tend to agglomerate but this can be overcome by the addition of a small amount of $CaCl_2$ (0.02 %) to boric acid (Willaert and Baron 1996).

Pattanapipitpaisal *et al.* (2001b) immobilized *Microbacterium* sp. NCIMB 13776 in polyvinyl alcohol (PVA). Three immobilization methods were studied (PVA-nitrate, PVA-borate, and PVA-alginate). Chromate reduction by immobilized cells was investigated in batch and continuous flow bioreactors. In batch, 1 mL of gel (75 mg wet weight cells mL^{-1}) or an equivalent amount of free cells were added to 10 mL AMM containing 100 μM chromate, whilst sparging with oxygen free N_2 (OFN). Pattanapipitpaisal *et al.* (2001b) found that free cells completely reduced chromate in 2 days, whilst PVA-borate and PVA-alginate cell beads took 4 days. PVA-nitrate cell beads reduced chromate poorly with a final concentration of chromate after 4 days of 55.6 μM. Decreased Cr(VI) reduction efficiency was probably due to inhibition by nitrate, which potentially could act as a competing electron acceptor (Pattanapipitpaisal *et al.* 2001b). Lower reduction rate by PVA-borate and PVA-alginate cell beads was attributed to diffusional constraints. Investigations into continuous Cr(VI) removal by *Microbacterium* sp. NCIMB 13776 occurred in 25 mL columns packed with 15 mL PVA-alginate cell beads (10.5 % wet weight cells mL^{-1}). Chromate solution comprising 50 μM chromate and 20 mM MOPS/ NaOH buffer, pH 7, was pumped through the column at a flow rate of 0.95 mL h^{-1}. The study showed that cell bead integrity was maintained for 20 days, with 90 – 95 % chromate removal (Pattanapipitpaisal *et al.* 2001a). Further column tests (Pattanapipitpaisal 2001) involved increasing the flow rate to 10.42 mL h^{-1} for 6 days. Approximately 25 % chromate was removed.

3.2.1.7 Gel entrapment with Lentikats®

Lentikats® is a new immobilization matrix based on polyvinyl alcohol. Lentikats® are non-toxic with good mechanical properties. The gelation process occurs under mild conditions so

loss in cell viability is generally negligible. The optimised geometry of Lentikats® means there will be minimal mass or heat transfer limitations (Fig. 4).

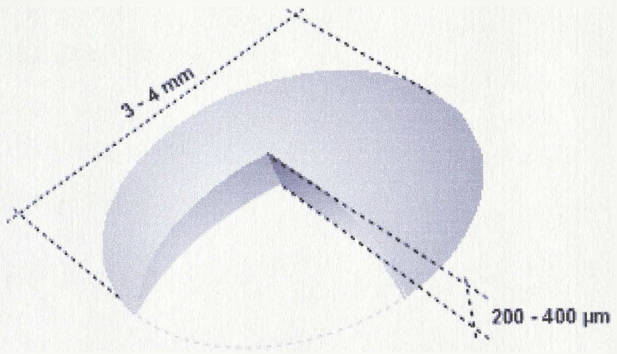


Fig. 4: Geometry of a Lentikat® (Taken from http://www.genialab.com).

Immobilization of cells in Lentikats® is inexpensive, and the immobilization matrix can be obtained as a bulk chemical for industrial applications (http://www.genialab.com): the exact composition is not available.

3.2.2 Entrapment with a preformed support

Entrapment of cells using a preformed support, such as cellulose, protects cells from the shear forces that exist within the bulk fluid in stirred reactors. However like cell adsorption, the cells are not totally separated from the systems effluent and can cause downstream processing difficulties. This type of entrapment offers more resistance to compression than gel immobilized systems and mass transport limitations are reduced (Willaert and Baron 1996).

3.3 Containment behind a barrier

For this category of cell immobilization, cells can be contained behind a preformed barrier (e.g. hollow fibre system) or the barrier can be formed around the cells. Unlike previous

techniques discussed this technique completely separates cells from the process effluent. Mass transfer limitations can reduce the efficiency of these systems as the supply of nutrients, and the removal of products occurs by diffusion through the barrier (Willaert and Baron 1996). Blockage of the membrane can occur through cell growth and in this case by $Cr(OH)_3$.

3.4. Self-aggregation of cells

This type of cell immobilization is support free and involves joining cells together to form a large 3D complex structure. Aggregation of cells occurs naturally or by the addition of artificial flocculation agents or cross-linking compounds (e.g. glutaraldehyde). Many cells aggregate naturally at some point in their life cycle.

3.5 Biofilm formation

Microbial cells firmly adhere to almost any surface in aquatic environments. Bacterial biofilm formation begins with the adhesion of a small number of bacterial cells to a surface. The immobilized cells grow, reproduce and produce extracellular polymers, which extend from the cell to form a matrix that provides the biofilm with structure (Costerton 1999).

A variety of microenvironments can exist in a biofilm. A thick biofilm, for example, may contain aerobic and anaerobic environments due to diffusional limitations (Characklis and Marshall 1990). Biofilms are composed of the biofilm, the overlying gas/ liquid layer, and the substratum on which the biofilm is immobilized. The biofilm component is composed of the base film and the surface film. The base film consists of a structured accumulation of cells, and is dominated by molecular transport. A transition between the bulk liquid and the base film is provided by the surface film, where gradients in the biofilms properties are most important (Characklis and Marshall 1990). The biofilm consists of a continuous liquid phase

that contains dissolved and suspended particulate materials, and a series of solid compartments composed of specific particulate materials (e.g. micro-organisms, extracellular material, inorganic particulate). The fluid dynamic regime governs mass and heat transfer from the bulk liquid component to the biofilm compartment. The gas compartment provides aeration and/ or removal of gaseous microbial reaction products (Characklis and Marshall 1990).

Net biofilm accumulation involves transport of cells to the substratum, adsorption of cells to the substratum, growth and other metabolic processes within the biofilm and detachment of portions of the biofilm. Desorption of cells from the biofilm may result from fluid shear forces among other physical, chemical and biological properties.

3.6 Factors affecting the activity of immobilized cell particles

3.6.1 Activity of immobilized cells

Generally the activity of immobilized cells is lower than for the same amount of freely suspended cells. One of the reasons for this reduced activity is mass transfer limitations (i.e. resistance to the transport of substrate, products, and nutrients). Fig. 5 shows the substrate concentration profile of an immobilized cell particle.

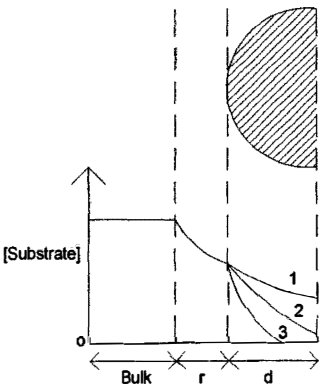


Fig. 5: Substrate concentration profile of an immobilized cell particle (Brodelius and Vandamme 1987).

Where, 1 = low cell loading. 2 = intermediate cell loading. 3 = high cell loading. S_{bulk} = substrate concentration in the bulk medium. r = thickness of stagnant region surrounding gel particle. d = radius of gel particle.

Mass transfer can be separated into internal and external mass transfer. Internal mass transfer is governed by the kinetics of the immobilized particle, and the physiochemical properties of the matrix, whilst external mass transfer is governed by reactor type, and the hydrodynamics of the bulk liquid. In the substrate concentration profile, the substrate concentration in the bulk is greater than at the external surface of the bead. Substrate supply from the bulk phase towards the bead is lower than the rate of substrate diffusion into the

bead. Fig. 5 also shows that the immobilized cells usually convert the substrate into product faster than it can be supplied through the bead surface. A gradual decrease in conversion rate is observed as the distance to the beads core gets closer due to decreasing substrate concentration (Brodelius and Vandamme 1987).

Mass transfer limitations increase with increasing size of the microbial aggregate/ support particle. The particles shape also influences the mass transfer resistance, principally by the ratio of external surface area to particle volume, as indicated in Table 5.

Table 5: Aspartase activities of immobilized *E.coli* cells formed in various shapes and their activity yields

Shape of gel	Surface area of gel (cm^2 g $cells^{-1}$)	Aspartase activity (uM h^{-1} g $cells^{-1}$)	Activity yield (%)
Bead (diameter = 3 mm)	124	30360	46.7
Cube (3x3x3 mm)	125	32130	46.4
Membrane (1x10x10 mm)	150	41120	63.3

(Taken from Brodelius and Vandamme 1987)

3.6.2 Concentration in the bulk liquid

When the substrate concentration in the bulk liquid is high, mass transfer resistances are decreased. This is because the substrate concentration can reach high enough concentrations in the immobilized particle so that microbial reactions can proceed at non-limited concentrations. When the concentrations of the substrate are low in the liquid medium, mass transfer resistances can become problematic (Mavituna 1986).

3.6.3 Effective diffusion coefficients

When the effective diffusion coefficients in the immobilized cell matrix become smaller than those in the bulk liquid phase, mass transfer limitations become problematic. The concentration of the diffusing species, the concentration of biomass, temperature, permeability of the carrier matrix, and the effect of products and substrates on the immobilization matrix affect the effective diffusion coefficient. Studies suggest that increased immobilized cell concentration and increased gel strength result in decreased diffusion coefficients (Mavituna 1986).

3.7 Operational considerations in the use of immobilized cells

3.7.1 Stability in immobilized bioreaction systems

The activity of an immobilized cell system often varies with operating time due to reversible and irreversible mechanisms. Cell activity may decline by reversible mechanisms such as blockage of channels and pores by accumulated cells or products, or inhibition of cell activity due to the accumulation of inhibitory materials. This can be visualised *in situ* in some cases using magnetic resonance imaging (see Appendix II). Irreversible mechanisms that affect immobilized cell activity include cell death and mechanical loss of cells from the carrier matrix, physico-chemical mechanisms where the cell-matrix link is broken resulting in cells diffusing out of the reaction system (Emery and Mitchell 1986).

3.7.2 Support matrix stability

If a packed-bed reactor is used, the flow properties of the system may break down because of fouling or because of disintegration of the support matrix. Scanning electron microscope

studies on *Laminaria* sp.-alginate beads showed cells were inactive in the centre of beads (diameter 2.9 ± 0.1 mm). Over time, interior voids appeared, caused by the build up of carbon dioxide, resulting ultimately in bead fracture and disintegration (Emery and Mitchell 1986).

To study support matrix stability using SEM, the sample must be dehydrated, so the natural, hydrated condition of the matrix is not observed. Magnetic Resonance Imaging (MRI) (Appendix II) would use intact cell beads, allowing non-invasive study of cell supports in reactors.

4.0 Objectives of the research programme

The overall goal of this programme was to develop, and define mathematically, an immobilized reactor system for the continuous removal of Cr(VI) from flows presented to immobilized biomass. Since simple metal analysis of inflow and outflow solutions gives information about only the "metal in" and "metal out", and no information about spatio-temporal processes within the reactor, a secondary objective was to use magnetic resonance imaging (MRI: Appendix II) to gain information about reactor homogeneity, integrity and chemistry that cannot be gained by other methods. The overall objective would be to provide the means to obtain macroscopic (bulk) chemical engineering flow and diffusional models to integrate with enzymatic and kinetic models governing events at the microscale.

4.1 Aims of this study

The aims of this study were as follows:

1) To develop a model system for meaningful comparison of chromate reduction by *Desulfovibrio vulgaris* NCIMB 8303 and *Microbacterium* sp. NCIMB 13776, selecting the best microorganism for bioprocess development.
2) To identify the most appropriate support for immobilization of *D. vulgaris* NCIMB 8303 and *Microbacterium* sp. NCIMB 13776, with respect to Cr(VI) reduction rate in continuous-flow packed-bed columns, matrix stability (mechanical) and column longevity, selecting the most appropriate support for bioprocess development.
3) To compare Cr(VI) reduction by resting cells of *D. vulgaris* NCIMB 8303 with that of palladised biomass (biologically produced Pd(0) (Bio-Pd(0))).
4) To compare Cr(VI) reduction by Bio-Pd(0) produced using different bacterial strains as host matrices.
5) To model Cr(VI) reduction by Bio-Pd(0) immobilized in continuous-flow packed-bed reactors (model of the 'black box').
6) To evaluate the potential of using biologically produced hydrogen as electron donor for Cr(VI) reduction by resting cells of *D. vulgaris* NCIMB 8303 and Bio-Pd(0).
7) To utilise MRI for visualisation of matrix homogeneity and stability and to differentiate between Cr(VI) and Cr(III) *in situ*.
8) To follow the reduction of Cr(VI) to Cr(III) *in situ* by MRI for spatio-temporal 4-D information to further delineate the 'black box' model developed in (5).

5.0 Layout of the thesis

This thesis is presented as a series of sections.

Section 1: General introduction containing background information relevant to the study.

Section 2 – 4: Results consisting of manuscripts that are published, or in submission. The manuscripts consist of individual introductions, materials and methods, results, discussion and conclusions. Each section is self-contained with bibliographies as part of the manuscripts themselves.

Section 5: Overall discussion, conclusions and suggested further work.

Appendix I: Symposium proceedings to the International Biohydrometallurgy Symposium 2003, Athens. Currently in press via a Greek Publisher.

Appendix II: A brief overview of the principles of magnetic resonance imaging, followed by a review of literature relevant to this project.

Appendix III: Humphries AC, Nott KP, Macaskie LE, Hall LD. *In situ* Magnetic Resonance Imaging of Cr(VI) and Cr(III)

Appendix IV: Supplementary Materials and Methods, providing information about bacterial strains used during this study. Assay methods for the determination of concentrations of Cr(VI), Pd(II) and protein are also detailed.

Appendix V: Macaskie LE, Baxter-Plant VS, Creamer NJ, Humphries AC, Mikheenko IP, Mikheenko, P, Penfold DW, Yong P 2005. Applications of bacterial hydrogenases in waste decontamination, manufacture of novel bionanocatalysts and in sustainable energy. Biochem. Soc. Trans. In press.

References cited in Introduction

Aubert C, Brugna M, Dolla A, Bruschi M, Giudici-Otriconi MT. 2000. A sequential electron transfer from hydrogenase to cytochromes in sulphate-reducing bacteria. Biochim Biophys Acta. 1476:85-92.

Bae WC, Kang TG, Kang IK, Won YJ, Jeong BC. 2000. Reduction of hexavalent chromium by *Escherichia coli* ATCC 334556 in batch and continuous culture. J Microbiol. 38:36-39.

Bagchi, D, Bagchi M, Stohs SJ. 2001. Chromium (VI)-induced oxidative stress, apoptotic cell death and modulation of p53 tumor suppressor gene. Mol Cell Biochem. 222:149-158.

Barnhart J. 1997. Occurrences, uses, and properties of chromium. Regul Toxicol Pharma. 26:S3-S7.

Baxter-Plant VS, Mikheenko IP, Macaskie LE. 2003. Sulphate-reducing bacteria, palladium and the reductive dehalogenation of chlorinated aromatic compounds. Biodegradation. 14:83-90.

Bickerstaff G. 1997. Immobilization of enzymes and cells: some practical considerations. Paisley, Scotland: Humana Press.

Bopp LH, Ehrlich HL. 1988. Chromate resistance and reduction in *Pseudomonas fluorescens* strain LB300. Arch Microbiol. 150:426-431.

Brodelius P, Vandamme E. 1987. Immobilized cell systems. Weinheim: Verlag Chemie.

Cary E. 1982. Chromium in air, soil and natural waters. In: Langard S, editor. Biological and environmental aspects of chromium. Oxford: Elsevier Biomedical Press.

Cervantes C, Campos-Garcia S, Devars F, Gutierrez-Corona H, Loza-Tavera J, Torres-Guzman C, Moreno-Sanchez R. 2001. Interactions of chromium with microorganisms and plants. FEMS Microbiol Rev. 23:335-347.

Cervantes C, Silver S. 1992. Plasmid chromate resistance and chromate reduction. Plasmid. 27:65-71.

Cetinkaya-Donmez G, Aksu Z, Ozturk A, Kutsal T. 1999. A comparative study on heavy metal biosorption characteristics of some algae. Process Biochem. 34:885-892.

Characklis W, Marshall K. 1990. Biofilms. New York: John Wiley and Sons.

Chen JM, Hao OJ. 1998. Microbial chromium (VI) reduction. Crit Rev Environ Sci Technol. 28:219-251.

Chibata I, Tosa T, Sato T, Takata I. 1986. Immobilization of cells in carrageenan. In: Mosbach K, editor. Immobilized enzymes and cells, Pt B. Orlando: Academic Press.

Clark DP. 1994. Chromate reductase activity of *Enterobacter aerogenes* is induced by nitrite. FEMS Microbiol Lett. 122:233-237.

Costerton JW. 1999. Introduction to biofilms. International Journal of Anti-microbial Agents. 11:217-221.

Deleo PC, Ehrlich HL. 1994. Reduction of hexavalent chromium by *Pseudomonas fluorescens* LB300 in batch and continuous cultures. Appl Microbiol Biotechnol. 40:756-759.

Eccles H. 1999. Treatment of metal contaminated wastes: why select a biological process? Trends Biotechnol. 17:462-465.

Eccles H. 1995. Removal of heavy metals from effluent streams – why select a biological process? Int Biodeter Biodegr. 35:5-16.

Emery AN, Mitchell DA. 1986. Operational considerations in the use of immobilized cells. In: Atkinson A, editor. Process Engineering aspects of immobilized cell systems, Pt B. Pergamon Press.

Gadd GM. 2001. Microbial metal transformations. J Microbiol. 39:83-88.

Gadd GM. 1988. Accumulation of metals by microorganisms and algae. Weinheim: Verlag Chemie.

Garbisu C, Alkorta I, Llama M, Serra J. 1998. Aerobic chromate reduction by *Bacillus subtilis*. Biodegradation. 9:133-141.

Gupta R, Ahuja P, Khan S, Saxena RK, Mohapatra H. 2000. Microbial biosorbents: meeting challenges of heavy metal pollution in aqueous solutions. Curr Sci India. 78:967-973.

Ishibashi YC, Cervantes C, Silver S. 1990. Chromium reduction in *Pseudomonas putida*. Appl Environ Microbiol. 56:2268-2270.

Kimbrough DE, Cohen Y, Winer AM, Creelman L, Mabuni C. 1999. A critical assessment of chromium in the environment. Crit Rev Env Sci Tec. 29:1-46.

Komori K, Rivas A, Toda K, Ohtake H. 1990. Biological removal of toxic chromium using an *Enterobacter cloacae* strain that reduces chromate under anaerobic conditions. Biotechnol Bioeng. 35:951-954.

Komori K, Wang PC, Toda K, Ohtake H. 1989. Factors affecting chromate reduction in *Enterobacter cloacae* strain HO1. Appl Microbiol Biotechnol. 31: 567-570.

Liu KJ, Shi XL. 2001. In vivo reduction of chromium (VI) and its related free radical generation. Mol Cell Biochem. 222:41-47.

Llovera S, Bonet R, Simonpujol MD, Congregado F. 1993a. Chromate reduction by resting cells of *Agrobacterium radiobacter* EPS916. Appl Environ Microbiol. 59:3516-3518.

Llovera S, Bonet R, Simonpujol, MD, Congregado F. 1993b. Effect of culture medium ions on chromate reduction by resting cells of *Agrobacterium radiobacter*. Appl Microbiol Biotechnol. 39:424-426.

Lloyd JR, Mabbett AN, Williams DR, Macaskie LE. 2001. Metal reduction by sulphate-reducing bacteria: physiological diversity and metal specificity. Hydrometallurgy. 59:327-337.

Lloyd JR, Yong P, Macaskie LE. 1998. Enzymatic recovery of elemental palladium using sulfate-reducing bacteria. Appl Environ Microbiol. 64:4607-4609.

Loujou E, Bianco O, Bruschi M. 1998. Kinetic studies on the electron transfer between various *c* type cytochromes and metal oxides. J Electroanalytic Chem. 452:167-177.

Losi ME, Amrhein C, Frankenberger WT. 1994. Factors affecting chemical and biological reduction of hexavalent chromium in soil. Environ Toxicol Chem. 13:1727-1735.

Lovley DR, Phillips EJP. 1994. Reduction of chromate by *Desulfovibrio vulgaris* and its c_3 cytochrome. Appl Environ Microbiol. 60:726-728.

Mabbett AN. 2001. The reduction and recovery of chromium (VI) from industrially polluted waste waters using sulphate-reducing bacteria. *PhD Thesis*. The University of Birmingham, England.

Mabbett AN, Lloyd JR, Macaskie LE. 2002. Effect of complexing agents on reduction of Cr(VI) by *Desulfovibrio vulgaris* ATCC 29579. Biotechnol Bioeng. 79:389-397.

Mavituna F. 1986. Activity of immobilized cell particles. In: Atkinson B, editor. Process engineering aspects of immobilized cell systems. Pergamon Press.

Mikheenko I. 2004. Nanoscale palladium recovery. *PhD Thesis*. The University of Birmingham, England.

Nowottny CW, Halwachs W, Schugerl K. 1997. Recovery of platinum, palladium and rhodium from industrial process leaching solutions by reactive extraction. Sep Purif Technol. 12:135-144.

Odom JM, Peck HD. 1984. Hydrogenase, electron transfer proteins, and energy coupling in the sulfate-reducing bacteria, *Desulfovibrio*. Ann Rev Microbiol. 38:551-592.

Odom JM, Peck HD. 1981. Hydrogen cycling as a general mechanism for energy coupling in the sulfate-reducing bacteria, *Desulfovibrio* sp. FEMS Microbiol Lett. 12:47-50.

Oh YS, Choi SC. 1997. Reduction of hexavalent chromium by *Pseudomonas aeruginosa* HP014. J Microbiol. 35:25-29.

Park CH, Keyhan M, Wielinga B, Fendorf S, Matin A. 2000. Purification to homogeneity and characterization of a novel *Pseudomonas putida* chromate reductase. Appl Environ Microbiol. 66:1788-1795.

Pattanapipitpaisal P. 2001. Bioreduction of chromate and detection of chromate resistance genes in Gram-positive and Gram-negative bacteria. *PhD Thesis*. The University of Birmingham, England.

Pattanapipitpaisal P, Brown NL, Macaskie LE. 2001a. Chromate reduction and 16S rRNA identification of bacteria isolated from a Cr(VI)-contaminated site. Appl Microbiol Biotechnol. 57: 257-261.

Pattanapipitpaisal P, Brown NL, Macaskie LE. 2001b. Chromate reduction by *Microbacterium liquefaciens* immobilized in polyvinyl alcohol. Biotechnol Lett. 23:61-65.

Peck HD, Lissolo T. 1988. Assimilatory and Dissimilatory Sulfate Reduction: Enzymology and Bioenergetics. In: Ferguson SJ, editor. Nitrogen and Sulfur cycles. Cambridge: Cambridge University Press.

Pettine M, Barra I, Campanella L, Millero FJ. 1998. Effect of metals on the reduction of chromium (VI) with hydrogen sulfide. Water Res. 32:2807-2813.

Romao CV, Pereira IAC, Xavier AV, LeGall J, Teixeira M. 1997. Characterization of enzymatic reduction of hexavalent chromium by *Escherichia coli* ATCC 33456. Appl Environ Microbiol. 59:3771-3777.

Shupack SI. 1991. The chemistry of chromium and some resulting analytical problems. Environ Health Persp. 92:7-11.

Srinath T, Verma T, Ramteke PW, Garg SK. 2002. Chromium (VI) biosorption and bioaccumulation by chromate resistant bacteria. Chemosphere. 48:427-435.

Sugiyama M. 1991. Effect of vitamins on chromium (VI)-induced damage. Environ Health Persp. 92:63-70.

Suzuki T, Miyata N, Horitsu H, Kawai K, Takamizawa K, Tai Y, Okazaki M. 1992. NAD(P)H-dependent chromium (VI) reductase of *Pseudomonas ambigua* G1 – a Cr(VI) intermediate is formed during the reduction of Cr(VI) to Cr(III). J Bacteriol. 174:5340-5345.

Tucker MD, Barton LL, Thomson BM. 1988. Removal of U and Mo from water by immobilized *Desulfovibrio desulfuricans* in column reactors. Biotechnol Bioeng. 60:88-96.

Voordouw G. 1988. Molecular biology of redox proteins in sulfate reduction. In: Ferguson SJ, editor. Nitrogen and sulfur cycles. Cambridge: Cambridge University Press.

Vorlop K, Klein J. 1986. Entrapment of microbial cells in chitosan. In: Mosbach K, editor. Immobilized enzymes and cells, Pt B. Orlando: Academic Press.

Wang YT, Shen H. 1997. Modelling Cr(VI) reduction by pure bacterial cultures. Water Res. 31:727-732.

Wang PC, Toda K, Ohtake H, Kusaka I, Yabe I. 1991. Membrane-bound respiratory system of *Enterobacter cloacae* strain HO1 grown anaerobically with chromate. FEMS Microbiol Lett. 78:11-16.

Wang PC, Mori T, Toda K, Ohtake H. 1990. Membrane-associated chromate reductase-activity from *Enterobacter cloacae*. J Bacteriol. 172:1670-1672.

White C, Sayer JA, Gadd GM. 1997. Microbial solubilization and immobilization of toxic metals: key biogeochemical processes for treatment of contamination. FEMS Microbiol Rev. 20:503-516.

White C, Wilkinson SC, Gadd GM. 1995. The role of microorganisms in biosorption of toxic metals and radionuclides. Int Biodeter Biodegr. 35:17-40.

Willaert R, Baron G. 1996. Gel entrapment and micro-encapsulation: methods, applications, and engineering principles. Rev Chem Eng. 12:5-205.

Yong P, Rowson NA, Farr JPG, Harris IR, Macaskie LE. 2003. A novel electrobiotechnology for the recovery of precious metals from spent automotive catalysts. Environ Technol. 24:289-297.

Yong P, Rowson NA, Farr JPG, Harris IR, Macaskie LE. 2002. Bioreduction and biocrystallization of palladium by *Desulfovibrio desulfuricans* NCIMB 8307. Biotechnol Bioeng. 80:369-379.

Zayed AM, Terry N. 2003. Chromium in the environment: factors affecting biological remediation. Plant Soil. 249:139-156.

SECTION 2

RESULTS:

Chromate reduction by *D. vulgaris* NCIMB 8303 and *Microbacterium* sp. NCIMB 13776



SECTION 2.1

"Reduction of Cr(VI) by *Desulfovibrio vulgaris* and *Microbacterium* sp".

Journal: ***Biotechnology Letters***

24: 1261 – 1267 (2002)

Biotechnology Letters **24**: 1261–1267, 2002.
© 2002 *Kluwer Academic Publishers. Printed in the Netherlands.*

Reduction of Cr(VI) by *Desulfovibrio vulgaris* and *Microbacterium* sp.

A.C. Humphries & L.E. Macaskie*
School of Biosciences, The University of Birmingham, Edgbaston, B15 2TT, UK
**Author for correspondence (Fax (44)-121-414-6557; E-mail: L.E.Macaskie@bham.ac.uk)*

Received 27 March 2002; Revisions requested 15 April 2002; Revisions received 21 May 2002; Accepted 22 May 2002

Key words: bioremediation of Cr(VI), chromate reduction, *Desulfovibrio* sp., *Microbacterium* sp.

Abstract

Many industrial wastes contain Cr(VI), a carcinogen and mutagen, the toxicity of which can be ameliorated by reduction to Cr(III). *Microbacterium* sp. NCIMB 13776 and *Desulfovibrio vulgaris* NCIMB 8303 reduced Cr(VI) to Cr(III) anoxically using 25 mM sodium citrate buffer (pH 7), with 25 mM sodium acetate and 25 mM sodium formate as electron donors at 30 °C, under which conditions the rates of reduction of 500 μM sodium chromate were 77 and 6 nmol h^{-1} mg dry cell wt for *D. vulgaris* and *Microbacterium* sp., respectively, these being increased to 127 and 17 nmol h^{-1} mg dry cell wt in the presence of 20 mM MOPS/NaOH buffer.

Introduction

Many wastes contain hexavalent chromium [Cr(VI); CrO_4^{2-})], which is toxic, carcinogenic and mutagenic (Komori *et al.* 1989). The bioconversion of Cr(VI) to Cr(III), which readily precipitates as $Cr(OH)_3$, has been suggested for the removal of Cr(VI) from contaminated waters (see Pattanapipitpaisal *et al.* 2001a). Many examples of microbial reduction of Cr(VI) exist, for example *Pseudomonas fluorescens* LB300 (Bopp & Ehrlich 1988), *Enterobacter cloacae* HO1 (Wang *et al.* 1989) and *Bacillus* sp. (Wang & Xiao 1995).

A new Gram-positive organism, identified as a species of *Microbacterium* (shown to be closely related to *M. liquefaciens* by 16S rRNA sequence homology and deposited as *Microbacterium* sp. NCIMB 13776: Pattanapipitpaisal *et al.* 2001b) is CrO_4^{2-}-resistant, reducing Cr(VI) using acetate as the electron donor (Pattanapipitpaisal *et al.* 2001a). This organism is facultatively anaerobic, reducing Cr(VI) only anaerobically, but cannot grow at the expense of Cr(VI) as the sole electron acceptor (Pattanapipitpaisal *et al.* 2001b).

In contrast to *Microbacterium* sp., the sulfate-reducing bacteria (SRB) are a group with a well-established ability to reduce metals (Lovley *et al.* 1993, Lovley & Phillips 1994, Lloyd *et al.* 1998a,b). This versatile group uses an organic compound (e.g. lactate) or H_2 as the electron donor and SO_4^{2-} as the electron acceptor. Certain metal ions can be used as electron sinks in lieu of sulfate, resulting in metal reduction and, indeed, metal ions can be used as electron acceptors to support growth (Tebo *et al.* 1998).

Although several microbial systems for Cr(VI) bioremediation have been proposed the challenge conditions are usually not comparable and therefore realistic comparison of their biotechnological potentials have not been made. For example, in the case of *Desulfovibrio vulgaris* NCIMB 8303 resting cells were added to a MOPS/citrate buffered solution containing 100 μM sodium chromate with formate as the electron donor (Mabbett *et al.* 2002), whereas cells of *Microbacterium* sp. NCIMB 13776 were used in acetate minimal medium (Pattanapipitpaisal 2001a, b). Previous studies on the reduction of Cr(VI) by *D. vulgaris* were made in bicarbonate buffer (Lovley & Phillips 1994); bicarbonate, or another complexing ligand, was subsequently found to be essential to ameliorate the toxicity of the Cr(III) product to the mediating enzyme(s) (Mabbett *et al.* 2002), but no such requirement was reported for the reduction of Cr(VI) by the *Microbacterium* sp. (Pattanapipitpaisal *et al.* 2001a, b). Taking these two examples, for the efficiency of Cr(VI) reduction to be compared a common challenge

Table 1. Effect of electron donor on initial rates of Cr(VI) reduction by *D. vulgaris* NCIMB 8303 and *Microbacterium* sp. NCIMB 13776.

Electron donor	Initial rate[a] of Cr(VI) reduction [nmol Cr(VI) reduced h^{-1} mg dry wt]	
	D. vulgaris	*Microbacterium* sp.
Acetate	24 ± 13	3 ± 0.4
Formate	63 ± 13	Negligible
Citrate	Negligible	4 ± 1.4
Acetate + formate	15 ± 5	3 ± 0.6
Acetate + citrate	21 ± 10	3 ± 0.8
Formate + citrate	56 ± 15	3 ± 0.9

Cells were challenged with 500 μM Cr(VI) with various electron donors (25 mM final concentration) singly or in mixtures as described in Materials and methods. Data are means ± SEM from 3 experiments.

[a]Initial rates were taken over the 1st h as gradients from linear regions of the appropriate graphs.

solution must be found that provides optimum conditions for Cr(VI) reduction by both bacteria and also sequesters the Cr(III) product. The first aim of this work was to develop a common solution for a realistic comparison prior to selection of the most appropriate bioremediation system.

A previous study showed that it is possible to 'interrogate' an intact bioreactor non-invasively in 3D using magnetic resonance imaging (MRI) (Paterson-Beedle *et al.* 2001). The accumulated metal used previously [La (III)] was MRI 'silent' but in contrast the Cr(III) ion has a magnetic moment of 3.8 BM (Bertini & Luchinat 1986) and preliminary tests (A.C. Humphries, K.P. Nott & L.E. Macaskie, unpublished work) have shown that Cr(III) [but not Cr(VI)] could be visualised by MRI [by the effect of the paramagnetic species on the proton signal (Paterson-Beedle *et al.* 2001)] albeit with low sensitivity, opening the way to investigation of the bioreduction reactions spatially and temporally *in situ*. Although metal deposition has been visualised using MRI (Paterson-Beedle *et al.* 2001) the use of this technique to follow biological redox reactions *in situ* is novel. The second objective, therefore, was to obtain the maximum rate of bioreduction of Cr(VI) to underpin further studies on temporal and spatial quantification of Cr(VI) bioreduction. In this context, the use of MOPS buffer as a 'molecular amplifier' was evaluated.

Materials and methods

Organisms and growth conditions

Desulfovibrio vulgaris NCIMB 8303 was obtained from Prof D.R. Lovley (University of Massachusetts, Amherst, MA). Cells were maintained routinely in butyl rubber-sealed 100 ml serum bottles in Postgate's medium C (Postgate 1979) under O_2-free N_2 (OFN). For experiments, growing cultures (OD_{600} 0.8 ± 0.2) were produced by withdrawing anaerobically 10 ml of an actively growing culture and adding it to 100 ml of fresh medium *C. Microbacterium* sp. NCIMB 13776 was as described previously (Pattanapipitpaisal *et al.* 2001a,b). Cells were maintained by routine plating on Luria broth-agar. For experiments, an actively growing starter culture was prepared by inoculating 50 ml of L-broth with a single colony from an L-agar plate. After 24 h of aerobic growth (orbital shaker), starter culture (10 ml) was used to inoculate 100 ml of fresh L-broth. Cells were shaken at 30 °C to the mid-exponential phase (24 h).

Preparation of cell suspensions

For harvesting cells were transferred anaerobically under OFN into 50 ml serum bottles and harvested by centrifugation (3800 *g*, 20 min, 22 °C) in the bottles, washed and centrifuged three times with anaerobic (degassed) stock solutions of 20 mM MOPS/NaOH buffer (pH 7–7.1 under OFN) to provide stock suspensions for resting cell experiments. The cells were stored at 4 °C until use (within 24 h of harvesting). The biomass concentration of the cell concentrates was estimated by measuring the OD_{600}, and conversion to dry cell weight via a previously determined calibration.

Reduction of Cr(VI) by resting cells

The reaction mixtures were set up in 12 ml serum bottles, sealed with butyl rubber stoppers. The final volume of the reaction mixture was 10 ml; sodium chromate was at 500 μM. The composition of the reaction mixture depended on the parameter being investigated and the bacterial strain used, and is stated where appropriate. For all experiments, bottles were out gassed with OFN for 5 min to remove O_2. Chromate reduction tests were initiated by the addition of resting cells to 0.5 mg dry cell wt ml^{-1}. The serum bottles were transferred to an MACS-MG anaerobic work station (Don Whitley Scientific Ltd.), with an atmosphere

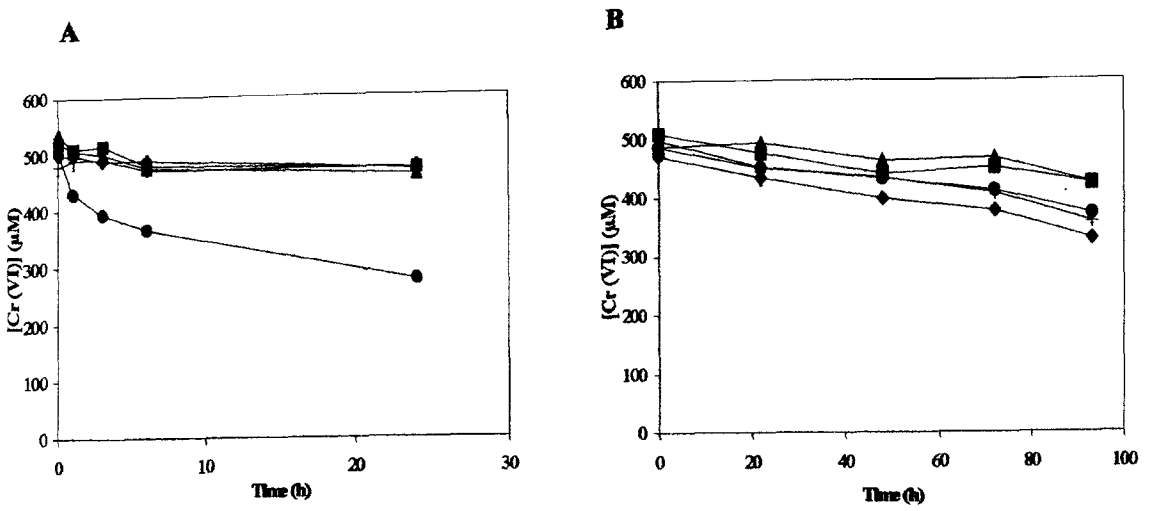


Fig. 1. Reduction of 500 μM Cr(VI) by resting cells of *D. vulgaris* (A) and *Microbacterium* sp. (B) at pH 7 and 30 °C using electron donors (25 mM each) as follows: ■, acetate; ▲, formate; ♦, acetate and citrate; ●, formate and citrate; + citrate. Error bars were within the dimensions of the symbols.

comprising 80% N_2, 10% H_2 and 10% CO_2. Controls for all experiments consisted of cells without electron donor and reaction solutions in the absence of cells. Samples were withdrawn periodically, via a syringe, and supernatants (100 μl) were analysed for residual Cr(VI) using diphenylcarbazide as described by Pattanapipitpaisal *et al.* (2001a, b). For investigating the effect of electron donor on Cr(VI) reduction the reaction solution contained mixtures of electron donors (25 mM final concentrations of each): sodium formate (pK_a 3.75), sodium acetate (pK_a 4.76) and sodium citrate (pK_a 3.13, 4.76, 6.40). The pH of the reaction mixture was adjusted to pH 7, and the incubation temperature was 30 °C or as stated. For investigating the effect of temperature and pH the electron donors for *D. vulgaris* were 25 mM (final concentration of each) sodium formate/sodium citrate (pH 7 with HCl) and for *Microbacterium* sp. were (25 mM final concentration of each) sodium acetate/sodium citrate (pH 7 with HCl) with temperatures and pH values as specified. For tests on the effect of pH, 25 mM sodium citrate buffer (pH 4, 5, 6, or 7 as appropriate) was used for washing and resuspension of cells (electron donors as above), with the pH checked at the end of each experiment. Where the effect of MOPS was investigated the cells were washed in 20 mM MOPS/NaOH buffer, pH 7, and resuspended with electron donors as above in the additional presence of 20 mM MOPS buffer (to pH 7 with NaOH).

To compare the efficiency of Cr(VI) reduction by *D. vulgaris* and *Microbacterium* sp. a common solution was used to provide optimum conditions for each organism. This comprised 25 mM sodium acetate, 25 mM sodium formate, 25 mM sodium citrate and 500 μM sodium chromate at pH 7 and 30 °C with or without MOPS/NaOH buffer, pH 7, as specified.

Results and discussion

Effect of electron donor

The first parameter investigated was whether acetate, formate and/or citrate could be used as electron donors for Cr(VI) reduction. No Cr(VI) reduction occurred in the controls, i.e. electron donor and cells were both required, and the electron donors *per se* did not effect Cr(VI) reduction spontaneously. The initial rates of Cr(VI) reduction, calculated over the first 1 h, are summarised in Table 1 and compared using a Student's *t*-test in Table 2.

Reduction of Cr(VI) by *D. vulgaris* was highest with formate, with an initial rate of Cr(VI) reduction of approx. 63 nmol h^{-1} mg dry cell wt. The presence of citrate did not enhance the initial rate (Table 1), probably because the concentration of Cr(III) product had not reached a toxic concentration (see below). A comparison of initial rates (Tables 1 and 2) showed that reduction was significantly higher in the

Table 2. Significance of electron donor on initial rates of Cr(VI) reduction.

D. vulgaris	*Acetate*	*Formate*	*Citrate*	*Acetate + formate*	*Acetate + citrate*
Formate	+				
Citrate	+	++			
Acetate + formate	−	+	+		
Acetate + citrate	−	+	+	−	
Formate + citrate	+	−	++	−	−
Microbacterium sp.	*Acetate*	*Formate*	*Citrate*	*Acetate + formate*	*Acetate + citrate*
Formate	++				
Citrate	−	+			
Acetate + formate	−	++	−		
Acetate + citrate	−	+	−	−	
Formate + citrate	−	+	−	−	−

Significant differences in rate over the 1st h were calculated using Student's *t*-tests (where shown): ++ denotes 99.99% significance, + denotes greater than 95% significance, − denotes less than 95% significance.

presence of formate with or without the presence of citrate. In the first 5 h approx. 27% of Cr(VI) was reduced when both citrate and formate were present, with 276 μM Cr(VI) remaining after 24 h (Figure 1). Other combinations of acetate, citrate and formate showed Cr(VI) reducing ability in the order formate > acetate ≈ acetate + citrate ≈ acetate + formate > citrate, suggesting that citrate *per se* cannot be used as an electron donor for Cr(VI) reduction by *D. vulgaris* NCIMB 8303, although previous work by Mabbett *et al.* (2002) showed that citrate was required for sustained Cr(VI) reduction by this organism. Although not metabolised, this complexing agent was necessary to chelate the Cr^{3+} product, forestalling inhibition of the enzyme(s) responsible for Cr(VI) conversion (Mabbett *et al.* 2002).

Therefore, in the system containing both formate and citrate, formate is the electron donor, whilst citrate acts as a protective ligand. From Table 1 Cr(VI) reduction by *Microbacterium* sp. occurred at the same initial rate [as confirmed by Student's *t*-test analysis (Table 2)] in all mixtures of citrate, formate, and acetate, except with formate alone, where negligible Cr(VI) reduction occurred. Citrate was not required in this case as a protective ligand (the *Microbacterium* sp. is Cr(VI) resistant: Pattanapipitpaisal *et al.* 2001b) but was used as the electron donor (Table 1). Loss of Cr(VI) by *Microbacterium*, sp. was slow, with an initial rate of Cr(VI) reduction by cells of approx. 3 nmol h^{-1}. mg dry cell wt, and approx. 450 μM of Cr(VI) remaining after 22 h. Longer incubations showed that the slow rate was sustained and the final removal of Cr(VI) after 93 h was approx. 330 μM (Figure 1), with overall reduction greatest when acetate and citrate were both present.

Effect of temperature and pH

The maximum rates of Cr(VI) removal were obtained at 37 °C for *D. vulgaris* and 30 °C for *Microbacterium* sp. (Table 3) but the differences in overall Cr(VI) removal were not significantly different between 30 °C and 37 °C over longer periods (24 h for *D. vulgaris* and 48 h for *Microbacterium* sp.), as confirmed by Student's *t*-test analysis. The effect of solution pH was investigated for pH 4, 5, 6, and 7. The results are illustrated in Figure 2, with the initial rates shown in Table 3. In both systems the efficiency of chromium reduction was greater at neutral than at acidic pH, although a Student's *t*-test showed that the differences in the initial rates for both bacteria were not highly significant. The initial rates of chromium reduction by *D. vulgaris* and *Microbacterium* sp. at pH 7 at 30 °C were 77 and 6 nmol h^{-1} mg dry cell wt, respectively.

Comparison of Cr(VI) reduction by D. vulgaris *and* Microbacterium *sp., and the effect of MOPS buffer*

The reduction of Cr(VI) by *D. vulgaris* NCIMB 8303 and *M. liquefaciens* sp. under identical conditions is illustrated in Figure 3A. In the initial 24 h *D. vulgaris* NCIMB 8303 reduced 186 μM Cr(VI), whilst *Microbacterium* sp. reduced 105 μM. Incorporation of MOPS into the mixtures significantly increased the rate of Cr(VI) reduction to 127 and 17 nmol h^{-1} mg

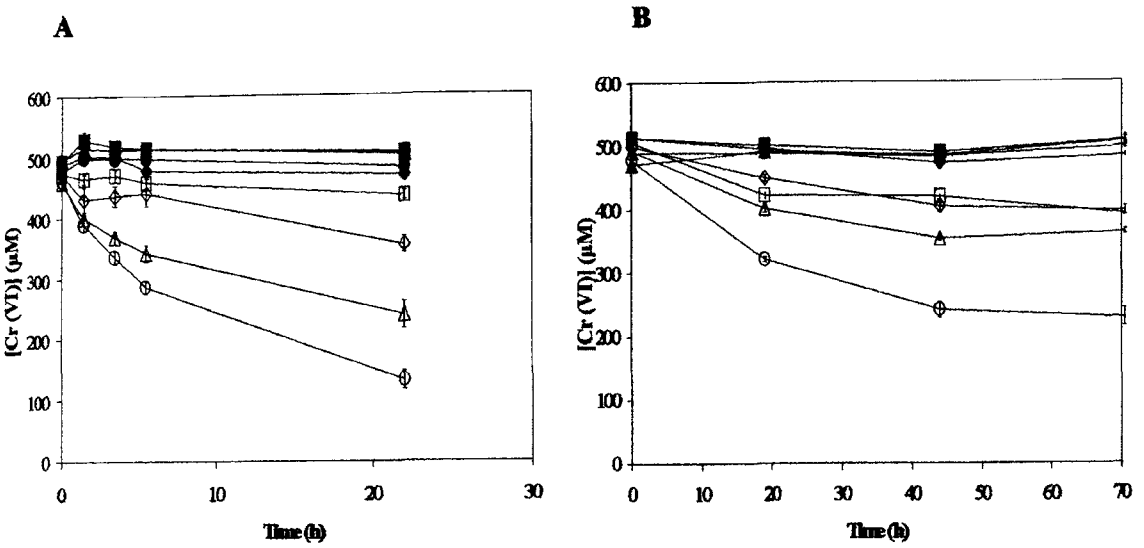


Fig. 2. Reduction of 500 µM Cr(VI) by resting cells of *D. vulgaris* (A) and *Microbacterium* sp. (B) at 30 °C, with 25 mM formate/25 mM citrate at pH: ♦, 4; ■, 5; ▲, 6; ● 7. Filled symbols: control; cells in the absence of electron donor. Open symbols: cells in the presence of electron donor. Error bars (where not shown) were within the dimensions of the symbols.

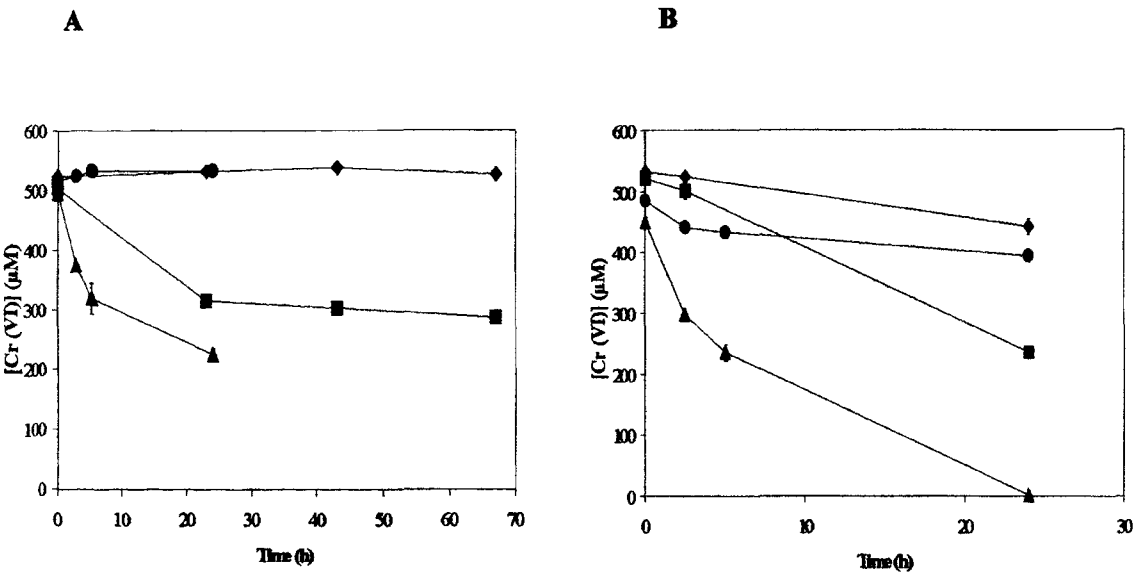


Fig. 3. Comparative reduction of 500 µM Cr(VI) by resting cells of *D. vulgaris* and *Microbacterium* sp. at pH 7 and 30 °C in a common matrix of (A) 25 mM citrate, 25 mM acetate, and 25 mM formate and (B), as (A) but with the incorporation of 20 mM MOP-NaOH. ●: *D. vulgaris* without electron donors; ♦: *Microbacterium* sp. without electron donors. ▲: *D. vulgaris* with electron donors; ■, *Microbacterium* sp. with electron donors. Error bars (where not shown) were within the dimensions of the symbols.

Table 3. Effect of temperature and pH on initial rates of Cr(VI) reduction by *D. vulgaris* NCIMB 8303 and *Microbacterium* sp. NCIMB 13776.

Temperature (°C) or pH	Initial rate of Cr(VI) reduction [nmol h^{-1} mg dry wt]	
	D. vulgaris	*Microbacterium* sp.
20°, pH 7	Not tested	1 ± 0.4
30°, pH 7	77 ± 11	6 ± 0.6
37°, pH 7	94 ± 8	2 ± 0.3
30°, pH 4	56 ± 25	4 ± 0.3
30°, pH 5	12 ± 12	4 ± 0.2
30°, pH 6	79 ± 10	6 ± 0.2

Cells were challenged with 500 μM Cr(VI) and incubated at various temperatures and pH values as described in Materials and methods. Data are means ± SEM from 2 (temperature tests) or 3 (pH tests) experiments. Rates were determined over the 1st h as described in Table 1.

dry cell wt for *D. vulgaris* and *Microbacterium* sp. respectively, and the former removed all of the Cr(VI) within 24 h (Figure 3B). It is interesting to note that MOPS *per se* appeared to promote reduction of Cr(VI). This, and other similar zwitterionic buffers, are commonly used in studies on biological interactions with metals since they complex metals minimally (Good *et al.* 1966), but these studies suggest that the presence of even these buffers should be taken into account.

Conclusions

From the results obtained, the optimum conditions for reduction of Cr(VI) by *D. vulgaris* are pH 7, 30–37 °C, in the presence of 25 mM sodium formate and 25 mM sodium citrate. The optimum system for *Microbacterium* sp. is pH 7, 30 °C, in the presence 25 mM sodium acetate and 25 mM sodium citrate. For comparative studies on Cr(VI) reduction by the two bacteria the suggested reaction solution is 25 mM sodium formate, 25 mM sodium citrate, 25 mM sodium acetate, and 500 μM sodium chromate, at pH 7, and 30 °C. Analysis of Cr(VI) reduction by *D. vulgaris* NCIMB 8303 and *Microbacterium* sp. NCIMB 13776 in the defined optimum solution matrix shows that the former system is significantly more efficient at Cr(VI) removal than the latter. Thus, assuming that provision of chelating agent is not likely to be problematic in industry, the use of SRB as commercial agents for the bioremediation of Cr(VI) is feasible and current studies aim to visualise the Cr(VI) to Cr(III) reduction by MRI to obtain kinetic data from within on-line bioreactors *in situ*. MOPS buffer, although not commercially realistic for industrial use, acts as a useful amplifier for the bioreduction, which should enable better visualisation of the process via MRI.

Acknowledgements

We wish to acknowledge the financial support of the EPSRC (studentship no. 00318650 to A.H.) and the Herchel Smith Endowment for funding to L.E.M., and to thank Dr K.P. Nott and Prof L.D. Hall (Herchel Smith Laboratory for Medicinal Chemistry, University of Cambridge) for the acquisition of preliminary MRI images.

References

Bertini I, Luchinat C (1986) *NMR of Paramagnetic Molecules in Biological Systems* (Physical Bioinorganic Chemistry Series). Benjamin/Cummings.

Bopp LH, Ehrlich HL (1988) Chromate resistance and reduction in *Pseudomonas fluorescens* strain LB300. *Arch. Microbiol.* **155**: 4426–4431.

Good NE, Winget GD, Winter W, Connolly TN, Izawa S, Singh RMM (1966) Hydrogen ion buffers for biological research. *Biochemistry* **5**: 467–474.

Kaim W, Schwederski B (1994) *Bioinorganic Chemistry: Inorganic Elements in the Chemistry of Life*. Chichester: John Wiley and Sons.

Komori K, Wang P, Toda K, Ohyake H (1989) Factors affecting chromate reduction in *Enterobacter cloacae* HO1. *Appl. Microbiol. Biotechnol.* **31**: 567–570.

Lloyd JR, Nolting HF, Sole VA, Bosecker K, Macaskie LE (1998a) Technetium reduction and precipitation by sulfate-reducing bacteria. *Geomicrobiol. J.* **15**: 45–58.

Lloyd JR, Yong P, Macaskie LE (1998b) Enzymatic recovery of elemental palladium by using sulphate reducing bacteria. *Appl. Environ. Microbiol.* **65**: 4607–4609.

Lovley DR, Phillips EJP (1994) Reduction of chromate by *Desulfovibrio vulgaris* and its c_3 cytochrome. *Appl. Environ. Microbiol.* **60**: 726–728.

Lovley DR, Widman PK, Woodward JC, Phillips EJP (1993) Reduction of uranium by cytochrome c_3 of *Desulfovibrio vulgaris*. *Appl. Environ. Microbiol.* **59**: 3572–3576.

Mabbett AN, Lloyd JR, Macaskie LE (2002) The effect of complexing agents on the reduction of Cr(VI) by *Desulfovibrio vulgaris* ATCC 29579. *Biotechnol. Bioeng.*, in press.

Paterson-Beedle M, Nott KP, Macaskie LE, Hall LD (2001) Study of biofilm within a packed-bead reactor by three-dimensional magnetic resonance imaging. *Meth. Enzymol.* **337**: 285–305.

Pattanapipitpaisal P, Brown NL, Macaskie LE (2001a) Chromate reduction by *Microbacterium liquefaciens* immobilised in polyvinyl alcohol. *Biotechnol Lett.* **23**: 61–65.

Pattanapipitpaisal P, Brown NL, Macaskie LE (2001b) Chromate reduction and 16S rRNA identification of bacteria isolated from a Cr(VI)-contaminated sites. *Appl. Microbiol. Biotechnol.* **57**: 257–261.

Postgate, JR (1984) *The Sulphate-Reducing Bacteria*. Cambridge: Cambridge University Press.

Tebo BM, Obraztsova AY (1998) Sulfate-reducing bacterium grows with Cr(VI), U(VI) and Fe(III) as electron acceptors. *FEMS Microbiol. Lett.* **162**: 193–198.

Wang P, Mori T, Komori K, Sasatsu M, Toda K, Ohtake H (1989) Isolation and characterisation of an *Enterobacter cloacae* strain that reduces hexavalent chromium under anaerobic conditions. *Appl. Environ. Microbiol.* **55**: 1665–1669.

Wang Y, Xiao C (1995) Factors affecting hexavalent chromium reduction in pure cultures of bacteria. *Water Res.* **24**: 2467–2474.

SECTION 2.2

"Reduction of Cr(VI) by immobilized cells of *Desulfovibrio vulgaris* NCIMB 8303 and *Microbacterium* sp. NCIMB 13776".

Journal: *Biotechnology and Bioengineering*

Accepted

This paper was produced entirely from work done by A. C. Humphries except for Magnetic Resonance Imaging of continuous-flow packed-bed columns, which was completed by K. P. Nott and L. D. Hall at the Herchel Smith Laboratory for Medicinal Chemistry (University of Cambridge, UK).

Reduction of Cr(VI) by immobilized cells of *Desulfovibrio vulgaris* NCIMB 8303 and *Microbacterium* sp. NCIMB 13776

A. C. Humphries[1], K. P. Nott[2], L. D. Hall[2] and L. E. Macaskie[1]*.

[1] *School of Biosciences, The University of Birmingham, Edgbaston, B15 2TT, UK.*

[2] *Herchel Smith Laboratory for Medicinal Chemistry, University of Cambridge, School of Clinical Medicine, University Forvie Site, Robinson Way, Cambridge, CB2 2PZ, UK.*

**Author for correspondence*

(Fax (44)-121-414-5925, e-mail: L.E.Macaskie@bham.ac.uk)

Keywords: Chromate reduction, *Microbacterium, Desulfovibrio.*

Abstract: Hexavalent chromium, a carcinogen and mutagen, can be reduced to Cr(III) by *Desulfovibrio vulgaris* NCIMB 8303 and *Microbacterium* sp. NCIMB 13776. This study examined Cr(VI) reduction by immobilized cells of the two strains in a common solution matrix using various entrapment matrices. Chitosan and PVA-borate beads did not retain integrity and supported low or no reduction of Cr(VI) by the cells. A commercial preparation (Lentikats®) was stable but also did not support Cr(VI) reduction. *K*-carrageenan beads were stable in batch suspensions but gel integrity was lost after only 5 h in a flow-through system in the presence of 100 μM Cr(VI). The best immobilization matrices were agar and agarose, where the initial rates of reduction of Cr(VI) (from 500 μM solution) for *D. vulgaris* NCIMB 8303 and *Microbacterium* sp. NCIMB 13776 were 127 (agar) and 130 (agarose), and 15 (agar) and 12 (agarose) nmol h^{-1} mg dry cell wt^{-1} respectively. The higher removal of Cr(VI) by *D. vulgaris* was also seen in 14 mL packed-bed flow-through columns, where, at a flow rate of 2.4 mL h^{-1}, the percentage removal of Cr(VI) was approx. 95 % and 60 % for *D. vulgaris* and *Microbacterium* sp., respectively (agar-immobilized cells). The Cr(VI) reducing activities of *D. vulgaris* and *Microbacterium* sp. were lost after 159 and 140 h, respectively. Examination of the beads for structural integrity within the columns *in situ* using magnetic resonance imaging after 24 and 100 h of continuous operation against Cr(VI) (with negligible Cr retained within the columns) showed that agar beads were more stable with time. The most appropriate system for development of a continuous bioprocess is thus the use of *D. vulgaris* NCIMB 8303 immobilized in an agar gel matrix.

Introduction

Environmental pollution by hexavalent chromium (CrO_4^{2-}) in marine and urban sediments and waters originates predominantly from industrial sources, with its widespread use in, for example, leather tanning, electroplating and textile manufacturing (Smith and Gadd 2000). Detoxification of Cr(VI), a mutagen and carcinogen, to less cytotoxic Cr(III) can be achieved chemically or biologically. Chemical reduction is expensive and requires addition of chemicals, whereas biological reduction by Cr(VI) reducing bacteria is potentially economically favourable because the methods involved are relatively cheap and simple (Pattanapipitpaisal *et al.* 2001b). Importantly, the use of toxic reagents is not required and native, non-hazardous micro-organisms can be used (Cervantes *et al.* 2001).

Many Cr(VI) reducing microbial systems have been identified; examples include *Pseudomonas fluorescens* LB300, which reduces Cr(VI) under aerobic and anaerobic conditions (Bopp and Ehrlich 1988). *Agrobacterium radiobacter* EPS-916 which is capable of reducing Cr(VI) aerobically (Llovera *et al.* 1993), and *Enterobacter clocae* strain HO1 which only reduces Cr(VI) under anaerobic conditions using a limited selection of electron donors (Komori *et al.* 1989).

This study focuses on two microorganisms, *Desulfovibrio vulgaris* NCIMB 8303 and *Microbacterium* sp. NCIMB 13776. A member of the obligatory anaerobic sulfate-reducing bacteria (SRB), *D. vulgaris* NCIMB 8303 has a well-established ability to reduce metals (Lovley 1993; Lovley and Phillips 1994; Lloyd *et al.* 1998a; 1998b), including Cr(VI), if a complexing agent is incorporated to chelate Cr(III) (Mabbett *et al.* 2002). The SRB use an organic compound (e.g. formate) or molecular H_2 as the electron donor and SO_4^{2-} as the electron acceptor in dissimilatory sulfate reduction. Certain high valence metal ions, such as Tc(VII) or Cr(VI) can be used as electron sinks in lieu of sulfate resulting in metal reduction (Lloyd *et al.* 2001; Mabbett *et*

al. 2002) although the ability of SRB to grow at the expense of chromate has only been demonstrated in one case (Tebo and Obraztsova 1998).

In contrast to the SRB *Microbacterium* sp. NCIMB 13776 is a newly identified Gram-positive organism, which has been shown to be closely related to *Microbacterium liquefaciens* by 16S rRNA sequence homology (Pattanapipitpaisal *et al.* 2001a). This organism grows facultatively aerobically, but reduces Cr(VI) only anaerobically using acetate or citrate as the electron donor (Humphries and Macaskie 2002), and cannot grow at the expense of Cr(VI) as the sole electron acceptor (Pattanapipitpaisal *et al.* 2001b).

The literature abounds with examples of new organisms which can reduce Cr(VI) (for example see Badar *et al.* 2000; Mabbett and Macaskie 2001; Neal *et al.* 2002; Srinath *et al.* 2002) but such reports are of limited significance if the rate of reduction, and its durability, are not compared under similar conditions to those described using established organisms. As a first step towards a unified system for evaluation, a common reaction matrix was developed (Humphries and Macaskie 2002) that provides optimum conditions for Cr(VI) reduction by the published strain (*D. vulgaris*: Lovley and Phillips 1994; Mabbett *et al.* 2002) and the new strain (in this example *Microbacterium* sp.). This solution contains acetate/formate (electron donors), citrate (additional electron donor and complexing ligand for Cr^{3+}) and MOPS buffer (pH 7). Under these conditions, at a cell concentration of 0.5 mg dry cell wt mL^{-1}, the rates of Cr(VI) reduction by resting free cells of *D. vulgaris* and *Microbacterium* sp. were compared (Humphries and Macaskie 2002) but no information is available regarding the longer-term stability of Cr(VI) reduction in immobilized cell bioreactors or, indeed of the most appropriate type of immobilization matrix, which formed the first objective of this study.

For industrial purposes, Cr(VI) reduction by freely suspended cells is disadvantageous because of difficult biomass/ effluent separation (White *et al.* 1995). These problems can be overcome by the use of immobilized cell packed-bed reactors. However, in practice neither the *D. vulgaris* nor the *Microbacterium* sp. were found to form good biofilm on solid supports (polyurethane foam (TM30:Reticel, Belgium) in preliminary tests, precluding the use of simple biofilm bioreactors; therefore, the second objective of this study was to identify an efficient and durable encapsulation system for Cr(VI) reduction.

A previous study has shown that magnetic resonance imaging (MRI) can be used to "interrogate" an intact bioreactor non-invasively *in situ* (Nott *et al.* 2001; Paterson-Beedle *et al.* 2001). The previous studies used biofilm of a *Citrobacter* sp. immobilized on reticulated foam sponge matrices or ceramic supports, but preliminary tests showed that gel beads (comprising mostly water and therefore difficult to see visually but highly amenable to proton magnetic resonance imaging) could be visualised in 3D using MRI within reactor vessels (A. C. Humphries, K.P.Nott, and L. E. Macaskie, unpublished). In the present studies the product of Cr(VI) reduction is Cr(III) which precipitates only slowly as $Cr(OH)_3$ (see Mabbett *et al.* 2002 for discussion). Precipitate formation would therefore occur distally from the site of reduction in a flow-through column and it is possible that accumulation of $Cr(OH)_3$ would disrupt bead integrity. On the other hand, since gel beads are often crosslinked by multivalent cations (Bickerstaff 1997), formation of nascent Cr^{3+} could reinforce bead integrity. Therefore, the third objective was to examine bead integrity spatially within the bioreactor in 3D before and during reduction of Cr(VI). The Cr(III) ion has a magnetic moment of 3.8 BM (Bertini 1986) and can alter the proton signal; paramagnetic species are widely used as contrast agents in MRI (see Paterson-Beedle *et al.* 2001; Nott *et al.* 2002 for discussion) and preliminary tests illustrated that

1 mM Cr(III) added contrast in visualisation of biofilm matrices, as compared to Cr(VI) (A. C. Humphries, K. P. Nott and L. E. Macaskie, unpublished). This introduces the possibility of using the liberated Cr(III) as a contrast agent *in situ* within the reactors to better visualise the integrity within the beads under load. Such information cannot be gained by withdrawal of the beads and visual examination alone, and MRI offers the opportunity to visualize the bioreactor internally at any point in space or time. Hence, the Cr(VI) reduction system is also a potentially useful tool to illustrate the potential application of MRI methods to process optimisation and intensification.

Materials and Methods

Organisms and growth conditions

Desulfovibrio vulgaris NCIMB 8303 was originally obtained from Prof. D. R. Lovley (University of Massachusetts, Amherst, MA, USA). Cells were maintained routinely in butyl rubber-sealed 100 mL serum bottles in Postgate's medium C (Postgate 1979) under O_2-free N_2 (OFN). For experiments, growing cultures (to OD_{600} 0.8 ± 0.2) were produced by withdrawing anaerobically 10 mL of an actively growing culture and adding it to 100 mL of fresh medium C. *Microbacterium* sp. NCIMB 13776 was as described previously (Pattanapipitpaisal *et al.* 2001a 2001b). Cells were maintained by routine plating on Luria broth-agar. For experiments, an actively growing starter culture was prepared by inoculating 50 mL of L-broth (Sigma) from a single colony on an L-agar plate. After 24 h of aerobic growth (orbital shaker), starter culture (10 mL) was used to inoculate 100 mL of fresh L-broth. Cells were shaken (*Microbacterium* sp.) or incubated statically under OFN (*D. vulgaris*) at 30 °C to the mid-exponential phase (24 h).

Preparation of cell suspensions

For harvesting, cells of each strain were transferred under OFN into 50 mL serum bottles and harvested by centrifugation (3800 g, 20 min, 22 °C) in the bottles, washed and recentrifuged three times with anaerobic (degassed) stock solutions of 20 mM MOPS-NaOH buffer (pH 7 under OFN) to provide stock concentrated suspensions for resting cell experiments. The cells were stored at 4 °C until use (within 24 h of harvesting). The biomass concentration of the cell concentrates was estimated by measuring the OD_{600}, and conversion to dry cell wt via a previously determined calibration.

Immobilization of cells

Chitosan beads (Vorlop and Klein 1987): A 1 % (w/v) viscous chitosan-acetate solution was prepared by mixing 100 mg chitosan (Sigma) with 9.9 mL deionized water and 70 µL glacial acetic acid (80 °C, with stirring). The chitosan-acetate solution was degassed with OFN, with all subsequent manipulations done in a MACS-MG anaerobic workstation (Don Whitley Scientific Ltd). To prepare beads cell concentrate (0.9 mL) was added to 8.2 mL chitosan-acetate solution to give a cell concentration of 1.25 mg dry cell wt mL^{-1}. Cell suspension was dropped from a 2.5 mL syringe fitted with a 21G needle into 50 mL of 2 % (w/v; aq.) polyphosphate (Sigma) solution (pH 8.2). After 4 h beads were collected with a nylon net and washed thoroughly with degassed deionized water.

Polyvinyl alcohol (PVA)-borate beads (Pattanapipitpaisal *et al.* 2001b): Polyvinyl alcohol (250 mg, Fluka) and medium viscosity sodium alginate (80 mg, Sigma) were mixed in 9 mL of deionized water, degassed with OFN and heated to 60 °C to dissolve the PVA. The solution was cooled to 35 °C and mixed with 1.0 mL cell concentrate (to cell concentration of 1.25 mg dry cell

wt mL^{-1}). Gel beads were made in the MACS-MG work station by extruding the cell suspension as drops from a 2.5 mL syringe fitted with a 21G needle into 50 mL degassed saturated boric acid (Sigma) solution containing 2 % (w/v) calcium chloride, and immersion for 24 h. Beads were washed thoroughly with degassed deionized water prior to use.

Agar, agarose, and k-carrageenan beads (Lopez *et al.* 1997): 200 mg agar, agarose (Sigma, type VII, low gelling temperature) or *k*-carrageenan were mixed with 9 mL deionized water, degassed with OFN, and autoclaved (121 °C, 20 min). The gel was allowed to cool to 40 °C before 1 mL cell concentrate was added to a cell concentration of 1.25 mg dry cell wt mL^{-1}. Gel bead formation was carried out in the MACS-MG workstation. The aqueous phase (degassed deionized water for agar and agarose cell beads, and 0.3 M KCl for *k*-carrageenan beads) and the oily phase (degassed olive oil) were placed in a 500 mL vessel in a ratio of 10:1 (v/v), respectively. The gel-cell mixture was extruded into the oily phase using a 2.5 mL syringe fitted with a 21G needle. The gel-cell beads passed into the aqueous phase and were collected using a nylon net. Beads were washed once with degassed Triton-X100 (Sigma) (0.01 % (v/v)) and three times with degassed deionized water or 0.3 M KCl as appropriate. Preliminary tests showed that the wash step did not affect bead integrity or function.

Lentikats®: Lentikat gel (geniaLab Biotechnologie, Braunschweig, Germany) was melted and 9 mL was withdrawn and transferred to a 12 mL serum bottle, degassed with OFN, and then transferred to the anaerobic work station. After cooling to 40 °C 1 mL cell concentrate was added to a final concentration of 1.25 mg dry cell wt mL^{-1}. After mixing, the Lentikat®-cell mixture was extruded as droplets onto pre-weighed petri dishes using a 2.5 mL syringe fitted with a 21G needle. Each plate was re-weighed, and left to dry at 30 °C in the anaerobic workstation until the

weight of each plate had reduced by 72 %. Once gelation was complete, 200 mL degassed Lentikat® stabiliser (geniaLab Biotechnologie: 3 g stabiliser powder 200 mL^{-1} deionized water) was poured over the Lentikat® immobilized cells and left for 30 min, allowing the Lentikats® to re-swell and come away from the petri dish. Lentikats®/ cells were transferred to a 500 mL vessel and stirred in Lentikat® stabiliser (geniaLab Biotechnologie) for 2 h (manufacturer's instructions) for maximum mechanical stability to be achieved. Lentikat® immobilized cells were washed thoroughly with degassed deionized water prior to use according to the manufacturer's protocol (Anon, 2001).

Chromate reducing activity of immobilized cell beads in batch suspensions

For batch reduction tests, the reaction mixtures were set up in the anaerobic work station (30 °C) in 12 mL serum bottles, sealed with butyl rubber stoppers. Cell beads (2 mL: equivalent to 2.5 mg dry cell wt) or free cells (equivalent to 2.5 mg dry cell wt) were suspended in 5 mL of a degassed solution comprising sodium acetate, sodium citrate and sodium formate (all at 25 mM) 20 mM MOPS-NaOH buffer and 500 μM sodium chromate (to pH 7), previously developed as optimal for both strains (Humphries and Macaskie 2002). Controls for all experiments comprised cell beads without electron donor, and reaction solutions without cells (cell free beads). Samples were withdrawn periodically, via syringe, and supernatants (100 μL) were analysed for residual Cr(VI) using diphenylcarbazide (specific for Cr(VI)) as described by Pattanapipitpaisal *et al.* (2001a; 2001b).

Chromate reducing activity of immobilized cell beads in continuous-flow reactors

Continuous Cr(VI) reduction tests used 14 mL flow-through packed bed reactors (water-jacketed glass columns; length 10 cm; i.d. 1.5 cm) containing 9 mL of agar, agarose, or *k*-carrageenan

immobilized cell beads (2.5 mg dry cell wt mL^{-1}). Sodium chromate solution (100 μM sodium chromate in sodium acetate, sodium citrate, sodium formate, MOPS-NaOH buffer, pH 7 as above) was fed continuously at a flow rate of 2.4 mL h^{-1} from the bottom of the column (30 °C). Samples of inflow and outflow solution were analysed for Cr(VI) using diphenylcarbazide as above.

Where mass balances of Cr were to be calculated, Cr(VI) in column input and outflow solutions was analysed using diphenyl carbazide as above, and parallel samples were analysed for total Cr using ICP-MS (H_2b Analytical Services Ltd, Capenhurst, UK). Cr(III) retained in the columns was estimated as the difference between total Cr in inlet and outlet solutions.

Examination of gel beads in bioreactors non-invasively using magnetic resonance imaging

Magnetic resonance imaging was done as described previously (Nott *et al.* 2001; Paterson-Beedle *et al.* 2001). Columns were withdrawn from the flow, the ends were sealed and the columns were introduced into a 2.35 Tesla super-conducting magnet (Oxford Instruments, Oxford, UK) connected to a Bruker Medzintechnik Biospec II imaging console (Karlsruhe, Germany). The 9.4 cm internal diameter 'bird cage' radio-frequency (RF) probe used to transmit and receive signal, and the 14.5 cm internal diameter gradient set used for spatial discrimination were both built 'in house'. ^{1}H images were acquired using a Spoiled GRASS (Hashemi 1997) sequence (repetition time (TR)/ echo time (TE)/ flip angle (θ) 50 ms/7.5 ms/30 °) with 400 μm isometric pixel resolution; total scan time was 13 min and 39 sec.

Results and Discussion

Preliminary evaluation of support matrices

Immobilized cells of both types of organism were reacted with Cr(VI) solution over 24 h. Observation of bead integrity and results of Cr(VI) removal tests are detailed in Table 1. With chitosan the immersion step in polyphosphate caused the beads to shrink to approximately half their original size (originally approx. 3 mm diameter), and coalesce. No Cr(VI) reduction occurred with either strain in the chitosan matrix and this was omitted from the remainder of the study.

The PVA borate beads were unstable, dissolving after 24 h, although the beads reduced some Cr(VI) (see Table 1). The instability was probably attributable to complex formation between the perfusing citrate (required to complex the Cr^{3+} product as it is formed : Mabbett *et al.* 2001) and the calcium ions cross-linking the gel matrix (Bickerstaff 1997). This infers that Cr^{3+} was not able to substitute for Ca^{2+} as a crosslinking ion although this was not specifically tested; it is likely that Cr^{3+} was unavailable due to its retention in the citrate complex (formation constants for Cr(III)-citrate complexes are given in Mabbett *et al.* 2002). Formation constants are usually determined in non-physiological matrices. Chelation of Cr^{3+} into the citrate complex would tend to suppress formation of $Cr(OH)_3$ but other studies have shown that at pH 7 hydroxylation behaviour eventually predominates and Cr(III) is precipitated from solution over time (Mabbett *et al.* 2002; Mabbett 2003). The use of PVA-borate beads was not considered further.

Cr(VI) reduction by cells immobilized in stable matrices

Although the commercial 'Lentikats®' immobilization matrix was stable (Table 1) Lentikats®-*D. vulgaris* cells did not reduce Cr(VI) significantly (Table 2). The initial rates and residual Cr(VI) concentrations after 22 h were similar with and without electron donor (Table 2), and also

for cell-free Lentikats® (not shown), suggesting that this immobilization technique results in loss of Cr(VI) reducing ability, possibly attributable to the treatment with Lentikat® stabiliser; the composition of this proprietary solution is not available from the manufacturer. *Microbacterium* sp. appeared to reduce Cr(VI) in the Lentikats® matrix, but the activity, although significant, was less than that obtained in any of the other matrices.

D. vulgaris cells immobilized in agar, agarose and *k*-carrageenan in the presence of electron donors reduced Cr(VI) at approx. equal initial rates (approx. 130 nmol h^{-1} mg dry cell wt^{-1}; Table 2), with approx. 53, 63, and 36 μM Cr(VI) remaining in each after 22 h (Fig. 1). The rates were comparable to those seen with free cells (Table 2), suggesting that there is little diffusional constraint to access of formate, the electron donor for *D. vulgaris*. However, in each matrix electron donor-free controls showed significant Cr(VI) removal (not seen in free cells), possibly attributable to retention of Cr(VI) in the gel matrix. Students *t*-test analysis (Table 3) shows that the initial rates of Cr(VI) reduction by immobilized *D. vulgaris* cells with electron donors were significantly different from those obtained for cell beads without electron donors, and for cell-free beads (except in the case of carrageenan cell beads incubated in the presence and absence of electron donors). A similar comparison of the concentration of Cr(VI) remaining after 24 h, for free cells with those for agar, agarose, and *k*-carrageenan immobilized cells (with electron donors), showed no significant differences, suggesting that mass transfer was not rate limiting within these gels.

Cr(VI) reduction by *Microbacterium* sp. occurred at a significantly lower rate compared to *D. vulgaris*. Initial rates of reduction are summarised in Table 2. The highest rate occurred when

cells were immobilized in agar in the presence of electron donors (approx. 15 nmol h^{-1} mg dry cell wt^{-1}) and with 261 μM Cr(VI) remaining after 65.5 h (Fig. 1).

Chromate reduction by free cells of *Microbacterium* sp. with electron donors occurred at an initial rate of 22 nmol h^{-1} mg dry cell wt^{-1} (Table 2) with 93 μM Cr(VI) remaining after 65.5 h (Fig. 1), significantly greater than results obtained for immobilized cells. However, results obtained for Cr(VI) reduction by *D. vulgaris* cells immobilized in agar and agarose suggested mass transfer limitations did not occur in these gels (above). Indeed, taking the ratio between activity with and without electron donors for each organism gave a similar result for each organism for a given immobilization matrix, suggesting that formate (electron donor for *D. vulgaris*) and acetate (electron donor for *Microbacterium* sp.) perfused equally well. In the case of *k*-carrageenan beads the ratio of activity with and without electron donor was 1.3-fold and zero for the two organisms, suggesting that the matrix itself reduced Cr(VI).

Inspection of Fig. 1 shows that in each immobilization matrix the *Microbacterium* sp. only removed approx. 50 % of the Cr(VI) at 24 h, whereas *D. vulgaris* removed nearly all the Cr(VI) after 24 h. In this respect the performance of the immobilized and free cells was similar. The limitation to *Microbacterium* sp. was attributed to immobilization-specific factors, since free cells removed 80 % of the Cr(VI) after 65 h, comparably to that seen with *D. vulgaris* after 24 h (Fig. 1) and showing that the overall removal rate was ca. 3-fold lower.

The above suggests that *D. vulgaris* has the greater potential for bioprocess-removal of Cr(VI), having both the greatest activity overall and also the best retention of activity in the immobilized cell systems. It is possible that the *Microbacterium* system is differentially inhibited by the accumulation of Cr(III)-citrate within the beads. Therefore longer-term tests utilized a flow-

through system to check the activity of the cells, and also the matrix stability, under more prolonged load.

Chromate reducing activity of immobilized cell beads in continuous-flow reactors

D. vulgaris and *Microbacterium* sp. were immobilized in agar, agarose, and *k*-carrageenan for study of chromate reduction in continuous-flow packed-bed reactors. After an operating time of 5 h the *k*-carrageenan cell beads dissolved (c.f. the beads were stable in a batch system: see above). Therefore the *k*-carrageenan method was discarded at this stage; further tests used agar and agarose only.

The results of the continuous flow tests are shown in Fig. 2. It was observed that the initial extent of Cr(VI) removal was approx. 95 % and 60 % for agar-immobilized *D. vulgaris* (a) and *Microbacterium* sp. (b), respectively. Columns containing agarose-immobilized *Microbacterium* sp. (b) lost activity and at 40 h reduction was negligible. Columns containing agar-immobilized *Microbacterium* sp. began to lose activity after 65 h, with activity ceasing after 140 h. For agar-immobilized *D. vulgaris*, reduction occurred initially at approx. 95 %, lowering to 60 % by 24 h with complete loss of reduction after 159 h. Cr(VI) reduction by agar-immobilized *D. vulgaris* and *Microbacterium* was similar after the initial 24 h but with both strains it was observed that reducing ability was lower after 30 h when bacteria were immobilized in agarose, possibly attributable to cell wash-out as a result of loss of matrix stability and bead integrity (i.e. bead material was washed out of the reactor: see later).

Stability of the immobilization matrices under prolonged use

The above shows that the method of choice for a Cr(VI) bioremediation process would use *D. vulgaris,* with the most suitable immobilization matrices being agar and agarose. The matrices were examined *in situ* using MRI (using *D. vulgaris* immobilized cell columns) to establish their

respective structural integrities. The images show (Fig. 3) that the beads were clearly visible initially (Fig 3a,b) but by 24 h the integrity of agarose cell beads had diminished, whilst the structure of agar cell beads was largely unchanged (Fig. 3c,d) and their integrity was still maintained after 100 h (not shown). The loss of activity observed using the agarose-bead columns was therefore probably attributable to biomass loss over time and, indeed, the perfusate clearly showed material in the interstices, and fragmented beads (Fig. 3c; c.f. 3b). Bead fragmentation was not attributable to the accumulation of $Cr(OH)_3$ (below).

Fate of the chromium species in the reactor

For long-term assessment of remediation potential and reactor stability it is necessary to establish whether the liberated Cr(III) is eluted as the soluble citrate complex or whether the Cr(III) dissociates from the complex and precipitates as $Cr(OH)_3$ within the column. Analysis of the column outflows using ICP-MS (total Cr) showed that the concentrations of Cr_{total} in the exit solutions were 100 μM , i.e. minimal chromium was retained within the columns.

Conclusions

The immobilization matrices that gave the highest Cr(VI) reducing efficiency in batch suspensions containing *D. vulgaris* and *Microbacterium* sp. were agar and agarose, with reduction occurring at an initial rate of 130 and 15 nmol h^{-1} mg dry cell wt^{-1}, respectively (both matrices). Immobilization of cells did not appear to affect Cr(VI) reducing ability (as compared to free cells) suggesting low mass transfer limitations. In a continuous-flow system, Cr(VI) reduction initially occurs significantly more efficiently in *D. vulgaris* agar-immobilized cell columns but by 24 h similar results were obtained with each organism and by 159 h Cr(VI)

reduction had ceased in all columns. Continuous-flow studies showed that agarose is a poor immobilization matrix for application to Cr(VI) reduction.

In conclusion, although Cr(VI) reduction by agar immobilized cells of *D. vulgaris* and *Microbacterium* sp. in continuous mode occurred at approx. 60 % conversion, the longevity of the columns is relatively short; this is attributable to biochemical constraints since the agar beads retain excellent integrity and would be the immobilization matrix of choice for future studies on biosystem stability.

Acknowledgements

We wish to acknowledge the financial support of the EPSRC (studentship no. 00318650 to A. C. H) and the Herchel Smith Endowment for funding to L. E. M., K. P. N., and L. D. H.

References

Badar U, Ahmed N, Beswick AJ, Pattanapipitpaisal P, Macaskie LE. 2000. Reduction of chromate by microorganisms isolated from metal contaminated sites of Karachi, Pakistan. Biotechnol Lett. 22:829-836.

Bertini I, Luchinat C. 1986. NMR of paramagnetic molecules in biological systems. Menlo Park, CA: Benjamin/ Cummings.

Bickerstaff G, 1997. Immobilization of enzyme and cells: some practical considerations. In: Bickerstaff G, editor. Immobilization of enzymes and cells. First ed: Humana Press Inc. p 1 -12.

Bopp LH, Ehrlich HL. 1988. Chromate resistance and reduction in *Pseudomonas fluorescens* strain LB300. Arch Microbiol. 150:426-431.

Cervantes C, Campos-Garcia J, Devars S, Gutierrez-Corona F, Loza-Tavera H, Torres-Guzman JC, Moreno-Sanchez R. 2001. Interactions of chromium with microorganisms and plants. FEMS Microbiol Rev. 25:335-347.

Hashemi RH, Bradley, WG. 1997. MRI: The basics. Baltimore: Williams and Wilkins.

Humphries AC, Macaskie LE. 2002. Reduction of Cr(VI) by *Desulfovibrio vulgaris* and *Microbacterium sp.* Biotechnol Lett. 24:1261-1267.

Komori K, Wang PC, Toda K, Ohtake H. 1989. Factors affecting chromate reduction in *Enterobacter cloacae* Strain HO1. Appl Microbiol Biotechnol. 31:567-570.

Llovera S, Bonet R, Simonpujol MD, Congregado F. 1993. Chromate reduction by resting cells of *Agrobacterium radiobacter* EPS-916. Appl Environ Microbiol. 59:3516-3518.

Lloyd JR, Mabbett AN, Williams DR, Macaskie LE. 2001. Metal reduction by sulphate-reducing bacteria: physiological diversity and metal specificity. Hydrometallurgy. 59:327-337.

Lloyd JR, Nolting HF, Sole VA, Bosecker K. 1998a. Technetium reduction and precipitation by sulfate-reducing bacteria. Geomicrobiol J. 15:45-58.

Lloyd JR, Yong P, Macaskie LE. 1998b. Enzymatic recovery of elemental palladium by using sulfate- reducing bacteria. Appl Environ Microbiol. 64:4607-4609.

Lopez A, Lazaro N, Marques AM. 1997. The interphase technique: a simple method of cell immobilization in gel-beads. J Microbiol Meth. 30:231-234.

Lovley DR. 1993. Dissimilatory metal reduction. Ann Rev Microbiol 47:263-290.

Lovley DR, Phillips EJP. 1994. Reduction of chromate by *Desulfovibrio vulgaris* and its c_3 cytochrome. Appl Environ Microbiol. 60:726-728.

Mabbett AN, Lloyd JR, Macaskie LE. 2002. Effect of complexing agents on reduction of Cr(VI) by *Desulfovibrio vulgaris* ATCC 29579. Biotechnol Bioeng. 79:389-397.

Mabbett AN, Macaskie LE. 2001. A novel isolate of *Desulfovibrio* sp with enhanced ability to reduce Cr(VI). Biotechnol Lett. 23:683-687.

Mabbett AN, Yong, P., Farr. JPG., Macaskie, LE. 2004. Reduction of Cr(VI) by palladized biomass of *Desulfovibrio desulfuricans* ATCC 29577. Biotechnol Bioeng. In press.

Neal AL, Lowe K, Daulton TL, Jones-Meehan J, Little BJ. 2002. Oxidation state of chromium associated with cell surfaces of *Shewanella oneidensis* during chromate reduction. Appl Surf Sci. 202:150-159.

Nott KP, Paterson-Beedle M, Macaskie LE, Hall LD. 2001. Visualisation of metal deposition in biofilm reactors by three- dimensional magnetic resonance imaging (MRI). Biotechnol Lett. 23:1749-1757.

Paterson-Beedle M, Nott KP, Macaskie LE, Hall LD. 2001. Study of biofilm within a packed-bed reactor by three- dimensional magnetic resonance imaging. In: J. DR, editor. Methods in enzymology: microbial growth in biofilms, Pt B. San Diego; London. p 285-305.

Pattanapipitpaisal P, Brown NL, Macaskie LE. 2001a. Chromate reduction and 16S rRNA identification of bacteria isolated from a Cr(VI)-contaminated site. Appl Microbiol Biotechnol. 57:257-261.

Pattanapipitpaisal P, Brown NL, Macaskie LE. 2001b. Chromate reduction by *Microbacterium liquefaciens* immobilized in polyvinyl alcohol. Biotechnol Lett. 23:61-65.

Postgate JR. 1979. The sulphate-reducing bacteria. Cambridge: Cambridge Univerisity Press.

Smith WL, Gadd GM. 2000. Reduction and precipitation of chromate by mixed culture sulphate-reducing bacterial biofilms. J Appl Microbiol. 88:983-991.

Srinath T, Verma T, Ramteke PW, Garg SK. 2002. Chromium (VI) biosorption and bioaccumulation by chromate resistant bacteria. Chemosphere. 48:427-435.

Tebo BM, Obraztsova AY. 1998. Sulfate-reducing bacterium grows with Cr(VI), U(VI), Mn(IV), and Fe(III) as electron acceptors. FEMS Microbiol Lett. 162:193-198.

Vorlop KD, Klein J. 1987. Entrapment of microbial-cells in chitosan. Meth Enzymol. 135:259-268.

White C, Wilkinson SC, Gadd GM. 1995. The role of microorganisms in biosorption of toxic metals and radionuclides. Int Biodeterior Biodegrad. 35:17-40.

Table 1. First stage evaluation of different support matrices using beads in batch suspensions

Immobilization matrix	Bead integrity	Cr(VI) reduction by cell beads (22 h)
Chitosan	Beads shrank after the polyP step, and coalesced	No
PVA-borate	Beads dissolved after 24 h	Yes*
Lentikats®	Retained	No (Table 2)
k-Carrageenan	Retained	Yes (Table 2)
Agar	Retained	Yes (Table 2)
Agarose	Retained	Yes (Table 2)

Beads were prepared as described in Materials and Methods and challenged in the common solution matrix (500 μM Cr(VI)) as described. *Initial rate was 60 ± 8 and 6 ± 2 nmol h^{-1} mg cell dry wt^{-1} for *D. vulgaris* and *Microbacterium* sp., respectively. PVA-borate beads alone, or cell beads in the absence of electron donor, did not reduce Cr(VI) (Pattanapipitpaisal *et al.*, 2001a).

Table 2. Effect of immobilization of *D. vulgaris* NCIMB 8303 and *Microbacterium* sp. NCIMB 13776 on initial rates of Cr(VI) reduction in batch mode.

	Initial rate* of Cr(VI) reduction** [nmol Cr(VI) remove h^{-1} mg dry cell wt^{-1}]	
	D. vulgaris	*Microbacterium* sp.
Agar cell beads + e^- donors	127 ± 9.5	15 ± 1.2
Agar cell beads - e^- donors	68 ± 3.5	7 ± 2.3
Agarose cell beads + e^- donors	130 ± 9.3	12 ± 1.0
Agarose cell beads – e^- donors	66 ± 7.1	7 ± 1.4
Lentikats® cell particles + e^- donors	52 ± 5.9	6 ± 1.2
Lentikats® cell particles – e^- donors	46 ± 5.0	1 ± 0.9
k-carrageenan cell beads + e^- donors	131 ± 8.1	9 ± 0.9
k-carrageenan cell beads – e^- donors	103 ± 13.4	9 ± 1.2
Free cells + e^- donors	133 ± 26.7	22 ± 2.2
Free cells – e^- donors	Negligible	6± 1.6

Immobilized cells (in various matrices as described in Materials and Methods) were challenged with 500 μM Cr(VI) in the common solution matrix. The electron donors for *D. vulgaris* and *Microbacterium* sp. were formate and acetate, respectively (Humphries and Macaskie 2002). Data are means ± SEM from 3 independent experiments.

*Initial rates were determined over the first 1 h (*D. vulgaris)* or first 22 h (*Microbacterium*) from linear regions of appropriate graphs (see Fig. 1).

**For these tests it was assumed that Cr(VI) removed from solution was attributable to reduction of Cr(VI) to Cr(III); full mass balances were not done in these tests but later studies showed recovery of 100 % of the Cr (Cr(VI) plus Cr(III)) from the spent solution (see text).

Table 3. Significance of immobilization matrix on initial rates of Cr(VI) reduction by *D. vulgaris* (a) and *Microbacterium* sp. (b)

(a)	Agar beads + cells – e^- donor	Cell-free agar beads
Agar/cells + e^- donor	++	++
Agar/ cells – e^- donor		++

	agarose beads + cells – e^- donor	Cell-free agarose beads
agarose/cells + e^- donor	++	++
agarose/ cells – e^- donor		-

	Lentikats® beads + cells – e^- donor	Cell-free Lentikats® beads
Lentikats®/cells + e^- donor	-	-
Lentikats®/ cells – e^- donor		+

	carrageenan beads + cells – e^- donor	Cell-free carrageenan beads
carrageenan/cells + e^- donor	-	++
carrageenan/ cells – e^- donor		++

	cells – e^- donor	no cells
cells + e^- donor	++	++
cells – e^- donor		-

(b	agar beads + cells – e^- donor	Cell-free agar beads
Agar/cells + e^- donor	+	+
agar/ cells – e^- donor		-

	agarose beads + cells – e^- donor	Cell-free agarose beads
agarose/cells + e^- donor	+	+
agarose/ cells – e^- donor		-

	Lentikats® beads + cells – e^- donor	Cell-free Lentikats® beads
Lentikats®/cells + e^- donor	++	++
Lentikats®/ cells – e^- donor		-

	carrageenan beads + cells – e^- donor	Cell-free carrageenan beads
carrageenan/cells + e^- donor	-	+
carrageenan/ cells – e^- donor		++

	cells – e^- donor	no cells
cells + e^- donor	++	+
cells – e^- donor		-

Significant differences in rate over the 1st h (a) or 1ST 22 h (b) were calculated using students *t*-test: ++ denotes 99.99 % significance, + denotes greater than 95 % significance, - denotes less than 95 % significance.

Legends to Figures

Fig. 1. Reduction of 500 μM Cr(VI) by resting cells of *D. vulgaris* NCIMB 8303 (left panels) and *Microbacterium* sp. NCIMB 13776 (right panels) immobilized in agar (a,b), agarose (c,d), Lentikats® (e,f) and *k*-carrageenan (g,h), and free cells in suspension (i,j), with the same weight of biomass present throughout (see Materials and Methods). ■: Control; gel beads (or solution alone), in the presence of electron donor. ▲; Control: immobilized/ free cells without electron donor. ●: Immobilized/ free cells in the presence of electron donor. Data are means ± SEM from 3 independent experiments. Where no error bars are shown these were within the dimensions of the symbols.

Fig. 2. Continuous removal of Cr(VI) by cells of *D. vulgaris* (a) and *Microbacterium* sp. (b) immobilized in agar (●) or agarose (▲) beads in the presence (filled symbols) or absence (open symbols) of electron donors using the common solution matrix. Columns were set up as described in Materials and Methods and the flow rate was constant at 2.4 mL h^{-1}. The input concentration of Cr(VI) was 100 μM. The total Cr concentration in the exit solution was 100 μM throughout (see text). At the points arrowed (initially, and after 24 and 100 h) the columns were examined non-invasively using MRI using duplicate sets. Data are means ± SEM from 3 independent experiments. Where no error bars are shown these were within the dimensions of the symbols.

Fig. 3. Proton magnetic resonance imaging of the columns shown in Fig. 2. Agar cell-bead column at the outset (a) and after 24 h of continuous-flow (c). Agarose cell-bead column at the outset (b) and after 24 h of continuous-flow (d).

Fig. 1. *D. vulgaris* *Microbacterium* sp.

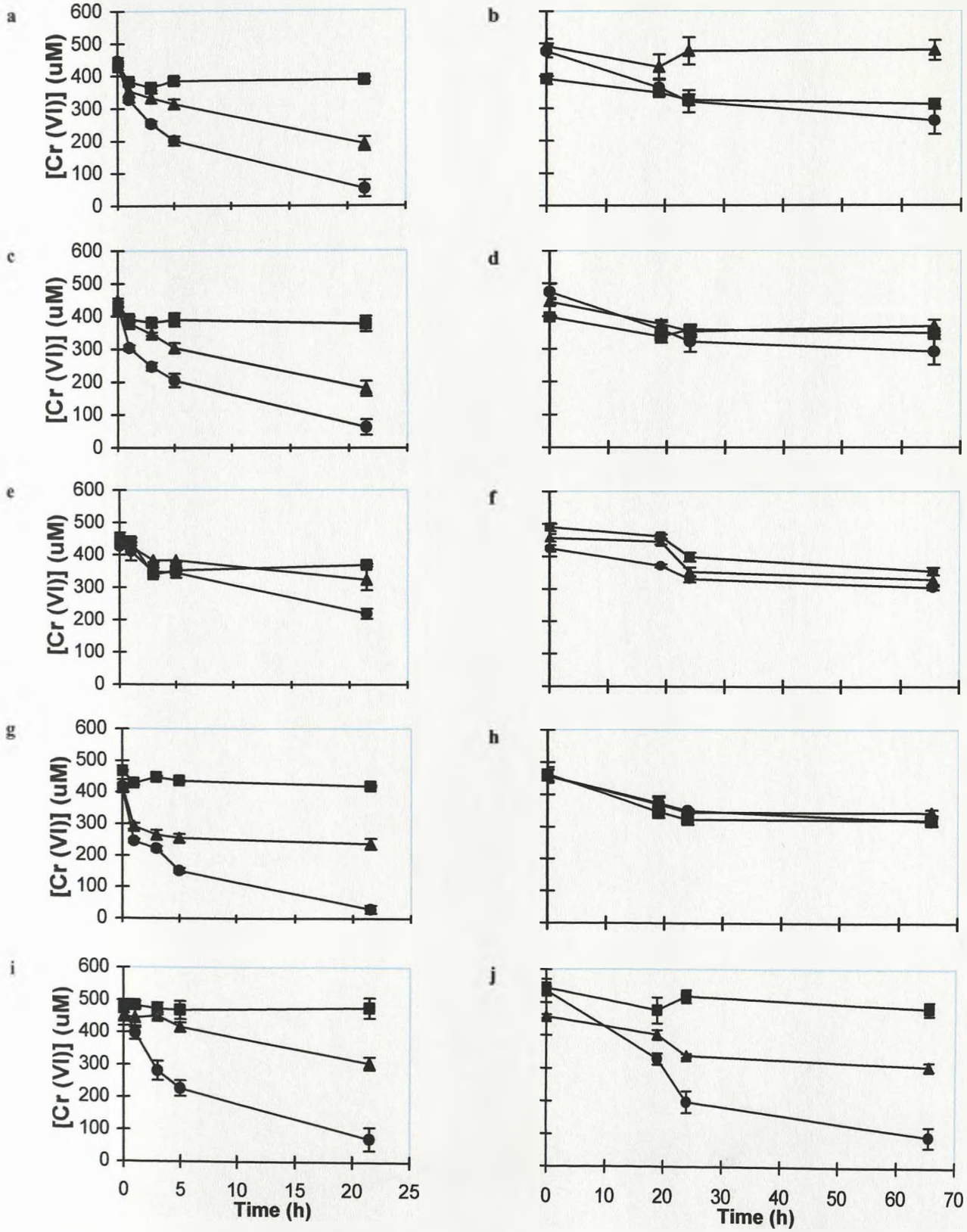


Fig. 2.

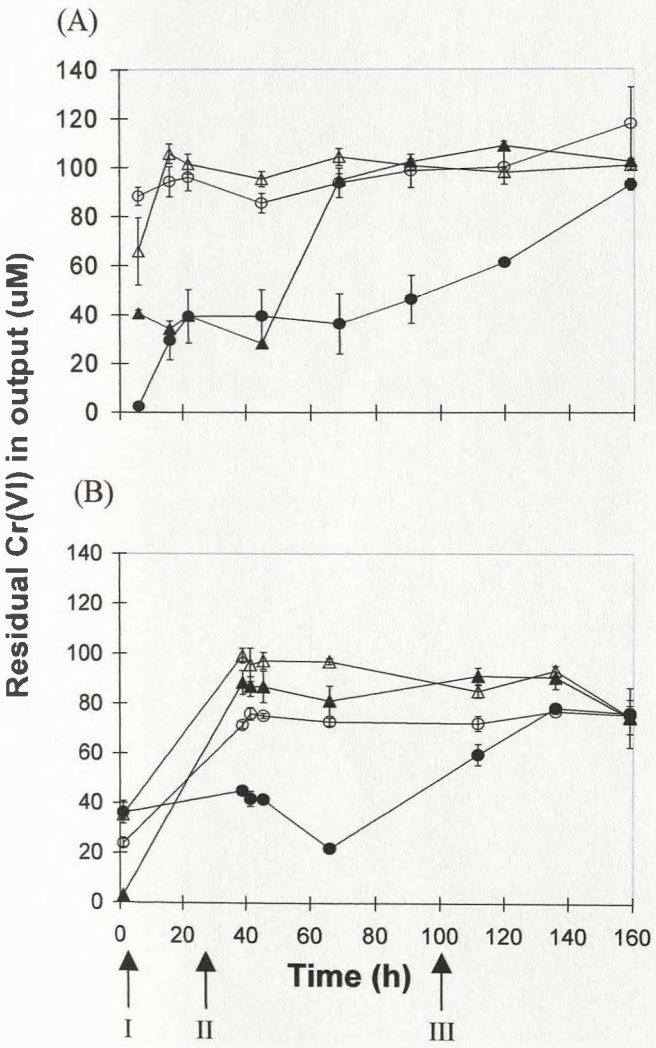
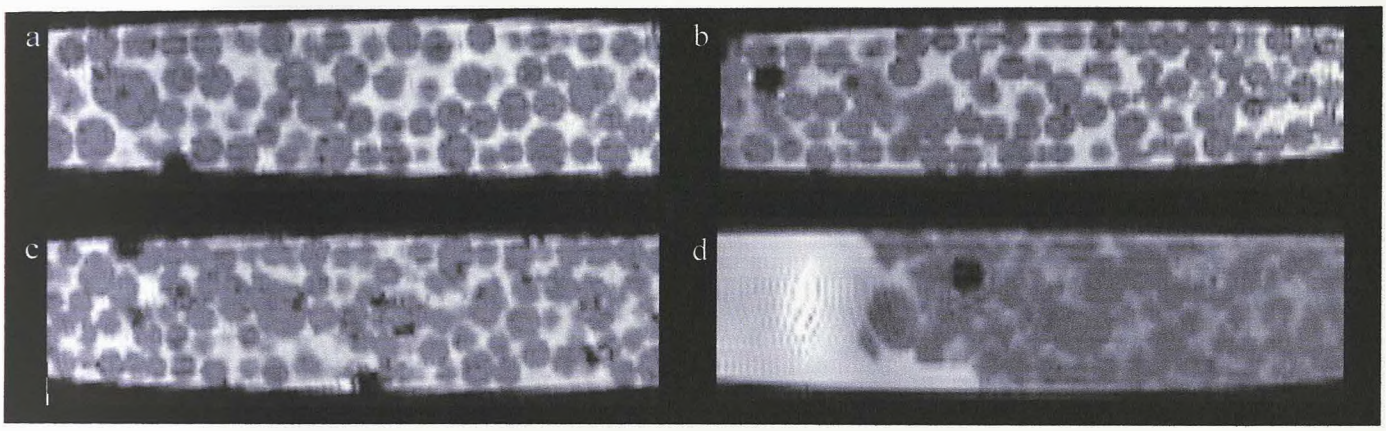

(A)
140
120
100
80
60
40
20
0
(B)
140
120
100
80
60
40
20
0
0
20
40
60
80
100
120
140
160
Time (h)
Residual Cr(VI) in output (uM)
I
II
III

Fig. 3.



SECTION 3

RESULTS:

Chromate reduction by palladised biomass

SECTION 3.1

"Continuous removal of Cr(VI) from aqueous solution catalysed by palladised biomass of *Desulfovibrio vulgaris* NCIMB 8303".

Journal: ***Biotechnology Letters***

26: 1529 – 1532 (2004)

This paper was produced entirely from work done by A. C. Humphries except for Magnetic Resonance Imaging of Bio-Pd(0) immobilized in agar and chitosan beads, which was completed by K. P. Nott and L. D. Hall at the Herchel Smith Laboratory for Medicinal Chemistry (University of Cambridge, UK).

Continuous removal of Cr(VI) from aqueous solution catalysed by palladised biomass of *Desulfovibrio vulgaris* NCIMB 8303

A. C. Humphries[1], K. P. Nott[2], L. D. Hall[2] and L. E. Macaskie[1*]

[1] *School of Biosciences, The University of Birmingham, Edgbaston, B15 2TT, UK*

[2] *Herchel Smith Laboratory for Medicinal Chemistry, University of Cambridge School of Clinical Medicine, University Forvie Site, Robinson Way, Cambridge, CB2 2PZ, UK*

**Author for correspondence*

(Fax (44)-121-414-6557, e-mail: L.E.Macaskie@bham.ac.uk

Keywords: Chromate reduction, bioinorganic catalyst, immobilization

Abstract: Growth decoupled cells of *Desulfovibrio vulgaris* NCIMB 8303 can be used to reduce Pd(II) to cell bound Pd(0) (Bio-Pd(0)), a bioinorganic catalyst capable of reducing hexavalent chromium to less toxic Cr(III), using formate as the electron donor. Magnetic resonance imaging showed that Bio-Pd(0), immobilized in chitosan and agar beads, is distinguishable from the surrounding gel and is evenly dispersed within the immobilization matrix. Agar-immobilized Bio-Pd(0) and "Chemical-Pd(0)" were packed into continuous-flow reactors, and challenged with a solution containing 100 μM Cr(VI) (pH 7) at a flow rate of 2.4 mL h^{-1}. Agar-immobilized Chemical-Pd(0) columns lost Cr(VI) reducing ability by 160 h, whereas columns containing immobilized Bio-Pd(0) maintained 90 % reduction until 680 h, after which reduction efficiency was gradually lost.

Introduction

Environmental pollution by hexavalent chromium, Cr(VI), in marine and urban sediments is due predominantly to industrial waste-water discharge. Cr(VI)-bearing water can be treated chemically (expensive) or biologically using resting cells of *Desulfovibrio vulgaris* NCIMB 8303 (Humphries and Macaskie 2002). For industrial applications continuous processes are generally more desirable because they are considered more efficient and cost effective (Thomas and Laval 1996).

The potential to use immobilized resting cells of *D. vulgaris* for continuous Cr(VI) reduction in packed-bed reactors was investigated. Conversion of Cr(VI) occurred at 60 % efficiency, but this was short lived, with conversion ceasing after 160 h (A. C. Humphries and L.E. Macaskie, unpublished). For industrial purposes reactors are engineered to operate at high efficiency for a considerable amount of time because running an immobilized cell reactor is inexpensive, but growing cells, immobilizing, filling, and emptying the reactor is expensive and frequent downtime is unacceptable (Bucke 1986).

An alternative approach is to use a catalyst for Cr(VI) reduction. Growth decoupled cells of *D. vulgaris* can reduce Pd(II) to cell bound Pd(0) at the expense of hydrogen via cellular hydrogenase activity (Yong *et al.* 2003), to produce a bioinorganic catalyst ('Bio-Pd(0)'), which comprises nanoparticles of Pd(0) scaffolded onto the bio-template offered by the microbial cell surface. Batch studies have shown that Bio-Pd(0) is substantially more efficient at Cr(VI) reduction than live cells of *D. vulgaris*, while Pd(0) made chemically by reduction of Pd(II) under H_2 without biomass had little activity (Mabbett and Macaskie 2002). A continuous-flow process was used previously for the reduction of Cr(VI) to Cr(III), with operation at pH 3, and mass balance analysis confirming quantitative recovery of Cr(III) in the exit solution (Mabbett 2001). However the Bio-Pd(0) was not held within a matrix and at

pH 7 the bioreactors lost activity, possibly attributable to fouling over time by accumulated colloidal $Cr(OH)_3$ (Mabbett 2001). The objective of this study was to investigate the potential to use immobilized Bio-Pd(0) in packed-bed reactors for continuous Cr(VI) reduction, and to develop a hybrid chemical/ bioreactor for long term effective operation.

Materials and Methods

Organisms, growth conditions and preparation of cell suspension

Desulfovibrio vulgaris NCIMB 8303 was originally obtained from Prof. D. R. Lovley (University of Massachusetts, Amherst, MA, USA). Cells were maintained routinely in butyl rubber-sealed 100 mL serum bottles in Postgate's medium C (Postgate 1979) under O_2-free N_2 (OFN). For experiments, growing cultures (to OD_{600} 0.8 ± 0.2) were produced by withdrawing anaerobically 10 mL of an actively growing culture and adding it to 100 mL of fresh medium C.

For harvesting, cells were transferred under OFN into 50 mL serum bottles and harvested by centrifugation (3800g, 20 min, 22 °C) in the bottles, washed and recentrifuged three times with anaerobic (degassed) stock solutions of 20 mM MOPS-NaOH buffer (pH 7 under OFN) to provide stock concentrated suspensions. The cells were stored at 4 °C until use (within 24 h of harvesting). The biomass concentration of the cell concentrate was estimated by measuring the OD_{600} and conversion to dry cell wt via a previously determined calibration.

Preparation of Bio-Pd(0)

The required volume of 2 mM Na_2PdCl_4 (98 %, Aldrich Chemicals, UK) (to pH 2 with nitric acid) was placed in a 200 mL serum bottle sealed with a butyl-rubber stopper. The required volume of cell concentrate was added to give a final mass ratio of dry cells:Pd of 3:1. The suspension was incubated at 30 °C for 1 h to allow Pd(II) biosorption (de Vargas *et al.* 2004).

The suspension was then out-gassed with H_2 for 15 min, resulting in deposition of Pd(0) on the cell surface. The suspension was left overnight to settle-out, before transferring to 50 mL serum bottles, and the Pd-coated cells were recovered by centrifugation at 3800g (10 min). The pellet was washed once with distilled H_2O, three times with acetone, and dried in a 60 °C oven to constant weight. The dried solid (Bio-Pd(0)) was ground to a fine powder with a pestle and mortar. For comparison "Chemical-Pd(0)" was prepared by gassing 200 mL of 2 mM Na_2PdCl_4 with hydrogen for 1 h, followed by washing, drying and grinding as for Bio-Pd(0).

Immobilization of Chemical and Bio-Pd(0) preparations

Agar beads (Lopez et al. 1997): 200 mg Agar-Agar (FSB Laboratory Supplies) was mixed with 10 mL distilled H_2O and autoclaved (121 °C, 20 min). The gel was allowed to cool to 40 °C before Bio-Pd(0) (25.0 mg) or Chemical-Pd(0) (6.25 mg) were added. The aqueous phase (distilled H_2O) and the oily phase (olive oil) were placed in a 200 mL vessel in a ratio 10:1 (v/v), respectively. The gel mixture was extruded into the oily phase using a 2.5 mL syringe fitted with a 21G needle. The gel beads passed into the aqueous phase and were collected using a nylon net. Beads were washed once with Triton-X100 (Sigma) (0.01 % (v/v)) and three times with distilled H_2O.

Chitosan beads (Vorlop and Klein 1987): A 1 % (w/v) viscous chitosan-acetate solution was prepared by mixing 100 mg chitosan (Sigma) with 9.9 mL deionized water and 70 µl concentrated glacial acetic acid (80 °C, with stirring). To prepare beads, 25.0 mg Bio-Pd(0) was added to 10 mL chitosan-acetate solution, and the solution was dropped from a 2.5 mL syringe fitted with a 21G needle into 50 mL of 2 % (wt/v; aq.) polyphosphate (Sigma) solution (pH 8.2). After 4 h beads were collected with a nylon net and washed thoroughly with deionised water.

Magnetic resonance imaging of Bio-Pd(0)-loaded columns

Magnetic resonance imaging (MRI) was used to image Bio-Pd(0) immobilized in chitosan and agar beads. For each test 10 beads were placed in a bijoux bottle containing 2 mL 20 mM MOPS-NaOH buffer, pH 7. The bottle was introduced into a 2.35 Tesla super-conducting magnet (Oxford Instruments, Oxford, UK) connected to a Bruker Medzintechnik Biospec II imaging console (Karlsruhe, Germany). The 9.4 cm internal diameter 'bird cage' radio-frequency (RF) probe used to transmit and receive signal, and the 14.5 cm internal diameter gradient set used for spatial discrimination were both built 'in house'. ^{1}H images were acquired using a Spoiled GRASS (Hashemi 1997) sequence (repetition time (TR)/ echo time (TE)/ flip angle (θ) 50 ms/ 7.5 ms/ 30 °) with 400 μm isometric pixel resolution.

Chromate reduction by Bio-Pd(0) in continuous-flow packed-bed columns

For continuous reduction studies, 9 mL Bio-Pd(0) agar beads or Chemical-Pd(0) agar beads were placed in a 14 mL flow-through water-jacketed glass column (i.d. 15 mm, length 10 cm). Solution comprising 100 μM sodium chromate, 25 mM each of sodium formate, sodium citrate, sodium acetate, and 20 mM MOPS-NaOH buffer, pH 7, was pumped up through columns (30 °C) at a flow rate of 2.4 mL h^{-1}. Samples were withdrawn every 24 h for 800 h and analyzed for residual Cr(VI) using diphenylcarbazide (Pattanapipitpaisal *et al.* 2001).

Results and Discussion

Bio-Pd(0) immobilized in agar and chitosan (2.5 mg mL^{-1}) was imaged using MRI (Fig. 1). The study showed some dark specks in the beads in the absence of Pd, probably attributable to air bubbles. The Bio-Pd(0)-supplemented beads were better defined, attributable to the functioning of paramagnetic Pd(0) as a contrast agent by virtue of the paramagnetic effect of the Pd(0) on the proton signal of water. Visualisation of individual Bio-Pd(0) particles was

below the limit of resolution of MRI (100–200 μM: Paterson-Beedle *et al.* 2001) but the Bio-Pd(0) supplemented beads were uniformly greyer then their unsupplemented counterparts (Fig. 1). Additional black specks were visible (Fig. 1); assignment of these to air bubbles or agglomerates of Bio-Pd(0) was not attempted but the images show an even dispersion of material within and between individual beads (i.e. the preparation was homogeneous). Similar results were obtained for Bio-Pd(0) immobilized in chitosan beads, although the beads were less well defined. The reason for this was not investigated further and since the chitosan beads were unstable, shrinking in size by half during the preparation process, their use was discontinued and further studies used agar-Bio-Pd(0) beads.

Bio-Pd(0) was immobilized in agar at a concentration of 2.5 mg mL^{-1} (3:1 dry cell:Pd(0) ratio), to allow comparison with resting cells of *D. vulgaris* (2.5 mg dry cell wt. mL^{-1} agar). For comparison Chemical-Pd(0) was immobilized in agar at a loading of 0.625 mg mL^{-1}. The time course for Cr(VI) reduction by Chemical-Pd(0) and Bio-Pd(0) in flow-through columns is shown in Fig. 2. Negligible removal of Cr(VI) occurred in controls (agar immobilized Bio-Pd(0) in the absence of electron donor, or agar beads in the presence of electron donors) with 80 % of the input Cr(VI) recovered in the column outflow within 28 h. Agar-immobilized Chemical-Pd(0) initially removed Cr(VI) at 100 % efficiency. By 28 h the removal efficiency was only 21 %, and was completely lost by 160 h. At 500 h the percentage of Cr(VI) removed is negative. This may be due to the saturation of Cr(VI) within the column leading to its appearance in the effluent. Bio-Pd(0) (2.5 mg mL^{-1} loading) initially removed Cr(VI) at 100 % efficiency and the activity was stable at approx. 90 % until 680 h (272 bed volumes), after which reduction ability gradually decreased until at 1334 h 53 % of Cr(VI) was reduced. The Cr(VI) removal by the Bio-Pd(0) supplemented column was not attributable to biosorption: periodic checks confirmed that the total Cr leaving the Bio-Pd(0) column was identical to the

input concentration (Mabbett *et al.* 2004, A.C. Humphries, unpublished) while Mabbett (2001) confirmed the recovery of Cr(III) in spent solutions following Bio-Pd(0) catalysis. This study shows that Bio-Pd(0) is a superior catalyst at pH 7 compared to Chemical-Pd(0) and that columns using agar beads as an immobilization matrix are stable in operation, with no fouling by accumulated Cr(III). The beads were still visible as intact beads after 1334 h of operation. Previous studies have shown that the crystal size of Bio-Pd(0) is approx. half that of Chemical-Pd(0), thus the reaction surface area is larger, and hence Cr(VI) reduction efficiency is greater using the palladised biomass (Yong *et al.* 2002). It is also noteworthy that reduction of Cr(VI) by palladised biomass was sustained as compared to the Chemical-Pd(0). The reason for this is unknown and is the subject of current investigations.

Palladium is an expensive metal, therefore using Bio-Pd(0) to reduce Cr(VI) on an industrial scale may appear uneconomical. However automotive catalyst leachates, electronic scrap and industrial processing wastes contain palladium. Previous studies have shown that *Desulfovibrio desulfuricans* NCIMB 8307 can be used to recover palladium from these wastes, without the catalytic activity of the Bio-Pd(0) produced being affected by the presence of other co-contaminants in the recovered solid (Mabbett 2001).

Acknowledgements

We wish to acknowledge the financial support of the EPSRC (studentship no. 00318650 to ACH) and the Herchel Smith Endowment for funding to LEM., KPN., and LDH.

References

Bucke C. 1986. Methods of immobilizing cells. In: Webb C, Black, G. M., Atkinson, B., eds. Process Engineering Aspects of Immobilized Cell Systems. First ed. Rugby: Institution of Chemical Engineers. p 20-30.

de Vargas I, Macaskie LE, Guibal E. 2004. Biosorption of palladium and platinum by sulfate-reducing bacteria. J Chem Technol Biotechnol. 79:49-56.

Hashemi RH, Bradley, WG. 1997. MRI: The basics. Baltimore: Williams and Wilkins.

Humphries AC, Macaskie LE. 2002. Reduction of Cr(VI) by *Desulfovibrio vulgaris* and *Microbacterium* sp. Biotechnol Lett. 24:1261-1267.

Lopez A, Lazaro N, Marques AM. 1997. The interphase technique: a simple method of cell immobilization in gel-beads. J Microbiol Methods. 30:231-234.

Mabbett AN. 2001. The reduction and recovery of chromium(VI) from industrially polluted waste waters using sulphate-reducing bacteria. *Ph.D Thesis* The University of Birmingham, England.

Mabbett AN, Macaskie LE. 2002. A new bioinorganic process for the remediation of Cr(VI) J Chem Technol Biotechnol. 77:1169-1175.

Mabbett AN, Yong P, Farr JPG Macaskie LE. 2004. Reduction of Cr(VI) by palladised biomass of *Desulfovibrio desulfuricans* ATCC 29577 Biotechnol Bioeng. in press.

Paterson-Beedle M, Nott KP, Macaskie LE, Hall LD. 2001. Study of biofilm within a packed-bed reactor by three- dimensional magnetic resonance imaging. In: Doyle. R. D. eds. Microbial growth in biofilms, Pt B. San Diego; London. p 285-305.

Pattanapipitpaisal P, Brown NL, Macaskie LE. 2001. Chromate reduction *by Microbacterium liquefaciens* immobilized in polyvinyl alcohol. Biotechnol Lett. 23:61-65.

Postgate JR. 1979. The sulphate-reducing bacteria. Cambridge: Cambridge Univerisity Press.

Thomas D, Laval JM. 1996. Enzyme technology. In: Balasubramanian D, Bryce CFA., Dharmalingam K, Green J, Jayaraman K, eds. Concepts in Biotechnology. First ed. Hyderabad: University Press (India) Ltd. p 114-134.

Vorlop KD, Klein J. 1987. Entrapment of microbial-cells in chitosan. Method Enzymol. 135:259-268.

Yong P, Rowson NA, Farr JPG, Harris IR, Macaskie LE. 2002. Bioreduction and biocrystallization of palladium by *Desulfovibrio desulfuricans* NCIMB 8307 Biotechnol Bioeng. 80:369-379.

Yong P, Rowson NA, Farr JPG, Harris IR, Macaskie LE. 2003. A novel electrobiotechnology for the recovery of precious metals from spent automotive catalysts Environ Technol. 24:289-297.

Legends to Figures

Fig. 1. MR images of Bio-Pd(0) immobilized in chitosan (left) and agar (right) beads prepared as described in Materials and Methods. The MRI scan protocol was 3D Spoiled GRASS TR/TE/θ 50 ms/ 7.5 ms/ 30 ° 200 μm pixel resolution.

Fig. 2. Continuous reduction of 100 μM Cr(VI) by agar-immobilized beads alone (♦) or supplemented with Bio-Pd(0) (■) or Chemical-Pd(0) (●). Data are means ± SEM from three experiments. Where no error bars are shown these were within the dimensions of the symbols.

Fig. 1

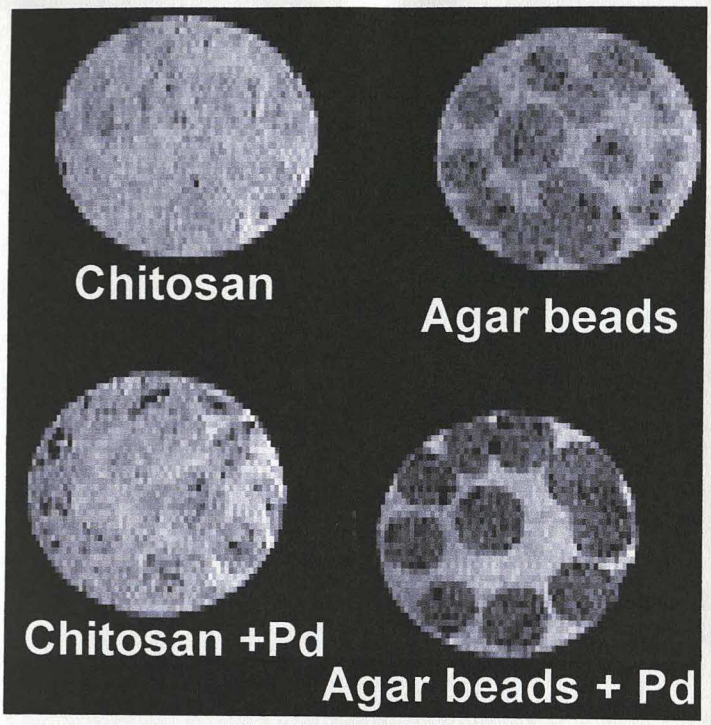
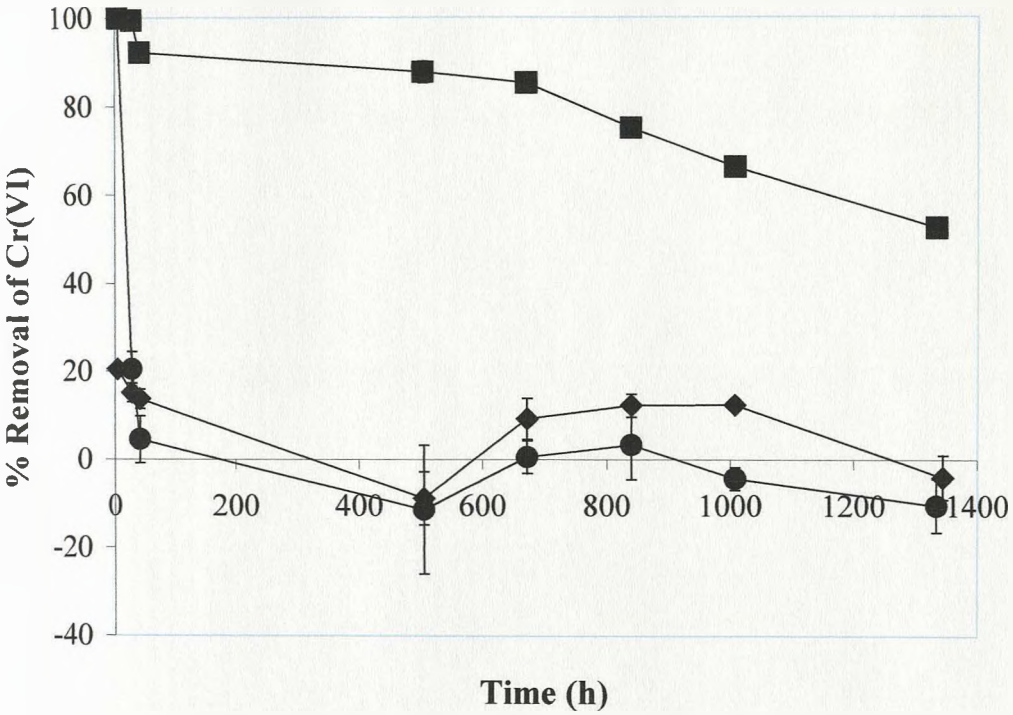


Fig. 2.


100
80
60
40
20
0
-20
-40
% Removal of Cr(VI)
0
200
400
600
800
1000
1200
1400
Time (h)

SECTION 3.2

"Reduction of Cr(VI) by palladised biomass of *Desulfovibrio vulgaris* NCIMB 8303".

Journal: ***Journal of Chemical Technology and Biotechnology***

Submitted

Reduction of Cr(VI) by palladised biomass of *Desulfovibrio vulgaris* NCIMB 8303

Andrea C Humphries and Lynne E Macaskie*

School of Biosciences, The University of Birmingham, Edgbaston, Birmingham, B15 2TT, UK.

**Author for correspondence* (E-mail: L.E.Macaskie@bham.ac.uk)

Abstract

Palladised biomass of *Desulfovibrio vulgaris* (Bio-Pd(0)) reduced Cr(VI) to Cr(III) at an initial rate four fold higher than chemically prepared Pd(0) metal. Optimal Cr(VI) reduction by suspended Bio-Pd(0) occurred at pH 3, whereas pH did not affect the rate of Cr(VI) reduction by Bio-Pd(0) immobilized in agar beads. The rate of Cr(VI) reduction was concentration-dependent below 300 μM, and application of enzyme kinetics, considering Bio-Pd(0) as an 'artificial enzyme', gave an apparent K_m of approx. 650 μM and V_{max} of 1667 nmoles h^{-1} mg $Pd(0)^{-1}$ for suspended Bio-Pd(0). The potential of Bio-Pd(0) as a method for the treatment of Cr(VI)-wastes is discussed.

Keywords: *bioinorganic catalyst, chromium, immobilization, kinetics*

Introduction

Chromium is a transition metal, existing in a variety of transition states ranging from +6 to -2, with the trivalent, Cr(III), and hexavalent, Cr(VI), states being predominant in solution (1). Cr(VI) is toxic, mutagenic and carcinogenic to humans and animals (2), whilst Cr(III) is less mobile and less toxic because biological membranes are relatively impermeable to it (3). Chromium is widely used industrially, endowing alloys or materials with properties of resistance to corrosion, temperature and decay, and conferring strength, hardness, permanence, and colour. For example, chromium is used in leather tanning, electroplating, and petroleum refining (4). Chromium-contaminated industrial effluents are conventionally treated using chemical methods, such as precipitation and ion exchange. However, these methods are relatively chemically and energetically intensive (5). As an alternative, Cr(VI) containing wastewaters may be treated biologically by reduction to Cr(III). Examples of Cr(VI) reducing microorganisms include *Shewanella alga* (6), *Pseudomonas putida* (7), *Microbacterium* sp (8) and *Desulfovibrio vulgaris* (9,10).

The optimum challenge conditions for Cr(VI) reduction by resting cells of *D. vulgaris* NCIMB 8303 and *Microbacterium* sp. NCIMB 13776 were defined (11), and immobilized resting cells were used for Cr(VI) reduction in continuous-flow packed-bed reactors, using agar as the immobilization matrix (12). This gave negligible mass transfer limitations and good structural integrity (12) but while conversion of (100 μM) Cr(VI) occurred at 60 % efficiency for both strains this was short lived, with activity ceasing after approx 160 h (12). For industrial purposes reactors should operate at high efficiency over extended periods, because growing cells, immobilizing, filling and emptying the reactor is expensive, and frequent downtime is unacceptable (13).

An alternative, more robust approach using a bioinorganic hybrid catalyst was pioneered. Growth-decoupled cells of *Desulfovibrio vulgaris* NCIMB 8303 can reduce Pd(II) to cell-bound Pd(0) at the expense of hydrogen via cellular hydrogenase activity (14,15) to produce a bioinorganic catalyst (Bio-Pd(0)), comprising Pd(0) nanoparticles supported on the surface of the bacterial cells (16). Continuous packed-bed reactors containing agar-immobilized Bio-Pd(0) challenged with an acetate-citrate buffered solution with formate as the electron donor removed 90 % of an input Cr(VI) solution of 100 μM for 680 h (17). One objective of this study was to identify the optimum conditions for Cr(VI) reduction by agar-immobilized Bio-Pd(0), with respect to temperature, pH and initial Cr(VI) concentration. The latter are important because bioprocesses are usually constrained to operate within physiologically permissive constraints but the use of an inorganic catalyst supported on dried biomass would overcome these restrictions and enable operation under the more extreme conditions which typify many industrial wastes. The areas in which Bio-Pd(0) would be superior to a completely microbial-based catalyst are discussed.

Materials and Methods

Organisms and growth conditions

Desulfovibrio vulgaris NCIMB 8303 was maintained and grown as described previously (10,11). For experiments, growing cultures (OD_{600} 0.8 ± 0.2) were produced by withdrawing 100 mL of actively growing culture and adding to 1 L fresh Postgate's medium C (18), followed by degassing with oxygen free nitrogen (OFN) for 20 min. The culture was harvested after 24 h (OD_{600} 0.8 ± 0.2).

Preparation of cell suspensions

Resting cells of *D. vulgaris* were prepared as described previously (11). Cell concentrate was stored under nitrogen at 4 °C suspended in 20 mM 3-(N-Morpholino)propanesulfonic acid (MOPS)/ NaOH buffer, pH 7, until use (within 24 h of harvesting). The biomass concentration of the cell concentrate was estimated by measuring the OD_{600}, and conversion to dry cell weight using a previously determined calibration.

Preparation of Bio-Pd(0) on cells of *D. vulgaris*, and immobilization in agar beads

The required volume of 2 mM Na_2PdCl_4 (98 %, Aldrich Chemicals, UK), adjusted to pH 2 with nitric acid, was placed in a 200 mL serum bottle sealed with a butyl-rubber stopper. The required volume of cell concentrate was added to give a final mass ratio of dry cells:Pd of 3:1. The suspension was incubated at 30 °C for 1 h to allow Pd(II) biosorption (19). The suspension was then out-gassed with H_2 for 15 min, resulting in deposition of Pd(0) on the cell surface. The suspension was left overnight under H_2 (no residual Pd(II) remained in the supernatant by assay: 15) before transferring to 50 mL serum bottles, and the Pd-coated cells were recovered by centrifugation (3800 g, 10 min). The pellet was washed once with distilled H_2O (dH_2O), three times with acetone, and placed in a 60 °C oven to constant weight. The dried solid ("Bio-Pd(0)") was ground to a fine powder with a pestle and mortar. For comparison "Chemical-Pd(0)" was prepared by gassing 200 mL of 2 mM Na_2PdCl_4 with hydrogen for 1 h, followed by washing, drying and grinding the black solid as for Bio-Pd(0). Immobilization of Bio-Pd(0) in agar beads was done as described previously (12).

Reduction of Cr(VI) by free and immobilized Bio-Pd(0) in batch suspensions

Reaction mixtures were set up in 12 mL serum bottles. The final volume of the reaction was 5 mL. Challenge solution comprised sodium chromate (500 μM or as specified in individual

experiments) and 25 mM each of sodium acetate, sodium formate, and sodium citrate in MOPS/ NaOH buffer (20 mM, pH 7, or as specified). All tests were done in air in triplicate on three separate occasions. Controls for all experiments consisted of Pd(0) in the absence of electron donor (formate). Samples were withdrawn periodically, via syringe, and the supernatant was analyzed for residual Cr(VI) using diphenylcarbazide (8). Previous studies showed negligible retention of Cr(III) product on the catalyst by assay of the solution (Humphries AC, Mikheenko IP, Macaskie LE, unpublished).

To study the effect of temperature and pH on Cr(VI) reduction, Bio-Pd(0) (1 mg Bio-Pd(0) mL^{-1}; equivalent to 0.25 mg Pd(0) mL^{-1}) and Chemical-Pd(0) (0.25 mg Pd(0) mL^{-1}) were suspended in the challenge solution at pH 1 - 9 and incubated at 22 °C or 30 °C as specified. The effect of pH on Cr(VI) reduction by agar-immobilized Bio-Pd(0) was further investigated at pH 3 and 7. For these tests, 2 mL Bio-Pd(0)-agar beads (2.5 mg Bio-Pd(0) mL $agar^{-1}$) were added to 5 mL challenge solution at the appropriate pH.

To study the effect of Cr(VI) concentration on the rate of its reduction, either free (1 mg Bio-Pd(0) mL^{-1}; equivalent to 0.25 mg Pd(0) mL^{-1}) or agar-immobilized Bio-Pd(0) (2 mL agar beads: 2.5 mg Bio-Pd(0) mL $agar^{-1}$) were challenged with the above solution, containing sodium chromate at a concentration of 100 - 500 μM, at pH 7 and 22 °C.

Results and Discussion

Reduction of Cr(VI) by free and immobilized Bio-Pd(0)

The optimum temperature for reduction of Cr(VI) by live cells was 30 °C (11), but operation at room temperature could be more economically attractive. Therefore, Cr(VI) reduction by suspended Bio-Pd(0) and Chemical-Pd(0) was studied at 22 and 30 °C. Negligible Cr(VI) reduction occurred in controls (Pd(0) in the absence of electron donor). The initial rate of Cr(VI)

reduction by Bio-Pd(0) was approx. 4 fold higher compared to Chemical-Pd(0) (Fig. 1). The crystal size, and therefore the surface area available for reaction of Chemical-Pd(0) is approx. twice that of Bio-Pd(0) (20) which explains the lower rate on the basis of the relative surface areas (1:4) assuming spheres (area 4 πr^2) of radii of 1 or 2 units (dimensionless). However, this does not explain why the reduction of Cr(VI) by the Chemical-Pd(0) did not proceed beyond approx. 20 % of that initially present (see later discussion). After 24 h, 318 ± 10 and 362 ± 10 μM Cr(VI) remained when Chemical-Pd(0) was incubated at 22 and 30 °C, respectively, i.e. this was temperature independent. It is important to note that although the reduction of Cr(VI) proceeded negligibly after 5 h using Chemical-Pd(0) the reaction went to completion after 24 h using the biomaterial (Fig 1). This is probably not attributable to the differences in particle sizes but may be attributable to the interactions between the metal and organic components of the hybrid material (see later). The initial rate of Cr(VI) reduction by Bio-Pd(0) was also not significantly different at 22 and 30 °C (initial rates: 587 ± 26 and 598 ± 18 nmol Cr(VI) h^{-1} mg $Pd(0)^{-1}$), respectively). All subsequent experiments were therefore carried out at 22 °C.

Cr(VI) reduction by suspended Bio-Pd(0) and Chemical-Pd(0) was investigated at pH 1 - 9 (Fig. 2). Negligible Cr(VI) reduction was seen in controls at all pH values (Pd(0) in the absence of electron donor). The initial rate of Cr(VI) reduction by Chemical-Pd(0) was largely independent of solution pH and was broadly optimal at pH 3 - 7. In contrast pH 3 was optimal for Cr(VI) reduction by suspended Bio-Pd(0), with no significant differences in the range pH 1 - 6, and with a lower rate at pH 7 and above. These results are in accordance with those of Mabbett (2001) but the effect of pH above 7 was not tested in the previous study. The solution pH did not change during the experiments, suggesting that the reaction solution was buffered by the formate

(pK_a 3.75), acetate (pK_a 4.76), citrate (pK_a 3.13, 4.76, 6.40) and MOPS (pK_a 7.2). To ensure consistency in the solution matrix all of these buffers were used in each test throughout the study. Some complexation of the Cr(III) product would be expected (the stability constants (log β_1) of the formate- acetate- and citrate- complexes of the Cr(III)-chelate were calculated at 1.93, 3.70 and 7.69, respectively, in a background solution of $NaClO_4$: 21) but the solution chemistry would not account for the differences seen between the Chemical-Pd(0) and Bio-Pd(0)-catalysed reactions.

Since the continuing conversion of Cr(VI) to Cr(III) could rely on the removal of nascent Cr(III) from the catalytic site, it follows that complexation (trapping) of Cr^{3+} with an adjacent ligand could facilitate further reduction of Cr(VI). Indeed, the incorporation of chelating ligands into the solution was found to promote Cr(VI) reduction by live cells of *Desulfovibrio vulgaris* to an extent which exactly correlated with the formation constant of the Cr(III)-ligand complex (10). In the present case it is possible that the 'naked' Chemical-Pd(0) was subject to inhibition by nascent Cr(III) at the catalytic site. In the case of Bio-Pd(0) the close proximity of biochemical ligands in the supporting biomatrix adjacent to the Pd(0) clusters may have provided a 'capture mechanism' for nascent Cr^{3+}. The possibility of this binding was suggested in other studies using magnetic resonance imaging (MRI), where a Gram negative biofilm-coated polyurethane reticulated foam cube was indistinct when challenged with Cr(VI) (in the absence of electron donor) but addition of Cr(III) to the biofilm gave a very clear MR image as compared to a similar foam cube without the biofilm layer (A.C. Humphries, K.P. Nott, L.E. Macaskie and L.D. Hall, unpublished). These images were similar to those published previously using Cu^{2+} as a 'doping agent' to introduce image contrast in the biofilm (22); the magnetic moments of Cu^{2+} and Cr^{3+} are

1.7 - 2.2 and 3.8, respectively (23) and accordingly Cr^{3+} is an established contrast agent in MRI whereas Cr(VI) is 'MRI-'silent' (24). This suggests that binding of Cr^{3+} occurs onto Gram negative bacteria. Such biosorption would suggest that the biomass ligand sites intercept Cr(III). This could be expected since overall, the cell surface carries a net negative charge due to the presence of carboxyl, hydroxyl and phosphate groups, and can absorb substantial quantities of positively charged cationic metals (25). It could be suggested that these biomass-polymer ligands, or possibly coordinating amino groups of proteins (the Pd(0) clusters initially form at the loci of cellular hydrogenases: 15) remove nascent Cr^{3+} from the Pd(0) cluster. Cr^{3+} ions could then migrate across the cell surface in the same way that coordination of U(VI) onto the amine group of chitin was followed by its migration across fungal wall polymers to leave the initial coordinating N-ligand free for the next incoming U atom (26). Formation and precipitation of $Cr(OH)_3$ could similarly occur on the cell wall layers, but in the present case hydrolysis would be suppressed in the presence of the excess of citrate in the bulk solution, which may act as the final 'sink' for Cr(III), and tending to withdraw it from the biomass.

For further tests, Bio-Pd(0) immobilized in agar beads was challenged with a solution as above containing 500 μM sodium chromate, at pH values of 3 and 7 (Fig. 3). Approx. 25 % of the Cr(VI) was removed onto agar-immobilized Bio-Pd(0) without electron donor, probably attributable to absorption by the immobilization matrix. In contrast to suspended Bio-Pd(0) (Fig. 2), the reduction proceeded at broadly similar initial rates at pH 3 and 7 (540 ± 76 and 488 ± 48 nmol h^{-1} mg $Pd(0)^{-1}$, respectively), i.e. the advantage of the lower pH was not apparent (c.f. the rate with non-immobilized Bio-Pd(0) at pH 3 was > 1100 nmol mg^{-1} h^{-1} (Fig. 2)). The lack of pH effect was probably attributable to the local fluid environment differing substantially from the bulk environment (27). In particular, a slower rate of ingress of citrate may have retarded the

removal of the Cr^{3+} product from the catalyst. Mabbett (2001) showed Bio-Pd(0) functioned for only 24 h in a continuous-flow column at pH 7, whilst at pH 3 100 % conversion was achieved for several weeks providing an efficient and economic method for the reduction of Cr(VI) to Cr(III).

Effect of the initial concentration of Cr(VI) and implications with respect to Cr(VI) waste treatment

The effect of initial Cr(VI) concentration on the rate of its reduction was investigated (Fig. 4). Between 7 % (100 μM Cr(VI)) and 29 % (500 μM Cr(VI)) Cr(VI) was removed from solution when agar-immobilized Pd(0) was present in the absence of electron donor, attributable to absorption by the immobilization matrix. This complicated accurate calculation of initial rates (the background biosorption was subtracted from rate calculations) but in the presence of formate, the initial rate of Cr(VI) reduction decreased with Cr(VI) concentration, below a concentration of approx. 300 μM Cr(VI) in each case (Fig 4).

For the purpose of calculations the Bio-Pd(0) may be considered as analogous to an artificial enzyme. Enzymes are composed of amino acids that are used to construct binding sites with high specificity. However, these groups are poorly suited to binding and catalyzing redox reactions of small molecules like H_2. Metallocofactors are therefore incorporated into enzymes to provide the binding interactions for small molecules and to confer the catalytic capability needed to achieve redox transformations (28). Metalloproteins (e.g. hydrogenase), consist of one or more metals (e.g. Fe, Ni) associated with inorganic groups interacting through protein ligands (e.g. cysteine, histidine) (28). In this sense Bio-Pd(0) could be considered as an 'artificial enzyme'. The Pd-bionanocluster system is redox-active and can be considered as analogous to metalloenzymes; it is localized at the site of cellular hydrogenases (15) following initial coordination of Pd(II) with

amino groups as shown by X-ray photoelectron spectroscopy (29). Effectively it might be considered functionally as a 'hydrogenase amplifier' in the current context and therefore the possibility exists to model the system according to applied enzyme kinetics. Using a double reciprocal plot of data obtained using suspended Bio-Pd(0) at 100 – 300 μM Cr(VI) (1/S versus 1/V; S and V are substrate (Cr(VI)) concentration and reaction velocities, respectively), an apparent 'K_m' value ($K_{m\ app}$) of approx. 650 μM was obtained, with a maximum velocity of 1667 nmoles h^{-1} mg $Pd(0)^{-1}$ (R^2 = 0.95). The K_m value is the substrate concentration at which the reaction rate is half-maximal, with a low K_m value representing high affinity of an enzyme for its substrate and a high K_m a low affinity (30). Previously a K_m value for Cr(VI) reduction by resting (unpalladised) cells of *D. vulgaris* was calculated as 333 μM (31), suggesting unpalladised cells have a higher affinity for Cr(VI) than their palladised counterparts.

It is concluded that Bio-Pd(0) can be considered to be effective for Cr(VI) concentrations in the 0.6 - 1.6 mM region at pH 3, but would be less effective as a final 'polishing' step at neutral pH.. In this respect a bio-based system might be more effective for treatment of low Cr(VI) concentrations, whilst the Bio-Pd(0) based system would find use at toxic concentrations and under acidic conditions. Indeed, immobilization of Bio-Pd(0) in columns challenged continuously with 1 mM $NaCrO_4$ reduced Cr(VI) for only 24 h at pH 7, compared to 100 % reduction at pH 3 sustained for several weeks (33), confirming that the process is more efficient at pH 3. However for the previous experiments (33) Bio-Pd(0) was immobilized in columns as a 'plug' between two membranes, and similar results will not necessarily be obtained for continuous-flow packed-bed columns containing Bio-Pd(0) immobilized in agar beads, since the fluid environment inside agar beads is different from the bulk solution (27). Future studies will compare the efficiency of

Cr(VI) reduction by continuous-flow packed-bed columns containing agar-immobilized Bio-Pd(0) at pH 3 and 7.

Palladium is an expensive metal, therefore using Bio-Pd(0) to reduce Cr(VI) may appear uneconomic. However automotive catalyst leachates, electronic scrap and industrial processing wastes contain palladium. Previous studies have shown that *D. desulfuricans* NCIMB 8307 can be used to recover palladium from these wastes as Bio-Pd(0) without the catalytic activity of the Bio-Pd(0) produced being compromised by the presence of other co-contaminants in the recovered solid (32). Use of biorecovered palladium would mitigate the cost of Cr(VI) remediation, whilst permitting application outside the usual physiological constraints of microbial processes.

Acknowledgements

We wish to acknowledge the financial support of the EPSRC (Studentship Number: 00318650 to ACH.). LEM was supported by a Fellowship from the Royal Society.

References

1. Barnhart J. 1997. Occurrences, uses, and properties of chromium. Regul Toxicol Pharm. 26:S3-S7.
2. Komori K, Wang PC, Toda K and Ohtake H. 1989. Factors affecting chromate reduction in *Enterobacter cloacae* strain HO1. Appl Microbiol Biotechnol. 31:567-570.
3. Cervantes C and Silver S. 1992. Plasmid chromate resistance and chromate reduction. Plasmid. 27:65-71.
4. Laxman RS and More S. 2002. Reduction of hexavalent chromium by *Streptomyces griseus*. Miner Eng. 15:831-837.

5. Konovalova VV, Dmytrenko GM, Nigmatullin RR, Bryk MT and Gvozdyak PI. 2003. Chromium (VI) reduction in a membrane bioreactor with immobilized *Pseudomonas* cells. Enzyme Microb Tech. 33:899-907.

6. Guha H, Jayachandran K and Maurrasse F. 2001. Kinetics of chromium (VI) reduction by a type strain *Shewanella alga* under different growth conditions. Environ Pollut. 115:209-218.

7. Ishibashi Y, Cervantes C and Silver S. 1990. Chromium reduction in *Pseudomonas putida.* Appl Environ Microbiol. 56:2268-2270.

8. Pattanapipitpaisal P, Brown NL and Macaskie LE. 2001. Chromate reduction by *Microbacterium liquefaciens* immobilised in polyvinyl alcohol. Biotechnol Lett. 23:61-65.

9. Lovley DR and Phillips EJP. 1994. Reduction of chromate by *Desulfovibrio vulgaris* and its c_3 cytochrome. Appl Environ Microbiol. 60:726-728.

10. Mabbett AN, Lloyd JR and Macaskie LE. 2002. Effect of complexing agents on reduction of Cr(VI) by *Desulfovibrio vulgaris* ATCC 29579. Biotechnol Bioeng. 79:389-397.

11. Humphries AC and Macaskie LE. 2002. Reduction of Cr(VI) by *Desulfovibrio vulgaris* and *Microbacterium* sp. Biotechnol Lett. 24:1261-1267.

12. Humphries AC, Nott KP, Hall LD and Macaskie LE. 2005. Reduction of Cr(VI) by immobilized cells of *Desulfovibrio vulgaris* NCIMB 8303 and *Microbacterium* sp. NCIMB 13776. Biotechnol Bioeng. in press.

13. Bucke C, Methods of immobilizing cells. 1986. In: Webb C, Black GM, Atkinson B, editors. Process engineering aspects of immobilized cell system. Rugby: I. ChemE.

14. Yong P, Rowson NA, Farr JPG, Harris IR and Macaskie LE. 2003. A novel electrobiotechnology for the recovery of precious metals from spent automotive catalysts. Environ Technol. 24:289-297.

15. Mikheenko I. 2004. Nanoscale palladium recovery. *Ph.D Thesis*. The University of Birmingham, England.

16. Mikheenko I, Mikheenko P, Darlington CNW, Muirhead CM and Macaskie LE. 2001. Magnetic testing of Pd loaded bacteria. In: Ciminelli VST, Garcia Jr O, editors. Biohydrometallurgy: Fundamentals, Technology and Sustainable Development. Elsevier, Amsterdam.

17. Humphries AC, Nott KP, Hall LD and Macaskie LE. 2004. Continuous removal of Cr(VI) from aqueous solution catalysed by palladised biomass of *Desulfovibrio vulgaris* NCIMB 8303. Biotechnol Lett. 26:1529-1532.

18. Postgate, JR. 1979. The Sulphate-Reducing Bacteria. Cambridge University Press: Cambridge.

19. daVargas I, Macaskie LE and Guibal E. 2004. Biosorption of palladium and platinum by sulfate-reducing bacteria. J Chem Technol Biotechnol. 79:49-56.

20. Yong P, Rowson NA, Farr JPG, Harris IR and Macaskie LE. 2002. Bioreduction and biocrystallization of palladium by *Desulfovibrio desulfuricans* NCIMB 8307. Biotechnol Bioeng. 80:369-379.

21. Vinokurov EG, Bondar VV. 2001. Prediction of Stability Constants for Cr(III) and Cr(II) complexes. Russ J Coord Chem. 29:71-77.

22. Nott KP, Paterson-Beedle M, Macaskie LE and Hall LD. 2001. Visualisation of metal deposition in biofilm reactors by three-dimensional magnetic resonance imaging (MRI) Biotechnol Lett. 23:1749-1757.

23. Bertini I and Luchinat C. 1986. NMR of Paramagnetic Molecules in Biological Systems. CA Benjamin/Cummings Menlo Park CA.

24. Liu KJ, Shi XL. 2001. *In vivo* reduction of chromium (VI) and its related free radical generation. Mol Cell Biochem. 222:41-47.

25. Lloyd JR. 2002. Bioremediation of metals; the application of micro-organisms that make and break minerals. Microbiol Today. 29:67-69.

26. Tzesos M and Volesky B. 1982. The mechanism of uranium biosorption by *Rhizopus arrhizus*. Biotechnol Bioeng.. 24:385-401.

27. Bailey JE and Ollis DF. 1986. Biochemical Engineering Fundamentals. Verma K, Martin CC, editors. Singapore: McGraw-Hill Book Co.

28. Rees DC. 2002. Great metalloclusters in enzymology. Annu Rev Biochem. 71:221-246.

29. Macaskie LE 2004. In Final report: Selective Separation of Strategic and Precious Metals. EU Contract No GIRD-CT2000-00300.

30. Fulbrook PD. 1983. Practical applied kinetics. In: Godfrey T, Reichelt J, editors. Industrial Enzymology. Macmillan Publishers Ltd.

31. Mabbett AN, Macaskie LE. 2001. A novel isolate of *Desulfovibrio* sp. with enhanced ability to reduce Cr(VI). Biotechnol Lett. 23:683-687.

32. Mabbett AN. 2001. The reduction and recovery of chromium (VI) from industrially polluted waste waters using sulphate-reducing bacteria. *PhD Thesis*. The University of Birmingham, England.

33. Mabbett AN, Yong P, Baxter-Plant VS, Mikheenko IP, Farr JPG, Macaskie LE. 2001. Effective reduction and removal of Cr(VI) and reductive dehalogenation of chlorophenol by hybrid bioinorganic catalytic processes. In: Ciminelli VST, Garcia Jr O, editors. Biohydrometallurgy: Fundamentals, Technology and Sustainable Development. Elsevier, Amsterdam.

Legends to Figures

Fig. 1. Reduction of 500 μM Cr(VI) by suspended Bio-Pd(0) and Chemical-Pd(0) at 22 and 30 °C. Filled symbols: in the presence of electron donor. Open symbols: Controls (Pd(0) in the absence of electron donor). ♦: Bio-Pd(0) 30 °C ; ●: Bio-Pd(0) 22 °C ; ▲: Chemical-Pd(0) 30 °C ; ■: Chemical-Pd(0) 22 °C. Error is ± SEM from 3 independent experiments. Where no error bars are shown these were within the dimensions of the symbols.

Fig. 2. Effect of pH on the initial rate of reduction of 500 μM Cr(VI) by suspended Bio-Pd(0) (♦) and Chemical-Pd(0) (■) at 22 °C. Error is ± SEM 3 independent experiments.

Fig. 3. Reduction of 500 μM Cr(VI) by agar-immobilized Bio-Pd(0) at 22°C at pH 3 and 7. Filled symbols: in the presence of electron donor. Open symbols: Controls (in the absence of electron donor). ♦: pH 3 ; ■: pH 7. Error is ± SEM 3 from independent experiments.

Fig. 4. Effect of initial Cr(VI) concentration on the initial rate of Cr(VI) reduction by suspended (■) and agar-immobilized (♦) Bio-Pd(0). Open symbols: Controls, Cr(VI) reduction in absence of electron donor. Filled symbols: Cr(VI) reduction in presence of electron donor. Error is ± SEM from 3 independent experiments.

Fig. 1

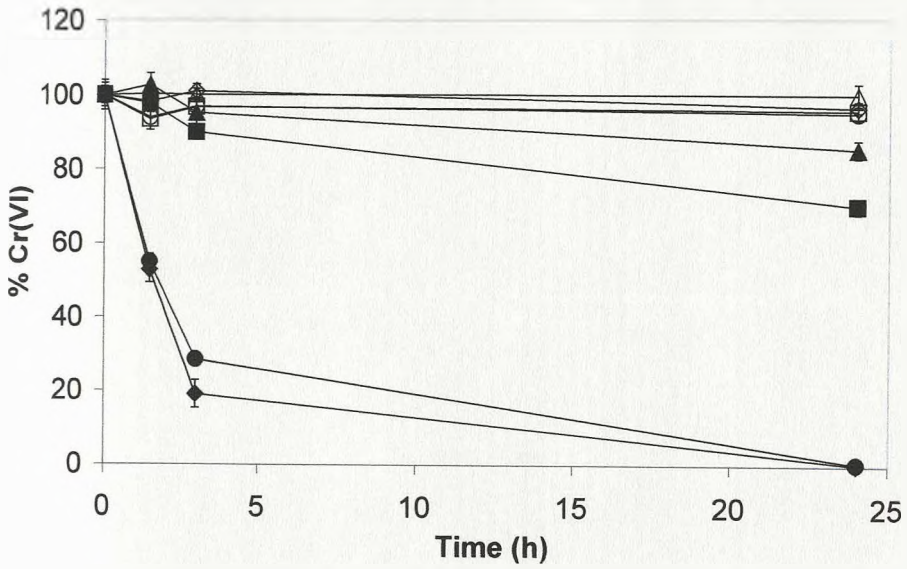


Fig. 2

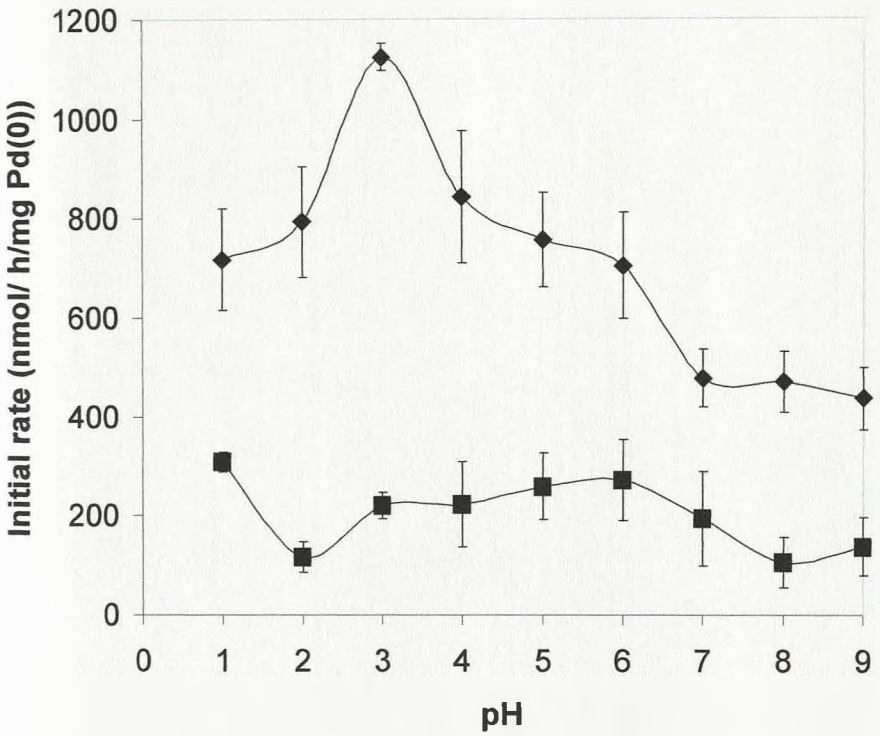

Initial rate (nmol/ h/mg Pd(0))
1200
1000
800
600
400
200
0
0
1
2
3
4
5
6
7
8
9
pH

Fig. 3

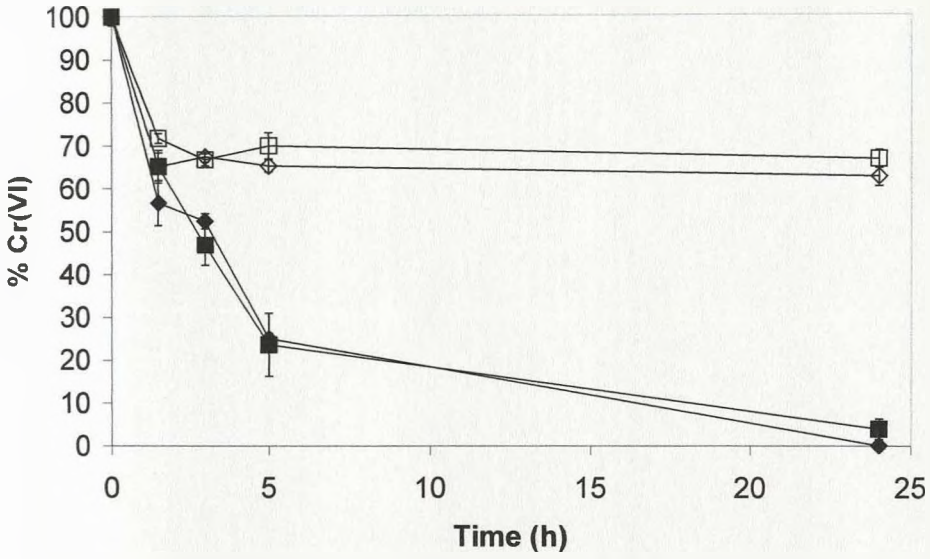
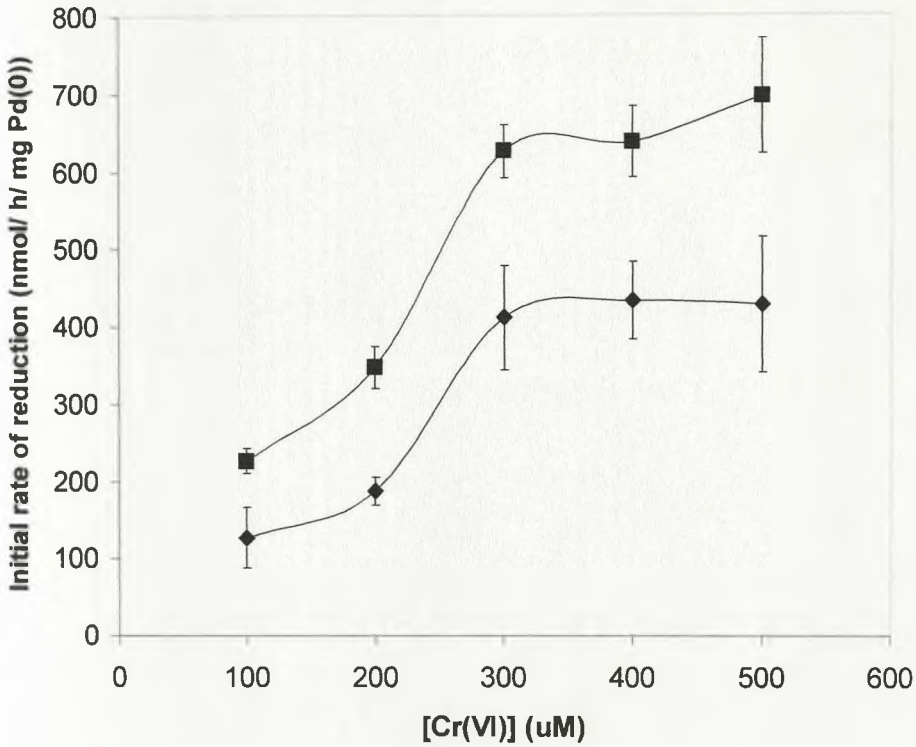


Fig. 4


Initial rate of reduction (nmol/ h/ mg Pd(0))
800
700
600
500
400
300
200
100
0
0
100
200
300
400
500
600
[Cr(VI)] (uM)

SECTION 3.3

"Chromate reduction by immobilized palladised bacteria".

Journal: ***Biotechnology and Bioengineering***

Submitted

This paper was produced entirely from work done by A. C. Humphries except for Transmission Microscopy, which was done by I. P. Mikheenko. Biosorption capacities for Pd(II) onto protonated biomass of *D. desulfuricans*, *D. vulgaris* and *E. coli* strains MC4100 and HD701 was investigated by I. deVargas, M. Climo and L. E. Macaskie.

Chromate reduction by immobilized palladised bacteria

A. C. Humphries, I. P. Mikheenko, L. E. Macaskie*

School of Biosciences, The University of Birmingham, Edgbaston, Birmingham, B15 2TT, UK

**Author for correspondence (E-mail:* L.E.Macaskie@bham.ac.uk*)*

Keywords: bioinorganic catalyst, chromium, immobilization, packed-bed reactor

Abstract

Resting cells of *Desulfovibrio vulgaris* NCIMB 8303, *Desulfovibrio desulfuricans* NCIMB 8307, and *Escherichia coli* strains MC4100 (wild type parental) and HD701 (HycA deficient hydrogenase upregulated mutant) were used for the hydrogenase-mediated reduction of Pd(II) to Pd(0). The resulting hybrid palladium bionanocatalyst (Bio-Pd(0)) was used in the reduction of Cr(VI) to the less environmentally problematic Cr(III) species. The reduction of Cr(VI) by free and agar-immobilized Bio-Pd(0) was evaluated. Investigations using catalyst suspensions showed that Cr(VI) reduction was highest (~ 170 nmol Cr(VI) h^{-1} mg Bio-Pd(0)$^{-1}$) when Bio-Pd(0) was produced using *D. vulgaris* or *D. desulfuricans*. Continuous-flow studies using *D. vulgaris* Bio-Pd(0) with agar as the immobilization matrix investigated the effect of Bio-Pd(0) loading, inlet Cr(VI) concentration, and flow rate on the efficiency of Cr(VI) reduction. Reduction of Cr(VI) was highest at a *D. vulgaris* Bio-Pd(0) loading of 7.5 mg Bio-Pd(0) mL^{-1} agar (3:1 dry cell wt: Pd(0)), an input [Cr(VI)] of 100 μM, and a flow rate of 1.75 mL h^{-1} (approx. 3.5 column volumes h^{-1}). A mathematical interpretation predicted the activity of the immobilized Bio-Pd(0) for a given set of conditions within 5 % of the value found by experiment. Considering the system as an 'artificial enzyme' analogue and application of applied enzyme kinetics gave an apparent K_m value ($K_{m\ app}$) of 430 μM Cr(VI) and a determined value of flow-through reactor activity which differed by 11% from that predicted mathematically.

Introduction

Chromium, a transition metal, exists predominantly in the trivalent and hexavalent form. Hexavalent chromium, Cr(VI), is a known carcinogen and mutagen (Costa 2003), which is actively transported into cells via an anion transport pathway (Shi *et al.* 1999). In contrast, the trivalent species, Cr(III), is relatively non-toxic and non-carcinogenic (Shi *et al.* 1999).

Hexavalent chromium has been used industrially for over 100 years (Chen and Hao 1998), with applications in, for example, the pigment, tanning, and electroplating industries (Dube *et al.* 2003). Discharge of Cr(VI) into the environment due to inadequate industrial waste treatment poses an environmental threat (Chen and Hao 1998). Conventional chemical methods for removing Cr(VI) from industrial wastewaters include anion exchange and chemical precipitation (Korngold *et al.* 2003). However, these are relatively expensive. As an alternative, Cr(VI) contaminated wastewater's may be treated biologically by reduction to Cr(III). Examples of microorganisms capable of reducing Cr(VI) include *Shewanella alga* (Guha *et al.* 2001), *Agrobacterium radiobacter* EPS-916 (Llovera *et al.* 1993), *Pseudomonas putida* (Ishibashi *et al.* 1990), *Escherichia coli* (Bae *et al.* 2000a,b) and *Desulfovibrio vulgaris* (Lovley and Phillips 1994; Mabbett *et al.* 2002). The latter is a member of the sulfate-reducing bacteria (SRB) which have a well-established ability to reduce a variety of metals. (Lovley and Phillips 1994; Mabbett *et al.* 2002). The SRB use an organic compound (e.g. formate) or molecular H_2 as the electron donor and SO_4^{2-} as the terminal electron acceptor in dissimilatory sulfate reduction. Certain high valence metal ions, such as Tc(VII) and Cr(VI), can be used as electron sinks in the absence of sulfate, with consequent metal reduction (Lloyd *et al.* 1999a; Lloyd *et al.* 2001; Mabbett *et al.* 2002), although growth at the expense of chromate has been demonstrated only in one case (Tebo and Obraztsova 1998).

The use of biological systems for continuous Cr(VI) reduction has several drawbacks. Cells must be cultivated and used within a relatively short time and the Cr(VI)-reducing activity may be short-lived. A previous study investigated Cr(VI) reduction by agar-immobilized cells of *D. vulgaris* NCIMB 8303 and *Microbacterium* sp. NCIMB 13776 in a continuous-flow packed-bed reactor. The Cr(VI) reducing activity of the columns was lost within 160 h (Humphries *et al.* 2004b). Industrial continuous systems are required to operate at high efficiency for extended periods because running an immobilized cell reactor is relatively economic, but growing cells, immobilizing, and filling the reactor is expensive and frequent downtime is unacceptable (Bucke 1986). Many biological systems are sensitive to alterations in pH, ionic strength or other parameters, which over a period of time may lead to reduced activity, and biosystems usually require physiologically compatible conditions (Thomas and Laval 1996).

An alternative, potentially more robust, alternative to bioreduction is to use a biologically-produced bioinorganic catalyst which, when dried and ground, was highly effective in the reduction of Cr(VI) (Mabbett *et al.* 2004). Growth-decoupled cells of *Desulfovibrio desulfuricans* NCIMB 8307 can be used to reduce Pd(II), via cellular hydrogenase activity (Mikheenko 2004), to cell-bound Pd(0) (Bio-Pd(0)) using H_2 as the electron donor (Lloyd *et al.* 1998). Recent studies showed that Bio-Pd(0) is more efficient at Cr(VI) reduction than live cells of *D. desulfuricans* or chemically reduced Pd(II), using either hydrogen or formate as the electron donor (Mabbett and Macaskie 2002). Pd(0) mediates homolytic bond cleavage of H_2, with the production of $H^{\bullet}$, which can then donate its electron to Cr(VI). Formate contains an electron pair, the negative charge of which is delocalised over the carboxyl group. This delocalised negative charge can come into close proximity with the Pd(0) surface, allowing chemisorption via interaction with vacant surface d-orbitals. This chemisorption destabilizes the formate molecule, weakening the

C-H bond, giving homolytic bond cleavage and entrapment of $H^{\bullet}$ by Pd(0), with consequent Cr(VI) reduction (Mabbett 2001; Mabbett *et al.* 2004).

As an alternative, *E. coli* could be used as the carrier biomass for Bio-Pd(0) since *E. coli* has good hydrogenase activity and has also been shown to reduce Pd(II) to Pd(0) (Mikheenko 2004). The ability of *E. coli* to reduce Tc(VII) anaerobically is well documented (Lloyd *et al.* 1997 a,b; Lloyd and Macaskie 1997) and growing cells of *E. coli* JCB387 were shown to accumulate Tc(VII) from solution and reduce it to a black precipitate using formate or H_2 as the electron donor (Lloyd and Macaskie 1997). Tc(VII) reduction was mediated via the activity of the hydrogenase 3 component of the formate hydrogenlyase (FHL) complex (Lloyd *et al.* 1997a). Resting cells of SRB have also been shown to couple formate or H_2 oxidation to Tc(VII) reduction via their cellular hydrogenase and are thought to have a simple FHL complex consisting of formate hydrogenlyase linked to hydrogenase via a cytochrome (see Lloyd *et al.* 1999b). Lloyd *et al.* (2001) compared Tc(VII) reduction by *D. vulgaris* NCIMB 8303 and *D. desulfuricans* NCIMB 8307, with similar rates observed between them when hydrogen (800 and 900 μmol Tc(VII) reduced g biomass^{-1} h^{-1}, respectively) or formate (150 and 200 μmol Tc(VII) reduced g biomass^{-1} h^{-1}, respectively) was used.

In a study comparing Tc(VII) reduction by *E. coli* strain MC4100 and *D. desulfuricans* NCIMB 8307, Tc(VII) reduction occurred at a faster rate with *D. desulfuricans* using either hydrogen or formate (800 and 150 μmol Tc(VII) reduced g biomass^{-1} h^{-1}, respectively) as electron donors, compared to *E. coli* strain MC4100 (12.5 (hydrogen) and 10.0 (formate) μmol Tc(VII) reduced g biomass^{-1} h^{-1}). In both cases, reduction was higher in the presence of H_2 than in its absence, suggesting hydrogenase was involved in both systems (Lloyd *et al.* 1999b). The lower activity of

E. coli MC4100 towards Tc(VII) reduction could be attributed to the lower hydrogenase activity in this organism as compared to *D. desulfuricans* (Lloyd *et al.* 1999b).

In order to further investigate the role of FHL in Tc(VII) reduction, mutants defective in various reductases were tested (Lloyd *et al.* 1997a). The *hyc* operon contains 9 genes (*hycA-I*) which are needed for synthesis of FHL. Tc(VII) reduction was unimpaired in only a *hycA* mutant, (which cannot synthesize the FHL repressor (HycA) and is, therefore upregulated with respect to FHL expression), where reduction of Tc(VII) was increased in the mutant strain compared to the parental *E. coli* strain. The upregulated strain (HD701) was adopted in the present study for the preparation of Pd(0) on the biomass in order to evaluate the role of hydrogenase in the reduction of Pd(II). Preliminary studies showed that the parental strain, *E. coli* MC4100, makes catalytically effective Bio-Pd(0) (Mikheenko 2004).

For industrial Cr(VI) reduction, retention of Bio-Pd(0) is important in order to limit downstream processing difficulties and maximize the potential use of the catalyst. The first objective of this study was to compare the catalytic efficacy of free and agar-immobilized Bio-Pd(0) produced using *E. coli* strains MC4100 (parental) and HD701 (*hycA* upregulated hydrogenase mutant), *D. vulgaris* NCIMB 8303, and *D. desulfuricans* NCIMB 8307, with respect to the ability of their respective Pd-bionanocatalysts to catalyze Cr(VI) reduction. The second objective was to evaluate reduction of Cr(VI) by the best Bio-Pd(0) in flow-through reactors and to characterize extended reactor performance with a view to potential industrial application.

Materials and Methods

Organisms and growth conditions

Desulfovibrio vulgaris NCIMB 8303 and *D. desulfuricans* NCIMB 8307 were maintained as described previously (Humphries and Macaskie 2002; Mabbett *et al.* 2002). For experiments, growing cultures (OD_{600} 0.8 ± 0.2) were produced by withdrawing 100 mL of actively growing culture and adding to 1 L fresh Postgate's medium C (Postgate 1979), followed by degassing with oxygen free nitrogen (OFN) for 20 min. The culture was harvested after 24 h (OD_{600} 0.8 ± 0.2).

E. coli strains MC4100 (parental) and HD701 (HycA-deficient mutant) were as described previously (Sauter *et al.* 1992; Lloyd *et al.* 1999b). Both strains were maintained aerobically at 30 °C on nutrient agar (Oxoid Ltd., UK) plates. Precultures were grown aerobically overnight in nutrient broth No. 2 (Oxoid) at 30 °C (Penfold *et al.* 2003). For experiments, growing cultures were produced by inoculating 1 L degassed fresh nutrient broth No. 2 with 100 µL preculture, followed by gassing with OFN for 20 minutes. Cultures were grown for 24 h in a 1 L closed anoxic bottle and maintained at 30 °C.

Preparation of cell suspensions

Resting cells of *D. vulgaris*, *D. desulfuricans* and *E. coli* were prepared as described previously (Humphries and Macaskie 2002). Cell concentrate was stored under nitrogen at 4 °C suspended in 20 mM 3-(N-Morpholino)propanesulfonic acid (MOPS)/ NaOH buffer, pH 7, until use (within 24 h of harvesting). The biomass concentration of the cell concentrate was estimated by measuring the OD_{600}, and conversion to dry cell weight using a previously determined calibration (A. C. Humphries, unpublished).

Preparation of Bio-Pd(0) on cells of *D. vulgaris*, *D. desulfuricans* and *E. coli*

The required volume of 2 mM Na_2PdCl_4 (98 %, Aldrich Chemicals, UK), adjusted to pH 2 with nitric acid, was placed in a 200 mL serum bottle sealed with a butyl-rubber stopper. The required volume of cell concentrate was added to give a final mass ratio of dry cells:Pd of 3:1. The suspension was incubated at 30 °C for 1 h to allow Pd(II) biosorption (deVargas *et al.* 2004). The suspension was then out-gassed with H_2 for 15 min, resulting in deposition of Pd(0) on the cell surface. The suspension was left overnight under H_2 (no residual Pd(II) remained in the supernatant by assay: Mikheenko 2004) before transferring to 50 mL serum bottles, and the Pd-coated cells were recovered by centrifugation (3800 g, 10 min). The pellet was washed once with distilled H_2O (dH_2O), three times with acetone, and placed in a 60 °C oven to constant weight. The dried solid ("Bio-Pd(0)") was ground to a fine powder with a pestle and mortar.

Transmission electron microscopy

Pellets of resting or palladised bacteria were rinsed twice with distilled water, fixed in 2.5 % (w/v) aqueous glutaraldehyde, washed once in distilled water and fixed in 1 % osmium tetroxide in 0.1 M phosphate buffer (pH 7, 60 min). Cells were dehydrated using an ethanol series (70, 90, 100, 100, 100 % dried ethanol; 15 min each step). After two 15 min washes in propylene oxide (1,2-epoxypropane), cells were embedded in epoxy resin (degassed under vacuum for 30 min) and the resin was left to polymerize for 24 h at 60 °C. Sections (100 – 150 nm thick) were cut from the resin block, placed onto a copper grid and viewed with a JEOL 120CX2 transmission electron microscope (TEM); accelerating voltage 80 kV.

Immobilization of Bio-Pd(0) preparations

Immobilization in agar beads (previously shown to retain integrity under continuous-flow) was done as described previously (Humphries *et al.* 2004a). The biomass content/ mL agar was 2.5 mg Bio-Pd(0) mL^{-1} or as described in individual experiments.

Chromate reduction by free and immobilized Bio-Pd(0) in batch suspensions

Reaction mixtures were set up in 12 mL serum bottles. Bio-Pd(0) beads (2 mL, 2.5 mg Bio-Pd(0) mL agar gel^{-1}) or free Bio-Pd(0) (5 mg) were suspended in 5 mL solution comprising 20 mM MOPS/ NaOH buffer and 25 mM each of sodium formate, sodium citrate, and sodium acetate, with 500 μM sodium chromate, pH 7. For anaerobic tests, reaction mixtures were degassed with OFN for 10 min before addition of chromate. Samples were withdrawn periodically (under OFN for anaerobic tests), via a syringe, and supernatants were analyzed for residual Cr(VI) using diphenylcarbazide (Pattanapipitpaisal *et al.* 2001).

Cr(VI) reduction by Bio-Pd(0) produced using *D. vulgaris*, *D. desulfuricans* and anaerobically grown *E. coli* in packed-bed continuous-flow columns

For continuous reduction studies, 4 mL Bio-Pd(0) agar beads (loading: 7.5 mg Bio-Pd(0) mL $agar^{-1}$; Pd(0) content: 1.87 mg mL $agar^{-1}$) were placed in a glass column (i.d. 12 mm, length 10 cm). Solution comprising 500 μM sodium chromate and 25 mM each of sodium formate, sodium citrate and sodium acetate, and 20 mM MOPS/ NaOH buffer, pH 7, was pumped upwards through the columns at a flow rate of 13.2 mL h^{-1}. Samples were withdrawn every 24 h for 108 h and analyzed for residual Cr(VI) using diphenylcarbazide (Pattanapipitpaisal *et al.* 2001). Control columns contained agar beads only.

Effect of inlet Cr(VI) concentration and Bio-Pd(0) loading and flow rate on the efficiency of Cr(VI) reduction

Packed-bed columns (as above) containing Bio-Pd(0) (*D. vulgaris*) agar beads (Bio-Pd(0) loading: 7.5 mg mL^{-1}) were challenged with the above solution containing sodium chromate at a concentration of 100 - 500 μM, at a flow rate of 13.2 mL h^{-1}. For testing the effect of Bio-Pd(0) concentration, Bio-Pd(0) (*D. vulgaris*) was immobilized in agar at loadings of 1.25, 2.5, 5.0, and 7.5 mg mL^{-1} (25 % of these amounts by mass as Pd(0)), and challenged with the above solution (with 100 μM sodium chromate) at various flow rates. Samples were withdrawn every 30 min at each flow rate until 3 consecutive concordant values were obtained. The flow rate giving 50 % removal of Cr(VI) ($FA_{1/2}$ value) was calculated to allow comparison between reactors. Columns containing agar beads were weighed prior to challenging with Cr(VI) solution, and again after, to allow calculation of column fluid volume. The residence time needed for 50 % Cr(VI) reduction ($RA_{1/2}$ value) was calculated by dividing the column fluid volume (0.5 mL) by the $FA_{1/2}$ value.

Where mass balances of Cr were to be calculated Cr(VI) in column input and outflow solutions was analyzed using diphenylcarbazide as above, and parallel samples were analyzed for total Cr using ICP-MS commercially (H_2b Analytical Services, Capenhurst, UK). The amount of Cr(III) retained in the columns was estimated as the difference between total Cr in the column inlet and outlet. No Cr(V) was detected in the system (Mabbett 2001).

Results and Discussion

Comparison of Cr(VI) reducing ability of Bio-Pd(0) produced with *D. vulgaris*, *D. desulfuricans* and *E. coli* strains

Previously the biosorption capacities for Pd(II) ($PdCl_4^{2-}$) onto protonated biomass of *D. desulfuricans*, *D. vulgaris* and *E. coli* strains MC4100 and HD701 were investigated (deVargas *et al.* 2004, M. Climo and L. E. Macaskie unpublished). In these biosorption experiments, resting cells were exposed to various concentrations of Pd(II) in the absence of electron donor and the biosorption capacity was calculated at equilibrium (deVargas *et al.* 2004). The highest capacity was seen in the hydrogenase upregulated *E. coli* strain HD701 (213.5 mg Pd/ g dry cell wt.) followed in the order *E. coli* strain MC4100 (181.2 mg Pd/ g dry cell wt.), *D. desulfuricans* (125.0 mg Pd/ g dry cell wt.) and *D. vulgaris* (106.3 mg Pd/ g dry cell wt.). This is noteworthy because the higher capacity of *E . coli* MC4100 cells for Pd(II) biosorption prior to H_2 addition (as compared to *D. vulgaris*) was inversely related to Bio-Pd(0) catalytic activity with respect to Cr(VI) reduction (see later). The biosorption step was essential for maximum accumulation of Pd(0) by subsequent bioreduction (Yong *et al.* 2002a) and the optimum pH was 2.0 – 2.5 (deVargas *et al.* 2004). This is because $PdCl_4^{2-}$ (the predominant species in solution) is sorbed most effectively at acidic pH, probably attributable to protonation of the biomass surface binding sites (deVargas *et al.* 2004). The biosorption time (1 h) was chosen for attainment of the biosorption equilibrium with minimum loss of metal-reducing hydrogenase activity (Mikheenko 2004). After 1 h at pH 2 purified periplasmic [NiFe] hydrogenase (*D. fructosovorans*) retained 32 % of its initial activity, but after 2 h the activity was negligible (Mikheenko 2004). Other studies have suggested that once the Pd-clusters reach a critical size enzymatically, reduction of more

Pd(II) is autocatalysed by the Pd(0) itself (see Yong *et al.* 2002b for discussion) until no more Pd(II) is present in solution.

Example electron micrographs of Pd-loaded cells of *D. desulfuricans*, *D. vulgaris* and *E. coli* strains MC4100 and HD701 are shown in Fig. 1 a - d, respectively. Mikheenko (2004) showed with *D. desulfuricans* that nucleation of Pd(0) occurs in the periplasmic space. The growing Pd(0) clusters then erupt through the outer membrane where they form dense agglomerates on the outer surface of the cell, attributable to subsequent autocatalytic reduction of Pd(II) from the bulk solution (Mikheenko 2004). Nucleation was attributed to the hydrogenase by the use of knock-out mutants in one or more of the hydrogenases of *D. fructosovorans* (Mikheenko 2004) and amine groups were suggested (by X-ray photoelectron spectroscopy: deVargas and Macaskie, 2004) to be involved in the initial uptake of Pd(II). Fig. 1 a - d shows the periplasmic location of Pd(0) deposit (arrowed) with the agglomerates processing outwards (double arrows). The loading of Pd(0) onto the cells was the same throughout (3:1 mass dry cell wt: mass of Pd) and the pattern of deposition reflects the distribution of the hydrogenases (Mikheenko 2004).

Lloyd *et al.* (1999) investigated Tc(VII) reduction by *E. coli* and *D. desulfuricans* NCIMB 8303 in a continuous-flow hollow-fiber membrane bioreactor. Reduction of Tc(VII) (80 %) occurred at flow rates of 0.7 mL h^{-1} (*E. coli* strain MC4100), 4 mL h^{-1} (*E. coli* strain HD701: hydrogenase upregulated mutant) and 11 mL h^{-1} (*D. desulfuricans*), reflecting the different activities of hydrogenase present in the *E. coli* strains and *D. desulfuricans*. *Desulfovibrio* has significantly more hydrogenase and hence by extrapolation probably more potential nucleation sites than *E. coli*. Fig. 1 a and b show that Pd(0) deposition is widespread in *D. desulfuricans* and *D. vulgaris*, with small crystals deposited uniformly throughout the periplasm. Pd deposition is less widespread in *E. coli* strains MC4100 and HD701 (Fig. 1 c, d) with extensive autocatalytic

projections visible (double arrows), attributable to the lower hydrogenase activity associated with this organism; the nascent depositing Pd(0) finds fewer nucleation sites, giving fewer, but larger, eventual deposits at the same biomass loading and with the same amount of available Pd(II). However, since the initial biosorption of Pd(II) was higher in the *E. coli* strains (see earlier) it must be assumed that some of the nucleation foci do not result in 'productive' nanocrystal growth, i.e. it can be suggested that only foci in close juxtaposition to hydrogenase can develop into Pd-nanocrystals and, ultimately, contribute to the cell surface 'decoration' seen in Fig. 1.

Reduction of Cr(VI) by palladised cells

The catalytic activity of the above Bio-Pd(0) samples, free in suspension and immobilized in agar, was evaluated in batch experiments. Negligible Cr(VI) reduction was seen in all controls where Bio-Pd(0) was present in suspension in the absence of electron donor, but approx. 20 % Cr(VI) was removed onto agar-immobilized Bio-Pd(0), attributable to absorption by the immobilization matrix (no biological activity was present since the catalyst was dried and ground: see Materials and Methods).

The rates of Cr(VI) reduction by Bio-Pd(0) produced using *D. vulgaris* and *D. desulfuricans* were similar, and higher compared to Bio-Pd(0) produced using *E. coli* strains MC4100 and HD701 (approx. 1.7 and 1.3 fold, respectively: Table 1). After 5 h, Bio-Pd(0) produced using *D. desulfuricans*, *D. vulgaris* and *E. coli* strain HD701 had reduced similar amounts of Cr(VI), significantly more than Bio-Pd(0) produced using *E. coli* strain MC4100 (Fig. 2). The lower rate of Cr(VI) reduction may reflect the lower hydrogenase activity present in *E. coli* and consequent display of fewer, larger agglomerates (Fig. 1 c, d). A 2-fold difference in particle diameter would give a 4-fold increase in catalytic surface area (assuming spherical particles and calculating surface area of a sphere). Using *Desulfovibrio* it was shown that cells containing a large number

of small deposits were catalytically more active compared to cells with larger but fewer agglomerations for the same deposited mass of Pd(0) (Mikheenko 2004). The rate of Cr(VI) reduction by Bio-Pd(0) produced using *E. coli* strains MC4100 and HD701 (Table 1) was significantly different (99.99 % significant difference by t-test analysis), suggesting that the higher activity of hydrogenase, which is upregulated in *E. coli* HD701 during pre-growth, affects the catalytic "quality" of Bio-Pd(0) produced upon the cells. Inspection of Fig. 1 suggests that cells of HD701 apparently had a higher proportion of small as compared to larger, extruded agglomerations but interpretation of EM data is not quantitative since only a few representatives of the population can be examined.

Using agar-immobilized Bio-Pd(0), the homogeneity of distribution of Bio-Pd(0) throughout the gel matrix was shown previously using magnetic resonance imaging (Humphries *et al.* 2004a). The initial rate of Cr(VI) reduction was reduced by 32 ± 3 % (pooled data for 4 strains, aerobic and anaerobic; mean ± SEM; n=8) when Bio-Pd(0) was immobilized in agar. A direct relationship between the amount by which immobilization affects Cr(VI) reduction and the amount of Cr(VI) reduced in the initial 1.5 h by corresponding non-immobilized Bio-Pd(0) is seen in Fig. 3 ($R^2 = 0.98$). The linear relationship of Fig. 3 suggests the effect of immobilization is chemical and not biological i.e. it is the matrix which affects the rate of reduction when the catalyst is immobilized, and not the Bio-Pd(0) *per se*. Fig. 3 suggests that immobilization results in diffusional limitations of either Cr(VI) and formate into, or Cr(III) out of, the agar bead. This may be attributed to diffusional constraints associated with the immobilization matrix, e.g. end product fouling by Cr(III) could occur if this cannot be removed effectively; local precipitation of $Cr(OH)_3$ could occur (discussed elsewhere: Mabbett 2001), blocking matrix pores and access to

embedded Bio-Pd(0). Attempts to visualise the process spatially using magnetic resonance (MR) imaging were unsuccessful. The Cr(III) ion can alter the MR proton signal; paramagnetic species are widely used as contrast agents in MRI (see Paterson-Beedle *et al.* 2001; Nott *et al.* 2002 for discussion) and it should be possible to visualise the appearance/ accumulation of Cr(III) species spatially with time. However this was not possible since the ferromagnetic Bio-Pd(0) (Mikheenko, 2004) was itself visualised by MRI (Humphries *et al.* 2004a) and it was not possible to differentiate between the MR effects of Cr(III) and Pd(0) on the proton signal of the surrounding water. However a mass balance analysis showed that negligible Cr was retained within the matrix overall, and it is suggested that the rate of scavenging of Cr(III) by the citrate 'trapping agent' and movement of the Cr(III)-citrate complex out of the gel may have been limiting (see later). Previous studies had suggested that only low diffusional limitations were present in agar beads (Humphries *et al.* 2004b). However, these studies focused on Cr(VI) reduction by resting live cells of *D. vulgaris*, shown previously to have a lower K_m value than palladised cells, and thus higher affinity for Cr(VI) (Mabbett and Macaskie 2001, A. C. Humphries and L. E. Macaskie unpublished). Therefore Cr(VI) reduction by palladised cells of *D. vulgaris* could be more affected by diffusional constraints which result in a lower concentration of Cr(VI) within the agar beads.

Chromate reduction by Bio-Pd(0) produced using *D. vulgaris*, *D. desulfuricans* and anaerobically grown *E. coli* in continuous packed-bed columns

The above suggested that Bio-Pd(0) produced on *Desulfovibrio* biomass is a better catalyst per unit of mass than corresponding Bio-Pd(0) carried on *E. coli*, even by using the superior hydrogenase-upregulated strain HD701 (Table 1). The respective efficiencies and longevities were compared using continuous-flow reactors. Agar-immobilized Bio-Pd(0), produced using *D.*

vulgaris, *D. desulfuricans* and the two *E. coli* strains, was packed into columns and challenged with a solution containing 500 μM sodium chromate at a flow rate of 13.2 mL h^{-1}. All column experiments were carried out in air since the effect of aerobic operation was small (Table 1). Columns containing Bio-Pd(0) produced using *D. vulgaris* and *D. desulfuricans* reduced Cr(VI) with similar efficiency, with approximately 50 % Cr(VI) reduction occurring after 24 h. Reduction efficiency was gradually lost until it stabilized at 20 % reduction after 96 h (Fig. 4). In contrast, columns containing Bio-Pd(0) produced using *E. coli* HD701 and MC4100 reduced Cr(VI) poorly in continuous-flow even though the batch test (Fig. 2) had suggested comparable activity between *E. coli* strain HD701 and *Desulfovibrio* spp. After 24 h only 16 % (*E. coli* strain HD701) and 10 % (*E. coli* strain MC4100) of Cr(VI) entering the columns was reduced, with reduction efficiency stabilizing at 5 % after 48 h (Fig. 4). At 24 h the difference between Bio-Pd(0) produced using *D. vulgaris* or *D. desulfuricans* and *E. coli* HD701 was approx. 3 fold.

Effect of inlet Cr(VI) concentration on the efficiency and longevity of reduction by Bio-Pd(0) produced using *D. vulgaris*

By imposing a flow rate constraint (thus effectively reducing the reaction time available for the Cr(VI)-Bio-Pd(0) interaction at the local concentration of Cr(VI) in each volumetric element) at a given input Cr(VI) concentration, the data becomes indicative of either the affinity of the Bio-Pd(0) for the Cr(VI) or the time required for dissociation of the Bio-Pd(0)-Cr(III) complex (see later). The reasons for the differences (see Fig. 4) may relate to the chemical nature of the subcellular 'environment' housing the Pd(0) nanoparticles in the two Gram negative genera. Inspection of Fig. 1 shows that the *Desulfovibrio* strains have many small particles distributed over the cell surface, whilst the *E. coli* strains, for the same amount of Pd per mass of biomass, have fewer, larger Pd-particles. A time-dependent diffusion of formate into, or $H^{\bullet}$ out of, the

Pd(0) could be involved to account for this (electron donor was present to excess; Pd(0) splits formate to yield hydrogen on the catalyst itself: see Mabbett et al 2004 for discussion). Since the *Desulfovibrio* Bio-Pd(0) was clearly superior to that of *E. coli* Bio-Pd(0) (Fig. 4) further studies focused on Bio-Pd(0) prepared on *Desulfovibrio vulgaris*.

Five columns containing *D. vulgaris* Bio-Pd(0) immobilized in agar at a loading of 7.5 mg mL^{-1} (1.875 mg mL $Pd(0)^{-1}$) were challenged with chromate (100 - 500 μM) in the presence of excess electron donor (formate), at a flow rate of 13.2 mL h^{-1}. Duplicate columns challenged with chromate in the absence of electron donor gave negligible removal of Cr(VI). Removal of Cr(VI) by palladised biomass over time is shown in Fig. 5. After 24 h the amount of Cr(VI) removed was linearly related ($R^2 = 0.998$) to the input concentration of Cr(VI) up to an input concentration of 300 μM Cr(VI) (Table 2). This, therefore suggested that 300 μM was the saturating concentration of Cr(VI), which is in agreement with earlier studies using free and agar-immobilized *D. vulgaris* Bio-Pd(0) in batch suspensions (A. C. Humphries and L. E. Macaskie unpublished).

High Cr(VI) reduction values were observed at the beginning of column operation, but over time the concentration of Cr(VI) in the effluent increased, with reduction ceasing after 120 h (500 μM), 168 h (400 μM), 216 h (300 μM), and 288 h (200 μM $[Cr(VI)]_{inlet}$). These duration's correspond to the time when approximately the same amount of Cr(VI) had passed through the columns (approx. 0.7 mmoles). Loss of Cr(VI) reduction may therefore be due to gradual 'poisoning' or fouling of the Bio-Pd(0) catalyst by Cr(III) (i.e. $Cr(OH)_3$). Indeed, columns using *D. desulfuricans* Bio-Pd(0) maintained at pH 3 (at which pH Cr(III) would be maintained as soluble Cr^{3+}) gave 100 % reduction of Cr(VI) over several weeks (Mabbett 2001). To establish

whether the liberated Cr(III) is eluted as the soluble citrate complex or whether Cr(III) dissociates from the citrate complex and precipitates as $Cr(OH)_3$ within the columns ICP-MS analysis was used to determine the total Cr concentration in inlet and outlet column samples. The concentrations of Cr_{total} in the inlet and outflow were approx. equal (i.e. chromium is retained minimally in the columns). However a small amount of Cr(III) retention over many hours could accumulate to inhibitory concentrations.

The data in Fig. 5 were fitted with trend lines, the equations for which (Table 3; eqns. 1 - 5) follow the form

$$\% \text{ Reduction at time t (h)} = (\text{gradient x time}) + \text{intercept} \quad (6)$$

Plotting the intercept value of Equations (1) – (5) against the $[Cr(VI)]_{inlet}$ and fitting a trend line gives a line with equation (correlation coefficient 0.94)

$$\text{Intercept} = -0.06[Cr(VI)]_{inlet} + 73.02 \quad (7)$$

Plotting the $[Cr(VI)]_{inlet}$ against the gradients of Equations (1) – (5) gives a line with equation (correlation coefficient 0.99):

$$\text{Gradient} = -0.11\text{Ln}[Cr(VI)]_{inlet} + 0.36 \quad (8)$$

Incorporating Equations (7) and (8) into Equation (6) gives an overall equation relating the % Cr(VI) reduction at time t, with $[Cr(VI)]_{inlet}$ and time:

$$\% \text{ Reduction at time t} = (-0.11\text{Ln}[Cr(VI)]_{inlet} + 0.36)\text{time} + (-0.06[Cr(VI)]_{inlet} + 73.02) \quad (9)$$

Time is in h and $[Cr(VI)]_{inlet}$ in units of μM. Equation (9) allows the percentage of Cr(VI) reduced to be calculated for any time between 0 and 96 h, and for any $[Cr(VI)]_{inlet}$ between 100 and 500 μM, at a flow rate of 13.2 mL h^{-1} and a Bio-Pd(0) loading of 7.5 mg mL^{-1}. Using equation (9) to predict values for % Cr(VI) reduction gave figures within 5 % of those experimentally determined (Table 4). Thus, although the column activity decreased with time

(possibly attributable to a gradual fouling by $Cr(OH)_3$: see above) this can be calculated into a working definition of reactor activity at any chosen time (eqn 9), with an accuracy of within 5 %.

Effect of flow rate and Bio-Pd(0) (*D. vulgaris*) loading on the efficiency of Cr(VI) reduction

Bio-Pd(0) was immobilized in agar at different loadings for study of chromate reduction in continuous packed-bed columns. Each column was challenged at various flow rates as described in Materials and Methods. Controls for all experiments consisted of columns containing agar beads (no Bio-Pd(0)) and duplicate Bio-Pd(0) columns challenged with 100 μM sodium chromate in the absence of electron donor. No Cr(VI) reduction occurred in the control columns. The percentage removal of Cr(VI) relative to the flow rate is shown in Fig. 6 and this was used to compare the performance of Bio-Pd(0) immobilized in agar at concentrations between 1.25 and 7.5 mg mL^{-1}.

Negligible Cr(VI) was reduced using Bio-Pd(0) immobilized at a loading of 1.25 mg Bio-Pd(0) mL^{-1}). For higher concentrations of Bio-Pd(0) flow rate/ activity plots (Fig. 6) were used to find the flow rate at which 50 % Cr(VI) was reduced ($FA_{1/2}$ value). The $FA_{1/2}$ value was then used to calculate the $RA_{1/2}$ value (residence time for 50 % Cr(VI) reduction) for each column (Table 5). When the Bio-Pd(0) loading was increased from 5.0 to 7.5 mg mL^{-1} the $RA_{1/2}$ value only decreased slightly compared to when the loading was increased from 2.5 to 5.0 mg mL^{-1}. This may suggest that the efficiency of Cr(VI) reduction is limited either by mass transfer (of Cr(VI) and formate in, and Cr(III) out of the Bio-Pd(0) beads) or by the Bio-Pd(0) catalyst surface area available for reaction, i.e. functionally $V = V_{max}$.

Doubling the Bio-Pd(0) loading from 1.25 to 2.5, and from 2.5 to 5.0 mg mL^{-1} resulted in incremental increases in the % Cr(VI) reduced at a fixed flow rate of 2.91 mL h^{-1} (see starred sections on Fig. 6), suggesting that the rate of Cr(VI) reduction is directly related to the amount

of biocatalyst present. Halving the flow rate for any chosen Bio-Pd(0) loading resulted in progressively larger incremental increases in the % Cr(VI) reduced. For example at a Bio-Pd(0) loading of 2.5 mg mL agar^{-1}, increasing the flow rate from 5.82 to 11.64 mL h^{-1} resulted in an approx. 20 % drop in Cr(VI) reduction. Increasing the flow rate from 2.91 to 5.82 mL h^{-1} resulted in an approx. 10 % drop in Cr(VI) reduction (Fig. 6). These relationships suggested that it would be possible to develop a model to describe the system.

Modeling of immobilized Bio-Pd(0) processes

Enzymes are composed of amino acids that are used to construct binding sites with high specificity. However, these groups are poorly suited to binding and catalyzing redox reactions of small molecules like H_2. Metallocofactors are therefore incorporated into enzymes to provide the binding interactions for small molecules and to confer the catalytic capability needed to achieve redox transformations (Rees 2002). Metalloproteins (e.g.hydrogenase), consist of one or more metals (e.g. Fe, Ni) associated with inorganic groups interacting through protein ligands (e.g. cysteine, histidine) (Rees 2002). In this sense Bio-Pd(0) can be considered as an 'artificial' enzyme. The Pd-bionanocluster system is redox-active and could be considered as analogous to metalloenzymes because it is localized onto or near to cellular hydrogenases (Mikheenko 2004) and is probably held supported on a peptide-based matrix since coordination of the initial Pd(II) onto amino groups was shown by X-ray photoelectron spectroscopy (deVargas and Macaskie 2004). Effectively it could therefore be considered functionally as a 'hydrogenase amplifier' in the current context and in this case the possibility exists to model the system according to applied enzyme kinetics. This approach was tested as described below.

Under steady-state conditions the apparent kinetic parameters in continuous-flow packed-bed enzyme reactors can be calculated using an integrated form of the Michaelis-Menten equation (Macaskie *et al.* 1995, developed from Fulbrook, 1983):

$$E_oK_3 = F[S_oX + K_m.\ln(1/1\text{-}X)] \qquad (10),$$

where K_3 and K_m are intrinsic kinetic constants, S_o is the input substrate concentration, F is the flow rate of solution through the column, E_o is the 'total enzyme present' (dimensionless). X is the conversion factor defined as $(S_o\text{-}S)/S_o$, where S is the residual substrate concentration at time t (Macaskie *et al.* 1995). In this case it is assumed that $[S_o] \equiv [Cr(VI)]_{inlet}$ and $[S] \equiv [Cr(VI)]_{outlet}$. Given equation (10), then at two substrate concentrations S_{o1} and S_{o2},

$$E_oK_3 = F[S_{o1}X_1 + K_m.\ln(1/1\text{-}X_1)] \qquad (11);$$

$$E_oK_3 = F[S_{o2}X_2 + K_m.\ln(1/1\text{-}X_2)] \qquad (12).$$

Apparent K_m values ($K_{m\ app}$) were calculated by substitution into equation (11) and (12) using the data presented in Fig. 5 as follows. Flow rate and Bio-Pd(0) concentration were held constant (13.2 mL h^{-1} and 7.5 mg Bio-Pd(0) mL gel^{-1}, respectively) thus equations (11) and (12) can be simplified to (with $K_{m\ app}$ the only unknown):

$$[S_{o1}X_1 + K_{m\ app}.\ln(1/1\text{-}X_1)] = [S_{o2}X_2 + K_{m\ app}.\ln(1/1\text{-}X_2)] \qquad (13).$$

Corresponding values for X_1 and X_2 for Cr(VI) concentrations S_{o1} and S_{o2} were obtained from Fig. 6. A value for K_m as operating in the immobilized Bio-Pd(0) reactor ($K_{m\ app}$) was calculated by substitution into equation (13). A value for $K_{m\ app}$ of ~ 430 μM was achieved at low initial substrate concentration (below 300 μM). This value is lower than that calculated previously for free Bio-Pd(0) in batch suspension (0.6 - 0.7 mM: A. C. Humphries and L. E. Macaskie unpublished) and suggests that in a flow-through system the Cr(III) product could be removed more easily by the incoming supply of fresh citrate to complex Cr(III) away from the catalyst

The validity of using an enzyme kinetic approach to describe Cr(VI) reduction by continuous-flow packed-bed reactors containing agar-immobilized Bio-Pd(0) was then tested as shown in Table 6 by substituting in the $K_{m\ app}$ value calculated as above. Calculation of an 'unknown' E_{o2} gave a value within 11 % of the actual E_{o2} value known from the Bio-Pd(0) actually put into the reactor, suggesting that Bio-Pd(0) can be considered an 'artificial' enzyme for the application of enzyme kinetics to describe reactor activity. As such, it would become possible to compare directly reactors containing *D. vulgaris* Bio-Pd(0) against comparable bioreactors containing live biomass. A previous study (A. C. Humphries and L. E. Macaskie unpublished) suggested that $K_{m\ app}$ of live cells was lower than that for Bio-Pd(0). This suggests live cells would be better for a final 'polishing' step (a high affinity for low concentrations of Cr(VI)), whilst Bio-Pd(0) (low affinity for Cr(VI)) would be more applicable to industrial wastes at higher concentrations presented under non-physiological conditions such as acidic pH.

Relationship between hydrogenase activity and catalytic activity of the Bio-Pd(0) produced

The four strains used in this study, *E. coli* MC4100 and HD701, *D. desulfuricans* NCIMB 8307 and *D. vulgaris* NCIMB 8303, share the ability to reduce Pd(II) to Pd(0) in the presence of H_2. Bio-Pd(0) produced using the SRB strains was catalytically more active compared to Bio-Pd(0)

produced with *E. coli* strains MC4100 and HD701, possibly attributable to the deposition of smaller, more numerous Pd-particles (see earlier). *E. coli* strain HD701 produced Bio-Pd(0) that was catalytically more active than *E. coli* strain MC4100, which suggested a possible role for upregulated hydrogenase in controlling the 'quality' of the Bio-Pd(0) produced, but with a caveat as described below.

HycA is a regulatory protein in *E. coli*, negatively regulating FhlA, a transcriptional activator that is needed for expression of the *hyc, hyp, hyf* operons and the gene *fdhF* (Skibinski *et al.* 2002, Fig. 7). Of relevance to this study, the *hyc* operon encodes hydrogenase 3, which together with formate dehydrogenase H (Fdh-H encoded by the gene *fdhF*) forms the hydrogen evolving, membrane associated, formate hydrogenlyase system (FHL-1) (Jacobi *et al.* 1992). The *hyp* operon comprises several genes that are needed for the post-translational modification of hydrogenases 1-3 (Sauter *et al.* 1992). The role of hydrogenase 1 in *E. coli* is not well established, but it may play a role in hydrogen recycling, whilst hydrogenase 2 has a respiratory role by conserving energy released by hydrogen oxidation (Messenger and Green 2003). The *hyf* operon encodes hydrogenase 4, which, together with Fdh-H, forms a second formate hydrogenlyase pathway (FHL-2) in *E. coli*, which, unlike the FHL-1 system, is an energy-conserving proton-translocating system (Skibinski *et al.* 2002). Mutations in *hycA* have a pleiotrophic effect in *E. coli* with deletions resulting in increased activity of formate dehydrogenase H, and hydrogenases 1-4. The increased activity of Bio-Pd(0) produced using *E. coli* HD701 (compared to the parental strain) cannot therefore be attributed conclusively at this stage to any one hydrogenase and further studies are needed to relate the catalytic activity of Bio-Pd(0) produced by *E. coli* strains to increases in specific hydrogenase activities.

Potential applications of Bio-Pd(0) to industrial wastes containing Cr(VI): wider implications

Using Bio-Pd(0) to reduce Cr(VI) may appear uneconomic because palladium is an expensive metal. However palladium and other precious metals are readily available within automotive catalyst leachates, electronic scrap and industrial processing wastes. Previous studies have shown that *D. desulfuricans* and *E. coli* can be used to biorecover palladium from industrial wastes and leachates (Yong *et al.* 2003, Mabbett 2001, D. Sanyahumbi and L. E. Macaskie unpublished) without the catalytic activity of the consequent Bio-Pd(0) being adversely affected by the presence of other metal elements from the waste in the biorecovered material (Mabbett 2001).

The need for electron donor is another consideration. This study used formate because the concentration of this can be accurately known: the HCOOH is split by the Pd(0) to give hydrogen, or more correctly, free, highly reactive $H^{\bullet}$ (see Mabbett *et al.* 2004). Hydrogen itself is an excellent electron donor (Mabbett 2001). Hydrogen can be produced fermentatively by *E. coli* at the expense of industrial sugar wastes, mediated by the formate hydrogenlyase (FHL-1) system in the synthetic direction (c.f. for Pd(II) reduction hydrogenase acts catabolically, breaking down formate and hydrogen) (Penfold *et al.* 2003). This multienzyme complex catalyses the formation of H_2 and CO_2 via the oxidation of formate in a homeostatic response to the reduction in pH caused by end products of mixed acid fermentation (Penfold *et al.* 2003). *E. coli* HD701 is upregulated with respect to FHL expression (see earlier: Sauter *et al.* 1992) resulting in an enhanced ability to produce H_2 (Bio-H_2) compared to the parental strain (MC4100) (Penfold *et al.* 2003). Potentially a system for the treatment of three industrial wastes could be engineered in which Bio-H_2 produced from industrial sugar waste (waste 1) is used initially as an electron donor for palladium recovery from industrial liquid waste (waste 2) (Yong *et al.* 2003) to produce

Bio-Pd(0). Bio-H_2 and Bio-Pd(0) synthesized from waste sources could then be used in conjunction to remediate Cr(VI) containing wastewater (waste 3) (Macaskie *et al.* 2005, Humphries *et al.*, unpublished). Since the palladium and hydrogen are both sourced from waste from the precious metal (Mabbett *et al.* 2004) and food (Penfold *et al.* 2003) sectors, respectively, a substantial economic benefit would result from the conversion of these wastes into useful products, avoiding landfill taxes and ensuring compliance with current legislation on disposal of solid scrap. Use of biorecovered materials would mitigate against the cost of the Cr(VI) treatment process, whilst at the same time permitting application outside the confines of physiological constraints (Mikheenko 2004).

Acknowledgements

We wish to acknowledge the financial support of the EPSRC (Studentship Number 00318650 to ACH and Grant Number GR/NO8445 to IPM) . The authors would like to thank Professor A. Böck (Lehrstuhl fur Mikrobiologie der Universtat, Munich, Germany) for providing *E. coli* HD701. LEM was supported by an Industry Fellowship from the Royal Society.

References

Bae W, Kang T, Jung J, Park C, Choi S, Jeong B. 2000a. Purification and characterization of NADH-dependent Cr(VI) reductase from *Escherichia coli* ATCC 33456. J Microbiol Biotechnol. 10:580-586.

Bae WC, Kang TG, Kang IK, Won YJ, Jeong BC. 2000b. Reduction of hexavalent chromium by *Escherichia coli* ATCC 33456 in batch and continuous cultures. J Microbiol. 38:36-39.

Bucke C. 1986. Methods of immobilizing cells. In: Webb C, Black GM, Atkinson B, editors. Process Engineering Aspects of Immobilized Cell System. Rugby: Institution of Chemical Engineers. p20-30

Chen JM, Hao OJ. 1998. Microbial chromium (VI) reduction. Crit Rev Environ Sci Technol. 28:219-251.

Costa M. 2003. Potential hazards of hexavalent chromate in our drinking water. Toxicol Appl Pharmacol. 188:1-5.

deVargas I, Macaskie LE 2004. In Final Report, Selective Separation of Strategic and Precious Metals EU Contract No. GIRD-CT-2000-00300.

daVargas I, Macaskie LE, Guibal E. 2004. Biosorption of palladium and platinum by sulfate-reducing bacteria. J Chem Technol Biotechnol. 79:49-56.

Dube BK, Tewari K, Chatterjee J, Chatterjee C. 2003. Excess chromium alters uptake and translocation of certain nutrients in *Citrullus*. Chemosphere. 53:1147-1153.

Fulbrook PD. 1983. Practical applied kinetics. In: Godfrey T, Reichelt J, editors. Industrial Enzymology. Macmillan Publishers Ltd.

Guha H, Jayachandran K, Maurrasse F. 2001. Kinetics of chromium (VI) reduction by a type strain *Shewanella alga* under different growth conditions. Environ Pollut. 115:209-218.

Humphries AC, Nott KP, Hall LD, Macaskie LE. 2004a. Continuous removal of Cr(VI) from aqueous solution catalysed by palladised biomass of *Desulfovibrio vulgaris* NCIMB 8303. Biotechnol Lett. 26:1529-1532.

Humphries AC, Nott KP, Hall LD, Macaskie LE. 2004b. Reduction of Cr(VI) by immobilized cells of *Desulfovibrio vulgaris* NCIMB 8303 and *Microbacterium* sp. NCIMB 13776. Biotechnol Bioeng. in press.

Humphries AC, Macaskie LE. 2002. Reduction of Cr(VI) by *Desulfovibrio vulgaris* and *Microbacterium* sp. Biotechnol Lett. 24:1261-1267.

Ishibashi Y, Cervantes C, Silver S. 1990. Chromium reduction in *Pseudomonas putida*. Appl Environ Microbiol. 56:2268-2270.

Jacobi A, Rossmann R, Bock A. 1992. The *hyp* operon gene products are required for the maturation of catalytically active hydrogenase isoenzymes in *Escherichia coli*. Arch Microbiol. 158:444-451.

Korngold E, Belayev N, Aronov L. 2003. Removal of chromates from drinking water by anion exchangers. Sep Purif Technol. 33:179-187.

Llovera S, Bonet R, Simonpujol MD, Congregado F. 1993. Chromate reduction by resting cells of *Agrobacterium radiobacter* EPS 916. Appl Environ Microbiol. 59:3516-3518.

Lloyd JR, Mabbett AN, Williams DR, Macaskie LE. 2001. Metal reduction by sulphate-reducing bacteria: physiological diversity and metal specificity. Hydrometallurgy. 59:327-337.

Lloyd JR, Ridley J, Khizniak T, Lyalikova NN, Macaskie LE. 1999a. Reduction of technetium by *Desulfovibrio desulfuricans*: Biocatalyst characterization and use in a flowthrough bioreactor. Appl Environ Microbiol. 65:2691-2696.

Lloyd JR, Thomas GH, Finlay JA, Cole JA, Macaskie LE. 1999b. Microbial reduction of technetium by *Escherichia coli* and *Desulfovibrio desulfuricans*: Enhancement via the use of high-activity strains and effect of process parameters. Biotechnol Bioeng. 66:122-130.

Lloyd JR, Yong P, Macaskie LE. 1998. Enzymatic recovery of elemental palladium by using sulfate-reducing bacteria. Appl Environ Microbiol. 64:4607-4609.

Lloyd JR, Cole JA, Macaskie LE. 1997a. Reduction and removal of heptavalent technetium from solution by *Escherichia coli*. J Bacteriol. 179:2014-2021.

Lloyd JR, Harding CL, Macaskie LE. 1997b. Tc(VII) reduction and accumulation by immobilized cells of *Escherichia coli*. Biotechnol Bioeng. 55:505-510.

Lovley DR, Phillips EJP. 1994. Reduction of chromate by *Desulfovibrio vulgaris* and its c_3 cytochrome. Appl Environ Microbiol. 60:726-728.

Mabbett AN, Yong P, Farr PG, Macaskie LE. 2004. Reduction of Cr(VI) by palladised biomass of *Desulfovibrio desulfuricans* ATCC 29577. Biotechnol Bioeng. 87:104-109.

Mabbett AN, Lloyd JR, Macaskie LE. 2002. Effect of complexing agents on reduction of Cr(VI) by *Desulfovibrio vulgaris* ATCC 29579. Biotechnol Bioeng. 79:389-397.

Mabbett AN, Macaskie LE. 2002. A new bioinorganic process for the remediation of Cr(VI). J Chem Technol Biotechnol. 77:1169-1175.

Mabbett AN, Macaskie LE. 2001. A novel isolate of *Desulfovibrio* sp. with enhanced ability to reduce Cr(VI). Biotechnol Lett. 23:683-687.

Mabbett AN. 2001. The reduction and recovery of chromium (VI) from industrially polluted wastewaters using sulphate-reducing bacteria. *Ph.D Thesis*. The University of Birmingham, England.

Macaskie LE, Empson RM, Lin F, Tolley MR. 1995. Enzymatically-mediated uranium accumulation and uranium recovery using a *Citrobacter* sp immobilized as a biofilm within a plug-flow reactor. J Chem Technol Biotechnol. 63:1-16.

Macaskie LE, Baxter-Plant VS, Creamer NJ, Humphries AC, Mikheenko IP, Mikheenko, P, Penfold DW, Yong P. 2005. Applications of bacterial hydrogenases in waste decontamination, manufacture of novel bionanocatalysts and in sustainable energy. Biochem. Soc. Trans. 33: 76-79.

Messenger SL, Green J. 2003. FNR-mediated regulation of *hyp* expression in *Escherichia coli*. FEMS Microbiol Lett. 228:81-86.

Mikheenko I. 2004. Nanoscale palladium recovery. *Ph.D Thesis*. The University of Birmingham, England.

Nott KP, Paterson-Beedle M, Macaskie LE, Hall LD. 2001. Visualisation of metal deposition in biofilm reactors by three-dimensional magnetic resonance imaging (MRI). Biotechnol Lett. 23:1749-1757.

Paterson-Beedle M, Nott KP, Macaskie LE, Hall LD. 2001. Study of biofilm within a packed-bed reactor by three-dimensional magnetic resonance imaging. In: Doyle RD, editor. Microbial Growth in Biofilms, Pt B. San Diego; London. P 285-305

Pattanapipitpaisal P, Brown NL, Macaskie LE. 2001. Chromate reduction by *Microbacterium liquefaciens* immobilized in polyvinyl alcohol. Biotechnol Lett. 23:61-65.

Penfold DW, Forster CF, Macaskie LE. 2003. Increased hydrogen production by *Escherichia coli* strain HD701 in comparison with the wild-type parent strain MC4100. Enzyme Microb Technol. 33:185-189.

Postgate JR. 1979. The Sulphate-reducing Bacteria. Cambridge: Cambridge University Press.

Rees DC. 2002. Great metalloclusters in enzymology. Annu Rev Biochem. 71:221-246.

Sauter M, Bohm R, Bock, A. 1992. Mutational analysis of the operon (Hyc) determining hydrogenase-3 formation in *Escherichia coli*. Mol Microbiol. 6:1523-1532.

Shi XL, Chiu A, Chen CT, Halliwell B, Castranova V, Vallyathan V. 1999. Reduction of chromium (VI) and its relationship to carcinogenesis. J Toxicol Env Health Pt B Crit Rev. 2:87-104.

Skibinski DAG, Golby P, Chang YS, Sargent F, Hoffman R, Harper R, Guest JR, Attwood MM, Berks BC, Andrews SC. 2002. Regulation of the Hydrogenase-4 Operon of *Escherichia coli* by the σ^{54}-Dependent Transcriptional Activators FhlA and HyfR. J Bacteriol.184:6642-6653.

Tebo BM, Obraztsova AY. 1998. Sulfate-reducing bacterium grows with Cr(VI), U(VI), Mn(IV), and Fe(III) as electron acceptors. FEMS Microbiol Lett. 162:193-198.

Thomas JM, Laval JM. 1996. Enzyme Technology. In: Balasubramanian D, Bryce CFA, Dharmalingam K, Green J, Jayaraman K, editors. Concepts in Biotechnology. Hyderabad: University Press (India).

Yong P, Rowson NA, Farr JPG, Harris IR, Macaskie LE. 2003. A novel electrobiotechnology for the recovery of precious metals from spent automotive catalysts. Environ Technol. 24:289-297.

Yong P, Rowson NA, Farr JPG, Harris IR, Macaskie LE. 2002a. Bioaccumulation of palladium by *Desulfovibrio desulfuricans*. J Chem Technol Biotechnol. 77:593-601.

Yong P, Rowson NA, Farr JPG, Harris IR, Macaskie LE. 2002b. Bioreduction and biocrystallization of palladium by *Desulfovibrio desulfuricans* NCIMB 8307. Biotechnol Bioeng. 80: 369-379.

Table 1: Effect of Bio-Pd(0) bacterial source on initial rates of Cr(VI) reduction by Bio-Pd(0) in batch suspensions.

Bacterial strain	Initial rate[a] of Cr(VI) reduction (nmol Cr(VI) h^{-1} mg Bio-Pd(0)$^{-1}$)	
	Reduction in air	Reduction under OFN[b]
Bio-Pd(0) (*D. vulgaris*)	152 ± 7	175 ± 32
Bio-Pd(0) (*D. desulfuricans*)	166 ± 22	168 ± 15
Bio-Pd(0) (*E. coli* MC4100)	91 ± 15	115 ± 16
Bio-Pd(0) (*E. coli* HD701)	120 ± 10	140 ± 7

Bio-Pd(0) samples (prepared as described in Materials and Methods and shown in Fig. 1) were challenged with 500 μM Cr(VI), 25 mM each of formate, acetate, and citrate, 20 mM MOPS/ NaOH, pH 7. Data are means ± SEM from 3 experiments.

[a]Initial rates were taken over the 1ST 1.5 h as gradients from linear regions of the appropriate graphs.

[b]OFN = Oxygen Free Nitrogen

Table 2: Cr(VI) removal after 24 h by immobilized *D. vulgaris* Bio-Pd(0)

Initial Cr(VI) concentration (μM)	Removal of Cr(VI) from flow (μM)
100	61
200	112
300	156
400	164
500	168

Table 3: Equations relating $[Cr(VI)]_{inlet}$ to % Cr(VI) reduction

$[Cr(VI)]_{inlet}$ (μM)	Trend line equation*	Eqn. No.	Correlation coefficient
100	Y = -0.15X + 64.4	(1)	0.99
200	Y = -0.22X + 60.78	(2)	0.99
300	Y = -0.28X + 57.92	(3)	0.99
400	Y = -0.30X + 46.01	(4)	0.94
500	Y = -0.32X + 39.90	(5)	0.99

* Y denotes % Cr(VI) reduced and X time in hours

Columns were challenged with chromate solution at a flow rate of 13.2 mL h^{-1}.

Table 4: Comparison of experimentally determined and predicted values for % Cr(VI) reduction by agar-immobilized Bio-Pd(0) in flow-through packed-bed columns

Time (h)	[Cr(VI)] (μM)	% Cr(VI) reduction		% Difference
		Experimental	Calculated	
24	100	61.19	63.50	2.3
48	100	57.2	59.98	2.7
96	100	50.71	52.95	2.2
24	200	55.75	55.67	0.1
48	200	49.95	50.32	0.4
96	200	39.91	39.63	0.3
24	300	51.81	48.60	3.2
48	300	43.68	42.18	1.5
96	300	31.47	29.35	2.1
24	400	40.8	41.84	1.0
48	400	29.63	34.67	5.03
96	400	19.22	20.31	1.1
24	500	33.54	35.25	1.7
48	500	22.83	27.49	4.7
96	500	10.11	11.95	1.8

% Cr(VI) reduction was calculated using equation (9) (see text).

Table 5: Effect of Bio-Pd(0)/ agar loading on the flow rate at which 50 % Cr(VI) is reduced ($FA_{1/2}$ value) and the residence time needed for 50 % Cr(VI) reduction to occur ($RA_{1/2}$ value*)

Bio-Pd(0)/ agar loading (mg mL^{-1})	$FA_{1/2}$ value (mL h^{-1})	$RA_{1/2}$ value (min)
1.25	ND**	ND**
2.5	3.43	8.75
5.0	11.24	2.66
7.5	14.86	2.02

Columns were challenged at various flow rates with a solution comprising 100 μM Cr(VI), 25 mM each of formate, acetate, citrate, 20 mM MOPS/ NaOH, pH 7

*$RA_{1/2}$ value was calculated on the basis that 0.5 mL solution was present within columns at any one time (see Materials and Methods).

ND** = Not Determined as negligible reduction occurred.

Table 6: Comparison of expected and actual bioreactor activities

$$\frac{E_o K_3}{E_o K_3} = \frac{F[S_{o1}X_1 + K_m.\ln(1/1-X_1)]}{F[S_{o2}X_2 + K_m.\ln(1/1-X_2)]} \quad (14)$$

Relative Eo value	Value for X (Experimental data) at F = 13.2 mL h^{-1}
Eo_1 = 2.5 mg Bio-Pd(0) mL $agar^{-1}$	X_1 = 0.24
Eo_2 = 5.0 mg Bio-Pd(0) mL $agar^{-1}$	X_2 = 0.47

Calculated value for E_{o2} by substitution of known values for E_{o1}, X_1, X_2 ($K_{m\ app}$: 430 μM, S_o: 112 μM) = 5.56 mg Bio-Pd(0) mL $agar^{-1}$.

Deviation from expected value = 11 % (actual E_{o2} was 5.0 mg Bio-Pd(0) mL $agar^{-1}$: above)

The value for $K_{m\ app}$ (430 μM) was obtained as described in the text and substituted into eqn. 13. True values for E_{o1} and E_{o2} were known (applied conditions: 2.5 and 5.0 mg Bio-Pd(0) mL $agar^{-1}$, respectively). For calculation, the values X_1 and X_2 at S_o = 112 μM were obtained by experiment (Fig. 6). The 'unknown' E_{o2} determined by calculation (5.56 mg Bio-Pd(0) mL^{-1}) was compared against the actual E_{o2} (5.0 mg Bio-Pd(0) mL^{-1}).

Legend to Figures.

Fig. 1. Deposits of Pd(0) on the surface of *D. desulfuricans* (a), *D. vulgaris* (b), *E. coli* strain MC4100 (c), and *E. coli* strain HD701 (d). Cells were exposed to Pd(II) as described in Materials and Methods. The biomass: Pd ratio was 3:1 (see text). Bars are 1 μm.

Fig. 2. Aerobic vs. anaerobic batch reduction of 500 μM sodium chromate by free and agar-immobilized Bio-Pd(0) produced with **(A)** *D. vulgaris*, **(B)** *D. desulfuricans*, **(C)** *E. coli* strain HD701, **(D)** *E. coli* strain MC4100. Filled symbols: Bio-Pd(0) in the presence of electron donor. Open symbols: Control; Bio-Pd(0) in the absence of electron donor. ♦, Reduction by free Bio-Pd(0) in air; ●, Reduction by agar-immobilized Bio-Pd(0) in air; ■, Reduction by free Bio-Pd(0) under OFN; ▲, Reduction by agar-immobilized Bio-Pd(0) under OFN. Error is ± SEM from 3 experiments.

Fig. 3. Correlation between the % by which the amount of Cr(VI) reduced in the initial 1.5 h is affected by immobilization and the initial rate of Cr(VI) reduction by immobilized Bio-Pd(0). Open symbols: aerobic Cr(VI) reduction; Filled symbols: anaerobic Cr(VI) reduction. Each datum was obtained using one bacterial strain: ●, *D. desulfuricans*; ▲, *D. vulgaris*; ♦, *E. coli* HD701; ■, *E. coli* MC4100. Error is ± SEM from 3 experiments.

Fig. 4. Continuous Cr(VI) reduction by Bio-Pd(0) immobilized in agar (loading 7.5 mg mL^{-1}). Columns were challenged at a flow rate of 13.2 mL h^{-1} with 500 μM sodium chromate in the presence of electron donors. ●, *D. vulgaris* Bio-Pd(0); ■, *D. desulfuricans* Bio-Pd(0); ▲, *E. coli*

MC4100 Bio-Pd(0); ♦, *E. coli* HD701 Bio-Pd(0); ○ agar beads (no bio-Pd(0)). Error is ± SEM from 3 experiments.

Fig. 5. Continuous reduction of Cr(VI) by *D. vulgaris* Bio-Pd(0) immobilized in agar (7.5 mg mL^{-1}). Columns were challenged at a flow rate of 13.2 mL h^{-1} with a solution comprising either 100 (♦), 200 (■), 300 (▲), 400 (●), or 500 (*) μM sodium chromate in the presence of electron donors (see text). SEM was within 10 % of the values shown.

Fig. 6. Flow rate/ activity plots for Cr(VI) reduction by packed bed columns containing *D. vulgaris* Bio-Pd(0) immobilized in agar at loadings of 0 (*), 1.25 (●), 2.5 (▲), 5.0 (♦), and 7.5 (■) mg Bio-Pd(0) mL $agar^{-1}$ (25 % of these masses as Pd(0) metal). Columns were challenged at various flow rates with 100 μM sodium chromate, 25 mM each of sodium formate, sodium acetate, sodium citrate, and 20 mM MOPS/ NaOH buffer, pH 7, 20 °C. SEM was within 10 % of the given values. Arrow shows doubling the Bio-Pd(0) loading at a flow rate of 2.91 mL h^{-1} resulted in an incremental increase of approx. 35 % Cr(VI) reduction (starred). Doubling the flow rate from 2.91 to 5.81 and again to 11.61 mL h^{-1} resulted in a 10 and 20 % drop in Cr(VI) reduction activity, respectively (see text).

Fig. 7. Model depicting transcriptional regulation by HycA (adapted from Skibinski *et al.* 2002). Thick arrows indicate gene-product relationships. Dashed arrows show induction (+) or repression (-) effects. Regulatory proteins are shown boxed. Arrows above or below the operons or genes indicate transcriptional organisation.

Fig. 1

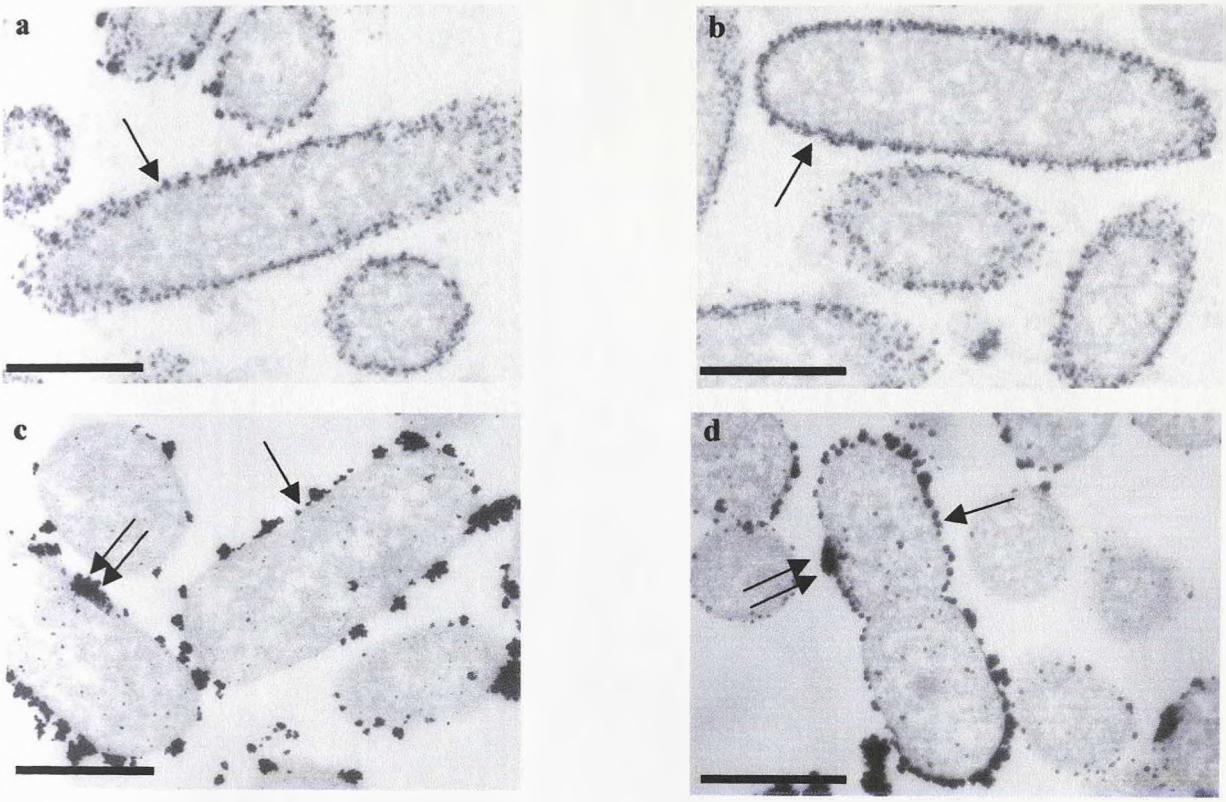


Fig. 2

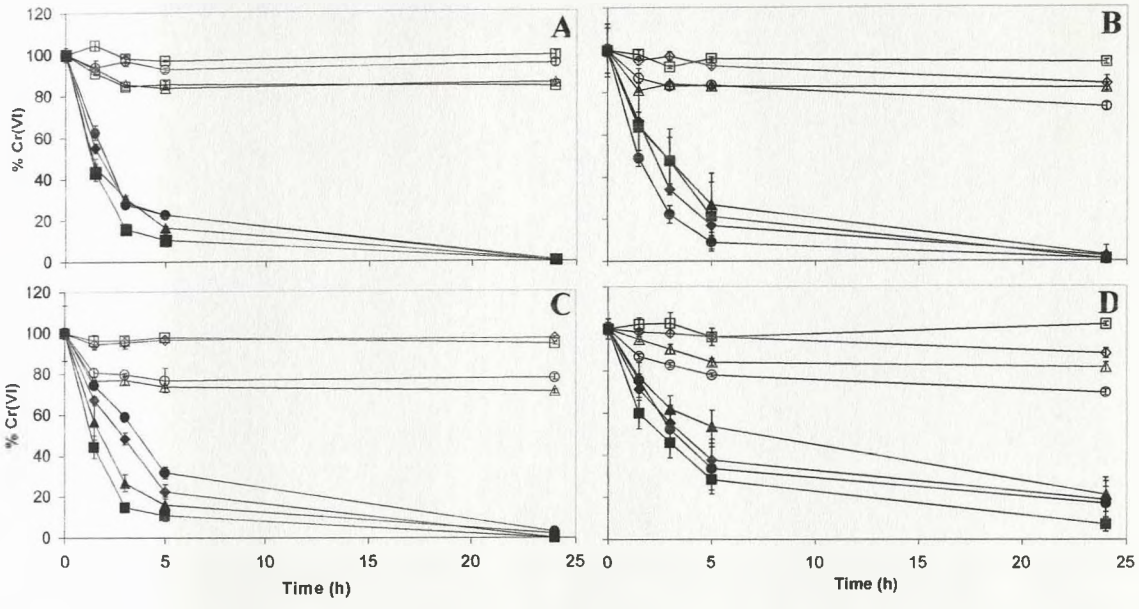


Fig. 3

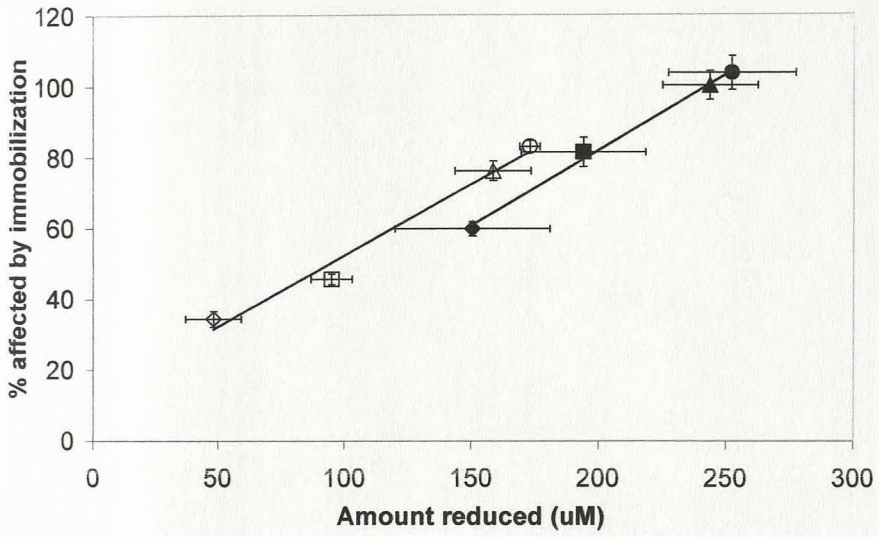

120
100
80
60
40
20
0
% affected by immobilization
0
50
100
150
200
250
300
Amount reduced (uM)

Fig. 4

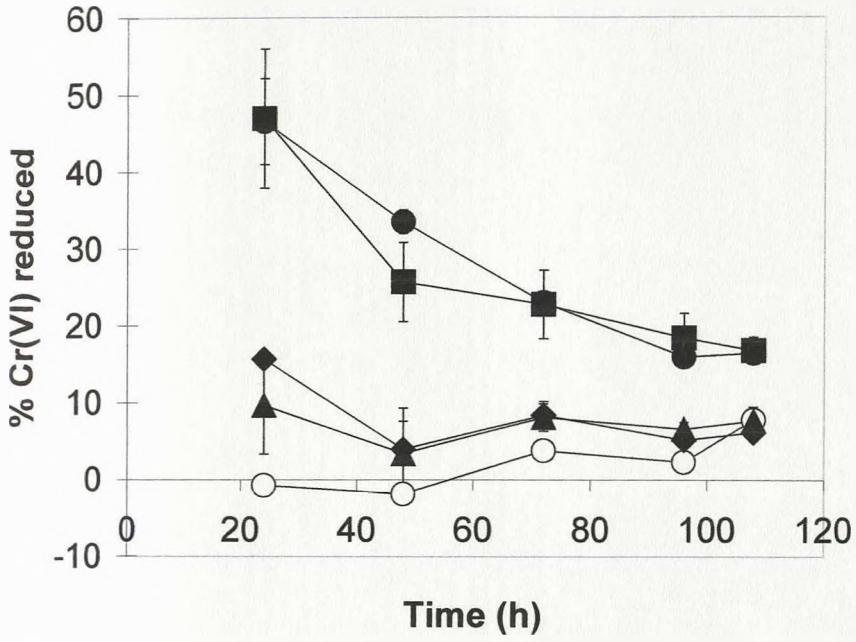


Fig. 5

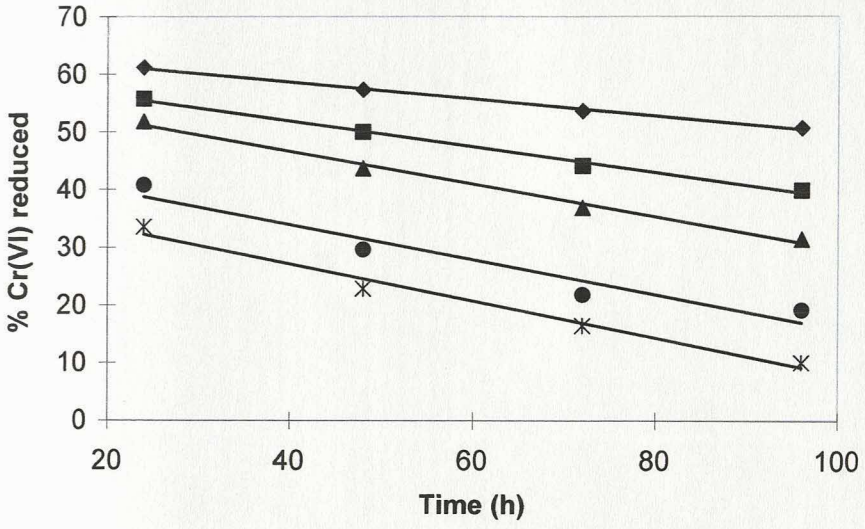


Fig. 6

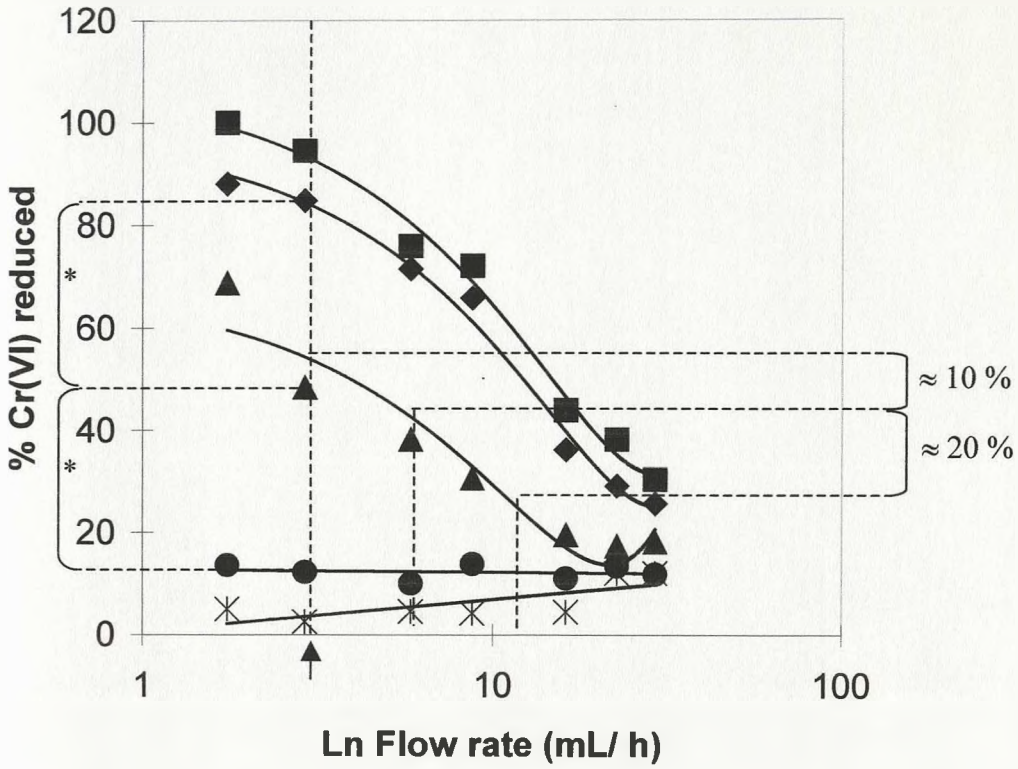
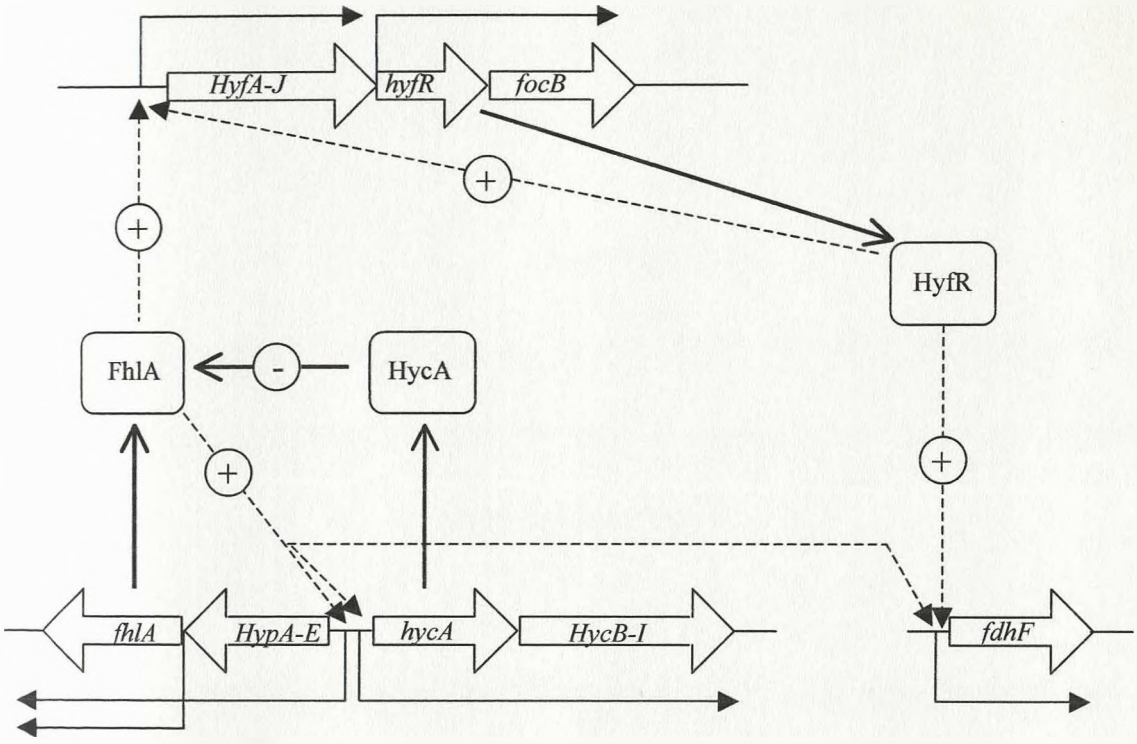


Fig. 7



SECTION 4

"Cr(VI) reduction by bio- and bioinorganic catalysis via use of Bio-H_2: a sustainable approach for remediation of wastes from the metal finishing and food processing sectors".

Journal: ***Journal of Environmental Science and Technology***

Submitted

Biohydrogen production was performed by D. W. Penfold. Analysis of Cr(VI) reduction was carried out by A. C. Humphries. The paper was written by A. C.Humphries.

Cr(VI) reduction by bio- and bioinorganic catalysis via use of Bio-H_2: a sustainable approach for remediation of wastes from the metal finishing and food processing sectors

A. C. Humphries, D. W. Penfold, L. E. Macaskie*

School of Biosciences, The University of Birmingham, Edgbaston, B15 2TT, UK

**Author for correspondence (Fax (44)-121-414-5925; E-mail: L.E.Macaskie@bham.ac.uk)*

Keywords: chromate reduction, palladium biocatalyst, Bio-Hydrogen

Abstract

Use of biologically-produced hydrogen (Bio-H_2) as an electron donor for Cr(VI) reduction by native and palladised cells of *Desulfovibrio vulgaris* NCIMB 8303 was demonstrated. Bio-H_2 was produced fermentatively by *Escherichia coli* HD701 (a strain upregulated with respect to formate hydrogenlyase expression) using glucose solution or two industrial sugar wastes as oxidisable substrates. Maximum Cr(VI) reduction occurred at the expense of Bio-H_2 using palladised biomass (Bio-Pd(0)), with negligible residual Cr(VI) remaining from a 500 μM solution after 2.5 h. Use of Bio-H_2 as the electron donor for Cr(VI) reduction by agar-immobilized Bio-Pd(0) in a continuous-flow system gave 90 % reduction efficiency at a flow residence time of 0.7 h, which was maintained for the duration of Bio-H_2 evolution by *E. coli* HD701. Since Bio-Pd(0) can be sourced from liquid wastes and precious metal scrap the potential is shown for the concurrent bio-treatment of industrial sugar wastes, precious metal scrap and Cr(VI).

Introduction

Contamination of the environment with Cr(VI) due to industrial wastewater discharge (e.g. during the manufacture of anticorrosive agents, leather tanning, and metal plating), in conjunction with other anthropogenic activities, is a major environmental problem (1). Cr(VI) is highly toxic but can be reduced to the less mobile, less toxic trivalent species, Cr(III) (2). This can be achieved chemically, but microbial-based Cr(VI) reducing systems may be used as an economical alternative. Examples of Cr(VI) reducing microorganisms include *Pseudomonas putida* (3), *Escherichia coli* (4), *Enterobacter cloacae* (5) and *Desulfovibrio vulgaris*. The latter, a member of the sulfate-reducing bacteria (SRB), has a well-established ability to reduce a variety of metals, including Cr(VI) (6-9) and also Pd(II) (10). The latter was also shown using *D. desulfuricans*, where deposition of cell-bound Pd(0) on cells (8) gave catalytically active bionanoparticles (see below).

Lovley and Phillips (7) showed that *D. vulgaris* NCIMB 8303 can completely reduce 500 μM K_2CrO_4 within 100 min using H_2 as the electron donor in bicarbonate buffer (7). The Cr(VI) reducing ability correlated with the extent to which the Cr(III) product could be removed by its chelation (9).

An alternative approach to Cr(VI) reduction is to use palladised biomass (Bio-Pd(0)) as a bio-inorganic catalyst which has the advantage that toxic concentrations of Cr(VI) and non-physiological pH can be used (11). Growth decoupled SRB cells can be used to reduce Pd(II), via cellular hydrogenase activity (10), to cell bound Pd(0) (Bio-Pd(0)) using H_2 as the electron donor (8,10). The resulting 'Bio-Pd(0)' was more efficient at Cr(VI) reduction than bacteria alone or than Pd(0) made by chemical reduction of Pd(II) under H_2 (9,10), e.g. Bio-Pd(0) (1:1 biomass:Pd) reduced 700 μM Na_2CrO_4 under H_2 (10,12), under which conditions an equivalent

mass of chemically reduced Pd(0) was ineffective. Bio-Pd(0) also reduced Cr(VI) continuously in a flow-through column (11,13), with Cr(III) recovered in the outflow solution (11).

Reduction of Cr(VI) by resting and palladised cells of *D. vulgaris* uses H_2 as the electron donor, supplied from a cylinder or generated electrochemically, and delivered through a H-transfer membrane (14), or from formate, which is split to give H_2 enzymatically via the formate hydrogenlyase (FHL) complex (see below), a vestigial form of which is thought to operate in the SRB (15) or via the Pd(0)-catalysed breakdown of formate to give highly reactive $H^{\bullet}$ (11). As a sustainable approach, H_2 can be produced fermentatively by *Escherichia coli* at the expense of industrial sugar waste, mediated by the FHL system synthetically. In this case the multi-enzyme complex catalyses the formation of $H_2 + CO_2$ via the oxidation of formate in a homeostatic response to the reduction in pH caused by end products of mixed acid fermentation (16). *E. coli* strain HD701 cannot synthesize the FHL repressor (Hyc A) and is, therefore up-regulated with respect to FHL expression (17), resulting in an enhanced ability to produce H_2 (16).

We investigated the potential to use biogenic H_2, made by *E. coli* strain HD701 via oxidation of industrial sugar wastes, as the electron donor to support Cr(VI) reduction by live (resting) and dried, palladised cells of *D. vulgaris* NCIMB 8303 in a second, coupled downstream reactor. For industrial purposes Cr(VI) reduction by free cells or biomass-bound nanoparticles is disadvantageous *per se* due to downstream difficulties in biomass/effluent separation (18). This can be overcome by the use of immobilized cells/ Bio-Pd(0) packed-bed reactors using agar beads as an immobilization matrix. This imposed low mass transfer limitations and the beads retained good structural integrity and gave an even dispersion of catalyst throughout (13). We report Cr(VI) reduction by agar-immobilized resting and palladised cells of *D. vulgaris* NCIMB

8303 in batch and continuous-flow modes and a new approach towards the integrated co-treatment of three classes of industrial waste.

Materials and Methods

Organisms and growth conditions

E. coli strain HD701, as described previously (16), was maintained aerobically at 30 °C on nutrient agar (Oxoid). Pre-culture medium was nutrient broth No. 2 (Oxoid). Cells were shaken aerobically overnight (100 rpm) at 30 °C. *D. vulgaris* NCIMB 8303 (11-13) was maintained routinely in butyl-rubber sealed 100 mL serum bottles in Postgate's medium C (9-11,13) under O_2-free N_2 (OFN). For experiments, growing cultures (OD_{600} 0.8 ± 0.2) were produced by withdrawing 100 mL of an actively growing culture and adding to 1 L of fresh medium C, followed by degassing with OFN for 20 min. The culture was harvested by centrifugation (4 °C) after 24 h (OD_{600} 0.8 ± 0.2) transferring cells anaerobically in a MACS-MG anaerobic workstation (Don Whitley Scientific Ltd). Cells were washed three times and resuspended in anaerobic (degassed) solutions of 20 mM 3-(N-Morpholinopropanesulfonic) acid (MOPS)/ NaOH buffer (pH 7). Cell concentrate was stored at 4 °C under N_2 until use (within 24 h). The biomass concentration was estimated by conversion of OD_{600} to dry cell wt via a previously determined calibration.

Hydrogen evolution by *Escherichia coli*

H_2 production was achieved in 320 mL (working volume: 310 mL) or 6 L (working volume: 5.5 L) reactors containing 40 % (v/v) phosphate buffered saline (PBS: 0.8 g l^{-1} NaCl, 0.2 g l^{-1} KCl, 1.43 g l^{-1} Na_2HPO_4 and 0.2 g l^{-1} KH_2PO_4, pH 7.3) and 50 % (v/v) inocula of an overnight culture of *E. coli* HD701. Carbon substrates were added at 10 % (v/v), consisting of glucose solution,

caramel or nougat waste (supplied by Cadbury Trebor Bassett Ltd, Birmingham, UK: Table 1). Cell suspensions were pre-gassed with argon for 1 h and were stirred and maintained at 30 °C. Evolved H_2 was passed through 1 M sodium hydroxide to remove CO_2. Other than CO_2, H_2 was the only gas found from glucose fermentation (by analysis using GC) and was passed into the Cr(VI) reduction reactor (H_2 flow rate as specified in individual experiments). Exit gas from the Cr(VI) reducing reactor was bubbled through olive oil to maintain a headspace of H_2 (Fig. 1), found necessary in preliminary tests.

Preparation of Bio-Pd(0) using *D. vulgaris*

The required volume of 2 mM Na_2PdCl_4 (98 %, Aldrich Chemicals, UK) (to pH 2 with HNO_3) was placed in a 200 mL serum bottle sealed with a butyl-rubber stopper. The required volume of *D. vulgaris* concentrate was added under OFN to give a 3:1 ratio (dry cell mass:Pd). The suspension was incubated for 1 h (30 °C) to allow biosorption of Pd(II) and formation of nucleation foci, followed by outgassing with H_2 (15 min) which gave complete reduction of Pd(II) (10) and deposition of Pd(0) on the biomass. The palladised cells were recovered by centrifugation (3800 g, 10 min), washed once in distilled H_2O, three times in acetone, and dried (60 °C) to constant weight. The black solid (palladised biomass) was ground to a fine powder with a pestle and mortar to comprise the bioinorganic catalyst (Bio-Pd(0)).

Transmission electron microscopy

Pellets of resting or palladised cells were rinsed twice with distilled water, fixed in 2.5 % (w/v) aqueous glutaraldehyde, washed once in distilled water and fixed in 1 % osmium tetroxide in 0.1 M phosphate buffer (pH 7, 60 min). Cells were dehydrated using an ethanol series (70, 90, 100, 100, 100 % dried ethanol; 15 min each step). After two 15 min washes in propylene oxide (1,2-epoxypropane), cells were embedded in epoxy resin (degassed under vacuum for 30 min) and the

resin was left to polymerise for 24 h at 60 °C. Sections (100 – 150 nm thick) were cut from the resin block, placed onto a copper grid and viewed with a JEOL 120CX2 transmission electron microscope (TEM); the accelerating voltage was 80 kV.

Immobilization of *D. vulgaris* resting cells and Bio-Pd(0)

200 mg Agar-Agar (FSB Laboratory supplies) was mixed with 9 mL deionised water, degassed with OFN, and autoclaved (121 °C, 20 min). The gel was allowed to cool to 40 °C before 50 mg Bio-Pd(0) (suspended in 1 mL deionised water) or 1 mL cell concentrate (equivalent to 25 mg dry cell wt) was added. Agar bead formation and bead preparation were carried out in the MACS-MG workstation as described previously (13,19,20). Homogeneity within the beads, and bead integrity under load were checked using magnetic resonance imaging (13,20).

Chromate reduction by *D. vulgaris* NCIMB 8303 and Bio-Pd(0) in batch mode

For batch reduction tests, reaction mixtures were set up in the anaerobic workstation (30 °C) in 14 mL jacketed glass columns. *D. vulgaris* cell beads (2 mL: equivalent to 5 mg dry cell wt), free cells (5 mg dry cell wt), Bio-Pd(0) beads (2mL: equivalent to 10 mg Bio-Pd(0)) or free Bio-Pd(0) (10 mg) were suspended in 10 mL of degassed 20 mM MOPS/ NaOH, and 25 mM sodium citrate buffer (pH 7). Columns were removed from the workstation and degassed with OFN for 15 min prior to the addition of 500 μM (final concentration) Na_2CrO_4. Controls for all experiments comprised free cells or Bio-Pd(0) suspensions, or agar-immobilized cells or Bio-Pd(0) in the absence of H_2, or reaction solution without cells/ Bio-Pd(0). Columns containing resting cells were set to 30 °C (optimum temperature for Cr(VI) reduction), whereas columns containing Bio-Pd(0) were maintained at 21°C (preliminary tests showed that higher reaction temperatures do not give a higher rate of Cr(VI) reduction using Bio-Pd(0): A. C. Humphries, unpublished). Cr(VI) reduction was initiated by the provision of H_2, either biologically produced

(Fig. 1a) or supplied from a commercial hydrogen cylinder (BOC) (flow rate as specified in individual experiments). Samples were withdrawn periodically, via a syringe, and supernatants (100 μL) were analysed for residual Cr(VI) using diphenylcarbazide (9,13,20).

Chromate reduction by Bio-Pd(0) in continuous mode

For continuous reduction tests, 4 mL Bio-Pd(0) beads (Bio-Pd(0) agar loading: 5.0 mg Bio-Pd(0) mL agar^{-1}) were placed in 12 mL serum bottles sealed with butyl-rubber stoppers. Challenge solution (100 μM Na_2CrO_4, 20 mM MOPS/ NaOH, 25 mM citrate, pH 7) was fed into the bottom of the serum bottle at a flow rate of 0.15 mL min^{-1} (Fig. 1b). The reaction volume was 6 mL; flow residence time was ~0.7 h. Controls comprised agar beads without Bio-Pd(0). Bio-H_2 (produced by *E. coli* in a 6 L working volume reactor from glucose solution) was used as the electron donor.

Results

Cr(VI) reduction by resting and immobilized cells of *D. vulgaris*

An example TEM of unpalladised resting cells of *D. vulgaris* is shown in Fig. 2a. Cr(VI) reduction by cell suspensions and immobilized cells using commercially available H_2 (flow rate of 60 mL h^{-1}: Fig. 3a) showed reduction for 3.5 h with ~ 175 μM Cr(VI) removed in each case. Loss in activity accompanied a fall in Cr(VI) reactor temperature from 30 °C to ~ 20 °C, attributable to the use of compressed gas (see later). Tests were repeated using Bio-$H_{2\ glucose}$ (Fig. 3b; Table 2) supplied to Cr(VI) reactors at a flow rate of ~ 15 mL h^{-1}. Negligible Cr(VI) removal occurred in cell free controls (not shown). Limited Cr(VI) removal, probably attributable to absorption by the immobilization matrix, occurred in agar bead controls, and using cell beads

without H_2 (Fig. 3b). In the presence of Bio-H_2 the suspended and immobilized cells removed 396 ± 29 and 390 ± 8 μM Cr(VI) respectively during the initial 5 h (Table 2a).

Immobilized cells of *D. vulgaris* were reacted with Cr(VI) solution over 6.5 h (Fig. 3b) using nougat and caramel wastes as oxidisable substrates for Bio-H_2 production by the *E. coli* reactor upstream. After 5 h 402 ± 22 μM and 455 ± 5 μM Cr(VI) was removed at the expense of Bio-$H_{2\ nougat}$ and Bio-$H_{2\ caramel}$, respectively (Table 2a).

Cr(VI) reduction by suspended and immobilized Bio-Pd(0)

An example TEM of palladised cells of *D. vulgaris* is shown in Fig. 2b. The Pd(0) is visible as cell-bound deposits identified as metallic Pd(0) by X-ray powder diffraction analysis (8,10). Cr(VI) reduction by free and immobilized Bio-Pd(0) using commercially available H_2 (flow rate of 60 mL h^{-1}) is shown in Fig. 3c. After 5 h 441 ± 52 μM and 496 ± 18 μM Cr(VI) (Table 2b) was removed from solution by free and immobilized Bio-Pd(0) respectively and, in contrast, to resting cells Cr(VI) reduction was maintained even at the lower temperature (Fig 3c; cf 3a).

Evolved Bio-$H_{2\ glucose/caramel}$ was used for Cr(VI) reduction by suspended and immobilized Bio-Pd(0) over 6.5 h (Fig. 3d). No Cr(VI) removal occurred in Bio-Pd(0)-free controls, or in the absence of Bio-H_2. In the presence of Bio-H_2 suspended Bio-Pd(0) removed 314 ± 6 μM (Bio-$H_{2\ glucose}$) and 340 ± 8 μM (Bio-$H_{2\ caramel}$) Cr(VI) from solution in the initial 5 h (Table 2b). This was not significantly different using immobilized Bio-Pd(0), with 354 ± 11 μM (Bio-$H_{2\ glucose}$) and 322 ± 14 μM (Bio-$H_{2\ caramel}$) Cr(VI) removed respectively (Table 2b). There was little difference in the rate of Cr(VI) removal overall by Bio-Pd(0) or an equivalent mass of free cells using Bio-$H_{2\ glucose}$ (Fig 3d, c.f. 3b).

Cr(VI) reduction by Bio-Pd(0) at the expense of Bio-H_2 (5.5 L reactor)

To investigate whether Cr(VI) reduction by immobilized Bio-Pd(0) was limited by the Bio-H_2 supply the *E. coli* reactor was scaled up to a working volume of 5.5 L (Fig. 3e, Table2) and with Bio-$H_{2\ glucose}$ or Bio-$H_{2\ caramel}$ generated, at flow rates of 289.2 ± 33.7 and 315.0 ± 37.2 mL h^{-1}, respectively. After 2.5 h negligible Cr(VI) remained (Fig 3e).

Cr(VI) reduction by Bio-Pd(0) in continuous mode

In previous studies continuous-flow reactors containing immobilized Bio-Pd(0) were shown to be more effective at Cr(VI) reduction over time in comparison to *D. vulgaris per se* (13,20). Therefore Bio-$H_{2\ glucose}$ (from the 5.5 L working volume *E. coli* reactor), was used to support continuous Cr(VI) reduction by immobilized Bio-Pd(0) (Fig. 1b, Fig. 4) at a Cr(VI) flow residence time of ~0.7 h. The efficiency of Cr(VI) reduction increased to 90 % after 4 h and was maintained for the duration of H_2 evolution, with no Cr(VI) reduction in the absence of Bio-H_2 (Fig 4).

Discussion

TEM of Pd-unchallenged cells (Fig. 2a) showed no electron-opaque areas, whilst Pd-challenged cells showed an array of cell surface-localized electron-opaque deposits (Fig. 2b), previously identified as elemental Pd(0) using EDAX (12) or XRD (8,10). Mikheenko (10) showed with *D. desulfuricans* that nucleation of Pd(0) occurs in the periplasmic space at loci corresponding to the location of hydrogenase activity. The growing Pd(0) clusters then erupt through the outer membrane, forming nanoparticles on the outer surface of the cell; hydrogenase activity is maintained for several hours at pH 2 (10).

The potential to use H_2 (commercial and biologically produced) as an electron donor for Cr(VI) reduction by suspended and agar-immobilized *D. vulgaris* and Bio-Pd(0) was shown. Immobilization did not affect the initial rate or level of Cr(VI) reduction attained by either preparation, suggesting that Cr(VI) reduction was not limited by diffusion of H_2/ Cr(VI) inward, or Cr(III) outward through the agar matrix.

In the presence of commercial H_2, Cr(VI) reduction by the resting cells ceased after 3.5 h, with a reduction in bioreactor temperature from 30 °C to approx. 20 °C. The ideal gas law states that pressure is related to temperature (i.e. the expanding H_2 gas cooled: 21), resulting in a drop in the Cr(VI) reactor temperature despite the water jacket for temperature control. Hence, for optimal performance, bottled H_2 would require pre-warming. Cr(VI) reduction by *D. vulgaris* cells using Bio-H_2 was approx. 2 fold greater, attributable to the 10 °C difference in temperature. Reduction of Cr(VI) by Bio-Pd(0) was independent of temperature between 20 °C and 30 °C (A. C. Humphries and L. E. Macaskie, unpublished).

Cr(VI) reduction by suspended and immobilized Bio-Pd(0) was faster when H_2 was supplied from a cylinder at a flow rate of 60 mL h^{-1} (Fig 3c) than when evolved by *E. coli* (310 mL reactor) (Fig. 3d), suggesting that the Cr(VI) reduction rate was limited by the H_2 supply (see Table 2). This was confirmed when the *E. coli* reactor was scaled up from 310 mL to 5.5 L (working volume), with hydrogen evolution correspondingly increasing to 289 (Bio-$H_{2\ glucose}$) and 315 (Bio-$H_{2\ caramel}$) mL h^{-1}. The rate of Cr(VI) reduction by agar-immobilized Bio-Pd(0) was significantly higher at the increased rate of H_2 supply, with negligible Cr(VI) remaining in solution after 2.5 h and, 90 % removal of Cr(VI) was sustained in a continuous flow reactor with the higher Bio-H_2 production for the duration of Bio-H_2 evolution.

Bio-H_2 was produced by *E. coli* using glucose solution, nougat and caramel wastes as oxidisable substrates, with H_2 evolved at rates of 16.3, 16.3, and 17.8 mL h^{-1}, respectively. These rates were not significantly different and therefore cannot account for the superiority of the Bio-$H_{2\ caramel}$ as compared to Bio-$H_{2\ glucose}$ or Bio-$H_{2\ nougat}$ shown in Fig. 3b. This enhancement was restricted to the live cells only (Fig. 3b; c.f. 3d, 3e). Further study of this phenomenon was outside the scope of this investigation but the possibility of the presence of a volatile agent which influences hydrogenase activity should be considered in follow-up studies, which would concentrate on full exit gas analysis with respect to the final gaseous discharges.

Comparison of Cr(VI) reduction by suspended and immobilized cells of *D. vulgaris* and Bio-Pd(0) suggests the latter is more efficient at Cr(VI) reduction in the presence of Bio-H_2 (i.e. more Cr(VI) is reduced per unit mass: Table 2). Also, Bio-Pd(0) would be more attractive industrially because it is more stable with respect to pH, temperature, and is stable in the presence of oxygen (A. C. Humphries, unpublished). Therefore the potential to use Bio-H_2 and Bio-Pd(0) together to treat Cr(VI) solution on a continuous basis was investigated, showing removal of Cr(VI) for the duration of the Bio-H_2 supply. A fed-batch reactor for semi-continuous sugar waste treatment was shown to prolong the H_2 evolution accordingly (D.W. Penfold, unpublished).

Palladium is an expensive metal, therefore using Bio-Pd(0) to reduce Cr(VI) may appear uneconomic. However automotive catalyst leachates, electronic scrap and industrial processing wastes contain Pd and other precious metals. Previous studies have shown that *D. desulfuricans* can be used to biorecover palladium from industrial wastes and leachates (14,23) without the catalytic activity of the consequent Bio-Pd(0) being affected adversely by the presence of other metallic elements in the biorecovered solid (12,23). A system for the treatment of three industrial wastes can therefore be engineered in which Bio-H_2 is used initially as the electron donor for

palladium recovery from industrial liquid waste (waste 1) (14) to produce Bio-Pd(0). Bio-H_2 $_{nougat}$ or Bio-H_2 $_{caramel}$ (waste 2) together with the waste-derived Bio-Pd(0) can then be used in conjunction to remediate Cr(VI) wastewater (waste 3). Since the palladium and hydrogen are both sourced from wastes from the precious metal (11) and food (16) sectors respectively a substantial economic benefit would result from the conversion of these wastes into two useful products, avoiding landfill taxes and ensuring compliance with current legislation on disposal of solid scrap. Use of the biorecovered materials would mitigate the cost of the Cr(VI) treatment process, while at the same time permitting application outside the usual confines of physiological constraints (10, 23). Finally, it has been shown (10; A.C. Humphries, I.P. Mikheenko & L.E. Macaskie, unpublished) that waste biomass of *E. coli* strain HD701 produced Bio-Pd(0) which was as effective in the reduction of Cr(VI) as Bio-Pd derived from *Desulfovibrio* spp, hence converting potentially high Biological Oxygen Demand (BOD) waste to new product and closing the loop. This minimises secondary waste production and the costs of biomass growth for the Pd(0) accumulation step.

Acknowledgements

We wish to acknowledge the support of the BBSRC (Studentship Number: 00/B1/E/0698 to DWP), the EPSRC (Studentship Number: 00318650 to ACH), both Research Councils for previous grant support (to LEM) which has made this work possible, and also the Royal Society for provision of a Industrial Fellowship to LEM. We also thank Professor A. Böck (Lehrstuhl für Mikrobiologie der Universität, Munich, Germany) for the use of *E. coli* strain HD701, Cadbury Trebor Bassett Ltd. (Bournville, Birmingham, UK) for provision of the nougat and caramel wastewaters, Dr. G. Thompson (Department of Civil Engineering, The University of Birmingham UK) for help with wastewater analyses and Dr V. S. Baxter-Plant (School of

Biosciences, The University of Birmingham, UK) for provision of the TEM images shown in Fig 2.

References

(1) Desjardin V, Bayard R, Huck N, Manceau A, Gourdon R. 2002. Effect of microbial activity on the mobility of chromium in soils. Waste Manage. 22:195-200.

(2) Neal AL, Lowe K, Daulton TL, Jones-Meehan J, Little BJ. 2002. Oxidation state of chromium associated with cell surfaces of *Shewanella oneidensis* during chromate reduction. Appl Surf Sci. 202:150-159.

(3) Ishibashi Y, Cervantes C, Silver S. 1990. Chromium reduction in *Pseudomonas putida*. Appl Environ Microbiol. 56:2268-2270.

(4) Bae WC, Kang TG, Kang IK, Won YJ, Jeong BC. 2000. Reduction of hexavalent chromium by *Escherichia coli* ATCC 33456 in batch and continuous cultures. J Microbiol. 38:36-39.

(5) Komori K, Rivas A, Toda K, Ohtake H. 1990. Biological removal of toxic chromium using an *Enterobacter cloacae* strain that reduces chromate under anaerobic conditions. Biotechnol Bioeng. 35:951-954.

(6) Lovley DR. 1993. Dissimilatory metal reduction. Annu Rev Microbiol. 47:263-290.

(7) Lovley DR, Phillips EJP. 1994. Reduction of chromate by *Desulfovibrio vulgaris* and its c_3 cytochrome. Appl Environ Microbiol. 60:726-728.

(8) Lloyd JR, Yong P, Macaskie LE. 1998. Enzymatic recovery of elemental palladium by using sulfate-reducing bacteria. Appl Environ Microbiol. 64:4607-4609.

(9) Mabbett AN, Macaskie LE. 2002. A new bioinorganic process for the remediation of Cr(VI). J Chem Technol Biotechnol. 77:1169-1175.

(10) Mikheenko I. 2004. Nanoscale palladium recovery. *Ph.D Thesis*. The University of Birmingham, England.

(11) Mabbett AN. 2001. The reduction and recovery of chromium (VI) from industrially polluted waste waters using sulphate-reducing bacteria. *Ph.D Thesis*. The University of Birmingham, England.

(12) Mabbett AN, Yong P, Baxter-Plant VS, Mikheenko I.P, Farr JPG, Macaskie LE. 2001. Effective reduction and removal of Cr(VI) and reductive dehalogenation of chlorophenol by hybrid bioinorganic catalytic processes. In: Biohydrometallurgy: Fundamentals, Technology and Sustainable Development Eds V.S.T. Ciminelli & O Garcia, Elsevier Holland. p 335-342.

(13) Humphries AC, Nott KP, Hall LD, Macaskie LE. 2004. Continuous removal of Cr(VI) from aqueous solution catalysed by palladised biomass of *Desulfovibrio vulgaris* NCIMB 8303. Biotechnol Lett. 26:1529-1532.

(14) Yong P, Rowson NA, Farr JPG, Harris IR, Macaskie LE. 2003. A novel electrobiotechnology for the recovery of precious metals from spent automotive catalysts. Environ Technol. 24:289-297.

(15) Peck HD. 1993. Bioenergetic strategies of the sulfate-reducing bacteria. In: Odom JM, Singleton R, editors. Sulfate-reducing bacteria: contemporary perspectives. Springer New York. p 41-76.

(16) Penfold DW, Forster CF, Macaskie LE. 2003. Increased hydrogen production by *Escherichia coli* strain HD701 in comparison with the wild-type parent strain MC4100. Enzyme Microb Technol. 33:185-189.

(17) Sauter M, Bohm R, Bock A. 1992. Mutational analysis of the operon (hyc) determining hydrogenase-3 formation in *Escherichia coli*. Mol Microbiol. 6:1523-1532.

(18) White C, Wilkinson SC, Gadd GM. 1995. The role of microorganisms in biosorption of toxic metals and radionuclides. Int Biodet Biodegr. 35:17-40.

(19) Lopez A, Lazaro N, Marques AM. 1997. The interphase technique: a simple method of cell immobilization in gel-beads. J Microbiol Methods. 30:231-234.

(20) Humphries AC, Nott KP, Hall LD, Macaskie LE. 2005. Reduction of Cr(VI) by immobilized cells of *Desulfovibrio vulgaris* NCIMB 8303 and *Microbacterium* sp. NCIMB 13776. Biotechnol Bioeng. in press.

(21) Levine IN. 1993. Physical Chemistry. Speer, J. B., Maisel, J., editors. McGraw-Hill Book Co: Singapore.

(22) Mabbett AN, Yong P, Farr JPG, Macaskie LE. 2004. Reduction of Cr(VI) by 'palladised'-biomass of *Desulfovibrio desulfuricans* ATCC 29577. Biotechnol Bioeng. 87:104-109.

(23) Macaskie LE, Baxter-Plant VS, Creamer NJ, Humphries AC, Mikheenko IP, Mikheenko P, Penfold DW, Yong P. 2005. Applications of bacterial hydrogenases in waste decontamination, manufacture of novel bionanocatalysts and in sustainable energy. Biochem Soc Trans. 33:76-79.

(24) Penfold DW, Macaskie LE. 2004. Production of hydrogen from sucrose by *Escherichia coli* strains carrying the pUR400 plasmid, which encodes invertase activity. Biotechnol Lett. in press.

Table 1. Waste composition

Component	Concentration in nougat waste	Concentration in resuspension medium	Concentration in caramel waste	Concentration in resuspension medium
Total soluble sugars (w/w)**	37.2 %	3.72 %	53.00 %	5.30 %
Total reducing sugars (w/w)	10.2 %	1.02 %	25.50 %	2.55 %
Total protein content (w/w)	0.5 %	0.05 %	1.90 %	0.19 %
Ammonium ion (mg L^{-1})	0.004	0.0004	2.20	0.22
Sulfide (mg L^{-1})	0.02	0.002	ND*	ND*

ND* - Not detected

Glucose was present at 1.8 % (w/v) in resuspension medium

**Note that *E. coli* HD701, as used, lacks invertase so cannot utilise the sucrose (cane sugar) components of the wastes. Introduction of the appropriate genes to enable sucrose utilisation for enhanced H_2 production is described elsewhere (24). Waste composition was analysed by D. W. Penfold and Dr. G. Thompson (School of Civil Engineering, The University of Birmingham, England).

Table 2. Effect of H_2 source and immobilization on Cr(VI) reduction.

a) **Resting cells of *D. vulgaris***	H_2 Flow rate ($mL\ h^{-1}$)	$[Cr(VI)]_{5h}$* (μM)	$[Cr(VI)]_{5h}$ unit mass^{-1} (μM mg dry cell wt^{-1})
Free cells + $H_{2(commercial)}$	60 ± 11.0	176 ± 10**	35 ± 2
Immobilized cells + $H_{2(commercial)}$	60 ± 11.0	174 ± 10**	35 ± 2
Free cells + Bio-$H_{2(glucose)}$	14.7 ± 1.5	396 ± 29	79 ± 6
Immobilized cells + Bio-$H_{2(glucose)}$	14.7 ± 1.5	290 ± 8	78 ± 2
Immobilized cells + Bio-$H_{2(nougat)}$	13.7 ± 1.1	402 ± 22	80 ± 4
Immobilized cells + Bio-$H_{2(caramel)}$	NT	455 ± 5	91 ± 1

b) **Bio-Pd(0)**	H_2 Flow rate ($mL\ h^{-1}$)	$[Cr(VI)]_{5h}$* (μM)	$[Cr(VI)]_{5h}$ unit mass^{-1} (μM mg $Pd(0)^{-1}$)
Free Bio-Pd(0) + $H_{2(commercial)}$	60 ± 11.0	441 ± 52	176 ± 21
Immobilized Bio-Pd(0) + $H_{2(commercial)}$	60 ± 11.0	496 ± 18	198 ± 7
Free Bio-Pd(0) + Bio-$H_{2(glucose)}$	14.7 ± 1.5	314 ± 6	126 ± 2
Immobilized Bio-Pd(0) + $H_{2(glucose)}$	14.7 ± 1.5	354 ± 11	142 ± 4
Free Bio-Pd(0) + Bio-$H_{2(caramel)}$	NT	340 ± 8	136 ± 3
Immobilized Bio-Pd(0) + $H_{2(caramel)}$	NT	322 ± 14	129 ± 6
Immobilized Bio-Pd(0) + excess Bio-$H_{2(glucose)}$	289.2 ± 33.7	408 ± 8***	163 ± 3
Immobilized Bio-Pd(0) + excess Bio-$H_{2(caramel)}$	315.0 ± 37.2	455 ± 6***	182 ± 2

$[Cr(VI)]_{5h}$* : Concentration of Cr(VI) removed from solution in initial 5 h.

**Reduction ceased after 3.5 h ***Negligible Cr(VI) remained in solution after 2.5 h.

Data are means ± SEM from 3 experiments.

NT -biohydrogen flow rate was not tested in the small reactor (Table 2a) but larger scale tests showed a comparable rate of production (Table 2b).

Legends to Figures:

Fig. 1. The Cr(VI) reducing dual reactor system for batch (a) and continuous (b) Cr(VI) reduction.

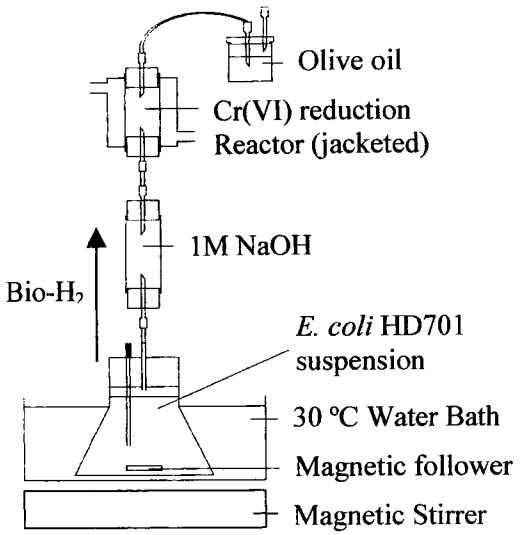
Fig. 2. Example TEM of (a) native and (b) palladised cells of *D. vulgaris*. Palladium was loaded onto the biomass at a mass ratio of 3:1 biomass:Pd (see text). Bar = 0.5 μm.

Fig. 3. Batch reduction of 500 μM Cr(VI) by suspended and immobilized resting cells of *D. vulgaris* NCIMB 8303 (a,b) or Bio-Pd(0) (c,d,e) using chemical hydrogen (a,c) or Bio-H_2 (b,d,e) as electron donor. Filled symbols: Cr(VI) removal in the absence of H_2; Open symbols: in presence of H_2/ Bio-H_2; o : free cells/ Bio-Pd(0) with H_2/ Bio-H_2 $_{glucose}$; Δ : immobilized cells/ Bio-Pd(0) with H_2/ Bio-H_2 $_{glucose}$; ◊ : immobilized cells/ Bio-Pd(0) with Bio-H_2 $_{nougat}$; □ : immobilized cells/ Bio Pd(0) with Bio-H_2 $_{caramel}$; x : free Bio-Pd(0) with Bio-H_2 $_{caramel}$. (b) and (c) used Bio-H_2 produced from the 310 ml reactor and (e) used Bio-H_2 produced from the 5.5 L reactor (H_2 flow rates as shown in Table 2). Data are means ± SEM from 3 experiments. Where no error bars are shown these were within the dimensions of the symbols.

Fig. 4. Continuous reduction of 100 μM Cr(VI) by agar-immobilized Bio-Pd(0) using Bio-H_2 as electron donor. Columns were set up as described in Materials and Methods, with Cr(VI) supplied at a flow rate of 0.15 mL min^{-1}. o : immobilized Bio-Pd(0) plus Bio-H_2 $_{glucose}$; ● : immobilized Bio-Pd(0) in the absence of H_2; ▲ : Volume of Bio-H_2 evolved. Data are means ± SEM from 3 experiments. Where no error bars are shown these were within the dimensions of the symbols.

Fig. 1

(a)


Olive oil
Cr(VI) reduction
Reactor (jacketed)
1M NaOH
Bio-H2
E. coli HD701
suspension
30 °C Water Bath
Magnetic follower
Magnetic Stirrer

(b)

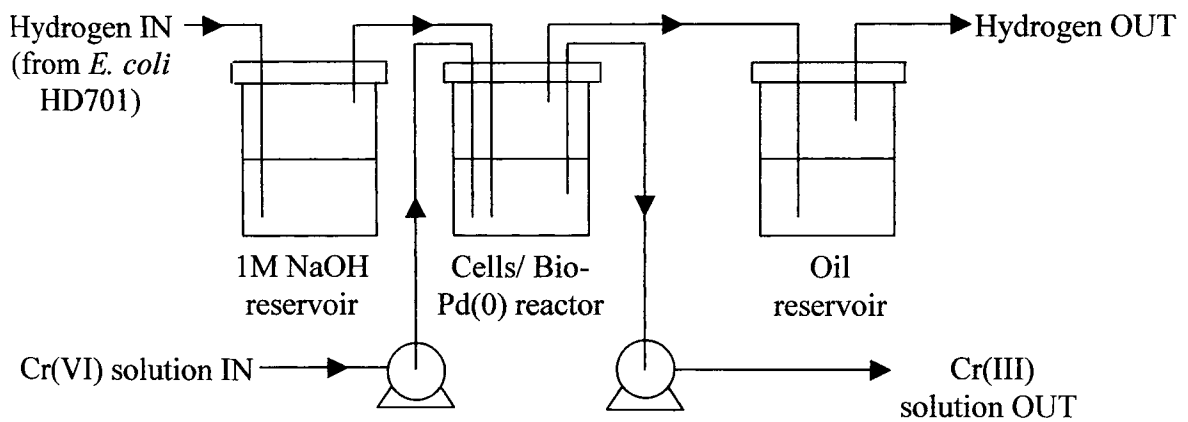

Hydrogen IN
(from E. coli
HD701)
Hydrogen OUT
1M NaOH
reservoir
Cells/ Bio-
Pd(0) reactor
Oil
reservoir
Cr(VI) solution IN
Cr(III)
solution OUT

Fig. 2

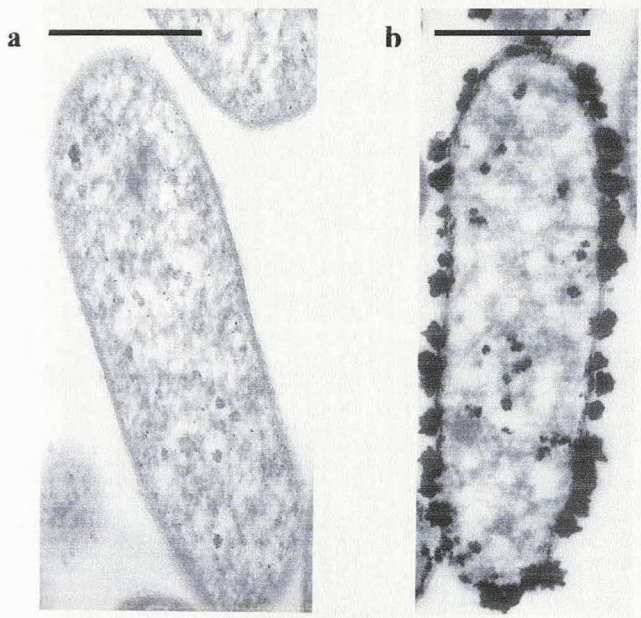


Fig. 3

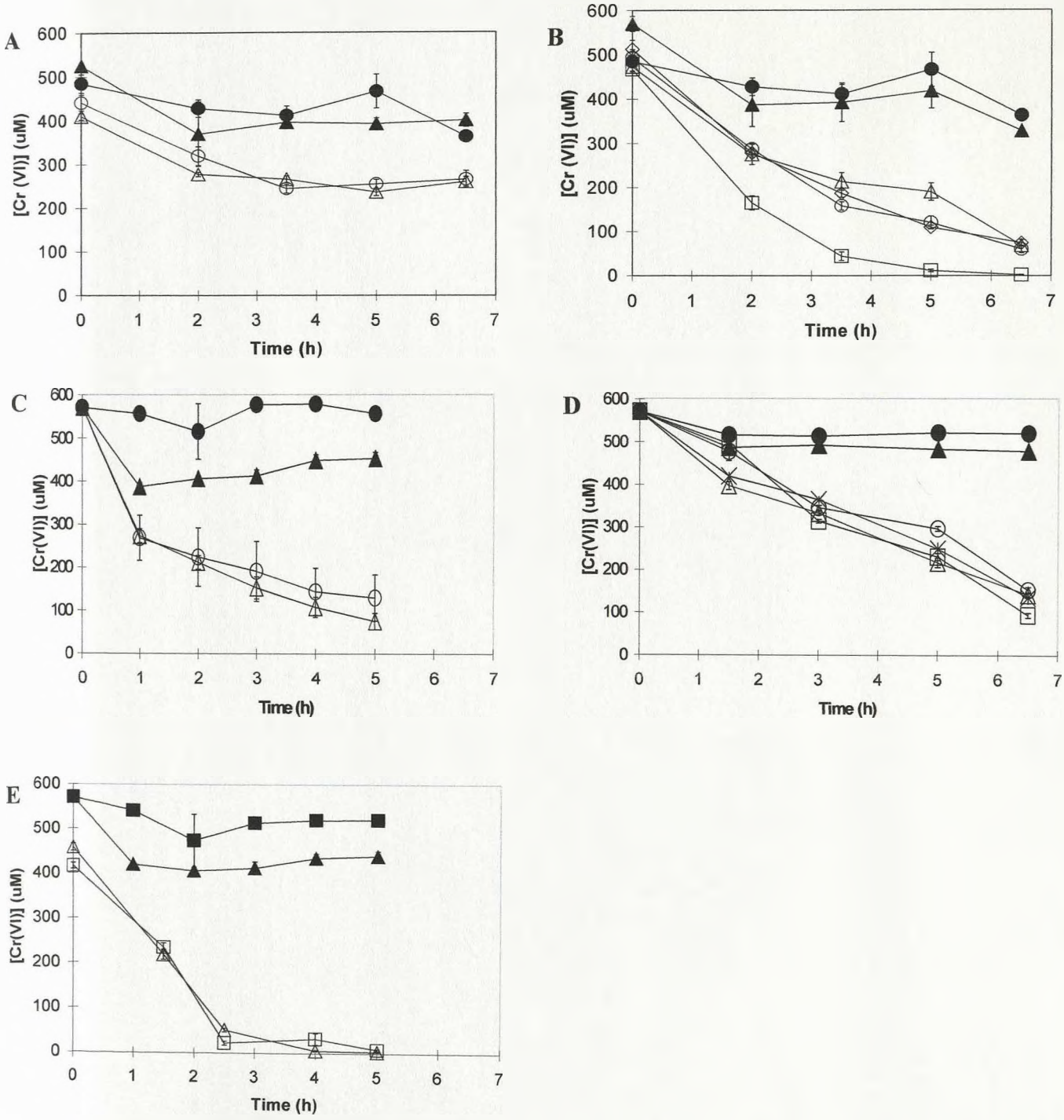
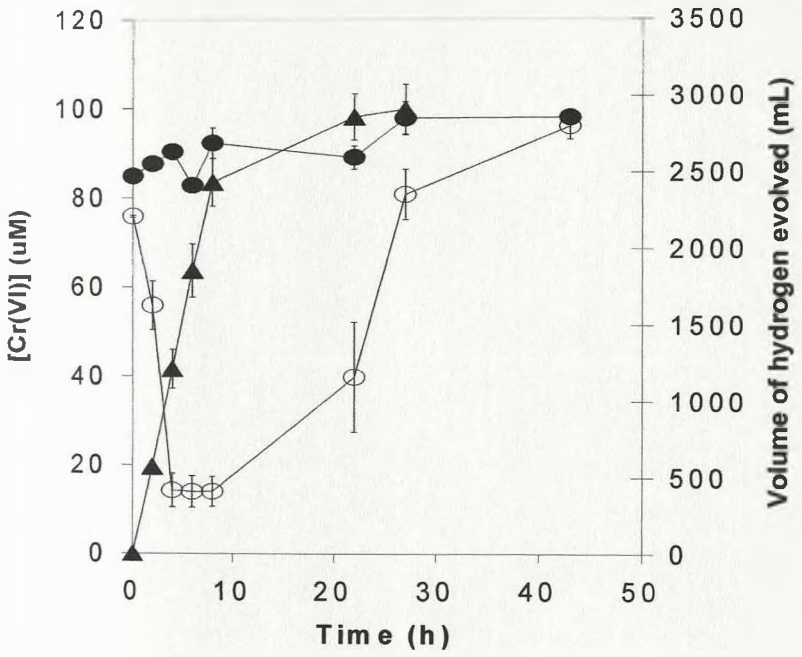


Fig. 4


120
100
80
60
40
20
0
[Cr(VI)] (uM)
3500
3000
2500
2000
1500
1000
500
0
Volume of hydrogen evolved (mL)
0
10
20
30
40
50
Time (h)

SECTION 5

Discussion

General Discussion

The overall goal of this research programme was to define mathematically a continuous-flow immobilized reactor system capable of removing Cr(VI) from solution. Additional information regarding reactor homogeneity, integrity and chemistry was gained through magnetic resonance imaging (MRI) and the final aim was to use MRI to define a Cr(VI) bioreactor spatio-temporally for model refinement.

Although several microbial systems for Cr(VI) bioremediation have been proposed previously, the challenge conditions are usually not comparable and therefore realistic comparison of their biotechnological potentials have not been made. For example, in the case of *Desulfovibrio vulgaris* NCIMB 8303 resting cells were added to a MOPS/ citrate buffered solution with formate as the electron donor (Mabbett *et al.* 2002), whilst cells of *Microbacterium* sp. NCIMB 13776 were used in acetate minimal medium (Pattanapipitpaisal *et al.* 2001). The initial objective of this study was to find a common challenge solution that provides optimum conditions for Cr(VI) reduction by resting cells of both *D. vulgaris* and *Microbacterium* sp. with respect to pH, temperature and electron donor **(Section 2.1)**. This reaction solution was defined as 500 μM sodium chromate, 25 mM each of sodium acetate (electron donor for *Microbacterium* sp.), sodium formate (electron donor for *D. vulgaris*) and sodium citrate, pH 7 and 30 °C. Citrate acted as an additional electron donor for Cr(VI) reduction by *Microbacterium* sp., and as a complexing ligand, which was found essential to ameliorate the toxicity of the Cr(III) product to the mediating enzymes of *D. vulgaris* (Mabbett *et al.* 2002). Using this reaction solution, *D. vulgaris* reduced Cr(VI) at an initial rate of approx. 4 fold greater than *Microbacterium* sp. Incorporation of MOPS increased the initial rate of reduction by *D. vulgaris* and *Microbacterium* sp.; although the reason for this is unknown.

Retention of cells by immobilization for industrial Cr(VI) bioremediation increases cell stability under more adverse conditions (e.g. pH), reduces the need for biomass/ effluent separation, and allows the process to be performed in continuous flow-through mode, consequently reducing process costs and reactor downtime. The immobilization strategy selected affects parameters such as overall catalytic activity, effectiveness of catalyst utilization, catalyst deactivation and cost (Bailey and Ollis 1986). The second objective of this project was therefore to identify the most appropriate immobilization method and to investigate the long-term stability of Cr(VI) reduction in immobilized-cell bioreactors **(Section 2.2)**. Preliminary studies investigated the potential of *D. vulgaris* and *Microbacterium* sp. to form biofilms on reticulated foam cubes, with neither strain forming adequate biofilms that could be utilised for continuous-flow studies.

Gel entrapment was chosen as an alternative. Generally gel entrapment produces immobilized cell systems with high biomass loadings, formed under mild conditions, maintaining high cell viability and Cr(VI) reducing efficiency (Willaert and Baron 1996). The physical and mechanical properties of the gel matrix are important, for example, pore size distribution and porosity determine the quantity of cells that can be immobilized in the support and the accessibility of the substrate to the immobilized cells (Bailey and Ollis 1986).

Resting cells of *D. vulgaris* and *Microbacterium* sp. immobilized in chitosan and Lentikats® did not reduce Cr(VI), attributable to reduced cellular metabolic integrity due to the relatively harsh immobilization procedure. Polyvinyl alcohol-borate (PVA-borate) beads, previously identified as a suitable and efficient immobilization matrix for *Microbacterium* sp. (Pattanapipitpaisal *et al.* 2001), were a poor support for resting cells of *D. vulgaris* and *Microbacterium* sp. The PVA-borate beads dissolved after 24 h of batch Cr(VI) reduction, attributable to complex formation between the perfusing citrate and Ca^{2+} ions cross-linking

the PVA-borate gel matrix (Bickerstaff 1997). Matrix stability and batch Cr(VI) reducing ability were however maintained when *D. vulgaris* and *Microbacterium* sp. were immobilized in agar, agarose and *k*-carrageenan.

The potential of agar, agarose and *k*-carrageenan-immobilized resting cells of *D. vulgaris* and *Microbacterium* sp. for Cr(VI) reduction in continuous-flow packed-bed reactors was investigated **(Section 2.2)**. *K*-carrageenan cell beads disintegrated after 5 h, attributable to citrate complexation of K^+ ions that stabilise the gel matrix (Leenen 2001). Agarose-immobilized *D. vulgaris* and *Microbacterium* sp. lost Cr(VI) reducing ability relatively quickly in conjunction with loss in bead integrity and cell wash-out from the reactor (as illustrated by magnetic resonance imaging (MRI)). In contrast, agar cell beads maintained integrity throughout. The initial extent of Cr(VI) reduction by agar-immobilized *D. vulgaris* and *Microbacterium* sp. was high, with minimal retention of Cr in columns (shown by ICP-MS mass balance analysis), but reduction ability was lost relatively quickly (ceasing after approx. 160 h). This was probably attributable to biochemical constraints (e.g. cell death, enzyme inactivation, end product inhibition) since the agar beads retain excellent integrity and were, therefore, the immobilization matrix of choice for further studies.

For industrial purposes reactors are engineered to operate at high efficiency for a considerable amount of time because running an immobilized-cell reactor is inexpensive, but growing cells, immobilizing, filling and emptying the reactor is expensive and frequent downtime is unacceptable (Bucke 1986). Additionally biological systems are sensitive to alterations in pH, ionic strength or other parameters, which over a period of time may lead to reduced activity (Thomas and Laval 1996). An alternative, more robust approach is to use a hybrid bioinorganic catalyst. Growth-decoupled cells of sulfate-reducing bacteria can reduce Pd(II) to cell bound Pd(0) at the expense of hydrogen via cellular hydrogenase activity (Yong

et al. 2002, Mikheenko 2004) to produce a bioinorganic catalyst (Bio-Pd(0)), comprising of nanoscale Pd(0) particles supported on the surface of the bacterial cells (Mikheenko *et al.* 2001). Batch studies have shown that Bio-Pd(0) is substantially more efficient at Cr(VI) reduction than comparable live cells of *D. vulgaris* (Mabbett and Macaskie 2002).

The potential to use agar-immobilized Bio-Pd(0) for Cr(VI) reduction in continuous-flow packed-bed reactors was investigated **(Section 3.1)**. Columns containing agar-immobilized Bio-Pd(0) reduced Cr(VI) at high efficiency for over 680 h (pH 7). Hence Bio-Pd(0) can be considered a superior catalyst for Cr(VI) reduction compared to resting cells of *D. vulgaris* (see above). With respect to homogeneity of the catalyst, magnetic resonance imaging of agar beads showed that Bio-Pd(0) is dispersed evenly throughout the matrix, although visualisation of individual Bio-Pd(0) particles was below the limit of resolution of MRI **(Section 3.1)**.

The challenge solution used in the above experiments was optimal with respect to resting cells of *D. vulgaris* and *Microbacterium* sp. Subsequently it was necessary to define the optimum conditions for Cr(VI) reduction by Bio-Pd(0) with respect to temperature, pH, initial Cr(VI) concentration and presence of oxygen **(Sections 3.2, 3.3)**. Bioprocesses are usually constrained to within physiologically permissive criteria, but the use of an inorganic catalyst held on dried biomass would remove this constraint, enabling operation under the more extreme conditions which typify many industrial wastes. Also, the composition of industrial wastewater is likely to vary with respect to pH and Cr(VI) concentration, and it is important to understand how these parameters affect the rate of Cr(VI) reduction. Cr(VI) remediation by Bio-Pd(0) was similar at 20 and 30 °C and was not significantly affected by the presence of oxygen. Consequently the process can be considered economically attractive compared to a process involving resting cells of *D. vulgaris*, which requires anaerobic conditions and an optimal temperature of 30 °C. The initial rate of Cr(VI) reduction increased linearly with

Cr(VI) concentration up to 300 μM for both suspended and agar-immobilized Bio-Pd(0). No further increase in reduction rate was observed above this concentration, suggesting the maximum Cr(VI) reduction rate was reached, even though this concentration was below the apparent maximum reduction rate (V_{max}) for Cr(VI) (see later).

The ability of microorganisms to reduce Pd(II) to Pd(0) is not confined to the sulfate-reducing bacteria. Previously Mikheenko (2004) showed that *E. coli* strain MC4100 could be used as the carrier biomass for Bio-Pd(0). The catalytic efficacy of free and agar-immobilized Bio-Pd(0) produced using *E. coli* strains MC4100 (parental) and HD701 (Hyc A deficient mutant, upregulated with respect to hydrogenase 1-4 expression), *D. vulgaris* NCIMB 8303 and *D. desulfuricans* NCIMB 8307 with respect to Cr(VI) reduction was studied **(Section 3.3)**. Investigations using batch suspensions suggested the initial rate of Cr(VI) reduction was similar when Bio-Pd(0) was produced using *D. vulgaris* or *D. desulfuricans*, and was higher compared to Bio-Pd(0) produced using *E. coli* strains MC4100 (1.7 fold) and HD701 (1.3 fold). The lower rate of reduction could be attributed to the lower hydrogenase activity present in the live cells of *E. coli*, and the consequent display of fewer nucleation sites and hence fewer, but larger Pd(0) agglomerates for the same amount of Pd(II) deposited. Using *Desulfovibrio* it was shown that cells containing a large number of small deposits were catalytically more active compared to cells with larger, but fewer agglomerates of Pd(0) (Mikheenko 2004) possibly attributable to respective catalyst surface areas. The higher reduction rate observed with Bio-Pd(0) produced using *E. coli* strain HD701 could be attributed to the higher hydrogenase activity of this strain (more foci for Pd(0) growth). Continuous-flow studies further illustrated the superior catalytic activity of Bio-Pd(0) produced using *Desulfovibrio* sp., which when immobilized in agar and packed into a column, initially achieved 50 % conversion (at 24 h: reducing to 20 % at 96 h) of Cr(VI). In

comparison *E. coli* strains MC4100 and HD701 Bio-Pd(0) initially achieved 10 and 16 % conversion, respectively. Cr(VI) reduction by Bio-Pd(0) produced using *E. coli* strain HD701 was slightly higher than that of strain MC4100. This was attributed to the higher hydrogenase activity of the upregulated strain, and the consequent display of more, smaller Pd(0) deposits. However, *E. coli* strain HD701 is upregulated with respect to hydrogenase 1-4, and it is not understood whether each or all of these hydrogenases has a role in Pd(II) reduction. Further studies would investigate the involvement of hydrogenase in Bio-Pd(0) synthesis through the use of hydrogenase specific mutations.

Since the *Desulfovibrio*-derived Bio-Pd(0) was superior to both *E. coli* MC4100 and HD701, Bio-Pd(0) produced using *D. vulgaris* was chosen for further study **(Section 3.3)**. The amount of Cr(VI) removed from columns was linearly related to input Cr(VI) up to 300 μM, suggesting this is the saturating concentration of Cr(VI), in agreement with batch studies (see above and **Section 3.2)**. Reduction efficiency decreased with increasing Cr(VI) concentration and with operating time irrespective of the Cr(VI) input concentration. Reduction ceased after approx. 0.7 mmoles of Cr(VI) had passed through columns, perhaps attributable to gradual 'poisoning' or fouling of the Bio-Pd(0) catalyst by Cr(III). Although the column activity decreased with time, the following equation was found to allow calculation of reactor activity (for any time between 0 – 96 h, Bio-Pd(0)-agar loading 7.5 mg mL^{-1}, flow rate 13.2 mL h^{-1}), with calculated values within 5 % of those experimentally determined:

$$\% \text{ reduction at time } t = (-0.11 \text{Ln}[Cr(VI)]_{inlet} + 0.36)\text{time} + (-0.06[Cr(VI)]_{inlet} + 73.02).$$

An additional way of modelling bioreactor activity was developed, in this case regarding the Bio-Pd(0) as an 'artificial enzyme'. Metallocofactors are incorporated into enzymes to provide binding interactions for small molecules (e.g. H_2), conferring the catalytic capability

needed to achieve redox transformations (Rees 2002). Metalloproteins (e.g. hydrogenase) contain one or more metals (e.g. Fe, Ni) connected with inorganic groups interacting through protein ligands (e.g. cysteine, histidine) (Rees 2002). The Pd-nanocluster system can be considered as analogous to metalloenzymes because it is redox-active, is localized onto or adjacent to cellular hydrogenases (Mikheenko 2004) and is probably held supported on a peptide-based matrix following an initial co-ordination of Pd(II) with amino groups as shown by x-ray photoelectron spectroscopy (I. deVargas and L. E. Macaskie, unpublished). In the current context, Bio-Pd(0) could effectively be considered functionally as a 'hydrogenase amplifier'. Application of Michaelis Menten kinetics to batch Cr(VI) reduction by suspended and agar-immobilized Bio-Pd(0) **(Section 3.2)** gave a $K_{m\ app}$ value of approx. 650 μM with a maximum velocity (V_{max}) of 1667 nmoles h^{-1} mg $Pd(0)^{-1}$. The $K_{m\ app}$ value is the substrate concentration at which the reaction rate is half-maximal, with a low K_m representing high affinity of an enzyme for its substrate, and a high K_m low affinity (Bailey and Ollis, 1986). In practice the rate of Cr(VI) reduction did not increase above an initial Cr(VI) concentration of 300 μM, and V_{max} was not reached (maximum reaction rates were approx. 630 and 460 nmoles h^{-1} mg $Pd(0)^{-1}$ for suspended and immobilized Bio-Pd(0), respectively). It is possible that irreversible inhibition of Bio-Pd(0) occurred, whereby the Cr(III) product bound to Bio-Pd(0), decreasing the concentration of active Bio-Pd(0), thus resulting in a lower reaction rate (Bailey and Ollis, 1986). This is reasonable to assume as Pd(0) is held supported on a peptide based matrix, and it has been shown previously that Cr(III) forms stable complexes with amino acids (Table 1).

Table 1. Stability constants of Cr(III) amino acid complexes (Vinokurov and Bondar, 2003).

Protonated form of ligand	logβ
Valine	8.3
Leucine	8.8
Serine	8.0
Aspartate	10.1
Arginine	8.0
Glycine	8.62

logβ denotes the stability constant calculated at 25 °C in a background solution of $NaClO_4$

Mabbett and Macaskie (2001) showed that suspended (non-palladised) resting cells of *D. vulgaris* had a K_m value for Cr(VI) of approx. 300 μM, suggesting that unpalladised cells have a higher affinity for Cr(VI) than Bio-Pd(0). Hence Bio-Pd(0) can be considered to be highly effective for Cr(VI) concentrations in the 0.6 – 1.6 μM region, but may be ineffective as a final 'polishing' step. For Cr(VI) concentrations below 0.6 μM, a bio-based system might be more effective.

Application of Michaelis-Menten kinetics to continuous-flow packed-bed columns **(Section 3.3)** gave $K_{m\ app}$ values which were dependent on the initial Cr(VI) concentration. At low substrate concentrations (100-300 μM), $K_{m\ app}$ was approx. 430 μM. This value is lower than for the batch system (above) suggesting that in a flow-through system, the Cr(III) product is removed more easily by the incoming supply of fresh citrate to complex it away from the catalyst. However, at initial substrate concentrations of 400 and 500 μM the $K_{m\ app}$ value apparently decreased. For a 'real' enzyme this would indicate competitive inhibition, whereby the inhibitor competes with the substrate for binding to the enzyme complex, altering enzyme shape and inhibiting product release (Dixon and Webb 1979). The inhibition mechanism for Bio-Pd(0) by Cr(III) is not fully understood and further studies are required to investigate the

reason for this apparent inhibition phenomenon, which is Cr(VI) concentration-dependent. Possibly the citrate cannot enter the matrix rapidly enough to remove Cr(III) which, in the absence of sufficient complexing ligand, may complex with amino acids present on the Pd(0) peptide support, fouling the catalyst and preventing further reaction.

The validity of using enzyme kinetics to describe Cr(VI) reduction (initial Cr(VI) concentration: 100 μM) by continuous-flow packed-bed reactors containing agar-immobilized Bio-Pd(0) was shown by substitution of the determined $K_{m\ app}$ back into the Michaelis-Menten equation **(Section 3.3)**. Prediction of E_0 (apparent amount of "enzyme" present) was within 11 % of values determined experimentally. Treatment of Bio-Pd(0) as an 'artificial enzyme' would then allow comparison of reactors containing *D. vulgaris* Bio-Pd(0) with comparable bioreactors containing live biomass.

A final consideration of this work was the use of hydrogen as an electron donor for Cr(VI) reduction by the bionanocatalyst. Commercial bottled H_2 contains traces of carbon monoxide which, over time, effectively acts as a catalyst poison. The use of formate in previous studies (above) was in order to know accurately the electron donor concentration and to remove effects attributable to the use of a 3-phase (solid-liquid-gas) system. For real industrial application, hydrogen would be useful if this could be produced as a clean gas in sufficient quantity, particularly from a renewable source. As a sustainable approach, H_2 can be produced fermentatively by *E. coli* strain HD701 at the expense of industrial sugar waste, mediated by the formate hydrogenlyase (FHL) system, here acting in the synthetic direction (c.f. earlier). The potential to use Bio-H_2, made by the upregulated *E. coli* strain HD701 using industrial sugar waste, as the electron donor for Cr(VI) reduction by resting and palladised cells of *D. vulgaris,* was investigated **(Section 4)**. Hydrogen produced by *E. coli*, using glucose solution, nougat and caramel waste as the oxidisable substrate, was successfully used to promote

Cr(VI) reduction by resting (unpalladised) and palladised cells of *D. vulgaris*. In the case of resting (unpalladised) cells, the Cr(VI) reduction rate was highest when hydrogen was produced upstream using caramel waste. However the hydrogen evolution rate was not significantly higher compared to when glucose solution and nougat waste were used and cannot account for the superiority of Bio-$H_{2\ caramel}$. Further studies should investigate the precise composition of the biogas, and should specifically investigate whether a volatile agent is present that could influence cellular hydrogenase activity of the downstream cells and thus Cr(VI) reduction by the live cells. The phenomenon is live biomass-associated, since the initial rate of Cr(VI) reduction by Bio-Pd(0) was similar using H_2 produced from glucose solution, nougat and caramel wastes. Comparison of Cr(VI) reduction by immobilized and suspended *D. vulgaris* and Bio-Pd(0) suggested the latter is more efficient at Cr(VI) reduction in the presence of Bio-H_2, on the basis of Cr(VI) reduced per unit mass. Therefore the potential to use Bio-H_2 and Bio-Pd(0) to treat Cr(VI) solution on a continuous basis was investigated, showing removal of Cr(VI) for as long as the Bio-H_2 supply was available. Development of a continuous Bio-H_2 reactor to work in conjunction with a downstream continuous-flow packed-bed reactor containing Bio-Pd(0) is underway.

Using Bio-Pd(0) to reduce Cr(VI) may appear uneconomic as palladium is an expensive metal ($216 per troy ounce: September 2004: http://www.platinum.matthey.com). However, palladium can be recovered from waste solutions such as automotive catalyst leachates, electronic scrap and industrial processing wastes. The catalytic activity of bio-palladium recovered from industrial waste leachates using *D. desulfuricans* is not affected by the presence of other metal contaminants in the biorecovered solid (Mabbett 2001).

The following system for the treatment of 3 industrial wastes can be suggested (Fig. 1). Bio-H_2, produced using industrial sugar waste, is used as an electron donor for palladium recovery

from industrial liquid waste (Yong *et al.* 2003, Mabbett *et al.* 2004) to produce Bio-Pd(0). Bio-H_2 and waste-derived Bio-Pd^0 are then used to remediate Cr(VI) wastewater. Since the palladium and hydrogen are both sourced from wastes from the precious metal (Yong *et al.* 2003) and food (Penfold *et al.* 2003) sectors, respectively, a substantial economic benefit would result from the conversion of these wastes into two useful products, avoiding landfill taxes and ensuring compliance with current legislation on disposal of solid scrap. Use of the biorecovered materials would mitigate the cost of the Cr(VI) treatment process, while at the same time permitting application outside the usual confines of physiological constraints (Mikheenko 2004).

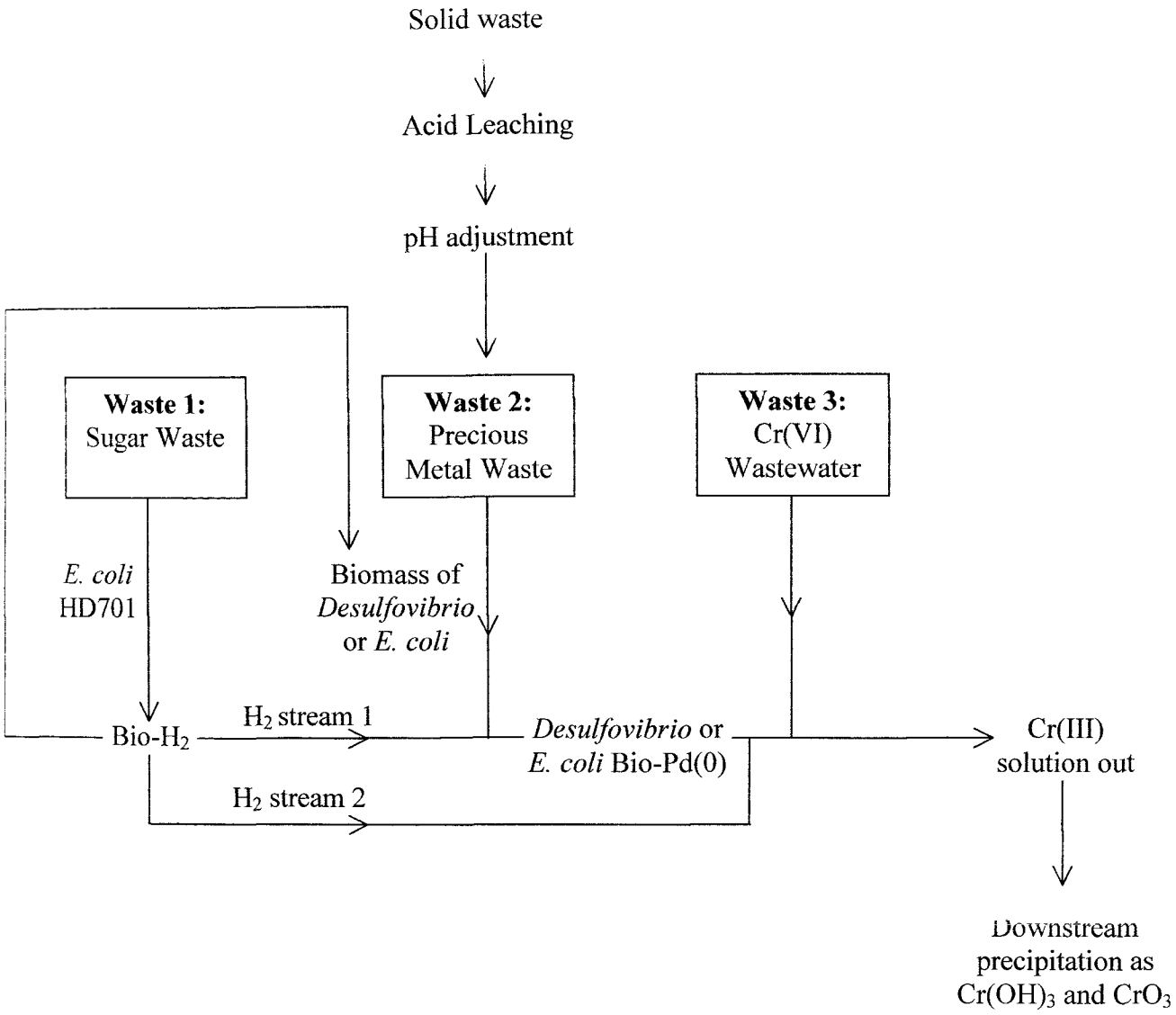


Fig. 1. System for the treatment of 3 industrial wastes (A.C. Humphries, D.W. Penfold, and L.E. Macaskie, unpublished).

Conclusions

This research programme has achieved the aims laid out in **Section 1**. As follows:

1) The optimum solution matrix for Cr(VI) reduction by both *D. vulgaris* NCIMB 8303 and *Microbacterium* sp. NCIMB 13776 is 500 μM Cr(VI), 25 mM each of acetate, formate, and citrate, and 20 mM MOPS/ NaOH, pH 7 and 30 °C.
2) The most appropriate matrix for immobilization of *D. vulgaris* and *Microbacterium* sp., with respect to Cr(VI) reduction rate and structural integrity, is agar.
3) Bio-Pd(0) represents a more robust, efficient and industrially attractive method for Cr(VI) reduction, compared to resting cells of *D. vulgaris* NCIMB 8303 and *Microbacterium* sp. NCIMB 13776.
4) Bio-Pd(0) produced using *D. vulgaris* NCIMB 8303 and *D. desulfuricans* NCIMB 8307 was a superior catalyst for Cr(VI) reduction, compared to Bio-Pd(0) produced using *E. coli* strains MC4100 and HD701.
5) Bio-Pd(0) can be treated as an 'artificial enzyme' to enable reactor modelling and comparison to living cell systems.
6) Biologically evolved hydrogen is a feasible alternative to commercially available hydrogen for Cr(VI) reduction by resting cells of *D. vulgaris* NCIMB 8303 and Bio-Pd^0.
7) MRI was successfully used to visualise the homogeneity of agar-Bio-Pd(0) beads, and to demonstrate agar beads retain structural integrity.
8) Aim number (8) could not be met within this study as detailed in 'further work'.

Further work

Through meeting the main aims of this research programme, several outstanding problems and new avenues of research have been highlighted.

1) Cr(VI) reduction by agar-immobilized Bio-Pd(0) in batch and continuous-flow systems was limited by inhibition, potentially by the Cr(III) product. The mechanism for this inhibition should be investigated further, and a method devised to prevent inhibition.

2) Investigation of Cr(VI) reduction is limited to a description of the overall reactor performance (i.e. the black-box approach) providing no information on biochemical, chemical or transport phenomena within the reactor. In this study, MRI was used to visualize polyurethane foam-immobilized *Serratia* sp. N14 after challenging with either 1 mM Cr(III) or 1 mM Cr(VI) **(Appendix III)**. Image analysis showed paramagnetic Cr(III) induced image contrast, and Cr(III) could be distinguished from Cr(VI), which is MRI 'silent'. Following further method development, Cr(VI) remediation could be studied non-invasively using MRI to quantify Cr(VI) reduction spatio-temporally.

3) Aim (8) was to follow the continuous reduction by agar-immobilized Bio-Pd(0) of Cr(VI) and Cr(III) *in situ* by MRI to further delineate the 'black box' model. This aim could not be achieved as Bio-Pd(0) itself gives an effect on the proton signal in MRI (as shown in Section 3.1) which swamps that of the Cr(VI) to Cr(III) conversion. A method needs to be developed to differentiate between the effect on the proton signal given by the Cr and Pd species. It is not known, as yet, whether this technology exists or indeed is feasible; identification of the ferromagnetic nature of Bio-Pd(0) (Mikheenko 2004) may facilitate this possibility. Further studies would also look to differentiate between Pd(II) and Pd(0) to allow the formation of Pd(0) to be followed *in situ*. Electron Paramagnetic Resonance

(EPR) may be used to help develop this method, and the newly-available technique of EPR imaging, a sister technique to MRI, may facilitate such investigations.

4) The use of continuous-flow packed-bed columns containing agar-immobilized Bio-Pd(0) is potentially an economical, efficient and environmentally friendly way of remediating Cr(VI) in polluted wastewaters. This study has only investigated Cr(VI) reduction using a model solution. In reality, industrial wastewater would contain additional compounds. For example electroplating wastewater contains other toxic metals (e.g. lead, cadmium), solvents, cyanides and acidic solutions (www.lenntech.com). Further studies are required to determine how the presence of these compounds affects Cr(VI) reduction. The use of the developed mathematical model will facilitate quantification of these effects.

References

Bailey JE, Ollis DF. 1986. Biochemical Engineering Fundamentals. Verma K, Martin CC, editors. Singapore: McGraw-Hill Book Co.

Bickerstaff G. 1997. Immobilization of enzymes and cells: some practical considerations. Paisley, Scotland: Humana Press.

Bopp LH, Ehrlich HL. 1988. Chromate resistance and reduction in *Pseudomonas fluorescens* strain LB300. Arch Microbiol. 150:426-431.

Bucke C. 1986. Methods of immobilising cells. In: Webb C, Black GM, Atkinson B, editors. Process engineering aspects of immobilised cell systems. Institution of Chemical Engineers.

Dixon M, Webb EC. 1979. Enzyme specificity. In: Enzymes. London: Longman group Ltd.

Kimbrough DE, Cohen Y, Winer AM, Creelman L, Mabuni C. 1999. A critical assessment of chromium in the environment. Crit Rev Environ Sci Technol. 29: 1-46

Komori K, Wang PC, Toda K, Ohtake H. 1989. Factors affecting chromate reduction in *Enterobacter cloacae* strain HO1. Appl Microbiol Biotechnol. 31:567-570.

Leenen E. 2001. Description of the support material. In: R. Wijffels, editor. Immobilized cells. Springer Lab Manual. Heidelberg: Springer.

Lloyd JR, Macaskie LE. 1997. Microbially-mediated reduction and removal of technetium from solution. Res Microbiol. 148:530-532.

Llovera S, Bonet R, Simonpujol MD, Congregado F. 1993. Chromate reduction by resting cells of *Agrobacterium radiobacter* EPS916. Appl Environ Microbiol. 59:3516-3518.

Mabbett AN, Yong P, Farr JPG, Macaskie LE. 2004. Reduction of Cr(VI) by 'palladised' biomass of *Desulfovibrio desulfuricans* ATCC 29577. Biotechnol Bioeng. 87:104-109.

Mabbett AN, Lloyd JR, Macaskie LE. 2002. The effect of complexing agents on the reduction of Cr(VI) by *Desulfovibrio vulgaris* ATCC 29579. Biotechnol Bioeng. 79:389-397.

Mabbett AN, Macaskie LE. 2002. A new bioinorganic process for the remediation of Cr(VI). J Chem Technol Biotechnol. 77:1169-1175.

Mabbett AN, Macaskie LE. 2001. A novel isolate of *Desulfovibrio* sp. with enhanced ability to reduce Cr(VI). Biotechnol Lett. 23:683-687.

Mabbett AN. 2001. The reduction and recovery of chromium (VI) from industrially polluted waste waters using sulphate-reducing bacteria. Ph.D Thesis. The University of Birmingham, England.

Mikheenko I. 2004. Nanoscale palladium recovery. Ph.D Thesis. The University of Birmingham, England.

Mikheenko I, Mikheenko P, Darlington CNW, Muirhead CM, Macaskie LE. 2001. Magnetic testing of Pd loaded bacteria. In: Ciminelli VST, Garcia Jr O, editors. Biohydrometallurgy: Fundamentals, Technology and Sustainable Development. Elsevier, Amsterdam.

Neal AL, Lowe K, Daulton TL, Jones-Meehan J, Little BJ. 2002. Oxidation state of chromium associated with cell surfaces of *Shewanella oneidensis* during chromate reduction. Appl Surf Sci. 202:150-159.

Nott KP, Paterson-Beedle M, Macaskie LE, Hall LD. 2001. Visualisation of metal deposition in biofilm reactors by three-dimensional magnetic resonance imaging (MRI). Biotechnol Lett. 23:1749-1757.

Pattanapipitpaisal P, Brown NL, Macaskie LE. 2001. Chromate reduction by *Microbacterium liquefaciens* immobilised in polyvinyl alcohol. Biotechnol Lett. 23:61-65.

Penfold DW, Forster CF, Macaskie LE. 2003. Increased hydrogen production by *Escherichia coli* strain HD701 in comparison with wild-type parental strain MC4100. Enzyme Microb Technol. 33:185-189.

Rees DC. 2002. Great metalloclusters in enzymology. Annu Rev Biochem. 71:221-246.

Thomas D, Laval JM. 1996. Enzyme technology. In: Balasubramanian D, Bryce CFA, Dharmalingham K, Green J, Jayaraman K, editors. Concepts in biotechnology. Hyderabad: University Press (India) Ltd.

Tzesos M, Volesky B. 1982. The mechanism of uranium biosorption by *Rhizopus arrhizus*. Biotechnol Bioeng. 24:385-401.

Willaert R, Baron G. 1996. Gel entrapment and micro-encapsulation: methods, applications, and engineering principles. Rev Chem Eng. 12:5-20.

Yong P, Rowson NA, Farr JPG, Harris IR, Macaskie LE. 2003. A novel electrobiotechnology for the recovery of precious metals from spent automotive catalysts. Environ Technol. 24:289-297.

Yong P, Rowson NA, Farr JPG, Harris IR, Macaskie LE. 2002. Bioreduction and biocrystallization of palladium by *Desulfovibrio desulfuricans* NCIMB 8307. Biotechnol Bioeng. 80:369-379.

Vinokurov EG, Bondar VV. 2003. Prediction of stability constants for Cr(III) and Cr(II) complexes. Russian Journal of Coordination Chemistry. 29:71-77.

APPENDICES

APPENDIX I:

"Chromate reduction by immobilized cells of *Desulfovibrio vulgaris* using biologically produced hydrogen"

This paper was presented at the **15TH International Biohydrometallurgy Symposium** 2003. Athens-Hellas (Greece). Biohydrogen production was done by D. W. Penfold. All other work was done by A. C. Humphries. This paper was written and presented by A. C. Humphries.

CHROMATE REDUCTION BY IMMOBILIZED CELLS OF *DESULFOVIBRIO VULGARIS* USING BIOLOGICALLY PRODUCED HYDROGEN.

A. C. Humphries[a], D. W. Penfold[a], C. F. Forster[b], L. E. Macaskie[a]*

[a]School of Biosciences, The University of Birmingham, Edgbaston, B15 2TT, UK

[b] School of Civil Engineering, The University of Birmingham, Edgbaston, B15 2TT, UK

**Author for correspondence (Fax (44)-121-414-6557; E-mail: L.E.Macaskie@bham.ac.uk)*

Abstract

Many industrial wastes contain Cr(VI), a carcinogen and mutagen, the toxicity of which can be ameliorated by reduction to Cr(III). Agar-immobilized cells of *Desulfovibrio vulgaris* NCIMB 8303 can reduce toxic Cr(VI) to less-toxic Cr(III) at the expense of metabolically produced hydrogen as the electron donor in a batch reactor under anaerobic conditions using H_2 produced by *Escherichia coli* HD701. Complete reduction of chromate (500 μM) was achieved within 24 h with an initial reduction rate of 302 nmol h^{-1} mg dry cell $wt.^{-1}$ using a coupled dual reactor system.

Introduction

Biological hydrogen can be economically produced by a process in which oxidisable sugar waste can be used to provide electron donors for hydrogen producing bacteria (1). Additional benefits of biological hydrogen production are that it can be coupled to waste bioremediation, for example conversion of Cr(VI) to Cr(III) using bacteria that can effect this reduction via hydrogenase activity.

E. coli strain HD701, which cannot synthesise the formate hydrogen lyase (FHL) repressor (Hyc A) and is, therefore, up-regulated with respect to FHL expression, has been constructed previously (2). The formate hydrogen lyase (FHL) complex comprises formate dehydrogenase and hydrogenase 3. The function of this complex is to convert formate, a metabolic end product of anaerobic fermentation, into CO_2 and H_2. This is a homeostatic response to reduce the acidity of the medium. In this respect, hydrogenase 3 is acting as a synthetic hydrogenase and is the source of reducing power for a second organism which is proposed to oxidise H_2 as a source of reducing power.

Environmental pollution by hexavalent chromium (CrO_4^{2-}) in marine and urban sediments and wastewaters originates predominantly from industrial sources, for example, leather tanning, electroplating and textile manufacture (4). Detoxification of Cr(VI), a mutagen and carcinogen, to less toxic Cr(III) can be achieved chemically or biologically. Chemical reduction is expensive and requires large amounts of chemicals, whereas biological reduction by Cr(VI) reducing bacteria is potentially economically favourable because the methods involved are cheap and simple (5). Additionally the use of toxic reagents are not required, and native, non-hazardous microorganisms can be used (6). Many Cr(VI) reducing microorganisms have been identified, with examples including, *Pseudomonas fluorescens*

LB300 (7, 8), *Agrobacterium radiobacter* EPS-916 (9), *Enterobacter cloacae* strain HO1 (10, 11), and *Desulfovibrio vulgaris* NCIMB 8303. The latter is a member of the sulphate-reducing bacteria (SRB) with a well-established ability to reduce a variety of metals, including Cr(VI) (12 - 17). The SRB use an organic compound (e.g. formate) or molecular H_2 as the electron donor and SO_4^{2-} as the electron acceptor in dissimilatory sulfate reduction. Certain high valence metal ions, such as Tc(VII) and Cr(VI), can be used as electron sinks in the absence of sulfate, with consequent metal reduction (16, 18). Previous studies have demonstrated that a complexing agent that is able to chelate Cr(III) must be present to permit Cr(VI) reduction by *D. vulgaris* (for example bicarbonate or citrate: (16)).

This study investigates the potential to use H_2, produced by *E.coli* HD701 from industrial sugar wastes, as the electron donor for Cr(VI) reduction by *D.vulgaris* NCIMB 8303. For industrial purposes, Cr(VI) reduction using freely suspended cells is disadvantageous because of downstream difficulties in biomass/ effluent separation (19). Consequently chromate reduction by agar-immobilized *D. vulgaris* NCIMB 8303 in batch mode was investigated, and compared to that of free cells. Agar was identified previously as the most suitable immobilization matrix for this purpose, imposing minimal mass transfer limitations and good structural integrity (A. C. Humphries, unpublished). The possibility of using H_2 produced by *E. coli* HD701 using nougat and caramel wastewater in a dual coupled reactor system was also investigated.

Materials and Methods

Organisms and growth conditions

E.coli strain HD701 was as described previously (2, 3). *E.coli* strain HD701 was maintained as previously described (1).

Desulfovibrio vulgaris NCIMB 8303 was obtained from Prof. D. R. Lovley (University of Massachusetts, Amherst, MA, USA). Cells were maintained routinely in butyl-rubber sealed 100 mL serum bottles in Postgate's medium C (20) under O_2-free N_2 (OFN). For experiments, growing cultures (OD_{600} 0.8 ± 0.2) were produced by withdrawing anaerobically 10 mL of an actively growing culture and adding it to 100 mL of fresh medium C. The culture was harvested after 24 h (OD_{600} 0.8 ± 0.2) for hydrogen production tests.

Preparation of cell suspensions

Resting cells of *D. vulgaris* were prepared by transferring cells anaerobically in a MACS-MG anaerobic workstation (Don Whitley Scientific Ltd) to closed centrifuge tubes and harvesting by centrifugation at 8000 rpm, 10 min, 4 °C. Cells were washed three times and resuspended with anaerobic (degassed) stock solutions of 20 mM MOPS/ NaOH buffer (pH 7). Cell concentrate was stored at 4 °C under N_2 until use (within 24 h of harvesting). The biomass concentration of the cell concentrate was estimated by measuring the OD_{600}, and conversion to dry cell wt. via a previously determined calibration (A. C. Humphries, unpublished).

Immobilization of cells

200 mg Agar-Agar (FSB Laboratory supplies) was mixed with 9 mL deionised water, degassed with OFN, and autoclaved (121 °C, 20 min). The gel was allowed to cool to 40 °C before 1 mL cell concentrate (*D. vulgaris*, as above) was added to give a cell concentration of 2.5 mg dry cell wt. mL gel^{-1}. Gel bead formation was carried out in the MACS-MG workstation. The aqueous phase (degassed deionised water) and the oily phase (degassed olive oil) (21) were placed in a 100 mL vessel in a ratio 10:1 (v/v), respectively. The gel-cell mixture was extruded into the oily phase using a 2.5 mL syringe fitted with a 21G needle. The gel-cell beads passed into the aqueous phase and were collected using a nylon net. Beads were

washed once with Triton-X100 (Sigma) (0.01% (v/v)) and three times with degassed deionised water (21).

Hydrogen evolution

Hydrogen production experiments used phosphate buffered saline (PBS) in 320 mL reactors (working volume of 310 mL) at 30 °C with 10 % (v/v) inocula of *E.coli* HD701 cells pre-grown in nutrient broth to an OD_{600} of 0.995 ± 0.005. Carbon substrates were used at 10 % of the total volume, and consisted of 100 mM glucose, nougat waste, or caramel waste (see below). Suspensions were gassed with argon for 1 h after inoculation and maintained at 30 °C, with stirring. Evolved hydrogen was passed through 1 M sodium hydroxide to remove carbon dioxide and into 30 °C column reactors containing the immobilized *D. vulgaris* and chromate reaction solution (Fig. 1A, B) at an approx. rate of 10 mL h^{-1}. The exit gas was bubbled through olive oil to extrude air from the system.

Chromate reduction by *D. vulgaris* NCIMB using biologically produced H_2 in batch mode

For batch reduction, the reaction mixtures were set up in the anaerobic workstation (30 °C) in 14 mL jacketed glass columns. Cell beads (2 mL: equivalent to 5 mg dry cell wt.) or free cells (equivalent to 5 mg dry cell wt.) were suspended in 10 mL of a degassed solution of 20 mM MOPS-NaOH, 25 mM sodium citrate, and 500 μM sodium chromate, pH 7. Columns were removed from the workstation and degassed with OFN for 15 min. Controls for all experiments comprised cells or cell beads in the absence of hydrogen, or reaction solution in the absence of cells. Columns were maintained at 30 °C. Chromate reduction was initiated by the provision of hydrogen to the cells, either biologically produced (Fig. 1) or supplied from a commercially available hydrogen-containing gas cylinder. Samples were withdrawn

periodically, via syringe, and supernatants (100 μL) were analysed for residual Cr(VI) using diphenylcarbazide (specific for Cr(VI) as described by 5, 6).

(A) (B)

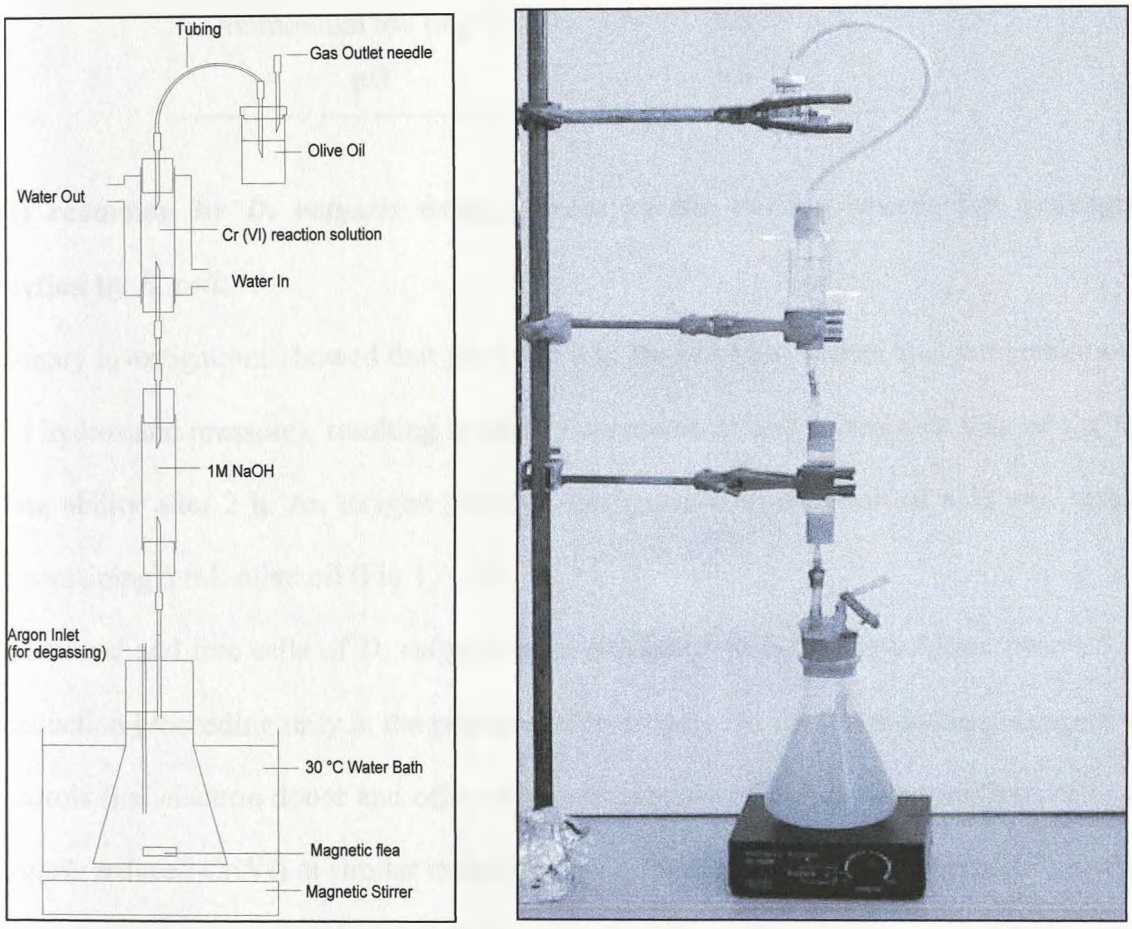


Fig. 1. The Cr(VI) reducing dual reactor system.

Results and Discussion

Nougat and Caramel Wastewater

Nougat wastes composition was as previously described (1). Caramel waste composition is shown in Table 1. Both wastes were stored at 4 °C.

Table 1. Caramel waste composition

Component	Concentration
Total soluble sugars (w/w)	53.0 %
Total reducing sugars (w/w)	25.5 %
Total protein content (w/w)	1.9 %
Ammonium ion (mg L^{-1})	2.2
pH	3.6

Cr(VI) reduction by *D. vulgaris* using glucose as the carbon source for hydrogen production by *E. coli.*

Preliminary investigations showed that gas entry into the reaction column was not continuous (due to hydrostatic pressure), resulting in loss of anaerobiosis and subsequent loss of Cr(VI) reducing ability after 2 h. An oxygen trap was incorporated in the form of a 12 mL serum bottle containing 5 mL olive oil (Fig 1 A, B).

Immobilized and free cells of *D. vulgaris* were incubated with Cr(VI) solution over 6.5 h, with reduction proceeding only in the presence of hydrogen. No Cr(VI) reduction occurred in the controls (i.e. electron donor and cells were both required). Free and immobilized cells of *D. vulgaris* reduced Cr(VI) at similar initial rates over the first 2 h at *ca.* 200 nmol h^{-1} mg dry cell $wt.^{-1}$). After 5 h, 120 ± 14.5 μM Cr(VI) remained in free cell suspensions, and 190 ± 19.9 μM Cr(VI) remained in immobilized cell reaction solutions (Fig. 2). The initial Cr(VI) reduction rates and final Cr(VI) concentrations are not significantly different (as determined by Students *t*-test analysis) for free and immobilized cells using biologically produced hydrogen as electron donor, suggesting that there are no mass or heat transfer limitations imposed by immobilization of *D. vulgaris* in agar gel.

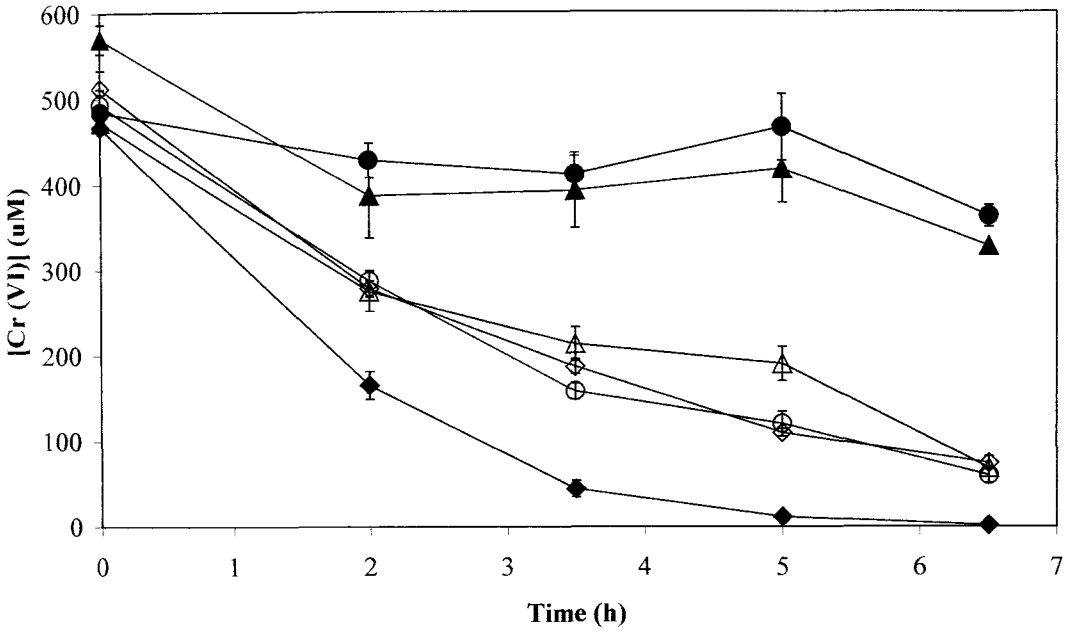


Fig. 2. Reduction of 500 μM Cr(VI) by free and agar-immobilized resting cells of *D. vulgaris* NCIMB 8303 using biologically produced hydrogen as electron donor.

Legend: o: Free cells plus bio-hydrogen; •: Free cells in the absence of hydrogen; Δ: Agar-immobilized cells plus bio-hydrogen; ▲: Agar-immobilized cells in the absence of hydrogen; ◊: Agar-immobilized cells plus bio-hydrogen produced using nougat wastewater; ♦: Agar-immobilized cells plus bio-hydrogen produced using caramel wastewater.

Cr(VI) reduction by *D. vulgaris* using chemical hydrogen

All Cr(VI) reduction tests were repeated using commercially available hydrogen supplied from a cylinder at the minimal flow rate that could be attained (*ca.* 60 mL h^{-1} (Fig. 3)). Reduction of Cr(VI) occurred at an initial rate of 150 nmol h^{-1} mg dry cell $wt.^{-1}$, with approx. 300 μM Cr(VI) remaining after 5 h for both free and immobilized cells. Student's *t*-test analysis showed Cr(VI) reduction by *D. vulgaris* using biologically produced hydrogen was significantly higher than when using chemical hydrogen at the higher gas flow rate. This

diminished reduction capacity may be due to temperature constraints, as chemical hydrogen is not pre-warmed prior to entry into the reaction solution. As a result of the high gas flow rate, it was observed that agar bead integrity was compromised, with the onset of bead disintegration occurring after 3.5 h.

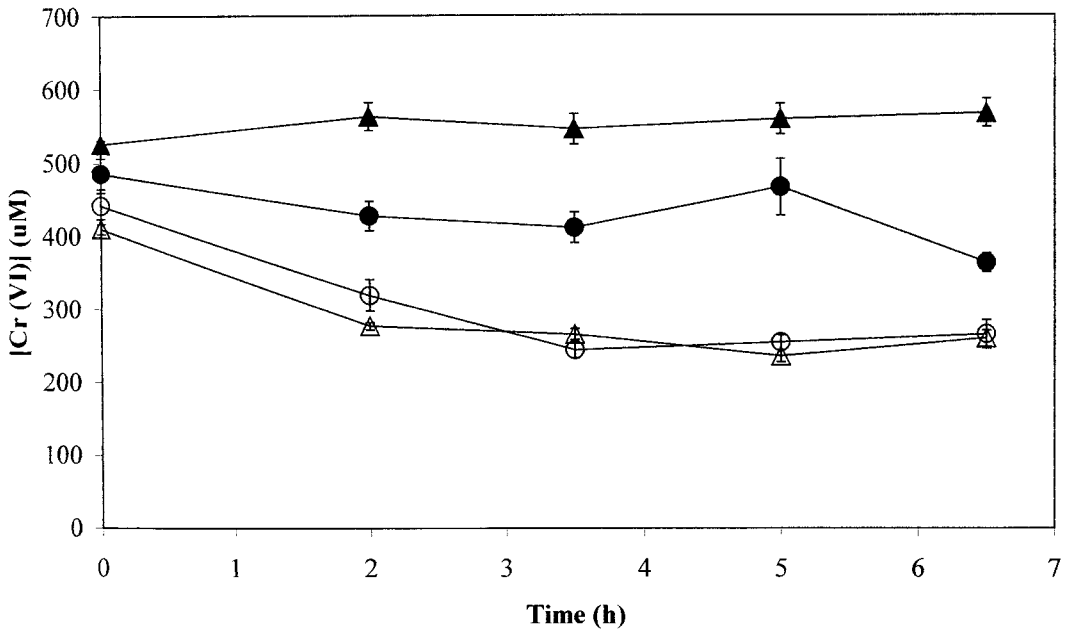


Fig. 3. Reduction of 500 μM Cr(VI) by free and agar-immobilized resting cells of *D. vulgaris* NCIMB 8303 using chemical hydrogen as electron donor.

Legend: o: Free cells plus bio-hydrogen; •: Free cells in the absence of hydrogen; Δ: Agar-immobilized cells plus bio-hydrogen; ▲: Agar-immobilized cells in the absence of hydrogen;

Cr(VI) reduction by *D. vulgaris* using nougat and caramel waste as carbon source for *E. coli*

Immobilized cells of *D. vulgaris* were reacted with Cr(VI) reaction solution over 6.5 h. Using nougat and caramel waste as a carbon source for the *E.coli* reactor (Fig. 2) gave a Cr(VI) removal rate of 234 ± 18.3 and 302 ± 14.5 nmol h^{-1} mg dry cell $wt.^{-1}$, respectively. After 5 h, 110 ± 4.3 μM and 2 ± 0.8 μM Cr(VI) remained in immobilized cell reaction solutions.

Reduction of Cr(VI) using hydrogen produced by *E.coli* fed with nougat waste gave statistically similar (as determined by Students *t*-test analysis) reduction rates as when provided with 100 mM glucose, whilst those obtained for *E.coli* fed with caramel waste are significantly higher. The latter is the only substrate to promote complete loss of Cr(VI) within 5 h (Fig. 2).

Conclusions

Hydrogen generated biologically by *E. coli* HD701, using glucose, nougat or caramel wastewater as a carbon source, can be used by *D. vulgaris* NCIMB 8303 as the electron donor for Cr(VI) reduction. The total amounts, and rates, of Cr(VI) reduction by *D. vulgaris* were significantly higher with biologically evolved hydrogen compared to chemical hydrogen. Chromate reduction using hydrogen generated by *E. coli* supplied with 100 mM glucose or nougat waste occurred at statistically similar rates with similar concentrations remaining after 6.5 h. In comparison, Cr(VI) reduction using hydrogen generated by *E.coli* using caramel waste occurred *ca.* 1.5 times faster, with Cr(VI) totally reduced after 6.5 h. The high rates of Cr(VI) removal using industrial sugar wastes as feedstock for *E.coli* hydrogen production demonstrate that this is an economically favourable and environmentally friendly system for the use of one starting material for remediation of another.

Acknowledgements

We wish to acknowledge the financial support of the BBSRC (Studentship Number: 00/B1/E/0698 to DWP.) and the EPSRC (Studentship Number: 00318650 to ACH.). The authors would like to thank Professor A. Böck (Lehrstuhl fur Mikrobiologie der Universitat,

Munich, Germany) for providing the strain of *E.coli* and Cadbury Trebor Bassett Ltd (Bournville, Birmingham, UK) for provision of the nougat and caramel wastewaters.

References

1. D. Penfold, C. Forster, L. E. Macaskie. *Enzyme Microbiol. Technol.* (in submission)
2. M. Sauter, R. Bohm, A. Bock. *Mol. Microbiol.* 6 (1992) 1523.
3. J. Lloyd, G. Thomas, J. Finlay, J. Cole, L. Macaskie. *Biotech. Bioeng.* 66 (1999) 122.
4. W. Smith, G. Gadd. *Journal of Appl. Microbiol.* 88 (2000) 983.
5. P. Pattanapipitpaisal, N. Brown, L. Macaskie. *Biotechnol. Letters.* 23 (2001) 61.
6. C. Cervantes, J. Campos-Garcia, S. Devars, F. Gutierrez-Corona, H. Loza-Tavera, J. Torres-Guzman, R. Moreno-Sanchez. *FEMS Microbiology Reviews.* 25 (2001) 335.
7. E. Chirwa, Y. Wang. *J. Environ. Eng.-ASCE.* 123 (1997) 760.
8. P. DeLeo, H. Ehrlich. *Appl. Microbiol. Biotechnol.* 40 (1994) 756.
9. A. Llovera, R. Bonet, M. Simonpujol, F. Congregado. *Appl. Environ. Microbiol.* 59 (1993) 3156.
10. K. Komori, A. Rivas, K. Toda, H. Ohtake. *Biotechnol. Bioeng.* 35 (1990) 951.
11. P. Wang, T. Mori, K. Toda, H. Ohtake. *J. Bacteriol.* 172 (1990) 1670.
12. D. Lovley. *Annu. Rev. Microbiol.* 47 (1993) 263.
13. D. Lovley, E. Phillips. *Appl. Environ. Microbiol.* (1994) 726.
14. J. Lloyd, P. Yong, L. Macaskie. *Appl. Environ. Microbiol.* 64 (1998) 4607.
15. J. Lloyd, V. Nolting, V. Sole, K. Bosecker, L. Macaskie. *Geomicrobiology Journal.* 15 (1998) 45.
16. A. N. Mabbett, J. Lloyd, L. E. Macaskie. *Biotechnol. Bioeng.* 79 (2002) 389.
17. A. C. Humphries, L. E. Macaskie. *Biotechnol. Letters.* 24 (2002) 1261.

18. J. Lloyd, A. N. Mabbett, D. Williams, L. E. Macaskie. *Hydrometallurgy.* 59 (2001) 327.

19. C. White, S. Wilkinson, G. Gadd. *Appl. Environ. Microbiol.* (1994) 726.

20. J. Postgate. The sulphate-reducing bacteria. (1979).

21. A. Lopez, N. Lazaro, A. Marques. *Journal of Microbiological Methods.* 30 (1997) 231.

APPENDIX II:

Principles of Magnetic Resonance Imaging

Appendix II gives an overview of the principles of Magnetic Resonance Imaging (MRI), followed by a summary of previous MRI investigations that are relevant to this study.

I wish to acknowledge Dr. Melanie Britton (School of Chemistry, The University of Birmingham), an expert in MRI, who has read through this Appendix to ensure it is factually correct.

1.0 Magnetic Resonance Imaging (MRI)

MRI is becoming increasingly recognised as a potential method used in studies on industrial processes, as it is non-invasive and non-destructive (Paterson-Beedle *et al.* 2001a). MRI can be used to study optically opaque systems, and aid in optimising product properties and processing operations *in situ*, for example, transport and reaction processes (Paterson-Beedle *et al.* 2001b). Examples of systems studied using MRI include physical and chemical heterogeneity in composite materials, and the transition of ceramics and glues from the liquid to solid state (Paterson-Beedle *et al.* 2001a). MRI was used during this project to image intact immobilized cell packed bed reactors to study support matrix stability, spatial heterogeneity of agar-immobilized Bio-Pd(0) and chromium speciation.

2.0 Principles of MRI

2.1 Nuclear spin and the magnetic moment

Nuclei with unpaired protons or neutrons have angular momentum and nuclear spin. The motion of this charge produces a magnetic moment, which has size and direction (denoted by an arrow). Consequently the nucleus acts like a small magnet, and effectively has a north and south pole. Nuclei with an even number of protons and neutrons exhibit no spin. The spin quantum number, I, quantifies the spin (Hutchison and Foster 1987). In MRI, nuclei with a spin quantum number of 1/2 are generally used.

2.2 Bulk magnetisation in a magnetic field

When placed in a magnetic field (B_0), a nuclear spin will align with the field. For nuclei with a spin quantum number of 1/2, one of two stable states can be taken. Either the nuclei will take the low energy state (parallel to the field) or the high energy state (in the opposite direction to the field), as illustrated in the diagram below.

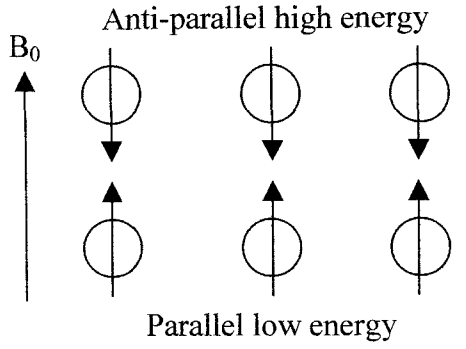


Fig. 1: Low and High energy alignment of nuclei with applied magnetic field (Taken from Westbrook and Kaut 1993).

Whether nuclei align parallel or anti-parallel to the magnetic field depends on the strength of the applied field and temperature (Westbrook and Kaut 1993). Nuclei with low thermal energy align with the field as they do not possess enough energy to oppose it. When a large number of spins are present in the sample, nuclei will be distributed randomly between the two energy states, but there will be a bias for the low energy state. The energy difference between the high and low energy states determines the frequency of radiation (the Larmor frequency, *f*) that will induce a transition between the two energy states.

2.3 Resonance

In the equilibrium state, the summed average of the magnetic moments (bulk magnetisation, M_0) is aligned with the static field, B_o. When energy is delivered to a nucleus at its Larmor frequency and orthogonal to B_o then the nucleus gains energy (more nuclei align anti-parallel to B_0) and resonates (Fig. 2).

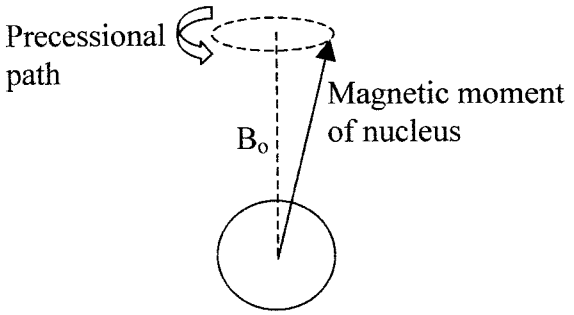


Fig. 2: Precession (Taken from Westbrook and Kaut 1993).

The energy supplied corresponds to the radiofrequency (RF) band of the electromagnetic spectrum (Westbrook and Kaut 1993). Following application of an RF pulse the magnetic moment moves away from B_o. The flip angle is defined as the angle by which the magnetic moment moves away from the direction of B_0. The magnitude of the flip angle depends on the amplitude and duration of the RF pulse. Typically the flip angle is 90° as it produces the largest signal. It should be noted that the static field, B_o, is aligned along the longitudinal axis/ plane, and the plane at 90° to B_o is termed the transverse plane (Westbrook and Kaut 1993). Additionally, following RF application, the magnetic moments in the transverse plane move into phase with each other. This means that the magnetic moments are in the same place on the precessional path around B_o. Fig. 3 illustrates the difference between magnetic moments being in phase and out of phase.

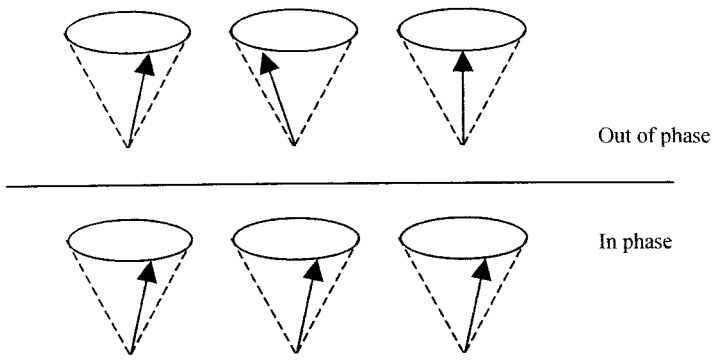


Fig. 3: Phase of magnetic moments around their precessional path (Taken from Westbrook and Kaut, 1993).

2.4 The MR signal

While the magnetisation is in the transverse plane it can induce a voltage into a coil of wire, known as the RF coil. If a receiver coil is placed in the transverse plane, following application of an RF pulse 'in phase' magnetisation cuts across the coil, producing magnetic fluctuations. The voltage produced is the magnetic resonance signal, the frequency of which is identical to the Larmor frequency. The magnitude of the signal depends on the amount of magnetisation present in the transverse plane (Westbrook and Kaut 1993).

2.5 The free induction signal

When the RF pulse is turned off, the bulk magnetisation loses energy by a process known as relaxation, so that it realigns with the static magnetic field. Consequently the magnitude of the resonance signal decreases. This decrease is the free induction decay signal (FID) (Westbrook and Kaut 1993).

2.6 Relaxation processes

Eventually the magnetisation will revert to M_0, the equilibrium state, by two distinct relaxation processes, each of which has its own time constant.

Longitudinal relaxation (also known as spin-lattice relaxation) involves the spin system losing energy to the molecular environment. It results in nuclei recovering their longitudinal magnetisation. Longitudinal relaxation has a time constant T_1 and the rate of relaxation is exponential (Westbrook and Kaut 1993).

Transverse relaxation involves the spin system losing no energy as a whole, but with spins exchanging energy among themselves. A loss in transverse magnetisation occurs as there is a gradual loss in phase coherence (i.e. nuclei precess at different rates) in the precessional motion of the spins. This process is known as spin-spin relaxation, and has a time constant of T_2. Loss of energy from the spin system by spin-lattice relaxation also causes decay in transverse relaxation. Time constant T_2 never exceeds T_1 (Hutchison and Foster 1987).

2.7 Pulse timing parameters

A pulse sequence is a combination of RF pulses and delays (such as the repetition time and the echo time). The repetition time (TR) is the time between RF pulses, and determines the amount of relaxation that occurs between pulses, and determines the amount of T_1 relaxation that occurs. The echo time (TE) is the time from the RF application to the peak of the signal induced in the coil. Fig. 4 illustrates the difference between TR and TE. The amount of T_2 relaxation that occurs is determined by the TE (Westbrook and Kaut 1993).

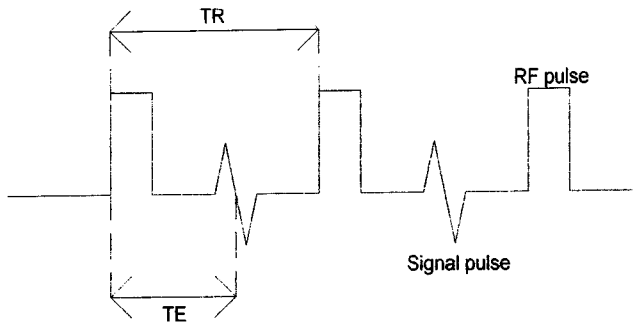


Fig. 4: A basic pulse sequence (Taken from Westbrook and Kaut 1993).

2.8 Spin Echo Imaging

Spin echo imaging initially involves the application of a 90° RF pulse. The 90° pulse rotates the magnetization into the transverse plane (Fig. 5a) and the magnetization begins to dephase. When visualised, this appears as a fan of individual *M*-components spread out in the transverse plane (Fig. 5b). Application of a 180° RF pulse rotates the magnetization by 180° about the x-axis. This results in the phases that were previously going too fast lagging behind (Fig. 5c). This results in the fan converging until after a further time, τ, all individual *M*-components will be back in phase (Fig. 5d). The signal produced at this time is called an echo (Hutchison and Foster 1987). Spin-echo is mainly used to measure T_2.

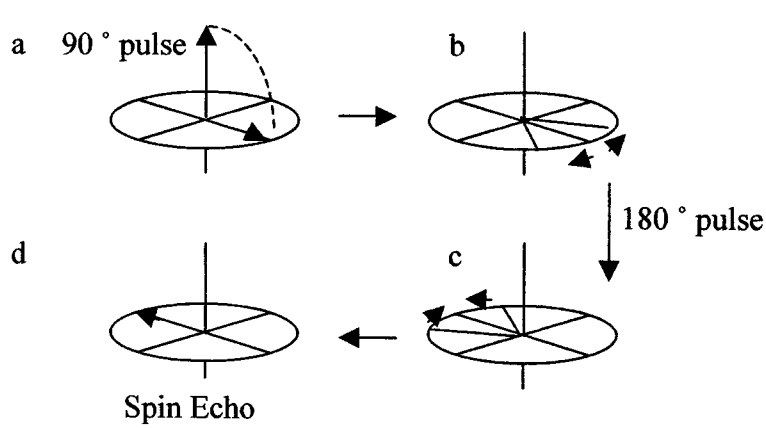


Fig. 5: The formation of a spin echo (Hutchison and Foster 1987).

2.9 Gradient Echo Techniques

As in spin echo imaging, gradient echo techniques use an RF excitation pulse to create transverse magnetization. However, instead of applying a second RF pulse to refocus the magnetization and form a spin echo, the dephasing transverse magnetization following the excitation pulse is collected and used to form an image (Westbrook and Kaut 1993). These sequences lend themselves well to imaging applications that require a short acquisition time. The main determinants of contrast in a gradient echo sequence are the users choices of flip angle, TE and TR.

2.10 Spoiled GRASS (SPGR) sequence

In SPGR, the transverse magnetization is prevented from returning to B_0 before the next RF pulse is applied. Using a short TE, image contrast is determined by the flip angle and TR.

2.11 Image contrast

When an image has areas of high signal, which appear white on an image, and areas of low signal, which appear black, then the image has contrast. High signals are produced when the nuclei in a sample have a large transverse component of magnetisation, and low signals are produced due to a low transverse component (Westbrook and Kaut 1993). Therefore image contrast depends on the relaxation times on the echo and repetition times and on the proton density of a sample (Paterson-Beedle *et al.* 2001b). Maximum signal detection is obtained when a short TE is used (to capture fully the transverse magnetisation before it decays) and long TR for full longitudinal recovery.

2.12 The use of metal ions as contrast agents

MR images can be improved by addition of contrast agents that influence proton density or proton relaxation. The development of contrast agents has focussed on compounds that affect $T_1$and T_2.

The most widely researched contrast agents have been paramagnetic materials; compounds that enhance the relaxation of surrounding protons, resulting in shortened T_1 and T_2 (Runge 1986). Paramagnetic substances have unpaired electrons in their outermost orbital, which induce a small magnetic moment. In the absence of an external magnetic field, these magnetic moments occur in a random pattern and cancel each other out. When an external magnetic field is present paramagnetic substances align with the direction of the field, and so the magnetic moments add together. Therefore the external magnetic field is affected in a positive way by paramagnetic substances by attraction to the field, resulting in a local increase in the magnetic field (Westbrook and Kaut 1993). Some transitional metals (e.g. iron, copper, and manganese) are strongly paramagnetic, usually in their reduced form (Oldendorf and Oldendorf 1988).

2.13 Use of paramagnetism as a way to determine metal speciation within a reactor

Paramagnetic substances can be used to;

1) 'Assay' metals that are paramagnetic by studying the intensity of the H^1 MRI signal produced (Fischer and Hall 1994).
2) Study metal binding to chelating agents. Binding of paramagnetic metal ions to macromolecules results in increased relaxation times (Lauffer 1987).
3) Follow differences in metal speciation where one valence and not another is paramagnetic (e.g. reduction of Fe(III) to Fe(II), or Cr(VI) to Cr(III)) (Fischer and Hall 1994).

3.0 Examples of MRI relevant to this project

Studies by Paterson-Beedle *et al.* (2001a) showed that it is possible to 'interrogate' an intact bioreactor non-invasively in 3D using MRI. *Serratia* sp. N14 expresses an acid-type phosphatase that liberates HPO_4^{2-} from a suitable organic phosphate donor. The liberated phosphate group can bind to metal ions to produce a cell surface metal phosphate precipitate (Paterson-Beedle *et al.* 2001a). The aims of the studies by Paterson-Beedle *et al.* were to characterise the spatial heterogeneity of metal removal, and to image any blockages that formed. The metal used in these studies for phosphate precipitation was La^{3+} because this is NMR 'silent'. Blockages were imaged due to exclusion of water from the blocked areas.

Polyurethane foam cubes with and without a biofilm coating were imaged using a 7 Tesla 9 cm vertical bore super-conducting magnet, using a gradient echo-sequence with a repetition time of 1000 msec, echo time of 7.5 msec, angle 45 °, and a spatial resolution of 156 μM x 156 μM x 156 μM. The total acquisition time was 9 h and 6 mins.

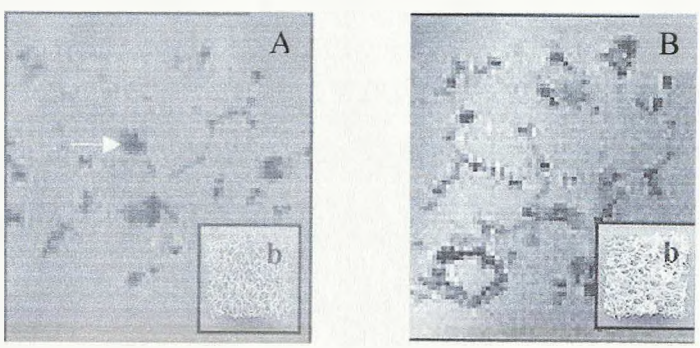


Fig. 6: A 2D slice through a 3D MRI data set of reticulated polyurethane foam in isotonic saline (inset: photograph of a single cube) in the absence (A) and presence (B) of *Serratia* biofilm in the absence of added metal (Taken from Paterson-Beedle *et al.* 2001a).

The foam *per se* gave zero signal compared to the surrounding isotonic saline. The foam structure was more visible when coated with biofilm (Fig. 6B) due to the proton signal from the water within the biofilm surrounding the foam matrix (Paterson-Beedle *et al.* 2001a).

In further studies polyurethane foam cubes with or without biofilm were packed in 13 mL glass columns, that were challenged with an upwards flow (10 mL h^{-1}) for 120 h. Challenge solutions contained 2 mM sodium citrate buffer, pH 6, and 5 mM sodium glycerol-2-phosphate supplemented with 1 mM $La(NO_3)_3$ and/ or 1 mM $CuSO_4.5H_2O$ as specified (Nott *et al.* 2001). In this case Cu^{2+} was applied to introduce contrast in the flow (see 2.12) and was not itself significantly removed into the biofilm (Nott *et al.* 2001). For MR imaging of columns a 2.35 Tesla 31 cm horizontal bore super-conducting magnet was used. A spoiled GRASS sequence was used to acquire 3D images, with a TR/ TE/ flip angle of 50 msec/ 7.5 msec/ 90 °, spatial resolution 312.5 μm x 312.5 μm x 312.5 μm, and a scan time of 13 min 39 seconds (Nott *et al.* 2001).

Columns (a) and (b) gave similar image contrasts as they do not contain Cu^{2+} (Fig. 7). Reactor (a) was not challenged with La^{3+}. The biofilm signal intensity was low against the challenge solution because of the biomass's high water content (greater than 90 %). Consequently the polyurethane foam can be seen as a dark matrix. Column (b) contains metal precipitate because it was challenged with La^{3+}. The precipitate is present as low signal intensity against the challenge solution. $LaPO_4$ is accumulated by the biofilm, resulting in reduced biofilm water content and proton signal. Columns (c), (d), and (e) all contain Cu^{2+} so are comparable in terms of image contrast. The presence of Cu^{2+} alters the MR properties of the challenge solution and water associated with the biofilm and precipitate. In contrast to columns (a) and (b), the biofilm and foam appear light (high signal intensity) against the challenge solution. In the absence of biofilm (and therefore no precipitate when challenged

with Cu^{2+} and La^{3+}), the foam matrix (c) is poorly visible. In the presence of biofilm and Cu^{2+} high signal intensity associated to the small amount of Cu^{2+} accumulated by the biofilm (d). When biofilm coated foam is challenged with Cu^{2+} and La^{3+}, the $LaPO_4$ precipitate is visualized as a white region at the column inlet (e).

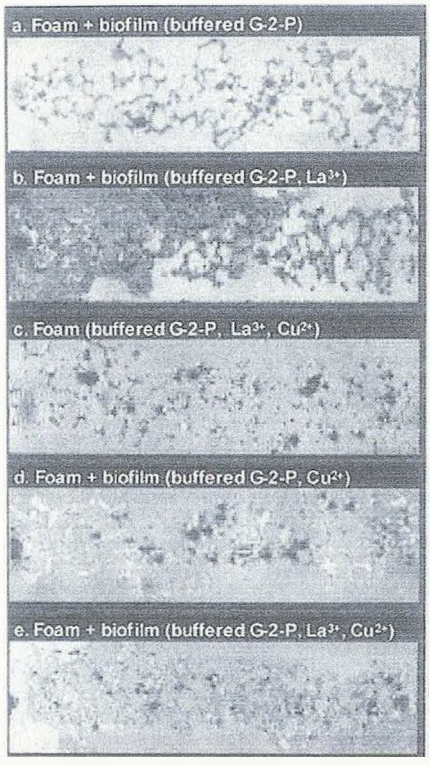


Fig. 7: 2D images of reactors packed with reticulated foam containing immobilized *Serratia* sp. biofilm and challenged with 2 mM citrate buffer, pH 6 in the presence of 5 mM glycerol-2-phosphate, and with or without metal: (a) metal unsupplemented flow (b) La^{3+} supplemented with no Cu^{2+} as contrast agent (c) control cell free reactor + La^{3+} + Cu^{2+} (note increased contrast) (d) Cu^{2+} supplemented (e) La^{3+} + Cu^{2+} supplemented (Nott *et al.* 2001).

References

Fischer A, Hall LD. 1994. Roles of paramagnetic substances in MRI: contrast agents, molecular amplifiers, and indicators of redox and pH mapping. MAGMA. 2:203-210.

Hutchison JMS, Foster MA. 1987. Practical NMR imaging. Oxford:IRL Press.

Lauffer RB. 1987. Paramagnetic metal complexes as water proton relaxation agents for NMR: theory and design. Chem Rev. 87:901-927.

Nott KP, Paterson-Beedle M, Macaskie LE, Hall LD. 2001. Visualisation of metal deposition in biofilm reactors by three-dimensional magnetic resonance imaging (MRI). Biotechnol Lett. 23:1749-1757.

Oldendorf W, Oldendorf W. 1988. Basics of magnetic resonance imaging. Martinus Nijhoff Publishing.

Paterson-Beedle M, Nott KP, Macaskie LE, Hall LD. 2001a. Three dimensional magnetic resonance imaging of *Serratia* biofilm reactors used for a metal accumulation process. In: Garcia O, editor. Ouro Preto: Elsevier.

Paterson-Beedle M, Nott KP, Macaskie LE, Hall LD. 2001b. Study of biofilm within a packed-bed reactor by three-dimensional magnetic resonance imaging. Method Enzymol. 337:285-305.

Runge V. 1986. Contrast agents in magnetic resonance imaging. In: Kulkami M, editor. Magnetic resonance imaging and spectroscopy. New York:Churchill Livingstone Publishers.

Westbrook C, Kaut C. 1993. MRI in practice. Oxford: Blackwell Scientific Publications.

APPENDIX III:

"Visualisation of the biosorption of Cr^{6+} and Cr^{3+} by Magnetic Resonance Imaging (MRI)"

All Magnetic Resonance Imaging and analysis was performed by Kevin Nott and Laurie Hall at the Herchel Smith Laboratory for Medicinal Chemistry (The University of Cambridge). Columns for imaging were prepared by A. N. Mabbett. This section was written by A. C. Humphries, with useful discussions with Dr Melanie Britton on application of MRI to visualise metal redox processes *in situ.*

Visualisation of the biosorption of Cr^{6+} and Cr^{3+} by Magnetic Resonance Imaging (MRI)

A. C. Humphries[1], A. N. Mabbett[1], K. P. Nott[2], L. E. Macaskie[1]*, L. D. Hall[2]

[1]*School of Biosciences, The University of Birmingham, Edgbaston, Birmingham, B15 2TT, UK.*

[2]*Herchel Smith Laboratory for Medicinal Chemistry, University of Cambridge, School of Clinical Medicine, University Forvie Site, Robinson Way, Cambridge, CB2 2PZ, UK.*

**Author for correspondence (Fax (44)-121-414-5925E-mail:* L.E.Macaskie@bham.ac.uk)

Abstract

Magnetic resonance imaging (MRI) was used to visualise *Serratia* sp. N14 immobilized on polyurethane foam after inclusion with Cr^{3+} or Cr^{6+} in a solution of 20 mM 3-(N-Morpholino)propanesulfonic acid (MOPS)-NaOH buffer (pH 5). Analysis of the signal intensities showed that biofilm was more contrasted against the challenge solution in the presence of paramagnetic Cr^{3+}, and that columns containing paramagnetic Cr^{3+} were distinguishable from Cr^{6+}, suggesting it may be possible to study Cr(VI) reduction non-invasively *in vivo* using MRI.

Keywords: chromium, magnetic resonance imaging, paramagnetic

Introduction

Magnetic Resonance Imaging (MRI) is becoming increasingly recognised as a potential method for studying industrial processes, as it is non-invasive and non-destructive (Lens and Hemminga 1998). MRI probes the physical state of matter and provides both spatial and chemical information (Hammer 1998). For example, MRI can be used to provide information about fluid flow (Dechter *et al.* 1991, Dijk *et al.* 1999), the transition of ceramics and glues from the liquid to solid state (Callaghan 1991), or mass transport in biofilms (Lewandowski *et al.* 1995).

The information gained from MR images can be improved by the addition of contrast agents, which influence the proton relaxation behaviour of water molecules. The most widely used contrast agents are paramagnetic compounds with unpaired electrons in their outermost orbital, which induce a small magnetic moment (Westbrook and Kaut 1993). Previous studies have demonstrated MRI is able to monitor the $Fe^{2+} \leftrightarrow Fe^{3+}$ equilibrium due to their differential effects on the relaxation times of water protons (Balcom *et al.* 1992).

MRI is able to monitor the biosorption and bioprecipitation of metal ions in a biofilm reactor. MRI was used to visualise polyurethane foam-immobilized *Serratia* in aqueous citrate buffer supplemented with glycerol-2-phosphate; *Serratia* sp. N14 expresses an acid-type phosphatase that liberates HPO_4^{2-} from a suitable organic donor (Nott *et al.* 2001). In the presence of La^{3+}, the foam matrix was more visible due to precipitation of $LaPO_4$, which is accumulated by the biofilm, resulting in reduction of the biofilm water content and hence the proton MRI signal; the $LaPO_4$ precipitated where it was produced, thereby effectively 'tagging' the location of the phosphohydrolase enzyme. Unlike with La^{3+}, Cr^{3+} and Cu^{2+} are not precipitated significantly as phosphates by the above phosphatase-mediated mechanism (Pattanapipitpaisal *et al.* 2002, Nott *et al.* 2001) and can therefore be used as MRI contrast

agents; when Cu^{2+} was present the contrast regime in the solution was altered significantly due to the paramagnetic properties of the Cu^{2+} ions. The foam matrix also became more visible due to a low level of Cu^{2+} biosorption by the biofilm (Nott *et al.* 2001).

In this preliminary study, the potential of the above MRI methodology to visualise Cr species *in situ* was investigated in the presence of *Serratia* sp. N14 biofilm. Such imaging, if successfully able to differentiate between soluble Cr^{6+} (MRI 'silent') and Cr^{3+} (paramagnetic, magnetic moment 3.8 BM: Bertini and Luchinat 1986) species, would provide potential to follow bioremediation spatially within a bioreactor in real time. The objective of the present study was to evaluate the feasibility for differentiation between Cr^{6+} and Cr^{3+} at physiologically realistic concentrations of metal.

Materials and Methods

Organisms, growth conditions and preparation of cell suspension

Serratia sp. N14 was grown as biofilm on polyurethane reticulated foam cubes (1 cm^3: TM30: Retiicel, Belgium) in an air-lift fermenter (Finlay *et al.* 1999).

Preparation of packed-bed reactor for MRI

Six biofilm-loaded foam cubes were packed into individual glass columns (i.d. 1.5 cm, length 9 cm) and challenged with flows supplemented with either 1 mM Cr^{3+} ($CrCl_3$) or 1 mM Cr^{6+} (Na_2CrO_4) in a carrier medium of 20 mM 3-(N-Morpholino)propanesulfonic acid (MOPS)-NaOH buffer and 5 mM glycerol-2-phosphate (G2P, pH 5). Reduction of Cr^{6+} did not occur (Pattanapipitpaisal *et al.* 2002) The approximate loading of biomass per column was ca. 72 mg bacterial protein, measured using the bicinchonic acid method (Nott *et al.* 2001). Each column was challenged with solutions at a flow rate of 10 mL h^{-1} for 1 week prior to MRI. Control columns contained polyurethane foam in the absence of *Serratia* biofilm.

Magnetic Resonance Imaging of columns

MRI of the columns used a 2.35 Tesla, 31 cm bore superconducting magnet (Oxford Instruments, UK) connected to a Bruker Medzintechnik Biospec II imaging console (Karlsruhe, Germany). The 9.4 cm internal diameter 'bird-cage' radio-frequency (RF) probe, and the 14.5 cm internal diameter gradient set used for spatial discrimination were both built 'in house'. ^{1}H images were acquired using a Spoiled GRASS sequence (Hashemi and Bradley 1997) (repetition time (TR)/ echo time (TE)/ flip angle (θ) 50 ms/ 7.5 ms/ 30 °) with 400 μM isometric pixel resolution.

Distribution of pixel intensity values for MR images (whole 3D image data set) were determined using CaMReS software written 'in house' at the Herchel Smith Laboratory for Medicinal Chemistry by Dr. N. J. Herrod. Data was displayed graphically using Microsoft Excel.

Results and Discussion

High resolution 2D slices of MR images taken from the 3D data set of the water in contact with the polyurethane foam, with and without immobilized *Serratia* biofilm are shown in Fig. 1. Histograms were plotted to quantify the difference in signal intensity of these images (Fig. 2). In the presence and absence of biofilm, paramagnetic Cr^{3+} has higher signal intensity than Cr^{6+} solution, as paramagnetic substances shorten the T_1 spin-lattice relaxation time.

Biofilm is visualised as low signal intensity against the challenge solution (biomass water content: ca 90 %). Consequently the polyurethane foam biofilm support can be visualised indirectly as a dark matrix (Fig. 1). Biofilm appears more distinct in the presence of Cr^{3+}, and it is reasonable to assume that metal ions have absorbed onto the biofilm, reducing the T_2 of the biofilm water.

This study shows that MRI can detect differences in signal intensity between Cr^{3+} and Cr^{6+} solution due to the different relaxivity and susceptibility of the two ions. Further method development is required to increase the sensitivity of this technique to enable visualisation and quantification of spatial and temporal variations in Cr^{3+} and Cr^{6+}. MRI may then be used non-invasively and non-destructively to provide spatial information that can be used for on-line quantification of Cr^{6+} reduction by immobilized bacteria in continuous-flow packed-bed columns.

Although this work demonstrates the potential of MRI to distinguish between Cr^{6+} and Cr^{3+}, the work is flawed. Only one image was produced and analysed for each experimental parameter. To be scientifically valid, additional images need to be analysed and conclusions drawn from the combined data. Glycerol-2-phosphate should not of been present as precipitation of Cr^{3+} as $CrPO_4$ did not occur. Incorporation of G2P introduces complications, since it may affect the Cr^{3+} signal (M. Britton, personal communication). Investigations into the potential to use MRI to distinguish between Cr^{6+} and Cr^{3+} should have focussed initially on a simple system that did not contain *Serratia* biofilm or the foam matrix (i.e. columns should only of contained Cr^{6+} or Cr^{3+} solution). Additional chemicals (e.g. MOPS) would then be added to assess whether addition of these compounds affects the MR image produced. Only after this preliminary work had been completed should additional parameters (i.e. foam matrix, *Serratia* biofilm) been introduced.

Acknowledgements

We wish to acknowledge the financial support of the EPSRC (Studentship Number: 00318650 to ACH), BBSRC (Studentship Number: 97/A1/E/03038 to ANM) and the Herchel Smith Endowment for funding LEM, KPN, LDH.

References:

Balcom BJ, Carpenter AT, Hall LD. 1992. Spatial and temporal visualization of two aqueous iron oxidation-reduction reactions by Nuclear Magnetic Resonance Imaging. *J. Chem. Soc. Chem. Commun.* 4:312-313.

Bertini I, :Luchinat C. 1986. NMR of paramagnetic molecules in biological systems. Menlo Park, CA: Benjamin/ Cummings.

Callaghan PT. 1991. Principles of Nuclear Magnetic Resonance Microscopy. Clarendon Press, Oxford.

Dechter JJ, Komoroski RA, Ramaprasad S. 1991. Use of presaturation for chemical-shift-selective imaging of individual fluids in sandstone and carbonate cores. *J. Magn. Reson.* 93:142-150.

Finlay JA, Allan VJM, Conner A, Callow ME, Basnakova G, Macaskie LE. 1999. Phosphate release and heavy metal accumulation by biofilm-immobilized and chemically-coupled cells of a *Citrobacter* sp. pre-grown in continuous culture. *Biotechnol. Bioeng.* 63:87-97.

Guha H, Jayachandran K, Maurrasse F. 2001. Kinetics of Cr(VI) reduction by a type strain *Shewanella alga* under different growth conditions. *Environ. Pollut.* 115:209-218.

Hammer BE. 1998. Industrial applications of nuclear magnetic resonance. *Sensor Review.* 18:245-251.

Hashemi RH, Bradley WG. 1997. MRI: The Basics. Baltimore: Williams and Wilkins.

Lens PNL, Hemminga MA. 1998. Nuclear Magnetic Resonance in environmental engineering: Principles and applications. *Biodegradation.* 9:393-409.

Lewandowski Z, Stoodley P, Altobelli SA. 1995. Experimental and conceptual studies on mass transport in biofilms. *Water Sci.* 31:153-162.

Lovley DR, Phillips EJP. 1994. Reduction of chromate by *Desulfovibrio vulgaris* and its c_3 cytochrome. *Appl. Environ. Microbiol.* 60:726-28.

Nott KP, Paterson-Beedle M, Macaskie LE, Hall LD. 2001. Visualisation of metal deposition in biofilm reactors by three-dimensional magnetic resonance imaging (MRI). *Biotechnol. Lett.* 23:1749-1757.

Pattanapipitpaisal P, Mabbett AN, Finlay JA, Beswick AJ, Paterson-Beedle M, Essa A, Wright J, Tolley MR, Badar U, Ahmed N, Hobman JL, Brown NL, Macaskie LE. 2002. Reduction of Cr(VI) and bioaccumulation of chromium by Gram positive and

Gram negative microorganisms not previously exposed to Cr-stress. *Environ. Technol.* 23:731-745.

Westbrook C, Kaut C. 1993. MRI in Practice. Oxford: Blackwell Scientific Publications.

Yong P, Macaskie LE. 1998. Bioaccumulation of lanthanum, thorium, and uranium, and use of a model system to develop a method for the removal of plutonium from solution. *J. Chem. Technol. Biotechnol.* 71:15-26.

Legend to Figures

Fig. 1. 2D slices taken from 3D MR image data sets (TR/ TE/ θ 50 ms/ 7.5 ms/ 30 °) of packed-bed columns. (A) polyurethane-immobilized *Serratia* with Cr^{6+} and G2P (B) polyurethane foam cubes with Cr^{6+} and G2P (C) polyurethane-immobilized *Serratia* with Cr^{3+} and G2P (D) polyurethane foam cubes with Cr^{3+} and G2P

Fig. 2. Variance in intensity of the solutions present in Fig. 1. against the number of image pixels present. Columns containing ●: polyurethane-immobilized *Serratia* with Cr^{6+} and G2P; ■: polyurethane foam cubes with Cr^{6+} and G2P; ○: polyurethane-immobilized *Serratia* with Cr^{3+} and G2P; □: polyurethane foam cubes with Cr^{3+} and G2P.

Fig. 1.

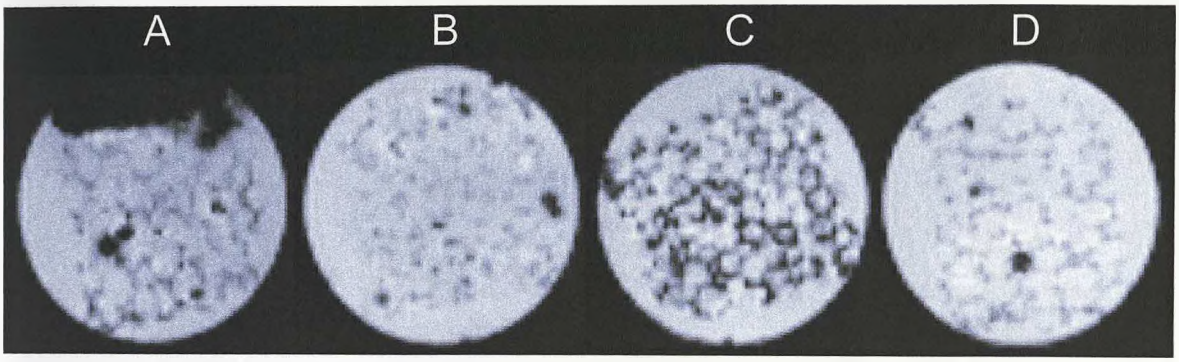
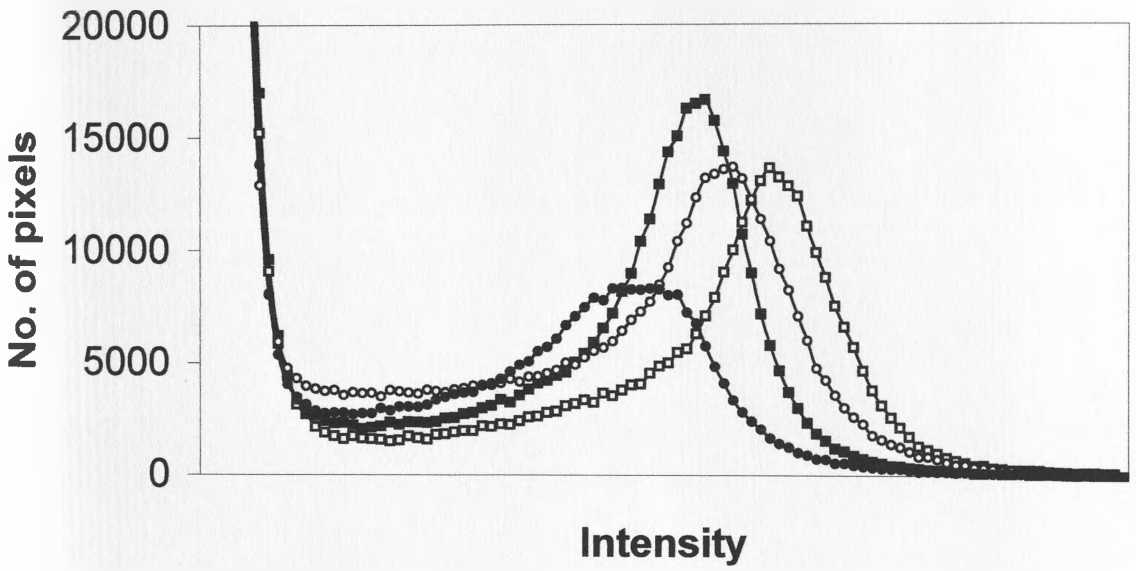


Fig. 2.



APPENDIX IV:

Supplementary Materials and Methods

1.0 Materials

1.1 Bacterial Strains

Microbacterium sp. NCIMB 13776 was isolated from a Pakistani tannery waste by P. Pattanapipitpaisal.

Desulfovibrio vulgaris NCIMB 8303 was obtained from Prof. D. R. Lovley (University of Massachusetts, Amherst, MA 01003, USA).

Desulfovibrio desulfuricans NCIMB 8307 was obtained from the American type culture collection.

Escherichia coli strains MC4100 (parental) and HD701 (HycA-deficient mutant) were provided by Prof. A. Böck (Lehrstuhl für Mikrobiologie de Universität, Munich, Germany).

1.2 Media

Microbacterium sp. NCIMB 13776 was maintained aerobically at 30 °C on L-agar plates. Bacterial cultures were grown aerobically overnight, with continuous agitation at 100 rpm, in L. broth, prepared by Central Services, School of Biosciences, The University of Birmingham, UK.

D. vulgaris NCIMB 8303 and *D. desulfuricans* NCIMB 8307 were maintained anaerobically in Postgate's medium B (PGB), with blackening of the iron salt indicative of growth. Postgate's medium C (PGC) was used for mass culture of cells, with citrate present to prevent precipitation of the iron salt.

Table 1: Composition of PGB

The concentration of each compound is given in g/ L.

KH_2PO_4	0.5
NH_4Cl	1.0
$CaSO_4$	1.0
$MgSO_4.7H_2O$	2.0
Sodium lactate	3.5
Yeast extract	1.0
Ascorbic acid	0.1
Thioglycollic acid	0.1
$FeSO_4.7H_2O$	0.5

Tap water 1 L, pH adjusted to pH 7.5 ± 0.2 with NaOH.

Table 2: Composition of PGC

The concentration of each compound is given in g/ L.

KH_2PO_4	0.5
NH_4Cl	1.0
Na_2SO_4	4.5
$CaCl_2.6H_2O$	0.06
$MgSO_4.7H_2O$	0.06
Sodium lactate	6.0
Yeast extract	1.0
$FeSO_4.7H_2O$	0.004
Sodium citrate.$2H_2O$	0.3

Distilled water to 1 L, pH 7.5 ± 0.2 with NaOH.

Both PGB and PGC were placed in 100 mL volumes into 120 mL glass serum bottles and sealed with butyl rubber seals. The media was degassed for 20 min with oxygen free nitrogen (OFN) prior to autoclaving at 121 °C for 20 min.

E. coli strains MC4100 and HD701 were maintained aerobically at 30 °C on nutrient agar No. 2 (Oxoid, UK) plates. Cells were grown aerobically overnight at 30 °C with continuous agitation at 100 rpm, in nutrient broth No. 2 (Oxoid).

2.0 General methods in Biochemistry

2.1 Assay for Cr(VI) – The Diphenylcarbazide method

Stock Solution A: 37.5 mg diphenylcarbazide + 7.5 mL acetone + 7.5 mL distilled water + 1.25 mL 3M sulphuric acid.

Stock Solution B: 4 mL Solution A + 96 mL distilled water.

1) Collect supernatant from cell suspension by centrifugation.
2) Mix 100 μL of sample supernatant (or Na_2CrO_4 standard) with 1.4 mL Solution B in a 1.5 mL cuvette. Leave at room temperature for 5 min.
3) Read absorbence at 540 nm (Pharmacia LKB, Novaspec II Spectrophotometer).

2.1.1. Cr(VI) calibration curve

Cr(VI) calibration curves were plotted using of Na_2CrO_4 standards (Fig. 1).

Error bars are within symbol dimensions.

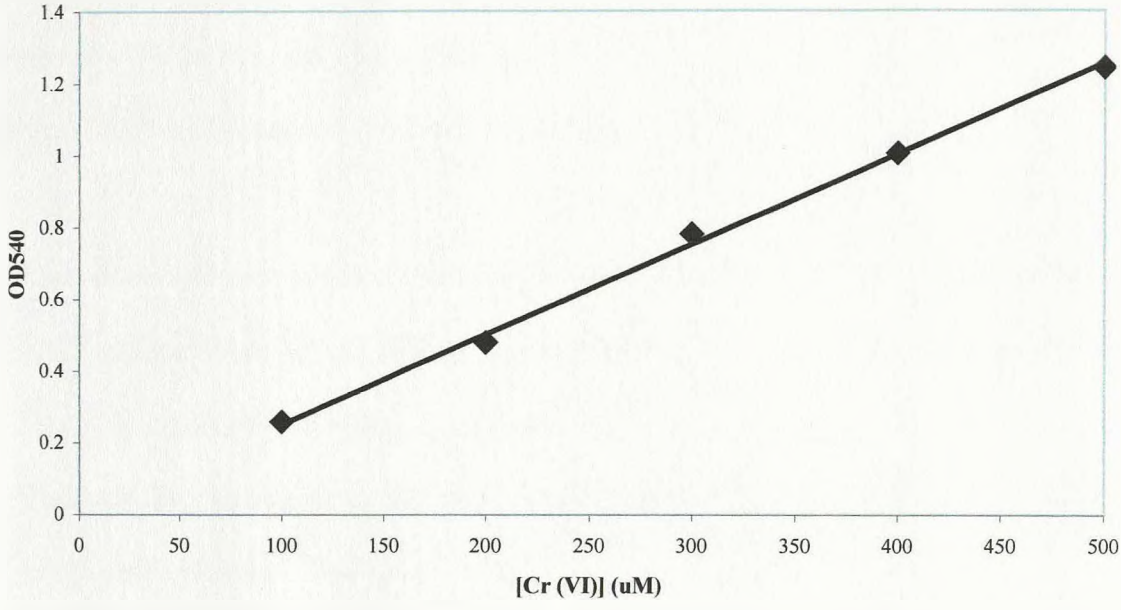


Fig. 1: Cr(VI) calibration curve

Equation of the line: $y = 0.0025x$; $R^2 = 0.9975$

y = Absorbance at 540 nm

x = [Cr(VI)] in μM

2.2 Determination of Protein concentration – The Bicinochoninic Acid method

This protein determination method was previously adapted from the Sigma protein test kit TPRO-562. Reaction mixtures were set up in 1.5 mL eppendorf tubes.

Solution A: Bicinchoninic acid (as supplied)

Solution B: 4 % (w/v) copper (II) sulfate solution

Solution C: 50 mL Solution A + 1.0 mL Solution B.

1) Appropriate volume of protein sample (depending on OD_{600} of cell culture; OD_{600} of 1.0 or 0.5 requires 50 or 100 µL of sample, respectively) or standard (Bovine Serum Albumin, Sigma) is pippetted into an eppendorf tube.
2) Make reaction volume up to 400 µL with distilled water.
3) Add 1.0 mL solution C and mix.
4) Incubate at 30 °C for 30 mins.
5) Mix and transfer to 1.5 mL cuvette and measure absorbence at 562 nm (Pharmacia LKB, Novaspec II Spectrophotometer).

2.2.1 Protein calibration curve

Protein calibration curves were plotted using Bovine Serum Albumin (BSA) as standard.

Error bars are within symbol dimensions.

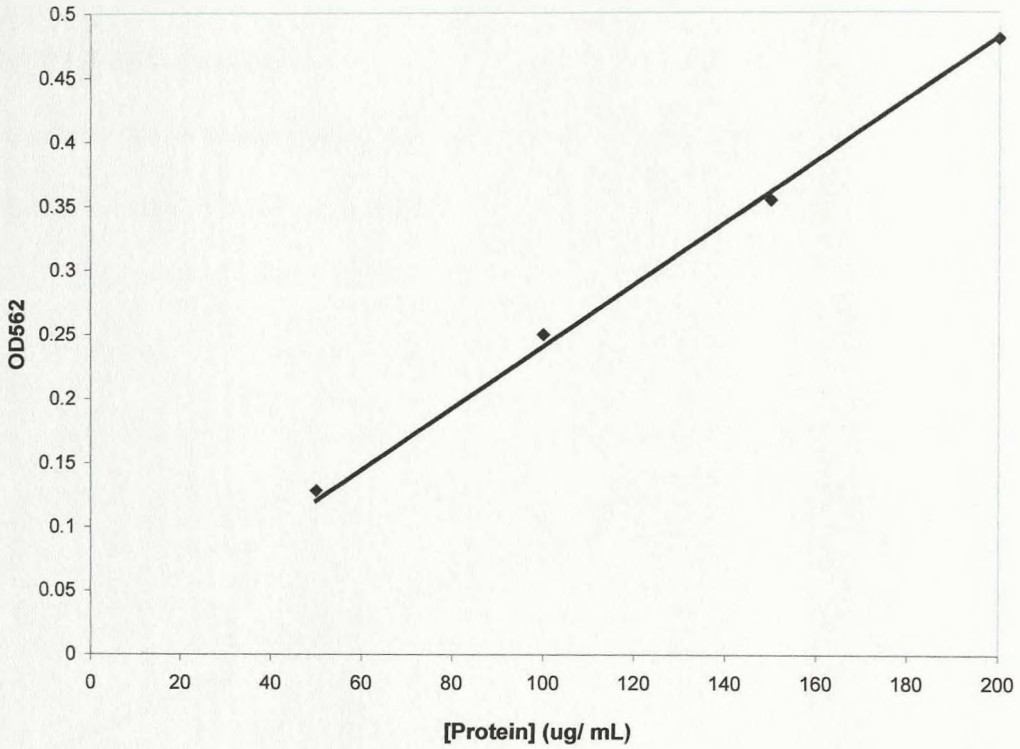


Fig. 2: Protein calibration curve

Equation of line: $y = 0.0024x$; $R^2 = 0.9972$

y = Absorbance at 562 nm

x = [Protein] in µg/ mL

2.3 Determination of Pd(II) concentration

The maximum height of the specific adsorption peak of $[PdCl_4]^{2-}$ at 420 nm depends linearly on the palladium salt concentration

2.3.1 Pd(II) Calibration curve

Pd(II) calibration curves were plotted using Na_2PdCl_4 as standard.

Error bars are within symbol dimensions.

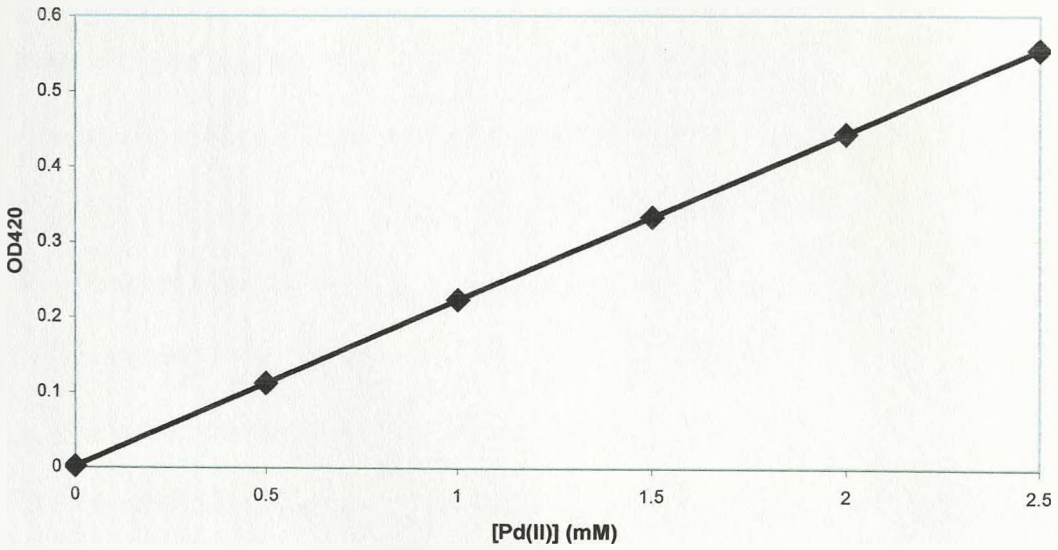


Fig. 3: Pd(II) calibration curve

Equation of line: $y = 0.222x - 0.002$; $R^2 = 0.98$

y = Absorbance at 420 nm

x = [Pd(II)] in mM

2.4 Cell density

The cell density of liquid culture was determined as optical density at 600 nm on a Pharmacia LKB, Novaspec II Spectrophotometer.

2.5 Determination of cell dry weight

1) Cells were harvested at 8000 rpm, 10 mins, 4°C, and washed three times with 20 mM MOPS/ NaOH buffer (pH 7).
2) Cells were resuspended in approx. 10 mL isotonic saline and centrifuged at 8000 rpm, 10 mins, 4°C, and washed twice in approx. 5 mL distilled water.
3) After the final wash, the cell pellet fraction was incubated at 35 °C, until constant weight.

2.6 Relationship between OD_{600}, protein concentration and dry cell weight

1) *D. vulgaris* NCIMB 8303 and *Microbacterium* sp. NCIMB 13776 were grown in their respective media to various values of OD_{600}.
2) The protein concentration at each of these OD_{600} values was measured using the Bicinchoninic acid method (above).
3) Dry cell weight was determined as above using 100 mL of culture for each OD_{600} value.
4) For each strain the dry cell wt. was approx. twice the protein concentration (i.e. a protein concentration of 200 μg mL^{-1} corresponds to a dry cell wt. of approx. 400 μg mL^{-1} for both *Microbacterium* sp. NCIMB 13776 and *D. vulgaris* NCIMB 8303.

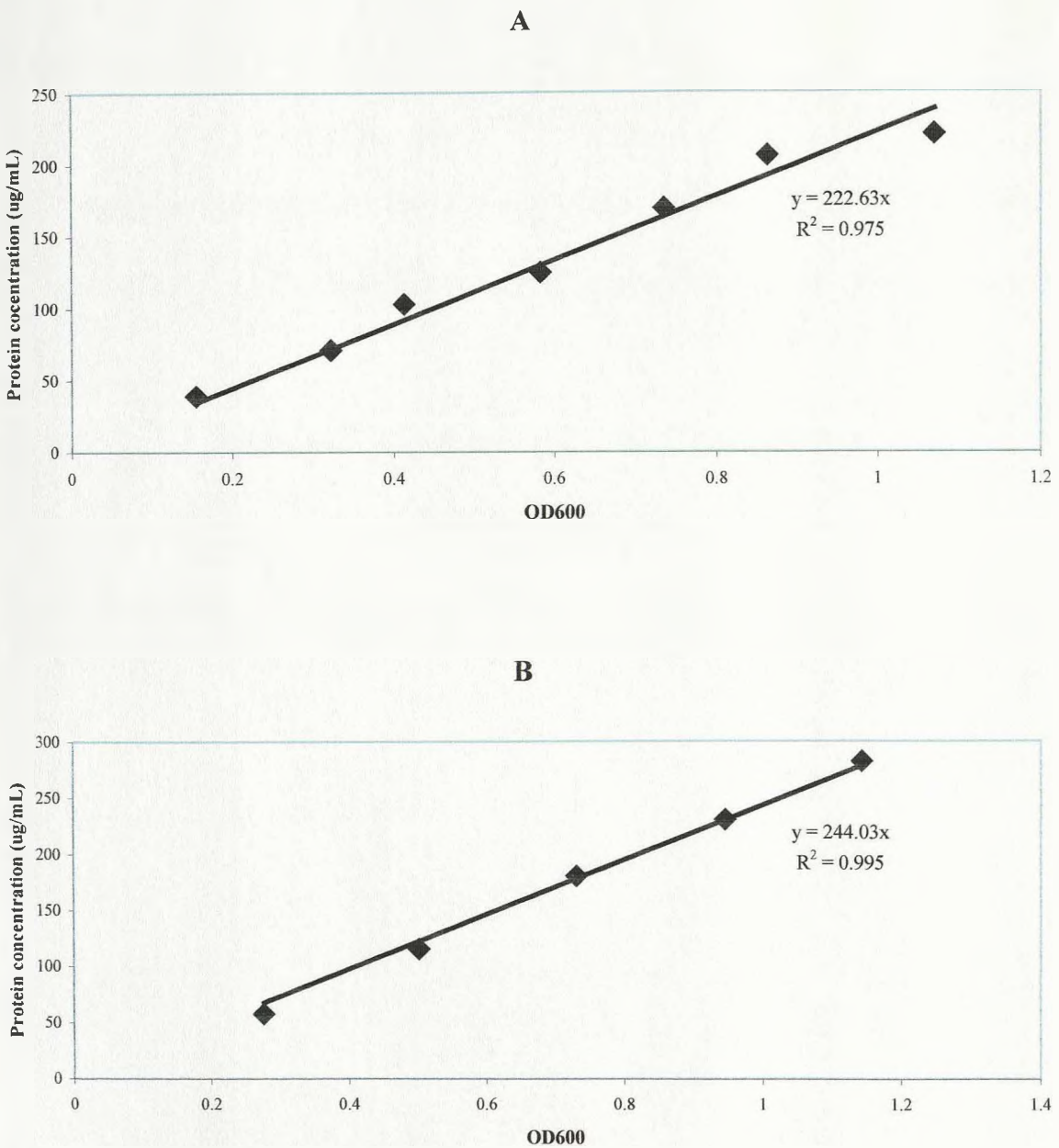


Fig. 4: Relationship between protein concentration and OD_{600} for (A) *D. vulgaris* NCIMB 8303 and (B) *Microbacterium* sp. NCIMB 13776

APPENDIX V:

"Applications of bacterial hydrogenases in waste decontamination, manufacture of novel bionanocatalaysts and in sustainable energy"

Journal: ***Biochemical Society Transactions***

33: 76 – 79 (2005)

This paper was written by L.E. Macaskie. The section entitled "Use of Bio-H_2 in sustainable waste treatment processes: closing the loop" was partly written using data from Section 4 of this thesis.

Applications of bacterial hydrogenases in waste decontamination, manufacture of novel bionanocatalaysts and in sustainable energy

L. E. Macaskie, V.S. Baxter-Plant, N.J. Creamer, A.C. Humphries, I.P.Mikheenko, D.W. Penfold, P. Yong

School of Biosciences, The University of Birmingham, Edgbaston, Birmingham, B15 2TT

Hydrogenases and bioreduction of metals

Many microorganisms are able to reduce toxic metals to less harmful forms by a variety of mechanisms including hydrogenase activity [1,2], e.g. in the reduction of U(VI) [3] and Se[IV] [4]. The ability to reduce the problematic radionuclide ^{99}Tc(VII) to insoluble ^{99}Tc(IV) was attributed to the activity of the hydrogenase-3 component of the formate hydrogenlyase complex in *Escherichia. coli* [5] and to the nickel-iron hydrogenase of *Desulfovibrio fructosovorans* [6]. Decontamination of Tc(VII) was also achieved by other *Desulfovibrio* spp. and demonstrated in flow-through decontamination processes [7,8]. Metal reductase activity was also extended to the reduction and recovery of precious metals from wastes at the expense of H_2 [9-11], and conclusively identified as hydrogenase-mediated by the use of mutants of *D. fructosovorans* deficient in one or more of the three major hydrogenases [12]. Pd(II) was reduced to Pd(0) which was held as biotemplated and supported metallic nanocrystals on the cell surface (Fig. 1).

Catalytic activity and properties of cell-bound Pd(0)

The microbially-reduced Pd(0) (Bio-Pd(0)) had a high catalytic activity, comparable to a commercial supported metal catalyst, in a standard hydrogenation reaction [13] and in its ability to reduce toxic Cr(VI) to less toxic Cr(III), at the expense of H_2, under conditions where bacteria alone or chemically-reduced Pd(0) were ineffective [14-17]. This activity was seen also in Bio-Pd(0) biorecovered from industrial wastes and harnessed at acidic pH [16,18]. Bio-Pd(0) was also able to reductively dehalogenate extensively polychlorinated biphenyls, which are recalcitrant to microbiological or chemical attack [19,20]. The reason for the high efficacy of the biomaterial is still under investigation but the Bio-Pd(0) has magnetic properties diagnostic of nanocrystals (Fig. 2). If the magnetic moment is examined as a function of the applied magnetic field a hysteresis is visible (Fig. 2) which is diagnostic of a ferromagnetic material and relates to the number of atoms at the surface of a cluster as compared to the number within the bulk, i.e. the property reflects that of predominantly surface-located atoms. From the magnetic data the size of the population subset of nanoparticles can be calculated; in this case as approx. 5 nm [12]. It is well known that nanoparticles have properties which differ from bulk crystals but chemical synthesis is difficult and expensive. Firstly, in the preparation of nanoparticles, nucleation must be achieved whilst growth is controlled to prevent the formation of larger particles. Secondly, the nanoparticles must be physically separated either by 'capping' (coating with a protective layer) or attachment to a support [21-23] during or following preparation. This prevents uncontrolled particle growth, which occurs either by coalescence, the fusing of two or more smaller particles to form a larger one, or by ripening, i.e. the growth of large particles by migration of material from smaller ones. Either of the two solutions above is required to preserve the nanoparticles and maintain their particular physical properties for any length of time. The bacterial system is unique

in that it provides nucleation functions, support on the biomatrix and, importantly, the rates and extents of nanocluster growth are controllable. Thus, according to requirements, Bio-Pd(0) can be prepared of variable nanoparticle size, which is illustrated by the magnetic (Fig 2), and also the catalytic [12] properties. The activity of Bio-Pd(0) was also extended to its use as an electrode material for low-temperature proton exchange fuel cell [24], which makes electricity from hydrogen.

Fuel cells and sustainable energy [25]

Low temperature proton exchange membrane (PEM) fuel cells use hydrogen as an energy vector. The incoming H_2 is split at the anode which comprises precious metal nanoparticles supported on electrically conducting graphite. Electrons derived from the H_2 generate current to power an electrical load. The protons from the H_2 move across an intermediate proton conducting layer and are reunited with the electrons from the circuit at the cathode and, with oxygen from the air, form H_2O as the only product. Consequently a fuel cell is environmentally-clean but the major disadvantage of the PEM fuel cell is that is requires a clean supply of hydrogen [25]. Provision of high quality, cheap H_2 is one of the objectives of the developing hydrogen economy. H_2 can be made by (e.g.) electrolysis of water or via anaerobic digestion of organic wastes [26,27]. In the latter case it is difficult to exclude other gaseous products (e.g. H_2S) which would poison the fuel cell catalyst, or methane (the end-product of anaerobic digestion), which is not used in a PEM fuel cell; a mixed gas stream would require a pre-filtration step.

Bioproduction of fuel cell quality H_2 by fermentation of industrial wastes

Enterobacterial strains, in common with other bacteria, synthesise hydrogen via the hydrogenase-3 component of the formate hydrogenlyase (FHL) complex. The FHL complex comprises formate dehydrogenase and hydrogenase-3 and its function is to oxidise formate (an end-product

of the mixed acid fermentation) to equimolar amounts of CO_2 + H_2, coupling formate oxidation by formate dehydrogenase H to proton reduction [28]. The conversion of formate is a homeostatic response to reduced acidic extracellular pH and a mechanism to dispose of the acidic end product of fermentation [29]. Expression of the FHL system is regulated via the constitutive repressor HycA, encoded by the *hycA* gene [29]. An *E. coli* strain HD701, which cannot synthesise the FHL repressor and is, therefore, up-regulated with respect to FHL expression, was constructed [29]. The up-regulated FHL expression allowed strain HD701 to reduce Tc(VII) at a higher rate (see above) as compared to its parental wild type *E. coli* MC4100 [30]. The hydrogenase-3 activity was also used synthetically in the generation of H_2 by fermentation of industrial confectionery wastes, using the upregulated mutant [31]. The head gas was passed through a NaOH trap to remove the CO_2 component; H_2 was the only component detected in the resulting gas stream and connection of the culture exit gas to a PEM fuel cell connected to a fan permitted continuous operation of the fan for the duration of H_2 evolution (10 h). Subsequent tests showed that is was not necessary to remove the CO_2 component of the culture exit gas, which could be passed directly into the fuel cell. The use of a monoculture ensures a constant gas composition and the use of an overproducing strain gives the maximum rate of H_2 production, which was several-fold greater than that of the parent culture [31]. However there are three potential drawbacks in the use of the monoculture. The first is overgrowth by contaminant organisms, since it would be very difficult to run the process aseptically at the industrial scale. The *E. coli* strain was used as resting cells in buffer, it lacked an additional nitrogen source and hence negligible biomass growth was supported using sugary waste substrates. This type of waste is often derived from cane sugar (sucrose) but *E. coli* does not possess invertase activity and a large proportion of the waste is not used, reducing bioprocess

efficiency. The genes encoding sucrose uptake and invertase activity were cloned into the H_2-overproducing strain, conferring the property of H_2 production from sucrose [32]. The industrial acceptability of a genetically modified organism remains to be proved. The third problem is that enterobacterial strains carry out mixed acid fermentation, that is, H_2 is produced along with other end-products. For maximum H_2 yield per mole of substrate an additional downstream fermentation step is required to convert organic acids; this could be an anaerobic digester (for a secondary H_2/CH_4 stream) or a photobioreactor for the production of an additional H_2 stream e.g. as a side reaction of nitrogenase activity by *Rhodobacter sphaeroides* in the presence of light at the expense of outflow from the *E. coli* reactor. This was shown to be feasible [32].

Use of Bio-H_2 in sustainable waste treatment processes: 'closing the loop'

The use of hydrogenases in biotechnology shows one important aspect: they can be harnessed in the synthetic direction (for Bio-H_2 production from wastes) or catabolically (at the expense of H_2) for the hydrogenase- mediated reduction of metals by bacteria (e.g. Pd(II) → Pd(0) (i.e. Bio-Pd(0))) or Bio-H_2 for the Pd(0)-catalysed reduction of Cr(VI), the reductive dehalogenation of PCBs or, indeed hydrogenation reactions for chemical manufacturing. Palladium metal splits H_2, not only in fuel cells (above) but within the Pd-crystal itself, to provide an excellent chemical catalyst. Therefore it should be possible to couple the Bio-H_2 production by *E. coli* strain HD701 to processes which consume H_2. A 2-stage bioreactor was constructed with the 1st stage fermenter as shown for the fuel cell and with the gas outlet connected to a 2nd stage reactor containing i) Cr(VI)-reducing bacteria and Cr(VI); ii) a reactor containing *D. desulfuricans* and Pd(II) or c) a reactor containing Bio-Pd(0) and Cr(VI). In all cases the Bio-H_2 supported the reaction similarly to H_2 from a commercial supply.

In conclusion, by coupling synthetic and catabolic hydrogenase activities it has been shown possible to co-treat wastes from the food industry, using the product (Bio-H_2) to treat precious metal waste solutions, producing a new class of bioinorganic catalyst (Bio-Pd(0)). This can be used in the treatment of a third (Cr(VI)) waste, produced by many chemical industries) or fourth (PCB) waste, providing the possibility to co-treat several classes of wastes from several industrial sectors simultaneously. In the field of sustainable energy bacterial hydrogenase activity can manufacture a key component of a fuel cell and the means (Bio-H_2) to generate electricity from it, while the use of Bio-Pd(0) as a hydrogenation catalyst could permit the use of H_2 as a chemical reactant at lower temperatures and pressures than are currently used, and hence a possible industrial application for Bio-H_2 here also. In this context it should be noted that for decoupling the rate of H_2 production from its consumption, temporally or spatially, a suitable H-store is necessary and hydrogen biotechnology and H-store development must proceed together to realise the hydrogen economy. H-stores are now becoming available that will accept H_2 at the low pressure of the culture head-gas (0.5-1.5 bar and at ambient temperatures [34] and these are currently being used in the coupling of the H-production and consumption steps, and in pooling the H-streams from dual synthetic bioreactor systems.

References

1. Lloyd, J.R. and Lovley, D.R. (2001). Microbial detoxification of metals and radionuclides. Curr. Op. Biotechnol. **12**, 248-253.
2. Lloyd, J.R., Macaskie, L.E. and Lovley, D.R. (2003) Applications of metal reducing microorganisms. Adv. Appl. Microbiol **53**, 85-119.
3. Woolfolk, C.A. and Whiteley, H.R. (1962) Reduction of inorganic compounds with molecular hydrogen by *Micrococcus lactilyticus.* J. Bacteriol. **84**, 647-658
4. Yanke, L.J., Bryant, R.D, and Laishly, E.J. (1995) Hydrogenase I of *Clostridium pasteurianum* functions as a novel selenite reuctase Anaerobe **1**, 61-67.
5. Lloyd, J.R., Cole, J.A. and Macaskie, L.E. (1997) Reduction and removal of heptavalent technetium from solution by *Escherichia coli.* J. Bacteriol. **179**, 2014-2021.
6. De Luca, G., Philip, P., Dermoun, Z., Rousset, M. and Vermeglio, A. (2001) Reduction of technetium (VII) by *Desulfovibrio fructosovorans* is mediated by the nickel-iron hydrogenase Appl. Environ. Microbiol. **67**, 4583-4587.
7. Lloyd, J.R., Mabbett, A.N., Williams, D.R. and Macaskie, L.E. (2001) Metal reduction by sulphate-reducing bacteria: physiological diversity and metal specificity. Hydrometall. **59**, 327-337.
8. Lloyd, J.R., Ridley, J., Khizniak, T., Lyalikova., Macaskie, L.E. (1999) Reduction of technetium by *Desulfovibrio desulfuricans*: biocatalyst characterisation and use in a flow-through bioreactor. Appl. Environ. Microbiol. **65,** 2691-2696.
9. Lloyd, J.R. Yong, P. and Macaskie, L.E. (1998) Enzymatic recovery of elemental palladium by using sulfate-reducing bacteria. Appl. Environ. Microbiol. **64**, 4607-4609.

10. Yong, P., Rowson, N.A., Farr, J.P.G., Harris, I.R. and Macaskie, L.E. (2002) Bioreduction and bio-crystallization of palladium by *Desulfovibrio desulfuricans* NCIMB 8307. Biotechnol. Bioeng. **80**, 369-379.

11. Yong, P., Rowson, N.A., Farr, J.P.H., Harris, I.R. and Macaskie, L.E. (2003). A novel electrobiotechnology for the recovery of precious metals from spent automotive catalysts. Environ. Technol. **24**, 289-297.

12. Mikheenko. I.P. (2004) Nanoscale Palladium Recovery. PhD Thesis, The University of Birmingham, UK.

13. Creamer, N.J., Mikheenko, I.P., Winterbottom, J.M., Wood, J and Macaskie, L.E. (2004) Catalytic palladium nanoparticles manufactured by sulphate-reducing bacteria. Proc. 7th Int. Conf on Nanostructured Materials Wiesbaden, Germany, June 20-24th 2004. p.169.

14. Mabbett, A.N. and Macaskie, L.E. (2002) A new bioinorganic process for the remediation of Cr(VI) J. *Chem. Technol. Biotechnol.* **77**, 1169-1175

15. Mabbett, A.N., Farr, J.P.G. and Macaskie, L.E. (2004) Reduction of Cr(VI) by palladized biomass of *Desulfovibrio desulfuricans* ATCC 29577. *Biotechnol. Bioeng.* **87**, 104-109.

16. Mabbett, A.N. (2001). The reduction and recovery of chromium (VI) from industrially polluted waste waters using sulphate-reducing bacteria. PhD Thesis, The University of Birmingham, UK

17. Humphries, A.C., Nott, K.P., Hall, L.D. and Macaskie, L.E. (2004) Continuous removal of Cr(VI) from aqueous solution catalysed by palladised biomass of *Desulfovibrio vulgaris* NCIMB 8303. *Biotechnol. Lett.* in press

18. Mabbett, A.N., Yong, P. and Macaskie, L.E. (2004) Biorecovered precious metals from industrial wastes: single step conversion of liquid waste to bioinorganic catalyst with environmental application. Biotechnol. Bioeng. In submission.

19. Baxter-Plant, V.S., Mikheenko, I.P. and Macaskie, L.E. (2003) Sulphate-reducing bacteria, palladium and the reductive dehalogenation of chlorinated aromatic compounds. *Biodegradation*, **14**, 83, 2003.

20. Baxter-Plant, V.S., Mikheenko, I.P., Robson, M., Harrad, S.J. and Macaskie, L.E. (2004) Dehalogenation of chlorinated aromatic compounds using a hybrid bioinorganic catalyst. Biotechnol. Lett. In press.

21. Choudhary, T. V. and Goodman, D. W. (2002) Oxidation catalysis by supported gold nano-clusters. Top. Catal. **21**, 25–34 (2002).

22. Mulvaney, P., Liz-Marzan, L. M., Giersig, M. and Ung, T. (2000) Silica encapsulation of quantum dots and metal clusters. J. Mat. Chem. **10**, 1259–1270 (2000).

23. Lopez-Quintela, M.A. (2003) Curr. Op. Coll. Interface Sci. **8**, 137-144, 2003.

24. Macaskie, L.E., Levine, C and Kendall, K.K. (2004) unpublished work

25. Larminie, J and Dicks, A (2000) Fuel Cells Explained. John Wiley and Sons, Chichester, UK

26. Mizuno, O., Disndale, R., Hawkes, F.R., Hawkes, D.L. and Noike T (2000) Enhancement of hydrogen production from glucose by nitrogen gas sparging Bioresource Technol. **73**, 67-75.

27. Mizuno, O., Ohara, T., Shinya, M and Noike, T (2000) Characteristics of hydrogen from bean curd manufacturing waste by anaerobic microflora. Wat Sci Technol **42**, 345-350

28. Rossman, R., Sawers, G and Bock, A. (1991) Mechanism of regulation of the formate-hydrogenlyase pathway by oxygen, nitrate and pH: definition of the formate regulon Mol. Microbiol. **5**, 2807-2814.

29. Sauter M., Bohm, R and Bock, A (1992) Mutational analysis of the operon (hyc) determining hydrogenase 3 formation in *Escherichia coli* Mol. Microbiol. **6**, 1523-1532.

30. Lloyd JR, Thomas GH, Finlay JA, Cole JA, Macaskie LE. (1999) Microbial reduction of technetium by *Escherichia coli* and *Desulfovibrio desulfuricans*: enhancement via the use of high activity strains and effect of process parameters. Biotechnol. Bioeng. **66**, 122-130.

31. Penfold, D.W., Forster, C.F., Macaskie, L.E.(2003) Increased hydrogen production by *Escherichia coli* strain HD701 in comparison with the wild type parent strain MC4100. Enz. Microb. Technol, **33**, 185-189.

32. Penfold, D.W. and Macaskie, L.E. (2004) Production of hydrogen from sucrose by *Escherichia coli* HD701 and FTD701 carrying the pUR400 plasmid, which encodes invertase activity. Biotechnol. Lett., in press

33. Penfold, D.W., Redwood, M. and Macaskie, L.E., unpublished work

34. Penfold, D.W., Macaskie, L.E. and Harris, I.R., unpublished work

Fig. 1: Accumulation of Pd(0) by *D. desulfuricans* at the expense of H_2. Inset: cell before exposure to Pd(II). Main panel: deposition of Pd(0). This starts at periplasmic loci corresponding to the sites of periplasmic and inner-membrane hydrogenase activity [12] and the nanoclusters grow in size, erupting through the outer membrane to 'decorate' the bacterial cells, forming 'Bio-Pd(0)' catalyst.

Fig. 2: Illustration of Bio-Pd(0) made on *D. desulfuricans* in two ways to give (top) small deposits with a high ferromagnetic component or (bottom) larger deposits with a small ferromagnetic component as evidenced by the magnitude of the hysteresis loops in the plot of magnetic moment versus applied magnetic field. In this way it is possible to influence the catalytic efficacy of the Bio-Pd(0). The magnetic properties were examined using a vibrating sample magnetometer and superconducting quantum interference device in the School of Physics, The University of Birmingham (thanks to P. Mikheenko for assistance with the magnetic measurements).

Fig. 1:

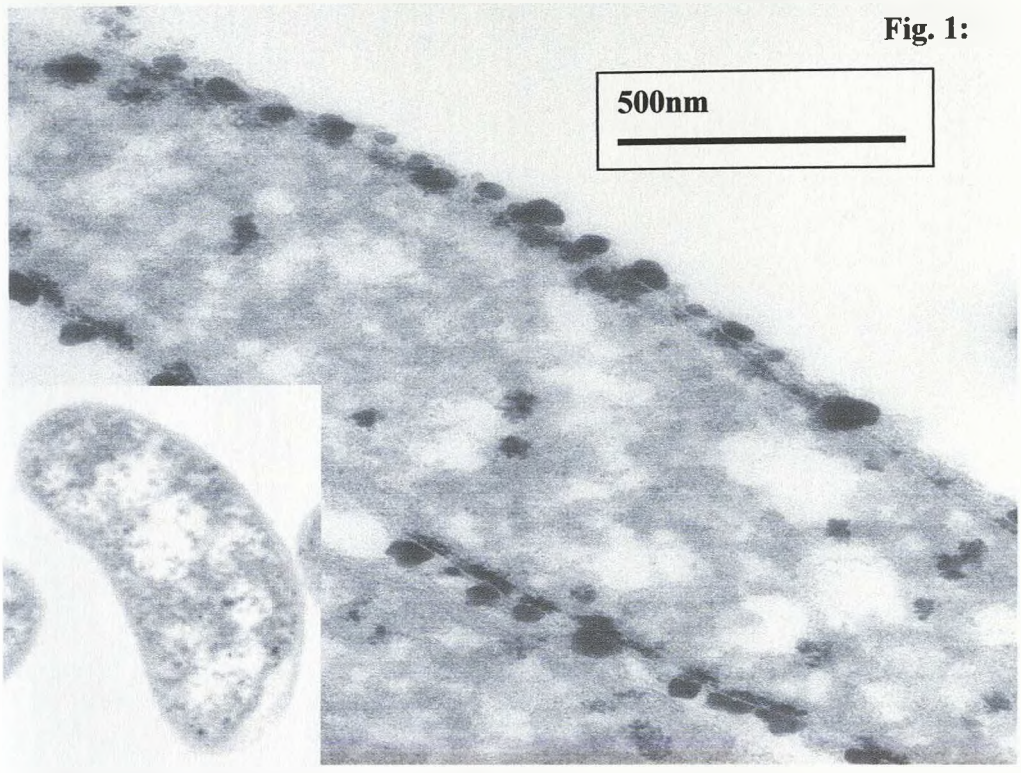
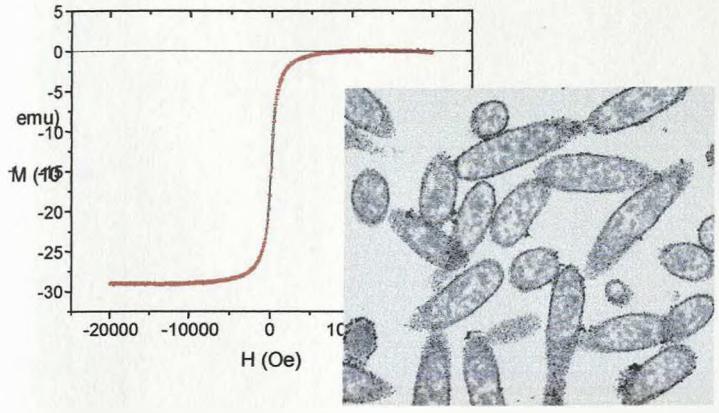
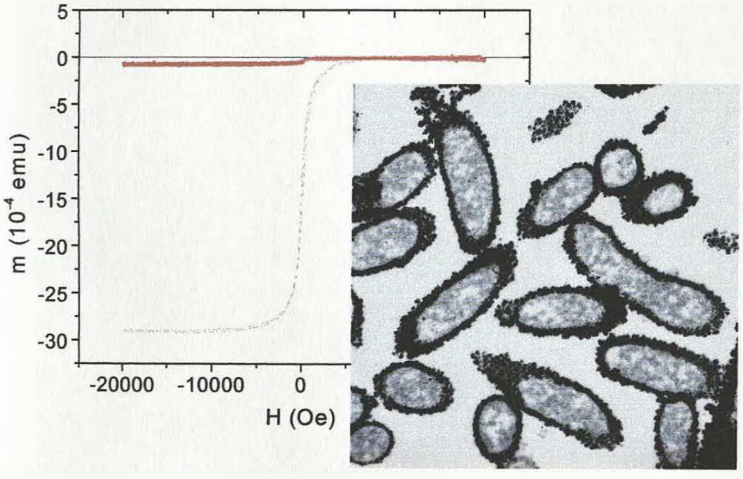


Fig. 2:



Pd(0) crystals in the Bio-Pd powder with large ferromagnetic component



Pd(0) crystals in the Bio-Pd powder with small ferromagnetic component